MECHANICAL RESPONSE OF SANDWICH PIPES SUBJECT TO HYDROSTATIC PRESSURE AND BENDING

by

Kaveh Arjomandi

Submitted in partial fulfillment of the requirements
for the degree of Doctor of Philosophy

at

Dalhousie University
Halifax, Nova Scotia
December 2010

© Copyright by Kaveh Arjomandi, 2010

DALHOUSIE UNIVERSITY

Department of Civil and Resource Engineering

The undersigned hereby certify that they have read and recommend to the Faculty of Graduate Studies for acceptance a thesis entitled "MECHANICAL RESPONSE OF SANDWICH PIPES SUBJECT TO HYDROSTATIC PRESSURE AND BENDING" by Kaveh Arjomandi in partial fulfillment of the requirements for the degree of Doctor of Philosophy.

Dated: 13 December 2010

External Examiner: _____

Research Supervisor: _____

Examining Committee: _____

_____

DepartmentalRepresentative: _____

DALHOUSIE UNIVERSITY

DATE: 13 December 2010

AUTHOR: Kaveh Arjomandi

TITLE: MECHANICAL RESPONSE OF SANDWICH PIPES SUBJECT TO HYDROSTATIC PRESSURE AND BENDING

DEPARTMENT OR SCHOOL: Department of Civil and Resource Engineering

DEGREE: Ph.D CONVOCATION: May YEAR: 2011

Permission is herewith granted to Dalhousie University to circulate and to have copied for non-commercial purposes, at its discretion, the above title upon the request of individuals or institutions.

_____

Signature of Author

The author reserves other publication rights, and neither the thesis nor extensive extracts from it may be printed or otherwise reproduced without the author's written permission.

The author attests that permission has been obtained for the use of any copyrighted material appearing in the thesis (other than the brief excerpts requiring only proper acknowledgement in scholarly writing), and that all such use is clearly acknowledged.

To my parents,

Aazam Enayati

and

Ali Arjomandi.

Table of Contents

List of tables x

List of figures xi

Abstract xviii

List of abbreviations used xix

Acknowledgements xxi

Chapter 1: Introduction 1

Chapter 2: Lierature Review 6

2.1. Loading applied to offshore pipelines 6

2.1.1. Loadings applied during the pipeline installation process 6

2.1.2. Loadings applied during the pipeline operation 9

2.2. Sandwich pipe systems 13

2.3. Buckling and collapse of pipelines 15

2.3.1. External pressure 16

2.3.2. Pure bending 23

2.4. High-grade steel pipelines 27

2.4.1. Manufacturing process 28

2.4.2. Numerical modeling of material yield anisotropy 29

2.4.3. Effect of yield anisotropy on the mechanical behavior of pipes 33

2.5. References 35

Chapter 3: Elastic Buckling Capacity Of Bonded And Unbounded Sandwich Pipes Under External Hydrostatic Pressure 41

3.1. Abstract 41

3.2. Nomenclature 42

3.3. Introduction 42

3.4. Motivation and aims 44

3.5. Analytical model 45

3.6. Equilibrium equations of the system 45

3.7. Characteristic equation of the system 49

3.8. Simplified solutions 50

3.8.1. Case A- Core layer can slide over the external pipe 51

3.8.2. Case B- Core layer is bonded to the external pipe 51

3.9. Results and discussion 52

3.10. Exact solution results 52

3.11. Accuracy of the simplified equations 56

3.12. Numerical results 59

3.13. Conclusions 64

3.14. References 65

Chapter 4: Stability And Post-Buckling Response Of Sandwich Pipes Under Hydrostatic External Pressure 68

4.1. Abstract 68

4.2. Nomenclature 69

4.3. Introduction 70

4.4. Motivation and the theory 72

4.5. Behavior of a sandwich pipe under hydrostatic external pressure 75

4.6. Finite Element models 78

4.7. Characteristic parameters 80

4.8. Parametric studies 85

4.9. Development of simplified practical equations 87

4.10. Results 88

4.11. Conclusions 91

4.12. Acknowledgments 93

4.13. References 93

Chapter 5: Influence Of The Material Plasticity On The Characteristic Behavior Of Sandwich Pipes 96

5.1. Abstract 96

5.2. Nomenclature 97

5.3. Introduction 97

5.4. Finite element model 100

5.5. Buckling and post-buckling response 103

5.5.1. Influence of the Lüder's banding 104

5.5.2. Influence of the core stiffness 107

5.5.3. Influence of yield strength 109

5.6. Conclusions 111

5.7. Acknowledgments 112

5.8. References 113

Chapter 6: A New Look At The External Pressure Capacity Of Sandwich Pipes 115

6.1. Abstract 115

6.2. Nomenclatures 116

6.3. Introduction 117

6.4. Theory and motivation 120

6.5. Parametric study 123

6.6. Finite element models 125

6.7. Parametric study results 128

6.7.1. Influence of the steel pipes thickness to radius (t/r)ratio 128

6.7.2. Influence of the core thickness..... 133

6.7.3. Influence of the steel pipes grade..... 136

6.8. A simplified and practical equation 137

6.8.1. Comparison with the experimental results..... 140

6.9. Optimization of the system parameters..... 141

6.10. Conclusion..... 145

6.11. Acknowledgement..... 147

6.12. References 147

Chapter 7: The Influence Of Intra-Layer Adhesion Configuration On The Pressure Capacity And Optimized Configuration Of Sandwich Pipes 150

7.1. Abstract 150

7.2. Nomenclature 151

7.3. Introduction 152

7.4. Theory and motivation 155

7.5. Parametric study..... 159

7.6. Finite element models 161

7.7. Parametric study results 162

7.7.1. Characteristic paths categories..... 163

7.7.2. Influence of the core thickness ratio 164

7.7.3. Influence of the external pipe's thickness to the radius ratio..... 168

7.7.4. Influence of the internal pipe's thickness to radius ratio 171

7.7.5. Influence of the core stiffness ratio..... 173

7.7.6. Influence of the internal and external pipes' steel grade 175

7.8. Simplified practical equations..... 178

7.8.1. Verification with the experimental results 182
7.9. Optimization of the system 183
7.10. Summary and conclusions 191
7.11. References 193
Chapter 8: Bending Capacity Of Sandwich Pipes 196
8.1. Abstract 196
8.2. Nomenclature 197
8.3. Introduction 198
8.4. Theory and motivation 203
8.5. Buckling behavior of sps under bending 207
8.5.1. Finite element models 207
8.5.2. Analysis results 209
8.6. Post-buckling behavior of sps under pure bending 215
8.6.1. Finite element models 215
8.6.2. Analysis results 219
8.7. Conclusion 228
8.8. References 231
Chapter 9: Conclusion 234
9.1. Conclusions 234
9.2. Recommendations for future work 241
References 243
Appendix A: Inner and Outer Pipes Stiffness Matrix 249
Appendix B: Core Material Stiffness Matrix 250
Appendix C: Copyright Agreement Forms 254
Jounral of Mechanics of Materials and Structures copyright agreement form 255

LIST OF TABLES

Table 4.1.The parameters considered in the parametric study and their range..... 85

Table 4.2. The value of constants to be used in Equation (4.9) for calculating CPIP pressure ($\Phi 1$) for pipes in category 1 88

Table 4.3.The value of constants to be used in Equation (4.9) for calculating limit equilibrium pressure ($\Phi 2$) for pipes in category 2..... 88

Table 6.1. Range of the parameters used in the parametric study. 125

Table 6.2. Values of the constants appearing in Equation (6.12) for calculating the pressure capacity of SPs..... 139

Table 6.3. Comparison of the experimental and numerical results produced by Estefen et al. [6.14] with the pressure capacities calculated by Equation (6.12).... 140

Table 7.1. Range of the parameters used in the parametric study. 160

Table 7.2. The value of constants of Equation (7.8) for calculating the pressure capacity of the FB SPs 180

Table 7.3. The value of constants of Equation (7.8) for calculating the pressure capacity of the OU SPs 180

Table 7.4. The value of constants of Equation (7.8) for calculating the pressure capacity of the IU SPs..... 181

Table 7.5. The value of constants of Equation (7.8) for calculating the pressure capacity of the BU SPs. 181

Table 7.6. Correlation of Stefen et al.[7.18] experimental results with the pressure capacity calculated from Equation (7.8) using constants for various intra layer properties..... 182

LIST OF FIGURES

Figure 2.1. Schematic presentation of the applied loads during S-Lay pipeline installation [from 2.1]. 7

Figure 2.2. Schematic presentation of applied loads during J-Lay pipeline installation [from 2.1]. 8

Figure 2.3. Schematic presentation of the reelship [from 2.1]..... 9

Figure 2.4. Internal and external pressure applied to an offshore pipeline..... 10

Figure 2.5. Uneven supports 10

Figure 2.6. Upheaval buckling [from 2.2]. 11

Figure 2.7. Ice keel gouging [from 2.2]. 12

Figure 2.8. Thaw settlement loading [from 2.2]. 13

Figure 2.9. A practical PIP configuration [from 2.4]..... 14

Figure 2.10. (a) Deformed and undeformed cross-section of the pipeline and (b) definition of midsurface displacements [from 2.7]. 16

Figure 2.11. Idealized geometry of the sandwich pipes..... 18

Figure 2.12. Non-dimensional collapse pressure for a sample SP system [from 2.12] 19

Figure 2.13. The buckling mode shapes of SP systems having $t1 = 9mm, tc = 115mm$ 20

Figure 2.14. Collapse cross-section of an aluminum SP system [2.16]..... 21

Figure 2.15. Propagation of section instability induced (a) during the installation process and (b) from the impact of an anchor [2.7]. 22

Figure 2.16. Pipe bending collapse modes [2.23]. 24

Figure 2.17. General stability behavior of pipes under pure bending..... 25

Figure 2.18. Schematic of the UOE manufacturing process. (a)Edge crimping. (b) U-ing. (c) O-ing. (d) Expansion process. [from 2.7]..... 29

Figure 2.19. Accuracy of the Hill's criteria in predicting the wrinkle half-wavelength vs. D/t from 15 experiments [from 2.48]..... 31

Figure 2.20. Deformation and load steps to simulate the material anisotropy and model the buckling behavior under the external hydrostatic pressure. (a) Bending. (b) Uniform contraction. (c) Unloaded cylinder. (d) Uniform expansion. (e) Final state. (f) External pressure. (g) Collapse. [from 2.51] 32

Figure 2.21. Influence of the yield anisotropy on: (a) critical stress (b) and axial half-wavelength at onset of wrinkling as a function of internal pressure for D/t 28.3 [from 2.46] 34

Figure 2.22. Effect of yield anisotropy on (a) bifurcation curvature (b) wrinkle half-wave as a function of the anisotropy variables [2.48]....35

Figure 3.1. The coordinate system and the idealized geometry.... 45

Figure 3.2. Histogram of t/r for the API Heavy and standard wall pipes with diameter greater than 0.1 m. 52

Figure 3.3. Ratio of the buckling capacity of the sandwich pipe to the external pipe as a function of geometric and material properties (a) Fully bonded (b) Core layer is disbonded from the external pipe (c) Core layer is disbonded from the internal pipe (d) Core layer is disbonded from both the internal and external pipes. 54

Figure 3.4. Ratio of the buckling capacity of the sandwich pipe to the external pipe as a function of geometric and material properties (a) Fully bonded (b) Core layer is disbonded from the external pipe (c) Core layer is disbonded from the internal pipe (d) Core layer is disbonded from both the internal and external pipes. 55

Figure 3.5. Sandwich pipe buckling mode numbers (a) Fully bonded (b) Core layer is disbonded from the external pipe (c) Core layer is disbonded from the internal pipe (d) Core layer is disbonded from both the internal and external pipes. 57

Figure 3.6. Error percentile resulting from the use of the SS [3.8,3.18] as a function of: (a) Ec/Ep and external pipe's t/r (b) Ec/Ep and r2/r1 58

Figure 3.7. Error percentile produced by the ATS for the case of fully bonded configuration, as a function of (a) Ec/Ep and external pipe's t/r (b) Ec/Ep and r2/r1.... 59

Figure 3.8. Error percentile produced by the ATS developed for the case of the external pipe sliding over the core as a function of (a) Ec/Ep and external pipe's t/r (b) Ec/Ep and r2/r1. 60

Figure 3.9. Buckling mode shape of the four studied PIP configurations. (a) Fully bonded (b) Core layer is disbonded from the external pipe (c) Core layer is disbonded from the internal pipe (d) Core layer is disbonded from both the internal and external pipes. 61

Figure 3.10. % Error produced by the simplified equations with respect to the FE results: (a) SS-Equation 16. (b) AST-Equation 19. (c) AST-Equation 18.... 63

Figure 3.11. The admissible range of parameters for which each of the simplified equations can predict the buckling pressure with less than 50% errors.... 64

Figure 4.1. Idealized geometry of a sandwich pipe. 73

Figure 4.2. Schematic of sandwich pipe characteristic paths. (a) for pipes with stiffening response after buckling; (b) for pipes with softening response during their post-buckling. 76

Figure 4.3. Geometry of the FE model. 78

Figure 4.4. Geometrical imperfection applied to the FE model 79

Figure 4.5. Effect of the characteristic parameters on the post-buckling behavior of sandwich pipes 81

Figure 4.6. Effect of the characteristic parameters on the post-buckling behavior of sandwich pipes 82

Figure 4.7. Pressure-Ovalization responses for sandwich pipes with various imperfections magnitude. (a) pipes with stiff core, (b) pipes with softer core. 84

Figure 4.8. Typical deformation of sandwich pipes with various interface adhesion configurations of the core layer and surrounding pipes. (a) Fully bonded (b) Core layer is disbonded from the external pipe (c) Core layer is disbonded from the internal pipe (d) Core layer is disbonded from both internal and external pipes. 86

Figure 4.9. Influence of the variation of the core thickness and stiffness and interface properties between the layers on the external pressure capacity of the pipe for a sandwich pipe with $t1/r1 = 0.07$, $t2/r2 = 0.05$ and $\nu c = 0.4$. (a) Fully bonded (b) Core layer is disbonded from the external pipe (c) Core layer is disbonded from the internal pipe (d) Core layer is disbonded from both internal and external pipes. 89

Figure 5.1. Idealized geometry of a sandwich pipe. 99

Figure 5.2. Mesh convergence study 101

Figure 5.3. Geometry and mesh configuration of the FE model 102

Figure 5.4. General steel stress-strain curve 105

Figure 5.5. Influence of the material plastic response on the buckling and post-buckling response of the pipe 107

Figure 5.6. Influence of the core stiffness on the buckling and post-buckling response. (a) $Ec/Ep = 0.1$(b) $Ec/Ep = 0.01$ (c) $Ec/Ep = 0.001$..... 108

Figure 5.7. Influence of the external pipe steel grade on the buckling, post-buckling and plastic strain contour response for the studied SP configuration. 110

Figure 5.8. Influence of the internal pipe steel grade on the buckling, post-buckling and plastic strain contour response for the studied SP configuration. 110

Figure 6.1. Idealized geometry of the sandwich pipes..... 120

Figure 6.2. Comparison of the pressure capacity calculated through different approaches for a sandwich pipe with $t2/r2 = 0.03$, $r2/r1 = 0.85$ and X60 grade steel internal and external pipes. 123

Figure 6.3. Distribution of API steel pipes with respect to the pipe thickness to radius ratio. 125

Figure 6.4. General geometry and FE mesh. 126

Figure 6.5. Influence of the steel pipe's thickness to radius ratio on the characteristic behavior of sandwich pipe with $r2/r1 = 0.8$ and X60 internal and external pipes (a)$Ec/Ep = 0.01$ (b) $Ec/Ep = 0.001$ 130

Figure 6.6. Equivalent plastic strain contours for the selected SP configurations. (a) $t1/r1 = 0.09$ (b) $t1/r1 = 0.05$, both with $Ec/Ep = 0.01$. (c) $t1/r1 = 0.09$ (d) $t1/r1 = 0.05$, both with $Ec/Ep = 0.001$. 131

Figure 6.7. Influence of steel pipe's thickness to radius ratio on the pressure capacity of SPs with various core stiffness ratios and $r2/r1 = 0.8$. 132

Figure 6.8. Influence of the core thickness on the characteristic behavior of sandwich pipe with $t1/r1 = t2/r2 = 0.05$, $Ec/Ep = 0.01$ and X60 grade steel internal and external pipes. Characteristic paths is shown up to the ovality magnitude of (a) 0.3. (b) 0.02. 134

Figure 6.9.Equivalent plastic strain contours at (a) the first proportional limit of the external pressure capacity (b) the ultimate external pressure capacity. 135

Figure 6.10. Influence of the core thickness on the pressure capacity of sandwich pipes with various core stiffness ratios and X60 internal and external pipes. (Left column) pipes with $t1/r1 = 0.07, t2/r2 = 0.03$. (Right column) pipes with $t1/r1 = t2/r2 = 0.05$. 136

Figure 6.11. Influence of the steel pipe's grade on the characteristic behavior of a sandwich pipe with $r2/r1 = 0.8$ and $Ec/Ep = 0.01$. 137

Figure 6.12. The optimization algorithm used for optimizing SP configurations at a given water depth and core material. 143

Figure 6.13. Optimization results of Equation (6.16) for α = 10 (a)$t1/r1$ (b) $t2/r2$ (c)$\sigma y1/\sigma y - X60$ (d)$\sigma y2/\sigma y - X60$. 144

Figure 7.1. Geometrical and material configuration of the SP system 156

Figure 7.2. (a) Characteristic behavior and (b) Maximum Equivalent Plastic Strain (PEEQ) of an SP configuration having the third category of characteristic path. .. 165

Figure 7.3. Influence of the core thickness on the characteristic behavior of SPs with fully bonded configuration. (a) Up to ovality magnitude of 30% (b) up to ovality magnitude of 2%. 166

Figure 7.4.Influence of the core thickness on the characteristic behavior of SPs having OU and IU configurations. Solid lines show the characteristic behavior of OU configurations and dashed lines illustrate the characteristic behavior of IU configurations. Symbol (^) represent the collapse point for OU configuration and symbol (v) shows the collapse point for the IU configuration. 167

Figure 7.5.Influence of the core thickness on the characteristic behaviorof SPs with BU configuration. 167

Figure 7.6.Influence of the core thickness on the pressure capacity of SPs with BU configuration. 168

Figure 7.7.Influence of external pipe's thickness to radius ratio on the characteristic behavior of SPs with (a) FB configuration (b) BU configuration..... 169

Figure 7.8.Influence of external pipe's thickness to radius ratio on the characteristic behavior of SPs having OU and IU configurations. Solid lines show the characteristic behavior of OU configurations and dashed lines illustrate the characteristic behavior of IU configurations. Symbol (^) represent the collapse point for OU configuration and symbol (v) shows the collapse point for the IU configuration. 170

Figure 7.9. Influence of external pipe's thickness to radius ratio on the pressure capacity of SPs. 170

Figure 7.10. Influence of internal pipe's thickness to radius ratio on the characteristic behavior of SPs with (a) fully bonded configuration (b) BU configuration. 171

Figure 7.11.Influence of internal pipe's thickness to radius ratio on the characteristic behavior of SPs having OU and IU configurations. Solid lines show the characteristic behavior of OU configurations and dashed lines illustrate the characteristic behavior of IU configurations. Symbol (^) represent the collapse point for OU configuration and symbol (v) shows the collapse point for the IU configuration. 172

Figure 7.12. Influence of internal pipe's thickness to radius ratioon the pressure capacity of SPs. 173

Figure 7.13.Influence of the core stiffness on the characteristic behavior of SPs with (a) fully bonded configuration (b) BU configuration..... 174

Figure 7.14.Influence of the core stiffness on the characteristic behavior of SPs with OU and IU configurations. Solid lines show the characteristic behavior of OU configurations and dashed lines illustrate the characteristic behavior of IU configurations. Symbol (^) represents the collapse point for OU configuration and symbol (v) shows the collapse point for the IU configuration. 174

Figure 7.15. Influence of the core stiffness on the pressure capacity of SPs..... 175

Figure 7.16. Influence of internal and external pipes' steel grade on the characteristic behavior of SPs having FB configuration. (a) FB configuration. (b) OU

configuration. (c) IU configuration. (d) BU configuration. Solid lines show the influence of changing in the steel grade of the external pipe on the characteristic behavior and dashed lines illustrate the effect of changing in the internal pipe steel grade on the characteristic behavior of pipes. Symbol (^) represent the collapse point for solid lines and symbol (v) shows the collapse point for dashed lines. 176

Figure 7.17. Influences of the internal and external pipes' steel grade on the pressure capacity of SPs. The solid lines with circular symbols demonstrate SP designs with internal pipe's steel grade of X80 and various external pipes' steel grades. Moreover the dashed lines with triangular symbols shows SP designs with external pipe's steel grade of X80 and various external pipes' steel grades. 178

Figure 7.18. Optimized external pipe's thickness to radius ratios for the water depth range between 1000 and 10000 meters considering various intra layer interaction properties. 186

Figure 7.19.Optimized internal pipe's thickness to radius ratios for the water depth range between 1000 and 10000 meters considering various intra layer interaction properties. 186

Figure 7.20. Optimized internal pipe to the external pipe's radius ratio for the SP configurations with Ec/Ep of 0.1. 187

Figure 7.21. External pipe's optimized steel grade..... 188

Figure 7.22. Internal pipe's optimized steel grade..... 188

Figure 7.23. Optimized manufacturing cost of various SP configurations..... 190

Figure 8.1. Idealized geometry and material properties of a SP system in the polar coordinate system..... 199

Figure 8.2. General stability behavior of different classes of cylindrical shells under pure bending..... 206

Figure 8.3. Mesh convergence study results for the SP system 208

Figure 8.4. Influence of the pipeline length on the buckling mode shapes of SP systems. 209

Figure 8.5. Influence of the L/D parameter on the buckling moment capacity of the SP systems. 210

Figure 8.6. The response of a practical range of SP configuration. (a) Deformation profile of the compression side of the pipes, along the pipeline axis, (b) Variation of the number of wrinkles along the pipeline axis, as a function of (L/D). 211

Figure 8.7. Influence of the core thickness on the buckling mode shape of the system. (a) Deformation profile of the compression side of the pipe. (b) Buckling mode shape of the system. 212

Figure 8.8. The influence of the core thickness on the buckling moment of the system. 213

Figure 8.9. Buckling mode shapes of the SP systems with core stiffness ratio of: (a) 0.0001. (b) 0.001. (c) 0.01. (d) 0.1. 214

Figure 8.10. Influence of the core stiffness ratio on the buckling moment of a sample SP system. 215

Figure 8.11. A SP system with its geometrical imperfection magnified 20 times..... 217

Figure 8.12. Influence of the core thickness on the characteristic behavior of a SP system having core stiffness ratio of (a) 0.001. (b) 0.01..... 220

Figure 8.13. The deformed shape and plastic strain of a SP system at the maximum bending capacity. (a) SP with core stiffness ratio is 0.001. (b) SP with core stiffness ratio is 0.01. 222

Figure 8.14. The deformed shape and maximum plastic strain of a sandwich pipe having FB intra-layer configuration at maximum bending capacity in SPs with two different size external pipe: (a) API size 16 (b) API size 20. 222

Figure 8.15. Influence of the pipeline length on the characteristic behavior of a SP system having core stiffness ratio of (a) 0.001. (b) 0.01..... 223

Figure 8.16. The deformed shape and maximum plastic strain of the sandwich pipe with various intra-layer configurations: (a) FB, (b) OU, (c) IU and (d) BU intra layer adhesion configurations. 224

Figure 8.17. Influence of the intra-layer interaction configuration on the Moment capacity and Curvature capacity of a SP with (a) $Ec/Ep = 0.001$. (b) $Ec/Ep = 0.01$. 225

Figure 8.18. Influence of the internal pipe's material yield anisotropy on the bending moment capacity of a SP system having core stiffness ratio of: (a) 0.001. (b) 0.01..... 227

Figure 8.19. Influence of the external pipe's material yield anisotropy on the bending moment capacity of a SP system having core stiffness ratio of: (a) 0.001. (b) 0.01..... 228

ABSTRACT

The recent substantial increase in world demand for energy and raw material resources has accelerated oil and gas exploration and production. At the same time, the depletion of onshore and shallow water oil resources presents a challenge to engineers to develop new means of harvesting and transporting oil and gas from harsh and remote areas. Sandwich Pipe (SP) is a relatively new design concept developed to address the transportation of oil in deep and ultra-deep waters as well as in cold environments. The main focus of this thesis is on the characterization of the structural performance of these novel systems.

Deep and ultra-deep water offshore pipelines are subjected to excessive hydrostatic external pressure during installation and operation. In this research, an innovative analytical solution was developed to evaluate the external pressure capacity of SPs by calculating the linear eigenvalues of the characteristic equations of the system. In the proposed solution, the interface condition between the layers of the system is accounted for in the governing equations. As well, a set of comprehensive parametric studies using the Finite Element (FE) method was developed to investigate both the elastic and plastic buckling response of SPs. The influence of various structural parameters such as the material, geometrical and intra-layer interaction properties on the characteristic behavior and the buckling pressure of SPs was examined. In addition to the proposed analytical solution, two sets of semi-empirical equations based on the FE analysis results were recommended in calculating the elastic and plastic buckling pressure of SPs.

As bending represents an important loading state in the installation and service life of SPs, it should be considered a governing loading scenario. In this thesis, the behavior of SPs under bending was investigated using a comprehensive set of parametric studies. SP systems with a wide practical range of physical parameters were analyzed using the FE method, and the influence of various structural parameters on the characteristic response and bending capacity of the system was explored, including pipe geometry, core layer properties, material yield anisotropy of high-grade steel pipes, and various intra-layer adhesion configurations.

LIST OF ABBREVIATIONS USED

D_{ij}	Laminated bending stiffness
E_c	Core material elastic modulus
E_p	Pipes elastic modulus
E_z	Elastic modules of the pipeline material along the pipeline axis
K_c	Core layer stiffness matrix
K_p	Pipes stiffness matrix
M	Moment
M_{cr-B}	Moment capacity of a pipe calculated from Eq. (2.14) and (2.18)
M_{cr}	Moment capacity of a pipe calculated from Eq. (2.15) and (2.19)
$M_{\theta\theta}$	Internal moment in the circumferential direction
$N_{\theta\theta}$	Internal force in the circumferential direction
P, P_e	External pressure
P_i	Internal pressure
P_{cr}	Pipe buckling pressure
P_{crs}	External pipe buckling pressure
R	Pipe radius
T	Tension
h	Constituent's thickness
n	Buckling mode number
r_1	Outer pipe nominal radius
r_2	Inner pipe nominal radius
t	Pipe wall thickness
t_1	Outer pipe wall thickness
t_2	Inner pipe wall thickness
v	Tangential deformation
w	Radial deformation
$\varepsilon_{\theta\theta}^{o}$	Membrane strain of the midsurface in the circumferential direction

$\kappa_{\theta\theta}$	Bending component of strain in the circumferential direction
ν_c	Core material Poisson's ratio
ν_p	Pipe material Poisson's ratio
Λ	Pipeline non-dimensional length calculated from Eq. (2.17)
σ_r	Radial stress
σ_{ij}	Stress components
σ_{rr}	Stress in the radial direction
σ_{zz}	Stress in the longitudinal direction
$\sigma_{\theta\theta}$	Stress in the circumferential direction
σ_{rr-y}	Yield stress in the radial direction
σ_{zz-y}	Yield stress in the longitudinal direction
$\sigma_{\theta\theta-y}$	Yield stress in the circumferential direction
$\tau_{r\theta}$	Tangential stress
ϕ	Stress function

ACKNOWLEDGEMENTS

The greatest love is a parents' love for their children, which is unconditional and priceless. I always received the most love and invaluable support from my family members. My deepest gratitude goes to my family, especially to my parents for giving me everything and expecting nothing.

During the past three years, I had the opportunity to develop my professional skills as a graduate student under the supervision of Professor Farid Taheri. In addition to all the technical and financial support I received from him, which enabled me to develop the research presented in this thesis, I had the chance to experience his precious friendship. For this, I wish to express my deepest thanks.

I also extend my sincere thanks to my current and former officemates, including Nikzad Nourpanah, Ramin Hosseinzadeh, Davood Rezaei, Sara Baftechi, You Lu, Mohammad Yahyaei, Julie Briand, Ahmed Shouman, Ramadan Esmaeel, Fathollah Taheri Behrooz, Shiva Eslami, Nur Hossein, Pejman Razi, Morteza Mehrzadi and Mobraka Mohamed for their support and friendship.

Finally, I sincerely appreciate the financial support I received from the Atlantic Innovation Fund through C-Core and also the financial assistance from Dalhousie University, which made it possible for me to continue my studies.

CHAPTER 1
INTRODUCTION

Modern harvesting of our world's limited oil and gas resources has been ongoing since the 18th century. Since then, the exponential increase in global demand for more energy and raw material resources has accelerated oil and gas production. As a result, shallow water oil and gas reserves are being depleted, and the need for deep water resources is growing fast. However, the oil and gas production and transportation facilities and techniques currently in use for shallow and accessible reserves are not feasible for deeper reservoirs located in harsh and remote environments. Consequently, engineers today face new challenges to improve traditionally used systems and develop new ones.

As pipelines are one of the main components of oil and gas transportation and harvesting systems, their configurations and performance must be improved in order to respond to the new requirements. Employing the traditional steel single-walled pipes is limited to a specific operational depth. Meanwhile, advances in material science, pipe manufacturing, installation methods and maintenance techniques allow engineers to develop new pipeline systems with a higher overall efficiency compared to traditional systems.

Pipe-in-Pipe (PIP) systems were developed to improve the thermal insulation properties of traditional single-walled steel pipes. PIP systems are composed of three concentric cylindrical elements. The internal pipe, also called the product pipe, is in contact with the product and facilitates the product flow. The external pipe, or sleeve pipe, is in contact with the surrounding environment and separates the core layer and internal pipe from the outside. The secondary boundary provided by the external pipe ensures containment of the product should the oil leak from the internal pipe.

Because PIP systems can be designed to fit the required thermal insulation properties, these systems have been employed in many practical offshore applications. However, in most of the PIP projects, the potential sandwich structure has been ignored and each component of the system has been individually designed based on its governing loads. Previous studies reveal that where the whole system to be considered as a

sandwich structure, a considerably lighter and a more cost-effective pipeline could be designed for a specific loading condition. As a result, the idea of Sandwich Pipes (SP) has been developed. In SP systems, a relatively soft core layer is sandwiched by relatively stiff internal and external pipes. The core layer in SP systems provides the required thermal insulation properties as well as the appropriate structural properties to transfer loads between the internal and external pipes. Thus, in SP systems, the core layer includes both structural and thermal properties.

Designing reliable and safe pipelines requires taking into consideration various load states under governing loads and environmental conditions. Load states of pipelines can be classified into two main categories with reference to the governing applied loads and the corresponding failure modes. The first category of load states includes excessive tensile stresses, which yields to rupture and fracture of the pipeline wall under the applied loads. The method used in designing and analyzing offshore pipelines should be capable of considering proper fracture models for the design states involved with large tensile stresses.

The second category includes load states involving large governing compressive stresses and strains. Pipelines which fall under this category typically buckle and collapse, locally or globally, at a critical state. The design criteria and analysis models used to simulate these load states should be able to consider the stability conditions involved with the problem. The main focus of this thesis is to investigate the stability behavior of Sandwich Pipes under the second category of load states. The following research was conducted to investigate the buckling and collapse behavior of SP systems under two major loading conditions: hydrostatic external pressure and pure bending.

The first chapter of this thesis provides an introduction to the research undertaken in this thesis and shows the outline and organization of the text.

In the second chapter, a brief review of previous research into characterizing the stability behavior of single and Sandwich Pipes is presented. In this chapter, an introduction to the applied loading conditions on offshore oil and gas pipelines during installation and operation is first presented, followed by a discussion of the constitutive components and design considerations of PIP and SP systems. Next, former studies investigating the behavior of offshore pipelines under pure bending and external pressure

are briefly reviewed, new advancements in the pipeline material and development of high-grade steel pipes are mentioned, and methods for modeling such material's behavior in numerical models are highlighted. Finally, former studies investigating the influence of using high-grade steel pipelines on the mechanical response of the system are reviewed.

In the third chapter, an analytical approach is used to develop exact and simplified solutions for establishing the buckling capacity of Sandwich Pipes subjected to externally applied hydrostatic pressure. A comprehensive finite element eigenvalue investigation is conducted to establish the performance of SPs with a wide range of material and physical properties and to verify the integrity of the proposed solutions. In the presented analytical and numerical solutions in this chapter, four different interlayer bonding configurations are considered. The details of calculating the parameters used to define the characteristic equation of the system are addressed. One of the important aims of the research outlined in Chapter 3 is extracting simplified solutions from the exact solution for use in practical designs. As a result, the simplified and exact solutions are compared and the accuracy of their results discussed. In addition, the error margins resulting from the use of the proposed simplified equations and those proposed by other researchers are established.

The fourth chapter presents a practical solution characterizing the behavior of SPs using the Finite Element (FE) method. In this chapter, a series of finite element parametric studies was developed to study the effects of significant structural parameters on the elastic buckling pressure of SPs. Using the results of FE analyses, a set of simplified practical equations is established for four different pipe configurations, accounting for the interaction properties between core layer and the surrounding pipes.

In the fifth chapter, a set of parametric studies is performed in order to investigate the influence of material plasticity on the buckling and post-buckling response of a possible design set of PIPs and SPs. As well, the external pressure capacity of PIP and SP configurations are compared. The influence of the stress-strain curve profile in the plastic regime on the response of SP systems is illustrated by considering several possible material properties. By adopting steel materials with various yield stresses, the influence of upgrading the steel grade of either the internal or external pipes in both SP and PIP systems is investigated.

The sixth chapter presents a numerical finite element solution to characterize the real behavior of SPs. In the FE models discussed in this chapter, appropriate forms of initial imperfection, material models, boundary conditions and FE parameters are considered. The results of a comprehensive parametric study on more than 3800 SP configurations having practical design parameters as well as the influence of a wide range of design parameters on the characteristic response are discussed. As the main objective of the research presented in this chapter, a set of practical and simplified equations for evaluating the plastic capacity of SPs is developed based on finite element analyses results. Finally, the outline of an optimization procedure is addressed and the results of the proposed method used for finding a set of hypothetical SP configurations for water depths up to 10,000 meters are presented.

In the seventh chapter, the influence of the intra-layer adhesion configuration on the plastic buckling pressure capacity of SPs is discussed. This chapter presents the results of more than 12,000 FE models developed to study the characteristic behaviour and pressure capacity of the systems, including all sources of nonlinearities. The general equation presented in Chapter 6 is calibrated for applications to alternative SP configurations in which the core layer could slide on the internal and/or external pipes. The accuracy of the developed equations is examined by comparing the pressure capacity calculated from the proposed equations with the FE and experimental results from the literature. Using the developed equations and the optimization method proposed in Chapter 6, the optimized structural parameters are evaluated for SPs with different intra-layer configurations and core stiffnesses for various operational water depths.

In Chapter 8, the behavior of SP systems under pure bending is characterized by examining a series of 3D FE models incorporating geometrical, material and contact nonlinearities. In the research presented in this chapter, both linear perturbation eigenvalue buckling analysis and nonlinear post-buckling analysis are used. Using the eigenvalue buckling analysis results, the influence of the length of the pipeline, core thickness and stiffness on both buckling moment and wrinkle wavelength are discussed. As well, the influences of the significant structural parameters on the buckling mode shape of the system are presented.

A proper geometrical imperfection was included in the models developed for the post-buckling analysis. Using the post-buckling analysis results, the influence of significant geometrical and material parameters on the pre-buckling, buckling and post-buckling behavior of a series of practical configurations is discussed. By presenting the results of the analysis of proper numerical models, the behavior of various intra-layer configurations is argued. Finally, the influence of employing steel pipes with yield anisotropy on the characteristic behavior of the system is examined, and the possible improvement of employing high grade steel pipes is analyzed.

The last chapter of this thesis, Chapter 9, is dedicated to the conclusions and to recommendations for an extension of this research into the future.

CHAPTER 2
LITERATURE REVIEW

In this chapter, an introduction to the pertinent applied loading states involved in the installation and operation of offshore oil and gas pipelines is first presented. The constitutive components and design considerations of Pipe-in-Pipe (PIP) and Sandwich Pipe (SP) systems are then discussed, followed by a brief review of some of the pertinent studies conducted previously in investigating the behavior of offshore pipelines under pure bending and external pressure. The literature review presents studies considering both pipelines and cylindrical shells. New advancements in the pipeline material and high-grade steel pipes are also mentioned and the methods for modeling such materials in the context of numerical modeling are discussed. Finally, notable studies that investigated the influence of the use of high-grade steel pipelines on the stability response of the system are reviewed.

2.1. LOADING APPLIED TO OFFSHORE PIPELINES

Offshore pipelines would be subjected to various loading conditions during their installation process and operation. In the following sections, the more significant loading conditions on offshore pipeline are discussed.

2.1.1. Loadings applied during the pipeline installation process

There are three common installation methods for offshore pipelines: the S-Lay, J-Lay and Reeling methods. Choosing the most appropriate method is usually based on the corresponding installation and maintenance costs of the pipeline, environmental conditions, and water depth. In the following sections, a brief review of the laying methods and the consequent exerted loads are presented.

A schematic profile of an offshore pipeline during the installation and the consequent loads during the S-Lay method is illustrated in Figure 2.1. In the S-Lay method, the pipeline installation process begins with joining and welding the pipes on the lay vessel in a horizontal position. After leaving the lay vessel, the pipeline acquires a controlled S-shape before lying in the seabed.

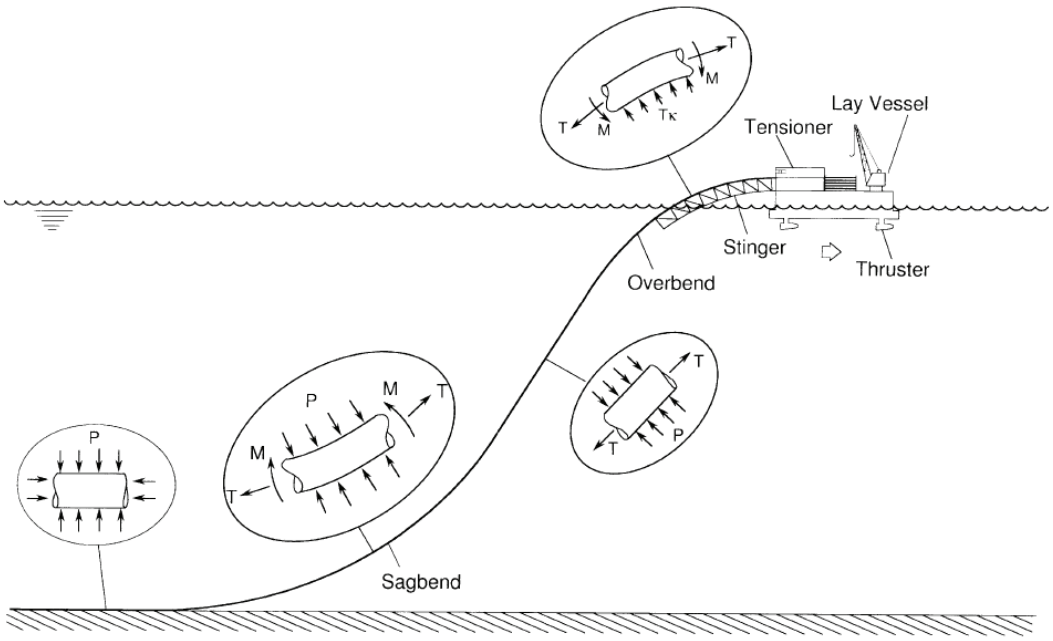

Figure 2.1. Schematic presentation of the applied loads during S-Lay pipeline installation [from 2.1].

During the S-lay installation process, the pipeline experiences various loading conditions before sitting on the seabed. Immediately after leaving the vessel, the pipeline comes in contact with a long boom-like structure called a stringer. The curvature applied to the pipeline in this regime is controlled by the stringer curvature. Like the applied curvature, the pipe is under excessive tension in this regime mainly due to the weight of the pipeline hanging from the ship between the stringer and the seabed.

After leaving the stringer, the pipe enters the overbend region, which is followed by a straightening region. As seen in Figure 2.1, in the sagbend section, the pipe starts to bend in the opposite direction of the stringer. Besides the excessive tensile and bending loads applied in this section, the pipe also undergoes large hydrostatic external pressure due to the water depth close to the seabed. After the sagbend region, the pipe sits on the seabed and experiences maximum hydrostatic external pressure and axial loads.

By increasing the water depths, the suspended length of the pipeline increases, and thus a larger magnitude of tension must be applied to the pipeline from the vessel. As a result, employing the S-lay method is limited to a specific length because of the excessive tension applied to the stringer in deep water. The J-Lay method is an alternative installation process which overcomes this problem and increases the installation depth.

In this method, the pipeline leaves the vessel from a nearly vertical position, as shown in Figure 2.2. As can be seen in the figure, by using this technique the pipeline profile is similar to a J shape. Moreover, in this method the pipeline does not experience the curvature controlled loads due to the stringer and the overbend region.

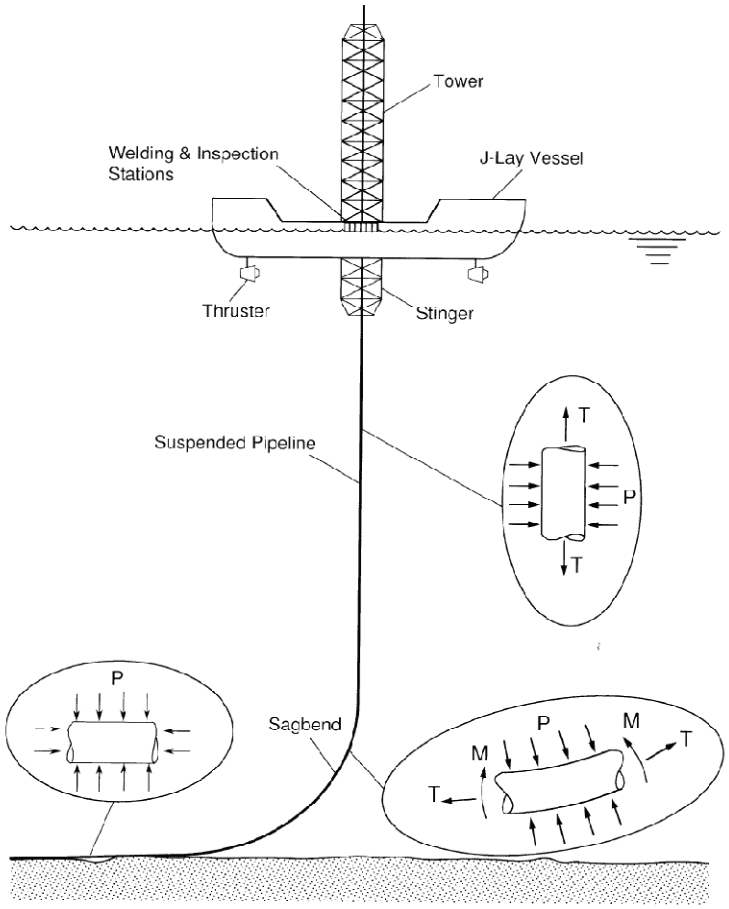

Figure 2.2. Schematic presentation of applied loads during J-Lay pipeline installation [from 2.1].

One of the most efficient and fastest installation methods is the reel vessel method. In this method, a kilometers-long pipe is usually made onshore and wound onto a large diameter drum to be installed on a reel vessel. Afterwards, the reel vessel gradually unspools the pipe at the installation site. One of the main limitations of this method is the pipe diameter, which is usually limited to API size-16 (a pipe with an outer diameter of 0.4064m). The pipeline steel grade also puts a restriction on this method, as the welding process can cause unacceptable work hardening in higher steel grades, which can cause problems in the reeling process. It should be mentioned that pipelines installed by reeling

vessels experience a large magnitude of plastic deformations because of the reeling and unspooling process. A schematic figure of the pipeline profile in the reeling ship is presented in Figure 2.3.

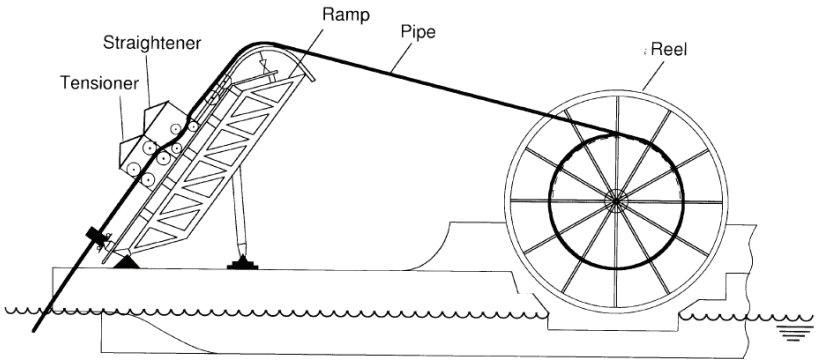

Figure 2.3. Schematic presentation of the reelship [from 2.1].

2.1.2. Loadings applied during the pipeline operation

An offshore pipeline experiences various mechanical loads during its operational life depending on the environmental, seabed and field conditions. Some of the most significant loading conditions are described below.

Internal and external pressure

Internal and external pressures induce hoop stress to the pipeline. In deep and ultra-deep waters, due to the large external pressure magnitude, the pipeline could be subjected to an excessive compressive hoop stress. Offshore pipelines must be designed to be stable under such high external pressure, without considering the positive effect of the internal pressure. Otherwise, the pipe would collapse during system shutdowns or during the installation process in which the positive effect of the internal pressure is removed. Moreover, the pipeline may be exposed to intense internal pressure from the carrying product. In such cases the burst pressure capacity of such pipelines should be designed to carry the projected operational internal pressure. Figure 2.4 illustrates an offshore pipeline cross-section under operational internal and external pressure, lying on the seabed.

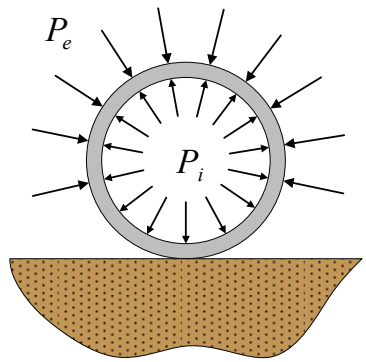

Figure 2.4. Internal and external pressure applied to an offshore pipeline.

<u>*Uneven supports*</u>

Pipelines lying on a rough seabed could experience uneven support, which could induce large deformation-controlled loads to the pipeline. An example of a pipeline laying on uneven supports is illustrated in Figure 2.5. As many of the oil fields in deep and ultra-deep water are located on a soft seabed, rock supports are commonly installed before installation of the pipeline to provide a solid foundation [2.2]. However, these supports would apply free spanning, and in some cases, uneven supports to the pipeline. It is imperative that such loading scenarios be considered in the design of the pipeline.

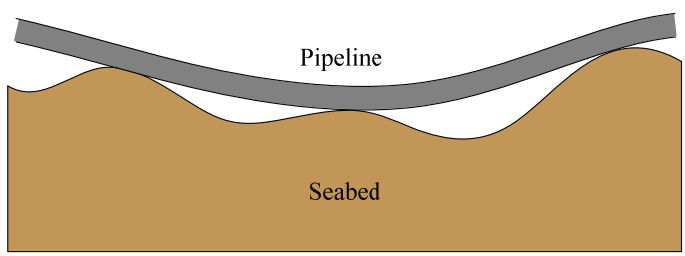

Figure 2.5. Uneven supports

<u>*Upheaval buckling*</u>

Figure 2.6.a shows an offshore pipeline after completing the installation process and initiating operation. It is convenient during the installation of offshore pipelines to trench and bury the pipeline in order to provide proper on-bottom stability and protect the pipeline from impact from anchors, trawl boards, ice gouging and strudel scour (Figure 2.6.b). However, because of the large difference in pressure and temperature of the

pipeline during installation and operation, the pipeline expands significantly during its operation. As a result, depending on the pipeline's structural and backfill soil properties and the depth of the trench, the pipeline experiences large vertical displacements, a phenomenon referred to as "upheaval buckling". Figure 2.6.c illustrates a pipeline suffering from upheaval buckling. Besides the instability issue, upheaval buckling pushes up pipeline through the covering soil and exposes it to impact from anchors and trawl boards.

Upheaval buckling occurs when the vertical loads due to the thermal and pressure expansions are larger than the resistance of the system. The pipeline stiffness, backfill soil weight and the pipeline weight contributing to the resistance of the system should be designed to prevent upheaval buckling.

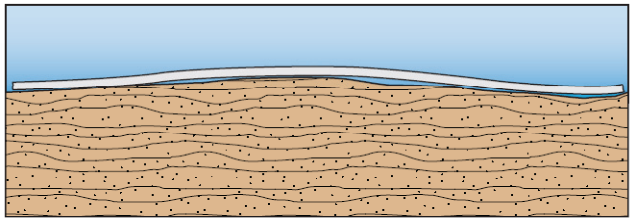

(a) As-laid

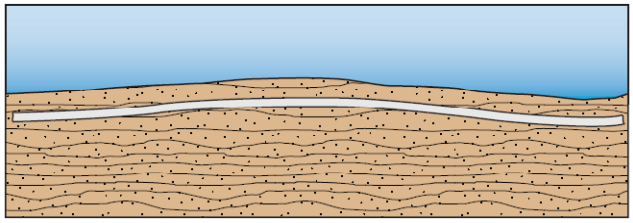

(b) Trenched and buried.

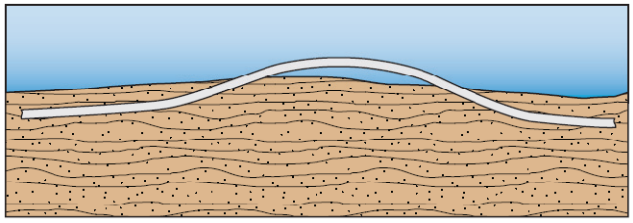

(c) Upheaval.

Figure 2.6. Upheaval buckling [from 2.3].

Ice keel gouging

Ice keel gouging is one of the main concerns for pipelines located in Arctic areas. During fall freeze-up and spring break-up, huge pieces of ice move in the sea, and some of these can cause gouges on the seabed. It is important that offshore pipelines located in a seabed susceptible to such gouges be located at a soil depth greater than the ice gouge depth. Figure 2.7 illustrates a schematic situation of the gouging of a seabed hosting an offshore pipeline. Pipelines located in such fields should be designed for a large deformation-controlled load applied by soil displacement due to gouging.

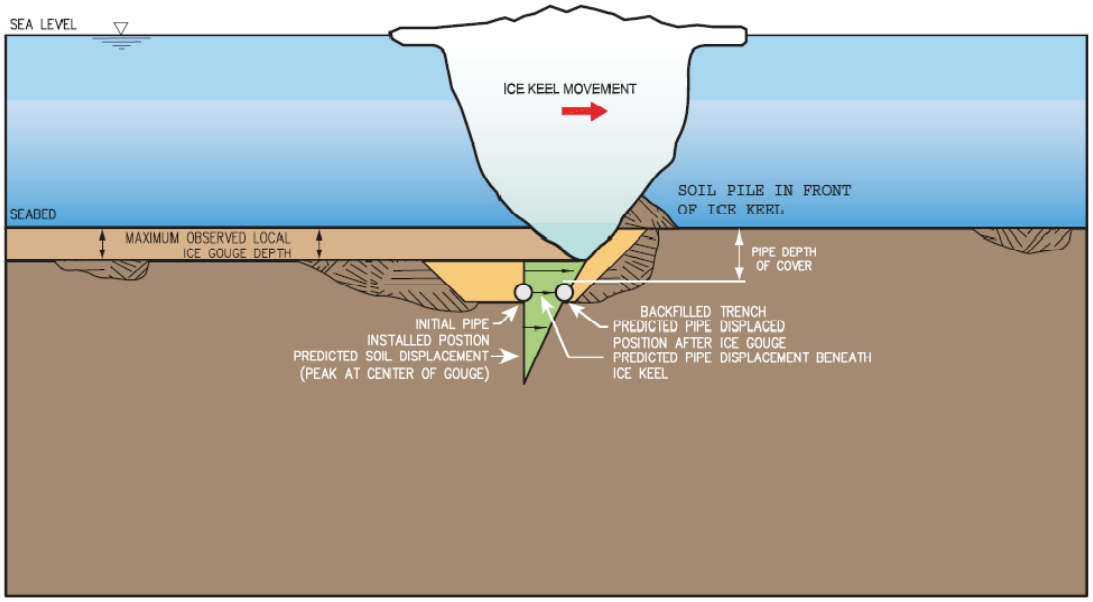

Figure 2.7. Ice keel gouging [from 2.3].

Thaw settlement loading

Thaw settlement is another scenario which would apply large deformation-controlled loads to offshore pipelines through the movement of the pipeline soil foundation. The near-shore shallow water soil which is the foundation of the pipeline may contain permafrost that includes a considerable amount of ice. The permafrost in the soil will be melted due to the temperature of the pipeline carrying a warm oil product. This would form a thaw bulb around the pipe and the soil foundation around the pipe will be melted. As a result, in fields where the foundation soil contains permafrost, a considerable magnitude of deformation-controlled loads would be exerted to the pipeline due to

foundation settlement. In such fields, the depth of the trench should be designed to decrease the amount of settlement. Figure 2.8 illustrates a schematic situation in which the pipeline foundation settles due to the forming of a thaw bulb around the pipe.

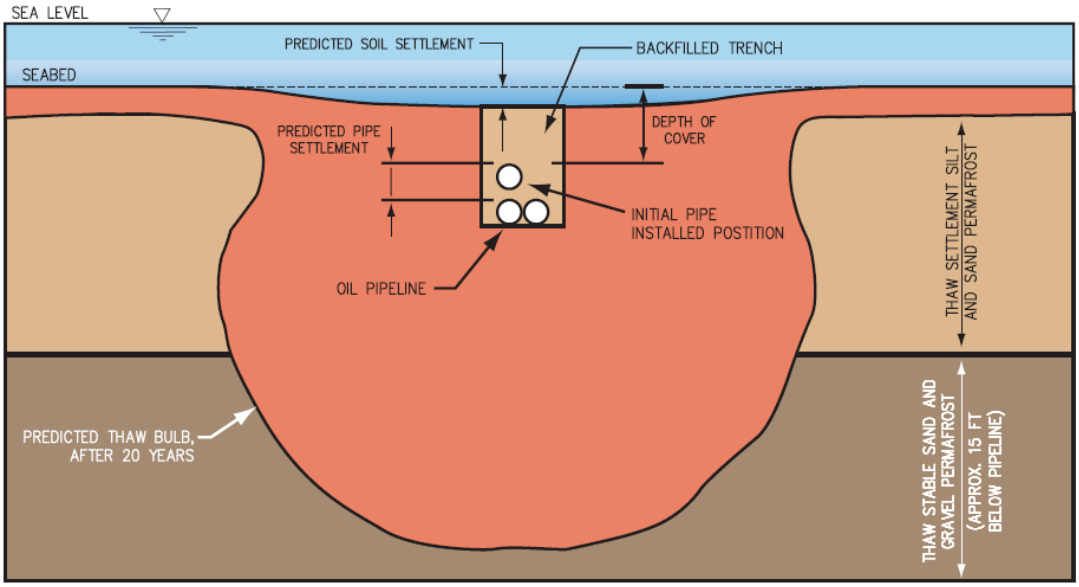

Figure 2.8. Thaw settlement loading [from 2.3].

2.2. SANDWICH PIPE SYSTEMS

In order to improve the thermal insulation properties of traditional single-wall steel pipes, the Pipe-in-Pipe (PIP) design configuration was developed. PIP systems are composed of three concentric cylindrical elements. The internal pipe, also called the product pipe, is in contact with the product and facilitates product flow. The core layer can be selected to act as a proper thermal insulator surrounding the internal pipe and as a host for structural and health monitoring systems, cathodic protection systems and/or the heating facilities. The outermost layer of the system, known as the external or sleeve pipe, separates the core layer and internal pipe from the surrounding environment. The secondary containment provided by the external pipe improves the assurance of the system in case of oil product leakage from the internal pipe. Figure 2.9 shows a practical configuration of a PIP.

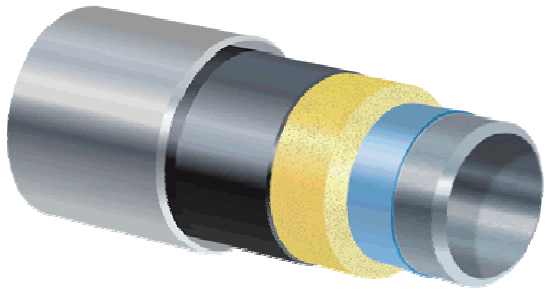

Figure 2.9. A practical PIP configuration [from 2.4].

Because of the capability of PIP systems to fit the required thermal insulation properties, they have been employed in many practical offshore applications. However, in most of the PIP projects, the potential sandwich structure has been ignored and each component of the system individually designed for the governing applied loads. For example, in designing a PIP system, the internal and external pipes are respectively designed in such a way so that the internal and external pressures are carried by the respective pipe, individually.

Previous studies reveal that if the whole system were to be considered as a sandwich structure, a considerably lighter and a more cost-effective pipeline could be designed for a specific loading condition [2.5]. As a result, the idea of Sandwich Pipe (SP) has been developed. In SP systems a relatively soft core layer is sandwiched by relatively stiff internal and external pipes. As will be discussed in the future chapters, a value of $E_c/E_p \geq 0.01$ (E_c being the stiffness of the core and E_p being the stiffness of the sandwiching pipes) would guaranty the formation of an effective sandwich structure. The core layer in SP systems provides the required thermal insulation properties as well as the appropriate structural properties to transfer loads between the internal and external pipes.

The idea of SP systems is a new take on the double-walled steel pipes and only a limited number of practical cases have been tested. Moreover, very few industrial projects have taken the advantage of SP relative to PIP systems, which are fairly commonly used. It should however be noted that the use of SP systems would become economically feasible only in circumstances when a combination of superior thermal and structural properties is required. Such a circumstance has not been experienced yet; however, it is believed that as the demand for exploration in deeper water depths and

harsher environment increases, the consideration of using SP systems would become inevitably eminent.

On the other hand, despite their novelty, PIP systems have already been widely used in several projects in the Arctic to test the required thermal installation properties. A few of these projects are mentioned below.

In the onshore Arco Alpine Colville River Crossing (AACRC) project, a PIP system was used with the Horizontal Directional Drilling (HDD) installation method. The PIP configuration was chosen for this project because of the compatibility of the system with the HDD method, its capability to provide a secondary containment for the product, its better resistance under bending, and its ability to be integrated with a leak detection system [2.6, 2.7].

PIP systems were also used in the BP Exploration Troika Towed Bundle Flowline (BETTBF), an offshore pipeline project. The PIP configuration was chosen for this project to provide the required thermal insulation properties as well as to control the buoyancy effect, improve the external pressure capacity of the system and improve the corrosion resistance of the system. In the employed PIP system, the annulus space between inner and outer pipes was pressurized with nitrogen, and bulkheads were used to separate annulus areas along the pipeline and thus improve the thermal insulation property should there be a loss of the outer pipe's integrity. The bulkheads also improve the structural integrity of the system under external pressure and during the installation process [2.6]. There are several other projects currently using PIP systems which, for the sake of brevity, are not mentioned here.

2.3. BUCKLING AND COLLAPSE OF PIPELINES

As mentioned previously, an offshore pipeline system would be subjected to various single and combined loads during the installation process and operation. The main focus of this research is on the behavior of SPs under hydrostatic external pressure and pure bending, which are two of the most significant governing loading conditions. In this section, the behavior of single-walled pipes and SPs under these two loading scenarios is discussed.

2.3.1. External pressure

Characterizing the stability behavior of cylindrical shells as the general geometry of pipelines under hydrostatic external pressure is a classic stability problem. Various approaches have been used to solve this problem. One of the most popular approaches is using the energy method for evaluating the buckling pressure of a pipeline.

Due to the symmetry in structural configuration and loading, this problem can be idealized as a 2-D plane strain problem of ring. The use of polar coordinates is also convenient to simplify the formulation of the problem. Figure 2.10 illustrates the deformed and undeformed cross-section of the pipeline as well as the definition of midsurface displacements.

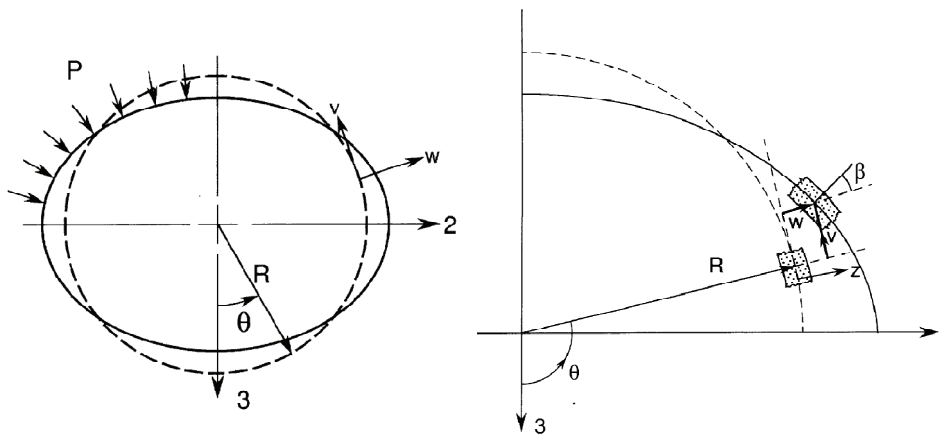

(a) *(b)*

Figure 2.10. (a) Deformed and undeformed cross-section of the pipeline and (b) definition of midsurface displacements [from 2.1].

The potential energy of the system under hydrostatic external pressure can be calculated by [2.1]:

$$\Pi = \int_0^{2\pi} \frac{1}{2}[N_{\theta\theta}\varepsilon_{\theta\theta}^{o} + M_{\theta\theta}\kappa_{\theta\theta}]Rd\theta + PR\int_0^{2\pi}\left[w + \frac{1}{2R}(v^2 + w^2 - vw' + v'w)\right]d\theta \tag{2.1}$$

Sander's shell equations can be used to describe the mid-surface strain-displacement relationships. Sander's kinematic equations are nonlinear and based on small strain and moderate rotation assumptions, which are appropriate for establishing the linear buckling equations. The kinematic equations in polar coordinate can be represented by:

$$\varepsilon_{\theta\theta} = \varepsilon_{\theta\theta}^{o} + zk_{\theta\theta} \tag{2.2}$$

$$\varepsilon_{\theta\theta}^{o} = \frac{w + v'}{r} + \frac{1}{2}\beta^2 \tag{2.3}$$

$$k_{\theta\theta} = \frac{\beta'}{r} \tag{2.4}$$

In these equations, β represents the rotation of a circumferential element located at the mid-plane of the pipes. β for an intermediate class of deformation (small mid-surface strains and small but finite rotations) can be defined by [2.8]:

$$\beta = \frac{v - w'}{r} \tag{2.5}$$

Moreover, magnitudes of force and moment can be calculated with respect to the ring displacement as [2.9]:

$$N_{\theta\theta} = \frac{Et}{\left(1 - v_p^2\right)}\varepsilon_{\theta\theta}^{o} \tag{2.6}$$

$$M_{\theta\theta} = \frac{Et^3}{12\left(1 - v_p^2\right)}k_{\theta\theta} \tag{2.7}$$

By substituting Equations (2.2), (2.4), (2.6) and (2.7) with Equation (2.1), the potential energy of the system can be calculated as a function of the displacement components. Using the variational calculus method, the equilibrium equations of the system can be derived. Finally, by calculating the eigenvalues of the system of equilibrium equations, the buckling pressure of the system can be calculated as [2.9]:

$$P_n = \frac{(n^2 - 1)}{12(1 + \rho)}\frac{E}{(1 - \nu^2)}\left(\frac{t}{R}\right)^3 \qquad , n = 2,3, \ldots \tag{2.8}$$

where:

$$\rho = \frac{1}{12}\left(\frac{t}{R}\right)^2 \tag{2.9}$$

The lowest eigenvalue of the system that corresponds to $n = 2$ is the buckling pressure of the pipe. In single-walled pipes, the ovalization mode ($n = 2$) is always the governing buckling mode. In practical cases, elastic buckling occurs where pipes have relatively high R/t; therefore, $\rho \ll 1$ is applicable in such cases and ρ can be neglected in comparison to one. By replacing $n = 2$ and neglecting ρ in Equation (2.8), the buckling pressure of the pipe can be calculated as:

$$P_{cr} = \frac{E}{4(1 - \nu^2)}\left(\frac{t}{R}\right)^3 \tag{2.10}$$

This equation includes some correction design factors and is widely used in pipeline design guidelines as the elastic buckling pressure capacity of a single-walled pipe.

Sandwich Pipes used in the oil and gas industry are generally long circular cylindrical structures consisting of two concentric steel pipes sandwiching a softer core layer. In such a configuration, the structural properties of the system, boundary conditions and applied loads along the pipeline longitudinal axis are uniform; therefore, similar to single-walled pipes, it would be admissible to consider the behavior of such a system, when subjected to hydrostatic external pressure, as a 2-D problem in the polar coordinates, as shown in Figure 2.11.

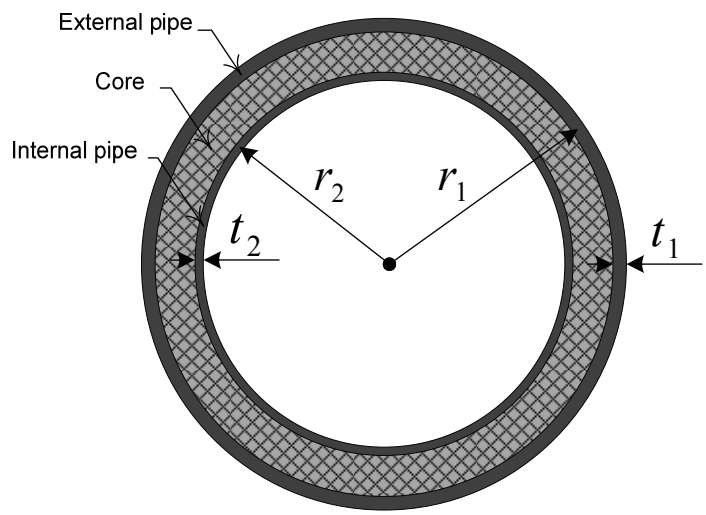

Figure 2.11. Idealized geometry of the sandwich pipes.

In the case of elastic structures, the elastic buckling pressure of a system represents its pressure capacity. Brush and Almroth [2.10] and Sato and Patel [2.11, 2.12] proposed an analytical solution for calculating the buckling capacity by simplifying the problem and determining the buckling pressure of a ring internally supported by an elastic foundation. They proposed the following equation:

$$P_{cr} = P_{crs} + \frac{1}{n^2 - 1} k \tag{2.11}$$

where:

$$k = E_c \frac{2n(\upsilon_c - 1) - 2\upsilon_c + 1}{4\upsilon_c^2 \ + \upsilon_c - 3} \tag{2.12}$$

and P_{crs} is the buckling pressure of the external pipe, obtained by:

$$P_{crs} = \left(\frac{t_1}{r_1}\right)^3 \frac{E_p(n^2-1)}{\left(1-v_p^2\right)\left(\left(\frac{t_1}{r_1}\right)^2+12\right)} \tag{2.13}$$

The buckling mode shape of Sandwich Pipes would be more complex than single-walled pipes. As mentioned previously, single-walled pipes always buckle by ovalizing the cross section corresponding to $n = 2$, while in SP systems the pipe would buckle in higher modes, depending on the structural parameters. Figure 2.12 illustrates the normalized buckling pressure of a set of SP systems as a function of changing the pipeline material and geometrical properties [2.12]. In this figure, q_{cr} and q^* are, respectively, the SP and external pipe buckling pressure, and a_1 and a_2 are, respectively, the external and internal pipes' radius. As can be seen in the figure, by increasing the core thickness or stiffness, the pipe buckles in the buckling modes correspond to higher values of n.

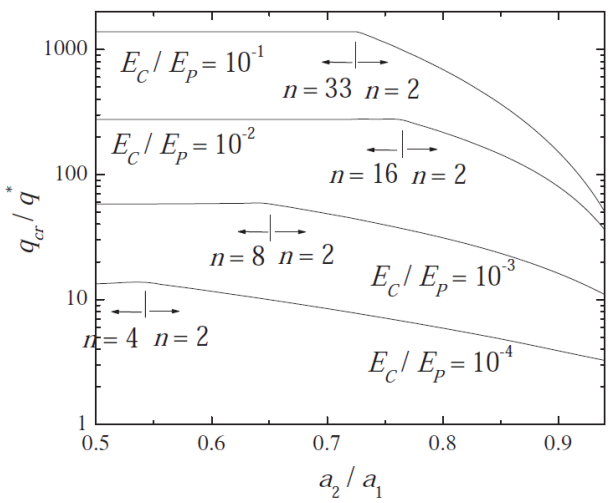

Figure 2.12. Non-dimensional collapse pressure for a sample SP system [from 2.12]

Figure 2.13 illustrates the buckling mode shape of a few SP configurations made of steel internal and external pipes and core materials having various stiffnesses. The buckling mode shapes in Figures 2.13.a and 2.13.b correspond to $n = 2$ and $n = 4$, respectively. Moreover, Figures 2.13.d, 2.13.e and 2.13.f show the buckling modes equivalent to $n = 6$, $n = 18$ and $n = 18$, respectively.

In another set of studies, Kardomateas and Simitses [2.13, 2.14] analytically studied the stability of long sandwich cylindrical shells (which can be considered as the general

configuration of SPs) under uniform external pressure. Ohga et al. [2.15] also investigated the reduced stiffness buckling of sandwich cylindrical shells under uniform external pressure, both numerically and analytically.

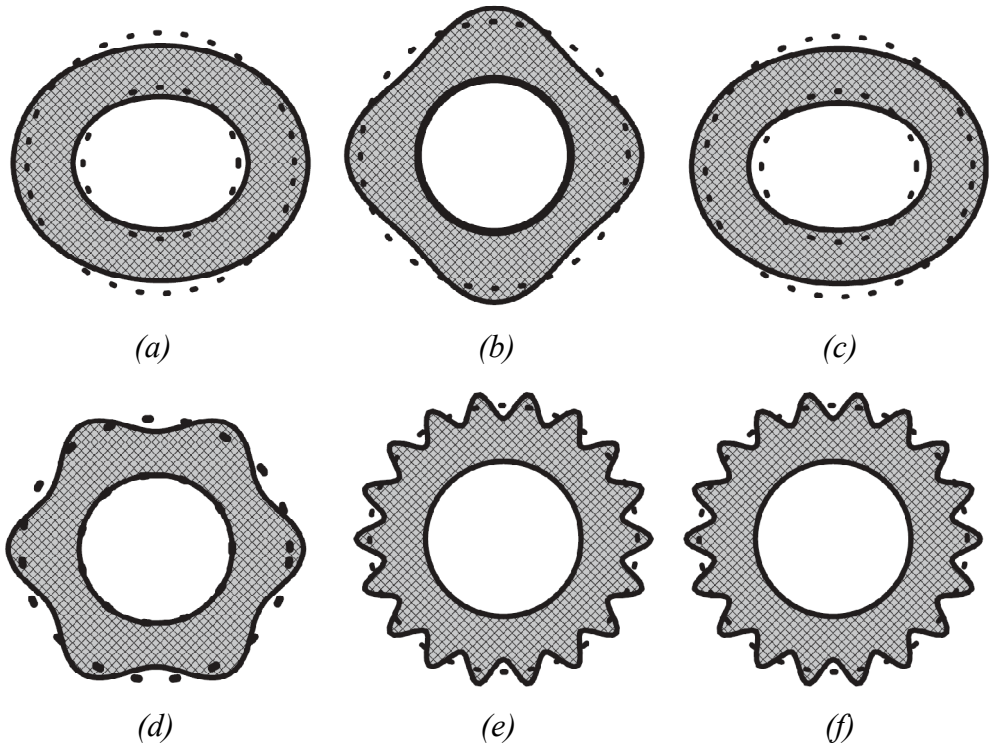

(a) $t_2 = 9mm$, $E_c = 2 \times 10^7 pa$. *(b)* $t_2 = 15mm$, $E_c = 2 \times 10^7 pa$.
(c) $t_2 = 9mm$, $E_c = 2 \times 10^8 pa$. *(d)* $t_2 = 15mm$, $E_c = 2 \times 10^8 pa$.
(e) $t_2 = 9mm$, $E_c = 2 \times 10^{10} pa$. *(f)* $t_2 = 15mm$, $E_c = 2 \times 10^{10} pa$.

Figure 2.13. The buckling mode shapes of SP systems having $t_1 = 9mm$, $t_c = 115mm$ *[from 2.12].*

One of the initial feasibility studies on employing sandwich pipes for deep and ultra-deep waters was conducted by Estefen et al. [2.5]. They explored the behavior of SPs under various loading scenarios, using numerical and experimental approaches. In their experimental research, they investigated the behavior of SP systems made from aluminum internal and external pipes and polypropylene or cement core layers. Figure 2.14 illustrates the collapse mode under the hydrostatic external pressure they captured in their experiments. They also conducted several numerical finite element studies to investigate the behavior of SP systems under combined external pressure and bending.

Figure 2.14. Collapse cross-section of an aluminum SP system [2.5].

Through a comparative study, Estefen et al. concluded that SP systems can be a viable design alternative for applications in water depths up to 3,000 meters. In another study, Castello et al. [2.16] compared PIP with SP systems designed for hypothetical oil filled with several core materials.

A vital structural parameter in SP systems is the adhesion properties between the core layer and its surrounding pipes. Castello and Estefen [2.16, 2.17] investigated the ultimate strength of Sandwich Pipes under combined external pressure and bending for several degrees of adhesion between the core layer and external pipe. As well, they investigated the effect of cyclic loads (applied during the reeling installation method) on the collapse pressure.

Several other researchers likewise investigated the behavior of SP systems under hydrostatic external pressure. However, for the sake of brevity, they are not included in this thesis.

In offshore pipelines subjected to hydrostatic external pressure, cross-section local buckling can propagate along the pipeline under an external pressure less than that of the elastic buckling pressure. This phenomenon is called buckle propagation, and the magnitude of the corresponding pressure is called the buckle propagation pressure. Buckle propagation pressure is described as the buckle propagation depth with the corresponding external pressure.

Figure 2.15.a illustrates how buckle propagation might occur during the installation process. As can be seen in the figure, if the pipeline buckles due to large loads applied during the installation in a depth greater than the buckle propagation depth, the instability would propagate along the pipeline. Figure 2.15.b shows another scenario in which local instabilities would propagate along the pipeline in the operational condition. In this case, the initial instability is formed due to the impact of an anchor on the pipeline.

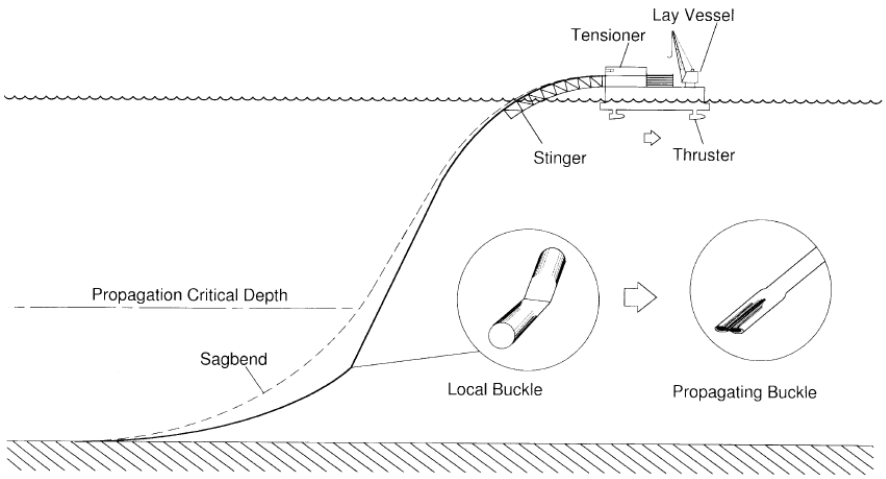

(a)

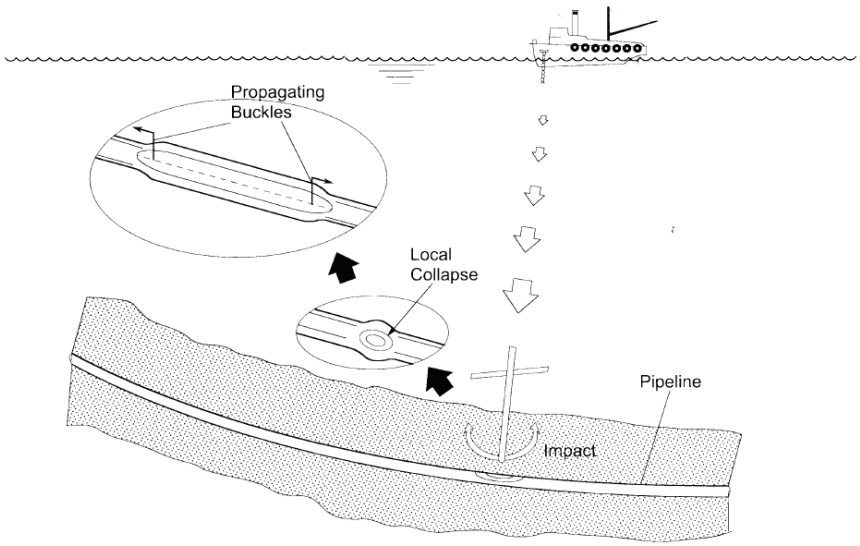

(b)

Figure 2.15. Propagation of section instability induced (a) during the installation process and (b) from the impact of an anchor [2.1].

A series of notable works by Kyriakides and his coworkers [2.18-2.21] have considered the buckle propagation phenomena in pipe-in-pipe systems from experimental, analytical and numerical perspectives. It should be noted, however, that investigating the development of a propagating buckle under the hydrostatic external pressure in SPs is not considered in this thesis. More information regarding this phenomena and design aspects of PIP systems susceptible to this type of instability can be found in the above-mentioned references.

2.3.2. Pure bending

Investigating the behavior of pipes under pure bending came to the attention of several researchers already at the beginning of 20th century. The general behavior of a pipe under bending can be classified into three categories, depending on the geometrical and material properties.

The main distinguishing characteristic behavior of pipes under pure bending is that the applied bending induces ovalization in the pipe's cross-section. Known as the Brazier effect, this ovalization reduces the stiffness of the system. By increasing the bending magnitude, the ovalization localizes in a zone which causes the collapse in pipe at a limit point. Figure 2.16.b illustrates such a collapse mode. This category of pipes is called Class I in this chapter. The stability problem of these systems was studied by Brazier for the first time in 1927 [2.22]. Brazier found that this category of cylinders collapses when the radially inward deflection reaches a value of 2/9 of the cylinder radius. The bending moment corresponding to such deformation can be calculated by [2.8]:

$$M_{cr-B} = \frac{2\sqrt{2}}{9}\frac{E\pi R t^2}{\sqrt{1-\upsilon^2}} \tag{2.14}$$

In the case of short pipes with large D/t, short wavelength wrinkles form in the longitudinal direction. By increasing the applied moment, the deformation magnitude of the ripples increases, followed by a catastrophic collapse at a limit load. The collapse mode of these pipes is shown in Figure 2.16.a. This category of pipes is classified as Class II in this text. Investigating the bifurcation buckling of cylindrical shells, including the longitudinal wrinkles, was initially considered by Flugge in 1932 [2.23]. However, the primary studies were restricted by inadequate computational capabilities of the era.

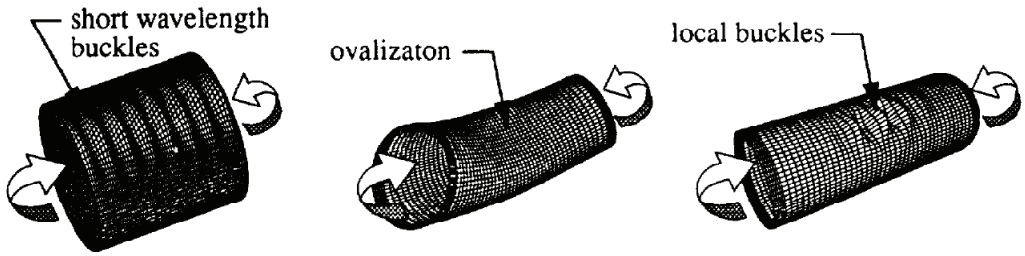

(a)
Compression buckling mode of short cylinders

(b)
Cross-section collapse mode of long cylinders

(c)
Interaction for cylinders of intermediate length

Figure 2.16. Pipe bending collapse modes [2.23].

In 1961, Seide and Weingarten found that the critical buckling stress for this class of cylindrical shells is essentially equal to the critical stress of the system under uniform axial compression [2.24]. Therefore, they recommended the following equation:

$$M_{cr} = S\sigma_{cr} = \pi R^2 t\sigma_{cr} \tag{2.15}$$

In this equation, S and σ_{cr} are respectively the elastic section modulus and the uniaxial compression critical stress that can be calculated from the following equation [2.8].

$$\sigma_{cr} = \frac{Et}{R\sqrt{3(1-\upsilon^2)}} \tag{2.16}$$

Kyriakides and Ju (2.25) and Ju and Kyriakides (2.26), through a series of experimental and numerical studies, developed a set of characteristic equations to describe both Class I and Class II types of behaviors. They defined deformation equations as incorporating three main features. First, the equations were capable of capturing the ovalization in the pipe's cross-section; second, the ovalization along the pipeline axis could be locally developed and; third, the equations are capable of simulating the wrinkle growth along the pipeline axis. They found that by employing this formulation, the characteristic behavior and buckling moment of cylindrical shells falling in the first and second classes of pipes can be accurately calculated.

Pipes with intermediate length and D/t values fall in the third category of pipes, here referred to as Class III. In this category, the instability modes consist of an interaction between the first and second class modes, and thus the method used to evaluate the instability limit moment should be capable of addressing this interaction.

The instability of such cylinders was first investigated by Axelrad in 1965 [2.27], who found that the moment capacity of these systems is a function of the ratios of the pipe's thickness and length to the radius. Calladine [2.28] suggested a non-dimensionalized geometrical parameter should be used to classify the behavior category of cylindrical shells as:

$$\Lambda \sim \sqrt{\frac{l^2 t}{R^3}} \tag{2.17}$$

It should be mentioned that, in contrast to the other two classes of pipes, the length parameter has a significant influence on the behavior of this category of pipes. Ju and Kyriakides (2.26) proposed a more complex series expansion to describe the deformation of such systems in comparison to the deformation equations used to describe the first and second classes. Generally, most of the studies developed to characterize the behavior of cylindrical shells are related to the first and the second categories of cylinders. As a result, and due to the complex behavior of the intermediate class, they are less discussed in the literature; nevertheless, advances in computational capabilities and numerical methods have made the investigation of the behavior of such systems more feasible.

A summary of the various classes of behaviors and the influence of geometrical properties (represented by parameter Λ) on classifying those behaviors is presented in Figure 2.17. As can be seen in this figure, the second class of pipes has the maximum bending capacity and the minimum deformability before reaching the buckling moment. The pre-buckling, buckling limit and post-buckling regimes in Figure 2.17.b are indicated by solid lines, solid symbols and dashed lines, respectively.

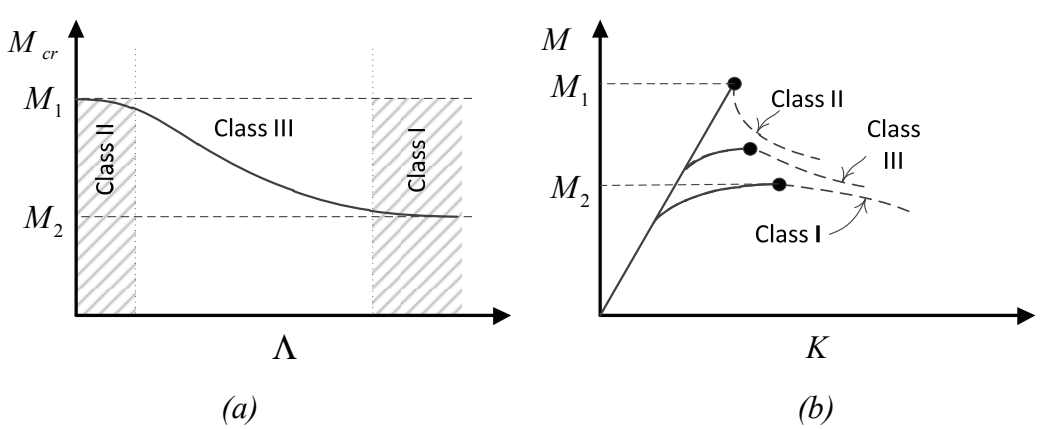

Figure 2.17. General stability behavior of pipes under pure bending. (After [2.23])

It should be noted that the first class of pipes, which would collapse due to excessive section ovality, would have the minimum bending capacity but the maximum deformability before buckling. M_1 and M_2 in these figures represent the minimum and maximum bending capacity of a system, respectively, which can be calculated by Equations (2.15) and (2.14) for a single-walled pipe. Former studies have revealed that, for conventional metallic pipes, the magnitude of M_1 is twice that of M_2 [2.23].

The behavior of multi-layered cylindrical shells made from anisotropic layers was investigated by several researchers. Fuchs et al. reported a state-of-the-art review in 1993 [2.23] regarding the analytical approaches developed to explore the behavior of laminated anisotropic circular cylinders under bending. Equations (2.18) and (2.19) illustrate the corresponding equations to Equations (2.14) and (2.15) for calculating the buckling moment of laminated cylindrical shells [2.23, 2.30 and 2.31]. These equations are developed for a symmetrical balanced laminate.

$$M_{cr-B} = 2\pi R\sqrt{\frac{8}{27}E_z t D_{22}} \tag{2.18}$$

$$M_{cr} = S\sigma_{cr} = 2\pi R\sqrt{E_z t D_{11}} \tag{2.19}$$

where E_z is the elastic modulus of the pipe along the pipeline axis and D_{11} and D_{22} are the corresponding laminate bending stiffness terms The equations for defining D_{11} and D_{22} can be found in any laminate composite text book (e.g. [2.31]).

Although Cylindrical Laminated Shells (CLS) and Sandwich Pipes are both multi-layered cylindrical structures, theories developed to characterize the behavior of CLSs are not applicable to SPs. The total thickness of Sandwich Pipes is at least 15% of the average radius, which is out of range of the parameters describing the classical first-order theories of laminated shells. To the author's knowledge, there is no analytical solution in the literature that can be applied to SP systems under bending due to the extreme complexity of the characteristic equations associated with such systems.

However, the behavior of SPs under bending has been investigated in a few numerical studies. As mentioned earlier, Estefen et al. [2.5] investigated the behavior of SP systems under combined external pressure and bending loads through both experimental and numerical studies. As well, the bending capacity and response function

of the Penguins pipeline, a 60km PIP system developed in the northern North Sea, was studied in a research by Carr et al. [2.32]. They experimentally tested the prototype scale of the pipe and captured the pipe's response as having a field joint. Due to the existence of field joints in the FE models, there was no need to consider any type of imperfection in analyzing the post-buckling behavior. However, they only captured the instability bending capacity limit corresponding to the extreme cross-section ovality, which is the most likely governing class of instability for pipes with field joints. It should be mentioned that, in their study, the core layer was bonded to both internal and external pipes. They concluded that instability occurred because of the formation of inward bulges in both the internal and external pipes.

2.4. HIGH-GRADE STEEL PIPELINES

Employing pipelines manufactured from new materials in applications where oil and gas are explored in deep waters and harsh remote offshore fields would improve the efficiency of the pipeline system. The demand for employing higher grade steel pipes, such as X80, X100 and X120 in large pipeline projects is increasing, especially in applications were the operating pressure is equal or greater than 150 [2.33]. More than a decade's worth of research has been carried out to understand the behavior of such pipes under various loading and environmental conditions. However, despite the recent technical advancements, more research is required to investigate the more complicated design configurations and loading conditions.

The major research carried out on high-grade steel pipelines started in the mid-1990s. One of the initial projects was the TAP project (Transporto gas Alta Pressione), which aimed to bring high pressure gas to the market via high grade (X80 and X100) long-distance pipelines through harsh environments [2.33]. After more than a decade, TransCanada Corp. earned an acceptance of X100 grade steel into the relevant Canadian Standards Association (CSA) code in 2002. This resulted in the incorporation of grade X100 (690 MPa) steel into the new edition of CSA Z245.1 [2.34].

In this section, a brief summary of the material properties of cold-formed steel pipes, such as high-grade steel made for oil and gas transportation purposes, is presented. The anisotropic material properties of high-grade steel pipes occur as a result of its

manufacturing process; therefore, the manufacturing process of such pipes is also briefly discussed. Afterwards, a short review of the numerical methods which can be used to model the yield anisotropic behavior of such pipes is discussed. Finally, a review of previous studies investigating the influence of such material property on the mechanical behavior of pipeline is presented.

2.4.1. Manufacturing process

The manufacturing of cold-formed pipes is not one of the main concerns of this study. However, due to the effect of the manufacturing process on a pipe's material behavior, a basic understanding of the manufacturing process would help to better grasp the material's characteristics. The steel plate production technology process has been improving since the mid-1980s through the use of the Thermo-Mechanical Controlled Process (TMCP) [2.35]. Likewise, high-grade steel pipes have been developed by the cold-forming of steel plates using the UOE process.

Figure 2.18 illustrates the four cold-forming steps in the manufacturing process of these pipes. The first step is crimping the plate edges into circular arches, which is shown in Figure 2.18.a. Next, the steel plate is formed into a U shape using a U press; this is followed by another press, which forms it into an O shape (Figures 2.18.b and 2.18.c). Finally, as illustrated in Figure 2.18.d, the O form is finished by expanding a number of dices on the internal side of the pipe. This expanding step produces a net compressive strain of 0.1-0.2% [2.1].

Applying plastic deformations in each manufacturing step affects the material's behavior due to the Bauschinger effect. Thus, pipes with X100 or higher grade steel would exhibit different response in the transverse direction as opposed to the longitudinal direction. A rough rule of thumb states that, by moving from the transverse to the longitudinal direction, pipe material loses about 10 ksi (70 MPa) in its tensile yield strength [2.34].

The cold-forming manufacturing process applies plastic strains to the original plate and thus changes the original material properties in the direction of the applied plastic deformations. The U and O steps induce large plastic strains in the circumferential direction, after which the E step induces large plastic deformations to the pipeline in both

the radial and hoop directions. Due to the Baushinger effect, the applied plastic deformations increase the tensile yield stress and decrease the compressive yield stress in the circumferential direction.

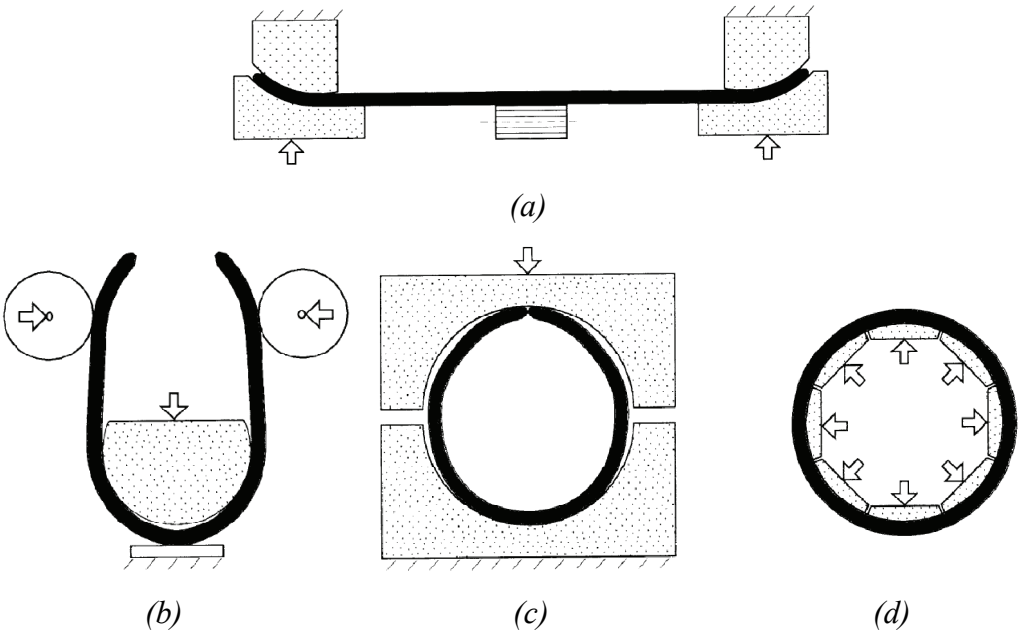

Figure 2.18. Schematic of the UOE manufacturing process. (a)Edge crimping. (b) U-ing. (c) O-ing. (d) Expansion process. [from 2.1]

2.4.2. Numerical modeling of material yield anisotropy

Several material models and numerical methods have been used by various researchers to simulate the yield anisotropic behavior of cold-formed pipes, including high-grade steel ones. In 1950, Hill [2.36] recommended a yield criterion for materials having various yield stresses in different directions. In a study by Martinez and Brown [2.37], a UMAT ABAQUS user subroutine that employs the Hill's yield criteria and a proper hardening model to predict the material anisotropy through the installation reel-lay process was developed.

In another numerical method, the plastic strains applied during the manufacturing process are applied to the pipeline material as a predefined plastic strain field [2.38]. In other words, in this method the manufacturing process of the pipeline is simulated by applying a proper material model modified by plastic strains. Some other material models considering the micro-structure of the material have also been proposed with other

researchers. For example, Liu and Wang [2.39, 2.40 and 2.41] proposed an advanced material model based on polycrystalline plasticity constitutive models, and Tanguy et al. [2.42] developed a constitutive model which considers both anisotropic behavior and ductile damage for an X100 pipeline steel.

More studies were done in order to compare the accuracy of the Hill's criteria with more complex criteria by Kuwabara [2.43]. Kuwabara studied the accuracy of various yield criteria in modeling steel sheets with yield anisotropy. In that study, the accuracy of Hill's yield criteria and several other more complicated yield criteria is compared. It can be concluded from their study that although more complicate criteria like Banabic-Balan-Comsa criteria yield more accurate results, the Hill's criteria has an acceptable accuracy and can be used in practice.

Employing Hill's yield criteria and applying the plastic strains using pre-defined field method in order to model the yield anisotropic behavior are the two most popular methods used for numerical modeling of cold-formed pipelines. In this section, a brief review of these two methods is presented.

Hill's anisotropy model

The yield potential function of Hill's plasticity model is a quadratic function of the normal and shear stress components [2.36]. This function, which is an extension of von Mises yield function, is presented in Equation (2.20).

$$f(\sigma) = \{F(\sigma_{22} - \sigma_{33})^2 + G(\sigma_{33} - \sigma_{11})^2 + H(\sigma_{11} - \sigma_{22})^2 + 2L\sigma_{23}^2 + 2M\sigma_{31}^2 + 2N\sigma_{12}^2\}^{1/2} \tag{2.20}$$

where F, G, H, L, M and N are the material constants and usually determined based on the ratio of yield strength in other orientations with respect to the reference direction, experimentally. These coefficients can also be determined based on the Lankford coefficients or the so-called R-values [2.38].

Several researchers used Hill's anisotropy yield function to model pipeline materials with anisotropic yield properties. Paquette and Kyriakides [2.44], Kyriakides et al. [2.45] and Bardi and Kyriakides [2.46, 2.47] used this method to study the behavior of aluminum tubes under axial compression and internal pressure. In these valuable works,

they used Hill's function with both flow and deformation theories of plasticity in an analytical approach. Their results showed that the response of a pipe could be accurately calculated by modeling the pipe using a combination of the deformation theory of plasticity and Hill's criterion. Figure 2.19 shows a comparison made by Bardi and Kyriakides between the measured experimentally and analytically calculated wrinkle half-wavelength for steel tubes under axial force and different D/t. In the figure λ_c is the wrinkle half-wavelength.

In another research, Corona [2.48] used the same method to study the bending behavior of aluminum pipes under bending. In this work, Hill's anisotropy criterion was incorporated in a flow theory used for the evaluation of pre-buckling and post-buckling responses. The bifurcation limit was also established by applying Hill's criteria into the deformation theory of plasticity.

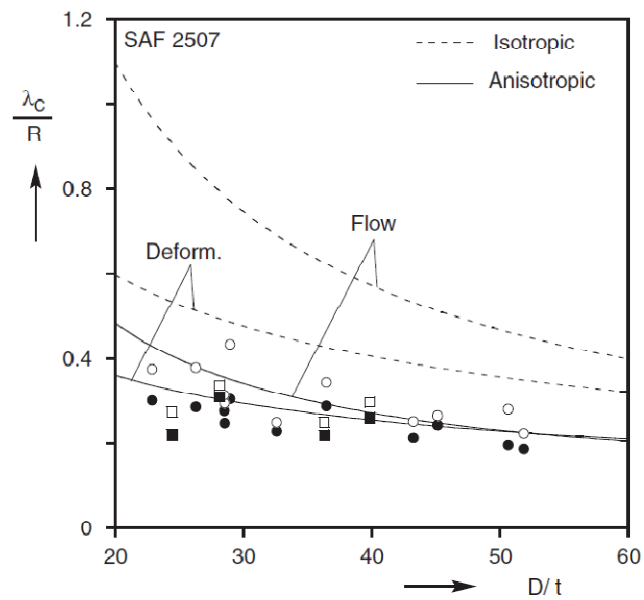

Figure 2.19. Accuracy of the Hill's criteria in predicting the wrinkle half-wavelength vs. D/t from 15 experiments [from 2.48]

<u>*Generating anisotropy by simulating the manufacturing process*</u>

As mentioned above, anisotropy in high-grade steel pipelines is due to the applied plastic deformations in the manufacturing process. Therefore, pipeline yield anisotropy can be modeled in the numerical method by applying the manufacturing plastic

deformations to the pipeline plate with the original isotropic material property. In the finite element method, this technique can be employed using two approaches. First, the plastic deformations can be applied using predefined strain fields. In another approach, the whole manufacturing process can be simulated by modeling a system of rigid pressing elements and a flexible pipeline plate. The plastic deformations in this second approach are applied to the pipeline plate by inducing the proper magnitude of deformations to the pressing elements using proper contact models.

Kyriakides et al. [2.49] used this approach to study the effects of the manufacturing process on the buckling pressure of X70 steel pipes. They also used it to solve the buckling pressure problem through an analytical approach. A summary of their modeling steps is shown in Figure 2.20. In this figure, steps *a* to *e* illustrate the manufacturing process and 2.20.f shows the application of the externally applied load, followed by the pipeline ovalization presented in Figure 2.20.g.

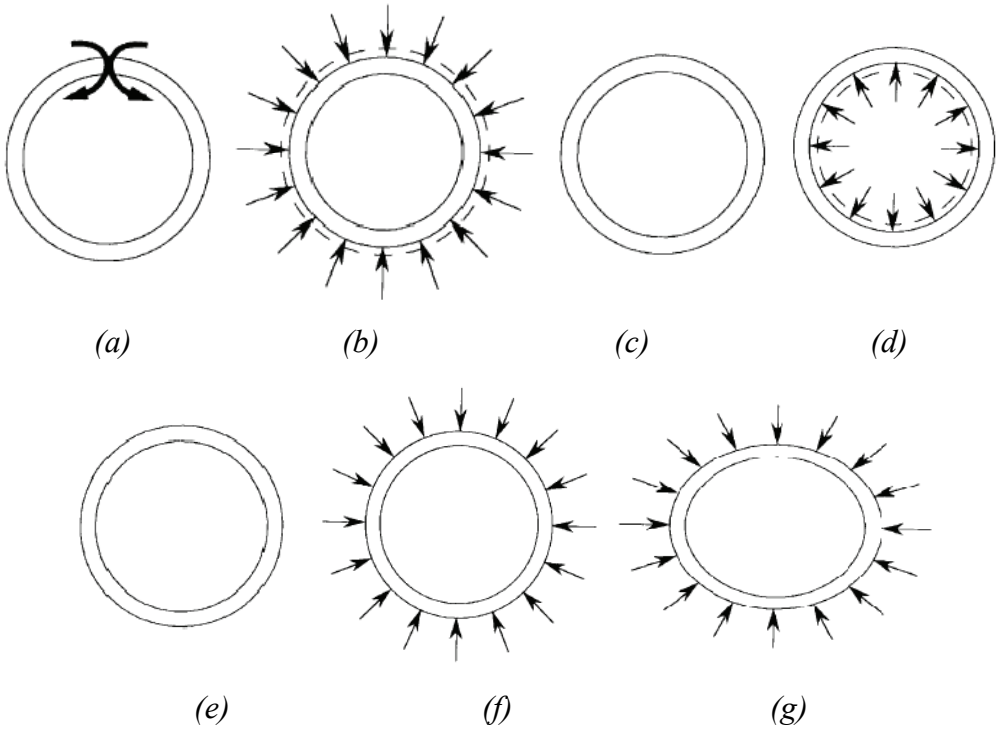

Figure 2.20. Deformation and load steps to simulate the material anisotropy and model the buckling behavior under the external hydrostatic pressure. (a) Bending. (b) Uniform contraction. (c) Unloaded cylinder. (d) Uniform expansion. (e) Final state. (f) External pressure. (g) Collapse. [from 2.49]

Isotropic, kinematic or a combination of these two hardening rules can be used in either of the above-mentioned methods. Using the isotropic hardening, the material can be defined with similar hardening in all directions. However, due to the Baushinger effect, high-grade pipe material would exhibit different hardening in different directions. While improving the models by using more complicated hardening rules like the kinematic or the nonlinear isotropic/kinematic hardening models might overcome this problem, these models require a comprehensive understanding of the material's behavior, and therefore access to more appropriate experimental test data and more complicated FE models. Lie and Wang [2.39-2.41] studied the effects of using isotropic or kinematic hardening models in the modeling of pipes under bending.

2.4.3. Effect of yield anisotropy on the mechanical behavior of pipes

Pipe under axial compression and internal pressure

Paquette and Kyriakides [2.44] studied the effect of material yield anisotropy on the behavior of a pipe under axial compression and internal pressure from experimental, numerical and analytical points of view. They calculated the critical stress, strain and wavelength of the wrinkles at the onset of wrinkling, using both mathematical and experimental methods. Paquette and Kyriakides used the classical plastic bifurcation theory based on the deformation theory of plasticity in their analytical approach. They also have created the material model through the flow theory of plasticity with isotropic and anisotropic hardenings using Hill's criterion. Figure 2.21 shows their results, comparing the experimental and numerical simulations of aluminum tubes manufactured through an UOE process. As can be seen in this figure, yield anisotropy would affect the behavior of the system significantly. Another interesting result that can be concluded from their work is that, by using Hill's quadratic anisotropic model, the real behavior of the pipe could be captured with acceptable accuracy compared to the experimental results.

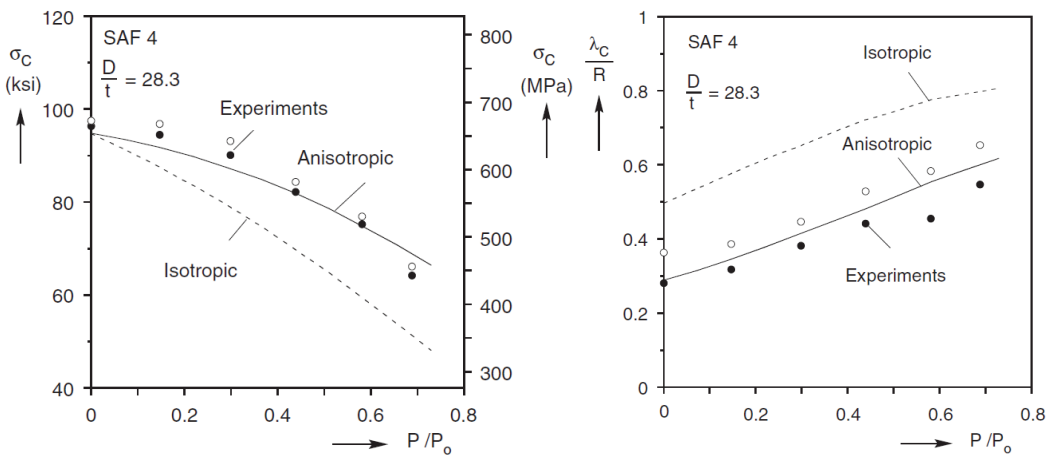

(a) *(b)*

Figure 2.21. Influence of the yield anisotropy on: (a) critical stress (b) and axial half-wavelength at onset of wrinkling as a function of internal pressure for D/t 28.3. [from 2.44]

In the above figures, σ_c is the critical stress and λ_c is the axial half-wavelength wrinkle at the onset of wrinkling.

<u>*Pipe under pure bending*</u>

The effect of the material yield anisotropy on the response of pipes under pure bending has been studied by Corona [2.48] from experimental, analytical and numerical aspects. In that study, the material anisotropy was incorporated into the flow theory used for pre-buckling and post-buckling calculations. In numerical models, it was assumed that the geometrical imperfection in the longitudinal direction is in the form of wrinkling. Moreover, the numerical models were developed with the assumption that the planes perpendicular to the pipeline axis remains plane after the deformation; however, they were allowed to ovalize.

Corona found that the material yield anisotropy had a significant effect on a pipe's behavior under pure bending. Figure 2.22 shows the results for the bifurcation curvature and the wrinkling half-wave as a function of the anisotropy variables, defined as:

$$S_r = \frac{\sigma_{rr}}{\sigma_{zz}} \tag{2.21}$$

$$S_\theta = \frac{\sigma_{\theta\theta}}{\sigma_{zz}} \tag{2.22}$$

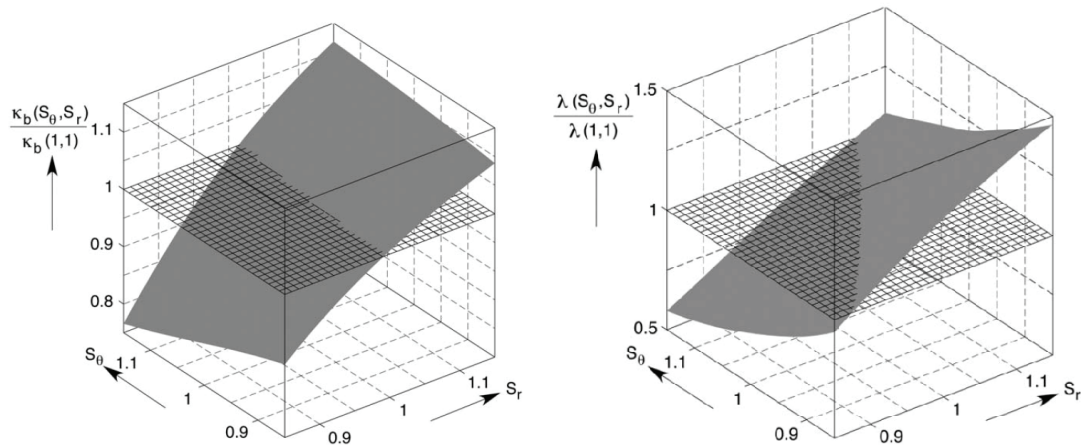

(a) *(b)*

Figure 2.22. Effect of yield anisotropy on (a) bifurcation curvature (b) wrinkle half-wave as a function of the anisotropy variables [2.48].

Another study on the behavior of high-grade steel pipes under bending was done by Suzuki et al. [2.50]. In this investigation, the behavior of X80 steel pipelines under bending was examined through a set of full-scale experiments as well as numerical simulations. The effect of the geometrical imperfection pattern used in the numerical models by comparing various modes of imperfection was also investigated. However, in their research, the yield anisotropy was not considered. A comparison of their experimental and FE results revealed an acceptable correlation between the pre-buckling and buckling regime, while in the post-buckling regime the FE results did not match the experiments.

REFERENCES

2.1. Kyriakides, S. and Corona, E. (2007). Mechanics of offshore pipelines (1st ed.). Elsevier, Amsterdam.

2.2. Vries G. D., Brennodden H., Meer, J. V. D., Wendel S. (2009). Ormen Lange Gas Field: Immediate Settlement of Offshore Rock Supports. *Journal of Offshore Mechanics and Arctic Engineering*. 131, 1-4.

2.3. Liberty Development Project (1999). *Evaluation of Pipeline System Alternatives: Executive Summary*, BP.

2.4. BREDERO SHAW, 2010. *PU Foam Insulated Pipe-In-Pipe.* [online] Available at: < http://www.brederoshaw.com/solutions/Pipe-In-Pipe.htm> [Accessed 16 September 2010].

2.5. Estefen, S. F., Netto, T. A., and Pasqualino, I. P. (2005). Strength analyses of sandwich pipes for ultra deepwaters. *Journal of Applied Mechanics, 72*(4), 599-608.

2.6. C-CORE, Colt Engineering Corp. Tri Ocean Engineering Ltd. and AGRA Earth & Environmental. (2000). *An Engineering Assessment of Double Wall versus Single Wall Designs for Offshore Pipelines in an Arctic Environment*. C-CORE Technical publication. St John's NF.

2.7. Meyer, K. J. (1999). Colville River Crossing. *Presented to: Alaskan Arctic Pipelines Workshop*, November 8-9, Anchorage, AK.

2.8. Farshad, M. (1994). *Stability of structures*. ELSEVIER, Amsterdam.

2.9. Timoshenko, S., and Goodier, J. N. (1970). *Theory of elasticity* (3rd ed.). McGraw-Hill, New York; Toronto.

2.10. Brush DO. and Almroth, B. (1975). *Buckling of bars, plates and shells*. McGraw-Hill, New York.

2.11. Sato, M. and Patel, M. H. (2007). Exact and simplified estimations for elastic buckling pressures of structural pipe-in-pipe cross sections under external hydrostatic pressure. *Journal of Marine Science and Technology, 12*(4), 251-262.

2.12. Sato, M., Patel, M. H., and Trarieux, F. (2008). Static displacement and elastic buckling characteristics of structural pipe-in-pipe cross-sections. *Structural Engineering Mechanics, 30*(3), 263-278.

2.13. Kardomateas, G. A. and Simitses, G. J. (2002). Buckling of long, sandwich cylindrical shells under pressure. *Proceedings of the International Conference on Computational Structures Technology*, 327-328.

2.14. Kardomateas, G. A. and Simitses, G. J. (2005). Buckling of long sandwich cylindrical shells under external pressure. *Journal of Applied Mechanics, 72*(4), 493-499.

2.15. Ohga, M., SanjeewaWijenayaka, A. and Croll, J. G. A. (2005). Reduced stiffness buckling of sandwich cylindrical shells under uniform external pressure. *Thin-Walled Structures, 43*(8), 1188-1201. Castello, X., Estefen, S. F., Leon H. R., Chad, L. C. and Souza, J. (2009). Design aspects and benefits of sandwich pipes for ultra deepwaters. *Proceedings of the 28th International Conference on Ocean, Offshore and Arctic Engineering,* OMAE2009 -79528, Hawaii, USA.

2.16. Castello, X. and Estefen, S. F., 2006. Adhesion effect on the ultimate strength of sandwich pipes. *International Conference on Offshore Mechanics and Arctic Engineering, OMAE2006-92481,* Hamburg, Germany.

2.17. Castello, X., and Estefen, S. F., 2008. Sandwich pipes for ultra deep-water applications. *Offshore Technology Conference,* OTC 197041*,* Houston, Texas, USA.

2.18. Kyriakides, S. and Netto, T. A. (2004). On the dynamic propagation and arrest of buckles in pipe-in-pipe systems. *International Journal of Solids and Structures, 41*(20), 5463-5482.

2.19. Kyriakides, S. (2002). Buckle propagation in pipe-in-pipe systems. Part I. Experiments. *International Journal of Solids and Structures, 39*(2), 351-366.

2.20. Kyriakides, S. and Netto, T. A. (2002). Dynamic propagation and arrest of buckles in pipe-in-pipe systems. *Proceedings of the International Conference on Offshore Mechanics and Arctic Engineering* – OMAE2002, 4, 199-205.

2.21. Kyriakides, S. and Vogler T.J. (2002). Buckle propagation in pipe-in-pipe systems. Part II. Analysis. *International Journal of Solids and Structures, 39*(2), 367-392.

2.22. Brazier, L. G. (1927). On the flexure of thin cylindrical shells and other 'thin' sections. *Proceeding of Royal Society of London*, Series A, 104-114.

2.23. Fuchs, J. P., Hyer, M. W., Starnes, J. H. (1993). Numerical and Experimental Investigation of the bending Response of Thin-Walled Composite Cylinders. *Department of Engineering Science and Mechanics, NASA Gran NAG-1-343, Interim Report 95*, The NASA-Virhina Tech Composite Program.

2.24. Seide, P., Weingarten, V. I. (1961). On the Buckling of Circular Cylindrical Shells Under Pure Bending. *Journal of Applied Mechanics*, 28, 112-116.

2.25. Kyriakides, S., Ju, G. T. (1992). Bifurcation and localization instabilities in cylindrical shells under bending. I. Experiments. *International journal of solids and structures,* 29(9), 1117-1142.

2.26. Ju, G. T., Kyriakides, S., (1992). Bifurcation and localization instabilities in cylindrical shells under bending. II. Predictions. *International journal of solids and structures,* 29(9), 1143-1171.

2.27. Axelrad, E. L. (1965). Pinpointing the Upper Critical Bending Load of a Pipe by Calculating Geometric Nonlinearity. AkademyNauk SSSR, IzvestiyaMekhanika, 4, 133-139.

2.28. Calladine, C. R. (1983). Theory of Shell Structures, Cambridge University Press, Cambridge, U. K., 614-621.

2.29. Fuchs, H. P., Hyer, M. W. (1992). The nonlinear bending response of thin-walled laminated composite cylinders. *Proceedings of the 33rd Structures, Structural Dynamics, and Materials Conference*, AIAA 92-2230, Dallas, TX, USA.

2.30. Kedward, K. T. (1987). Nonlinear collapse of thin-walled composite cylinders under flexural loading. *Proceeding of the 2nd International Conference on Composite Materials (ICCM2)*, 353-365, Toronto, Canada.

2.31. Reddy, J. N. (2003). *Mechanics of laminated composite plates and shells, theory and analysis, second edition*. CRC Press, Boca Raton.

2.32. Carr, M., Matheson, I., Peek, R., Saunders, P. and George, N. (2004). Load and resistance modeling of the Penguins pipe-in-pipe flowline under lateral buckling. *International Conference on Offshore Mechanics and Arctic Engineering – OMAE*.3, 39-47.

2.33. Spinelli, C., and Marchersani, F. (2004). TAP project. *Proceedings of the Biennial International Pipeline Conference, IPC, 1*, 757.

2.34. Canadian Standards Association (2002). *Steel Line Pipe*, Oil and Gas Industry Systems and Materials Standard CSA-Z245.1.

2.35. Pontremoli, M. (2005). A new generation of ultra-high strength X100/120 pipelines: A breakthrough for economic long-distance gas transportation. *Proceedings of the International Offshore and Polar Engineering Conference - ISOPE, 2005*, 31.

2.36. Hill, R. (1950). *Mathematical theory of plasticity*. New York: Oxford University Press.

2.37. Martinez, M. and Brown, G. (2005). Evolution of pipe properties during reel-lay process: Experimental characterization and finite element modeling. *Proceedings of the International Conference on Offshore Mechanics and Arctic Engineering - OMAE,* 419-429.

2.38. ABAQUS User's and Theory Manual. (2008). Version 6.8, Dassault Systèmes, RI, USA.

2.39. Liu, M., and Wang, Y. (2006). Modeling of anisotropy of TMCP and UOE linepipes. *Proceedings of the International Offshore and Polar Engineering Conference-ISOPE,* 221.

2.40. Liu, M., and Wang, Y. (2007). Modeling of anisotropy of TMCP and UOE linepipes. *International Journal of Offshore and Polar Engineering, 17*(4), 288.

2.41. Liu, M. and Wang, Y. (2007). Advanced modeling of plasticity of linepipe steels with anisotropic texture and complex loading history. *Proceedings of the International Offshore and Polar Engineering Conference-ISOPE,* 3093.

2.42. Tanguy, B., Luu, T. T., Perrin, G., Pineau, A. and Besson, J. (2008). Plastic and damage behavior of a high strength X100 pipeline steel: Experiments and modeling. *The International Journal of Pressure Vessels and Piping, 85*(5), 322.

2.43. Kuwabara, T., Comsa, D. S., Banabic, D. and Iizuka, E. (2002). Modeling anisotropic behavior for steel sheets using different yield criteria. *Key Engineering Materials, 233*, 841. Paquette, J. A., and Kyriakides, S. (2006). Plastic buckling of tubes under axial compression and internal pressure. *International Journal of Mechanical Sciences, 48*(8), 855. Corona, E. Yield anisotropy effects on buckling of circular tubes under bending. International Journal of Solids and Structures, 43(22), 7099.

2.44. Paquette, J. A., and Kyriakides, S. (2006). Plastic buckling of tubes under axial compression and internal pressure. *International Journal of Mechanical Sciences, 48*(8), 855. Corona, E. Yield anisotropy effects on buckling of circular tubes under bending. International Journal of Solids and Structures, 43(22), 7099.

2.45. Kyriakides, S., Bardi, F. C., and Paquette, J. A. (2005). Wrinkling of circular tubes under axial compression: Effect of anisotropy. *Journal of Applied Mechanics, 72*(2), 301.

2.46. Bardi, F. C., and Kyriakides, S. (2006). Plastic buckling of circular tubes under axial compression-part I: Experiments. *International Journal of Mechanical Sciences, 48*(8), 830.

2.47. Bardi, F. C., Kyriakides, S., and Yun, H. D. (2006). Plastic buckling of circular tubes under axial compression-part II: Analysis. *International Journal of Mechanical Sciences, 48*(8), 842.

2.48. Corona, E. (2006). Yield anisotropy effects on buckling of circular tubes under bending. *International Journal of Solids and Structures*, 43(22), 7099.

2.49. Kyriakides, S., Corona, E. and Fischer, F.J. (1991). On the effect of the UOE manufacturing process on the collapse pressure of long tubes. *Proceeding of Offshore Technology Conference*, OTC 6758, 531-543.

2.50. Suzuki, N., Kondo, J., Ishikawa, N., Okatsu, M., and Shimamura, J. (2007). Strain capacity of X80 high-strain line pipes. *Proceedings of the 26th International Conference on Offshore Mechanics and Arctic Engineering - OMAE, 3*, 475.

CHAPTER 3
ELASTIC BUCKLING CAPACITY OF BONDED AND UNBONDED SANDWICH PIPES UNDER EXTERNAL HYDROSTATIC PRESSURE*

Kaveh Arjomandi and Farid Taheri
Department of Civil and Resource Engineering, Dalhousie University

3.1. ABSTRACT

Sandwich pipes can be considered as a potentially optimum system for use in deepwater applications. Understanding the stability characteristic of these pipes under the governing loading conditions, with the aim of generating optimum design, has gained considerable interest in recent years. External hydrostatic pressure is a critical loading condition that a submerged pipeline would experience during its installation and operational period.

This article presents an analytical approach for estimating the bucking capacity of sandwich pipes with various structural configurations and core materials, subject to external hydrostatic pressure. The influence of adhesion between the core layer and internal or external pipes has also been a focus of this study. Beside an exact solution, two simplified equations are developed for estimating the buckling capacity of two configurations commonly used in practice. Details of both the exact and simplified analytical formulations are presented and the required parameters are defined. The efficiency and integrity of the proposed simplified solutions are compared with a solution developed by other researchers. A comprehensive series of finite element eigenvalue buckling analyses were also conducted to evaluate the accuracy and applicability of the proposed solutions.

Keywords: Sandwich pipes, pipe-in-pipe, stability, buckling, hydrostatic pressure.

---

* JOURNAL OF MECHANICS OF MATERIALS AND STRUCTURES, Vol. 5, No. 3, 2010, (391–408).

3.2. NOMENCLATURE

AST	Simplified solution developed in this study
E_c	Core material elastic modulus
E_p	Pipes elastic modulus
h	Constituent's thickness
K_c	Core layer stiffness matrix
K_p	Pipes stiffness matrix
n	Buckling mode number
P	External pressure
P_{cr}	Sandwich pipe buckling pressure
P_{crs}	External pipe buckling pressure
r_1	Outer pipe nominal radius
r_2	Inner pipe nominal radius
SS	Simplified solution developed by Brush and Almroth, and Sato and Patel
t_1	Outer pipe wall thickness
t_2	Inner pipe wall thickness
v	Tangential deformation
w	Radial deformation
ν_c	Core material Poisson's ratio
ν_p	Pipe material Poisson's ratio
σ_r	Radial stress
$\tau_{r\theta}$	Tangential stress
ϕ	Stress function

3.3. INTRODUCTION

As the shallow offshore oil reserves are depleting, the demand for deep water oil reserves is increasing. Extracting oil from deep waters would not be possible, unless new pipeline systems could be developed to accommodate the new loading and environmental conditions. High external hydrostatic pressure, pipeline buoyancy during installation and low water temperatures restrict the application of single metallic pipelines to a limited

depth. Sandwich pipes can be considered as potentially optimum design alternative in addressing the requirements in deep waters. Sandwich Pipe (SP) systems employ the structural and thermal insulation benefits provided by two stiffer pipes sandwiching a lighter-weight and less-stiff core material. Moreover, the secondary containment provided by the external pipe improves the reliability of the system in case of product leak.

A typical Pipe in Pipe (PIP) system consists of an internal pipe, a relatively thick lightweight core layer and an external pipe. Each layer in this system can be designed for a specific purpose. The internal pipe, also referred to as the product pipe, usually is designed to endure the internal pressure and to facilitate the transport of the product safely. Core layer's function could be different depending on the application. For example, it can be designed to perform as a thermal insulator, or to improve the structural performance of the pipeline, depending on the core's material properties and the interaction mechanism between the core layer and the surrounding pipes. Wide range of core materials such as plastics, gels, ceramics and composite materials can be used to achieve the system's thermal and structural requirements. The external pipe, also called the sleeve pipe, separates the internal and core layer from the surrounding environment. The sleeve pipe may individually carry the externally applied loads like in a PIP system or as the main part of a sandwich system like in a SP system. Furthermore, the external pipe provides a secondary containment for the product being transported, in case of leakage of the product through the inner pipe.

To design an optimum SP system, understanding of its structural behavior is a prerequisite. A great number of works have been done in recent years to clarify the structural characteristic of such a system under different loading conditions. Some of those works have considered the stability of a sandwich cylindrical shell, which can be a general geometry for a sandwich pipe. For example Kyriakides and his coworkers studied the buckle propagation phenomena [3.1-3.4] from both numerical and experimental perspectives. Kardomateas and Simitses [3.5,3.6] studied the buckling of long sandwich cylindrical shells under external pressure analytically. Ohga et al. [3.7] studied the reduced stiffness buckling of sandwich cylindrical shells under uniform external pressure both numerically and analytically. Sato and Patel [3.8] and Sato et al [3.9] studied the

buckling behavior of a PIP system under hydrostatic pressure and developed a simplified solution for estimating a PIP system's buckling capacity. Castello and Estefen [3.10, 3.11] and Estefen et al. [3.12] studied the feasibility of a sandwich pipe system for deep water applications with both numerical and experimental approach. In another study, Castello and Estefen [3.13] investigated the ultimate strength of sandwich pipes under combined external pressure and bending for several degrees of adhesion between core layer and external pipe. They also investigated the effect of cyclic loads applied during reeling installation method on the collapse pressure. Very recently, Castello et al. [3.14] also conducted an investigation, comparing PIP with SP systems designed for hypothetical oil field with several core materials. In this study they used polypropylene and polyurethane foams with various densities as the core material and investigated both the influence of their mechanical and thermal properties. In conclusion they found that the combination of steel and the foams could provide effective SP systems with good buoyancy and thermal insulation properties.

Furthermore, several other works have been done by other researchers in numerical modeling of a sandwich pipe considering various parameters, and loading and boundary conditions.

3.4. MOTIVATION AND AIMS

Our preliminary investigation indicated that most of the available simplified solutions developed for predicting buckling capacity of PIP systems subject to hydrostatic pressure produce results with very large margins of error under certain conditions. This fact prompted an analytical investigation, with the aim of developing exact and simplified solutions for establishing the buckling capacity of PIPs subject to externally applied hydrostatic pressure. Moreover, a comprehensive finite element investigation will also be conducted to establish the performance of PIPs with a wide range of material and physical properties, and to verify the integrity of the proposed solutions. In this work, four different interlayer bonding configurations will be considered. The parameters used to define the characteristic equation of the system will be outlined. An important aim of this investigation will also be extracting simplified solutions from the exact solution for use in practical design. As a result, the simplified

and exact solutions will be compared and the accuracy of their results will be discussed. Finally, the error margins resulting from the use of the proposed simplified equations and that proposed by other researchers will be established.

3.5. ANALYTICAL MODEL

A long, circular cylindrical shell, consist of three layers (steel, core, steel) is considered. Due to the symmetry in structural configuration and loading, this problem can be idealized as a 2-D plane strain problem. The use of polar coordinates would also aid in formulating the problem. Figure 3.1 shows the geometry and the polar coordinate system of the model.

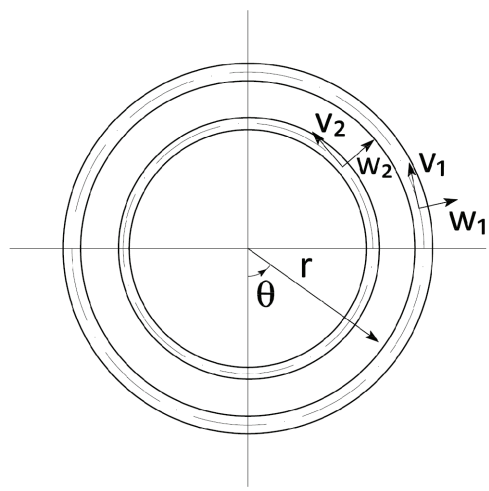

Figure 3.1. The coordinate system and the idealized geometry

3.6. EQUILIBRIUM EQUATIONS OF THE SYSTEM

The potential energy of the system can be used to derive the equilibrium equations. The corresponding potential energy can be represented by [3.15]:

$$\Pi = U_{P,1} + U_{P,2} + U_c + \mathrm{W_p} \tag{3.1}$$

where the potential energy of the internal and external pipes are given by:

$$U_{P,i} = \int_0^{2\pi} \frac{1}{2}\left[N_{\theta\theta,i}\varepsilon^o_{\theta\theta,i} + M_{\theta\theta,i}k_{\theta\theta,i}\right] r_i . d\theta \tag{3.2}$$

($i = 1,2$ for external and internal pipes, respectively)

in which $N_{\theta\theta}$ is the internal hoop force, $\varepsilon^{o}_{\theta\theta}$ is the circumferential strain of the centroid fiber, $M_{\theta\theta}$ is the internal moment and $k_{\theta\theta}$ is the curvature change in the centroid surface.

In equation (3.1), the effect of the core layer can be considered as the work done by the entire layer's stresses applied to the inner and outer pipes. These works can be represented by:

$$U_{C} = U_{c,1} + U_{c,2} \tag{3.3.a}$$

where:

$$U_{C,i} = \int_0^{2\pi} \left[\sigma_r\Big|_{a_i} . \; w\Big|_{a_i} + \tau_{r\theta}\Big|_{a_i} . \; v\Big|_{a_i} \right] a_i . d\theta \tag{3.3.b}$$

where $a_1 = r_1 - t_1/2$ and $a_2 = r_2 + t_2/2$.

The work done by the external hydrostatic pressure is given by [3.15]:

$$W_{P} = P \int_0^{2\pi} \left[w r_1 + \frac{1}{2}(v^2 + w^2 - vw' + v'w) \right] . d\theta \tag{3.4}$$

where ($'$) indicate the derivative of the variable with respect to θ.

Sander's shell equations are used to describe the strain-displacement relationships. Sander's kinematic equations are nonlinear and are based on small strain and moderate rotation assumptions, which are appropriate for establishing the linear buckling equations. The kinematic equations in polar coordinate can be represented by:

$$\varepsilon_{\theta\theta} = \varepsilon^{o}_{\theta\theta} + z k_{\theta\theta} \tag{3.5.a}$$

$$\varepsilon^{o}_{\theta\theta} = \frac{w + v'}{r} + \frac{1}{2}\beta^2 \tag{3.5.b}$$

$$k_{\theta\theta} = \frac{\beta'}{r} \tag{3.5.c}$$

In these equations, β represents the rotation of a circumferential element located at the mid-plane of the pipes. β for an intermediate class of deformation (small mid-surface strains and small but finite rotations) can be defined by [3.16]:

$$\beta = \frac{v - w'}{r} \tag{3.6}$$

Using the plane strain material constitutive relation, the force and moment intensities in (3.2) can be written as:

$$N_{\theta\theta} = C\varepsilon^{o}_{\theta\theta} \tag{3.7.a}$$

$$M_{\theta\theta} = Dk_{\theta\theta} \tag{3.7.b}$$

where $C = Et/\left(1 - \upsilon_p^2\right)$ and $D = Et^3/12\left(1 - \upsilon_p^2\right)$.

By substituting the kinematic and constitutive equations and using the variational calculus, the equilibrium equations of the system can be presented by the following four equations:

$$\alpha_{1,1}(w_1 + v_1')-\alpha_{2,1}(v_1 - w_1')''' + p(w_1'' + w_1)+a_1 \quad \sigma_r\Big|_{a_1} = 0 \tag{3.8.a}$$

$$\alpha_{1,1}(w_1 + v_1')'+\alpha_{2,1}(v_1 - w_1')'' + a_1 \quad \tau_{r\theta}\Big|_{a_1} = 0 \tag{3.8.b}$$

$$\alpha_{1,2}(w_2 + v_2')-\alpha_{2,2}(v_2 - w_2')''' - \ a_2 \quad \sigma_r\Big|_{a_2} = 0 \tag{3.8.c}$$

$$\alpha_{1,2}(w_2 + v_2')'+\alpha_{2,2}(v_2 - w_2')'' - a_2 \quad \tau_{r\theta}\Big|_{a_2} = 0 \tag{3.8.d}$$

where:

$$\alpha_{1,i} = \frac{C_i}{r_i} \quad ; \qquad \alpha_{2,i} = \frac{D_i}{r_i^3}(i = 1,2) \tag{3.8.e}$$

These Euler differential equations are written in terms of four independent variables u_1, v_1, u_2 and v_2, which represent the deformation of the internal and external pipes and four dependent variables $\sigma_r\Big|_{a_1}$, $\tau_{r\theta}\Big|_{a_1}$, $\sigma_r\Big|_{a_2}$ and $\tau_{r\theta}\Big|_{a_2}$. The dependent variables can be described as functions of independent variables, using the core properties. An elasticity approach is used here to characterize the core behavior.

The displacement function that could satisfy the equilibrium equations can be assumed as circumferentially periodic. Considering this assumption, the following stress function would satisfy the equilibrium equations (3.8):

$$\phi(r, \theta) = f_n(r)\cos n\theta \tag{3.9}$$

where n is the buckling mode number. To yield a possible stress distribution, the stress function must ensure that the following compatibility equation in polar coordinate is satisfied [3.17]:

$$\left(\frac{\partial^2}{\partial r^2}+\frac{1}{r}\frac{\partial}{\partial r}+\frac{1}{r^2}\frac{\partial^2}{\partial \theta^2}\right)\left(\frac{\partial^2 \phi}{\partial r^2}+\frac{1}{r}\frac{\partial \phi}{\partial r}+\frac{1}{r^2}\frac{\partial^2 \phi}{\partial \theta^2}\right)=0 \tag{3.10}$$

In order for ϕ to be an admissible solution of this equation, a general solution of f_n can be written as follows [3.17]:

$$f_n(r)=A_n r^{-n}+B_n r^{2-n}+C_n r^{2+n}+D_n r^n (n \geq 2) \tag{3.11}$$

in which the constants A_n, B_n, C_n and D_n are to be calculated from the distribution of forces and displacements at the boundaries. The stress and displacement components in polar coordinates are described as:

$$\sigma_r=\frac{1}{r}\frac{\partial \phi(r,\theta)}{\partial r}+\frac{1}{r^2}\frac{\partial^2 \phi(r,\theta)}{\partial \theta^2} \tag{3.12.a}$$

$$\tau_{r\theta}=-\frac{\partial}{\partial r}\left(\frac{1}{r}\left(\frac{\partial \phi(r,\theta)}{\partial \theta}\right)\right) \tag{3.12.b}$$

$$\widetilde{w}=\int \varepsilon_r . dr \tag{3.13.a}$$

$$\tilde{v}=\int (r\varepsilon_\theta - w). d\theta \tag{3.13.b}$$

Using these relations, stresses at the boundary of the core can be described as a function of deformation of the boundary. The following general core boundary conditions are considered:

$$\widetilde{w}\Big|_{a_1}=\widetilde{W_1}\cos n\theta \tag{3.14.a}$$

$$\tilde{v}\Big|_{a_1}=\widetilde{V_1}\sin n\theta \tag{3.14.b}$$

$$\widetilde{w}\Big|_{a_2}=\widetilde{W_2}\cos n\theta \tag{3.14.c}$$

$$\tilde{v}\Big|_{a_2}=\widetilde{V_2}\sin n\theta \tag{3.14.d}$$

$$\tau_{r\theta}\Big|_{a_1} = 0 \tag{3.14.e}$$

$$\tau_{r\theta}\Big|_{a_2} = 0 \tag{3.14.f}$$

Four different boundary conditions have been considered in here.

i. Core is fully bonded to both the internal and external pipes. In this configuration, general core boundary conditions (3.14.a, b, c and d) are satisfied.

ii. Core is unbounded to the outer pipe in the tangential direction, but it is fully bonded to the inner pipe; hence, boundary conditions (3.14.a, c, d, and e) are satisfied for this configuration.

iii. Core is unbounded to the internal pipe in the tangential direction, but is fully bonded to the external pipe; hence, boundary conditions (3.14.a, b, c, and f) are satisfied for this configuration.

iv. Core can slide freely on both the internal and external pipes; hence, boundary conditions (3.14.a, c, e and f) describe this configuration.

3.7. CHARACTERISTIC EQUATION OF THE SYSTEM

Characteristic equation of the system can be presented as:

$$[K_p + K_c]\{\delta\} = 0 \tag{3.15}$$

where K_p and K_c are pipes and core stiffness matrices, respectively, as defined in Appendices A and B. In this equation δ represents the deformation of the structure in the form of a vector representing the radial and circumferential deformations of the internal and external pipes. To obtain a nontrivial solution, the determinant of the coefficient matrix must be set to zero. By solving this eigenvalue equation, the buckling pressure of the sandwich pipe is determined.

The characteristic equation of a sandwich pipe is more complex than a single pipe. Because of this complexity, the mode number that yields the lowest buckling pressure would not necessarily correspond to mode number 2. In the system under investigation,

the first buckling mode ($n = 1$) corresponds to a rigid body motion; therefore the characteristic equation must be solved for higher buckling modes.

3.8. SIMPLIFIED SOLUTIONS

A simplified solution was developed independently by Brush and Almroth [3.18] and Sato and Patel [3.8] for calculating the buckling pressure of a sandwich pipe under externally applied hydrostatic pressure, hereafter abbreviated as (SS). The SS equation is:

$$P_{cr} = P_{crs} + \frac{1}{n^2 - 1} k \tag{3.16.a}$$

where:

$$k = E_c \frac{2n(\upsilon_c - 1) - 2\upsilon_c + 1}{4\upsilon_c^2 + \upsilon_c - 3} \tag{3.16.b}$$

$$P_{crs} = \left(\frac{t_1}{r_1}\right)^3 \frac{E_p(n^2 - 1)}{\left(1 - \upsilon_p^2\right)\left(\left(\frac{t_1}{r_1}\right)^2 + 12\right)} \tag{3.16.c}$$

This equation was developed by solving the buckling pressure of a ring supported internally by an elastic foundation. This would indicate that the continuity of the shear stresses between the core and external pipe is ignored. Furthermore, the above equation was developed based on the assumption that the core can be replaced by a set of springs. The solution has been improved in this study by considering a proper stress function representing the core layer's response. In the mathematical model developed in this study, the continuity of the inter layer deformations and stresses was considered, and the characteristic equation of the system, which included the response of both core and pipes, were solved simultaneously.

In this section a set of simplified equations will be developed with the assumptions that $r_2 \to 0$ and $h_2 \to 0$, indicating that the inner portion of the system (surrounded by the external pipe) is filled entirely by the core material. It is indeed recognized that this assumption may not be entirely correct, violating the exact proportional equivalency of the inner steel pipe in terms of the core material; however, as it will be seen later, this simplifying assumption would facilitate the solution of an otherwise complex equation.

Moreover, as it will also be shown, the produced solution will be capable of generating relatively accurate results.

The above assumption enables one to establish the buckling pressure of a sandwich pipe by satisfying the following equation:

$$\lim_{R\to 0}\left\{\lim_{h_2\to 0}\left[K_p + K_c\right]\{\delta\}\right\} = 0 \tag{3.17}$$

The accuracy of the proposed simplified solution is discussed in the next sections.

3.8.1. Case A- Core layer can slide over the external pipe

Using the abovementioned simplifying assumptions, the characteristic equation of the system was solved using the Mathematica software [3.19], leading to the following equation that can be used to establish the critical buckling capacity (pressure) of a sandwich pipe whose core layer is unbounded from the external pipe:

$$P_{cr} = P_{crs} + \frac{E_c}{[2n(1-\nu_c) + 2\nu_c - 1](1+\nu_c)} \tag{3.18}$$

This equation satisfies equation (3.17), using boundary conditions II or IV.

3.8.2. Case B- Core layer is bonded to the external pipe

Using the same method, the following buckling pressure has been calculated by solving equation (3.17) with category I boundary conditions.

$$P_{cr} = \frac{\xi_1}{\xi_2} \tag{3.19.a}$$

where:

$$\begin{aligned}\xi_1 = {} & 192E_c^2 a_1 {r_1}^3\left(\upsilon_p^2 - 1\right)^2 + E_p^2 {t_1}^4 n^2 \Lambda (n^2-1)(\Lambda+7)^2 \\ & + 2E_c E_p r_1 t_1\left(\upsilon_p^2 - 1\right)(\Lambda+7)\{{t_1}^2 n^2[n(\Lambda-1) - \Lambda - 1] \\ & - 6t_1 r_1[(n+1)^2 + (n-1)^2\Lambda] \\ & - 12{r_1}^2[n(\Lambda-1) - \Lambda - 1]\}\end{aligned} \tag{3.19.b}$$

$$\begin{aligned}\xi_2 = {} & r_1\left(\upsilon_p^2 - 1\right)(\Lambda+7)\{-12E_c {r_1}^2 a_1\left(\upsilon_p^2 - 1\right)[n(\Lambda-1) - \Lambda - 1] \\ & + E_p t_1 n^2 \Lambda({t_1}^2 + 12{r_1}^2)(\Lambda+7)\}\end{aligned} \tag{3.19.c}$$

Parameter Λ in this equation is defined as:

$$\Lambda = 4\nu_c - 3 \tag{3.20}$$

Please note that for the sake of brevity the simplified solutions developed above will be referred to as the ATS, hereafter.

3.9. RESULTS AND DISCUSSION

The histogram in Figure 3.2 illustrates the number of standard and heavy wall line pipes available in the API standard [3.20]. This histogram has been generated for the API pipes with radius greater than 0.1 m, which are the most widely used range for offshore pipeline applications. As shown in this graph, the thickness to radius ratio in API pipe charts varies between 0.02 to 0.18.

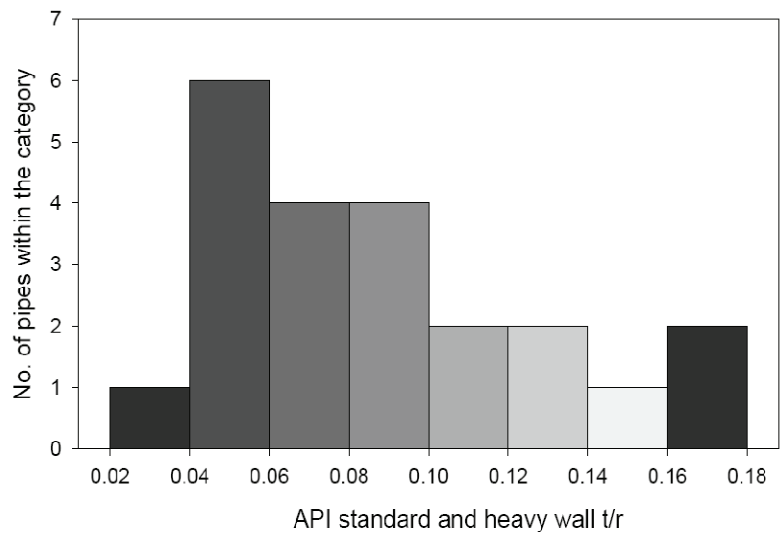

Figure 3.2. Histogram of t/r for the API Heavy and standard wall pipes with diameter greater than 0.1 m.

3.10. EXACT SOLUTION RESULTS

The ratio of the buckling pressure of an integral sandwich pipe to the buckling pressure of the external pipe of a SP system can be written as a function of the following non dimensionalized parameters:

$$\frac{P_{cr}}{P_{crs}} = f\left(\frac{E_c}{E_p}, \frac{t_1}{r_1}, \upsilon_p, \upsilon_c, n\right) \tag{3.21}$$

where P_{crs} is the buckling pressure of the external pipe, which can be calculated by equation (3.16.c). This ratio is used to present the results obtained from the proposed and the SS solutions, hereafter.

Figure 3.3 shows the variation of the buckling pressure of a sandwich pipe with respect to the change in pipe geometry (r_2/r_1) and pipe material properties (E_c/E_p) in the above mentioned practical range. As stated, the sandwich pipes' buckling pressures in these figures have been normalized with respect to that of the external pipe. These graphs have been developed for a sandwich pipe with internal and external pipe thickness to radius ratio of 0.05. In this study, Poisson's ratio of core and pipes have been taken as 0.5 and 0.3, respectively. As can be seen, the continuity of the shear stresses between pipes and core layer would significantly affect the buckling resistance of the pipe under external pressure. As expected, the fully bonded configuration provides the greatest buckling capacity in comparison to the other configurations. Moreover, the configuration in which the core layer and surrounding pipes are free to slide on one other exhibits the lowest buckling pressure. The difference between the buckling pressure of these two extreme configurations can be more than 100 times for certain values of r_2/r_1 and E_c/E_p.

Figure 3.3.a shows that for the fully bonded configuration, the buckling pressure of the sandwich pipes with a wide range of $\mathrm{r_2/r_1}$ and $\mathrm{E_c/E_p}$, does not get significantly affected by the variation in $\mathrm{r_2/r_1}$ parameter. This fact was used as the basis for driving the simplified equations based on the assumption that the equivalent structure would be a pipe (the external pipe) filled with the core material. The same conclusion can be made by considering Figure 3.3.b, for the lower range of $\mathrm{r_2/r_1}$. As also seen, buckling pressure in the other configurations is significantly dependent on the internal pipe diameter.

The other interesting results are associated to the pipe configuration in which its core and inner pipe can slide on one another. As can be seen in Figure 3.3.c, there is no consistent trend for the buckling pressure within the studied range of parameters. By comparing Figure 3.3.c and Figure 3.5.c, which illustrate the buckling mode numbers for the same configuration, it can be realized that the chaotic behavior of the graph in Figure 3.3.c is because of the oscillation in the buckling mode response of the pipe. It duly noted that the actual buckling mode response of such sandwich pipes would not be exactly the

same as what has been captured in our investigation. Indeed, the discrepancy between what has been considered as the general buckling mode shape in this study with what would happen in reality become more significant in sandwich pipes in which the core can freely slide on the internal pipe. This phenomenon is believed to be the cause the oscillation in the calculated buckling pressures corresponding to the different buckling mode shapes. It should be noted that for the sake of consistency, the logarithmic scale has been used in these figures, which indeed magnifies the chaotic trend (see also Page 10 of the revised manuscript).

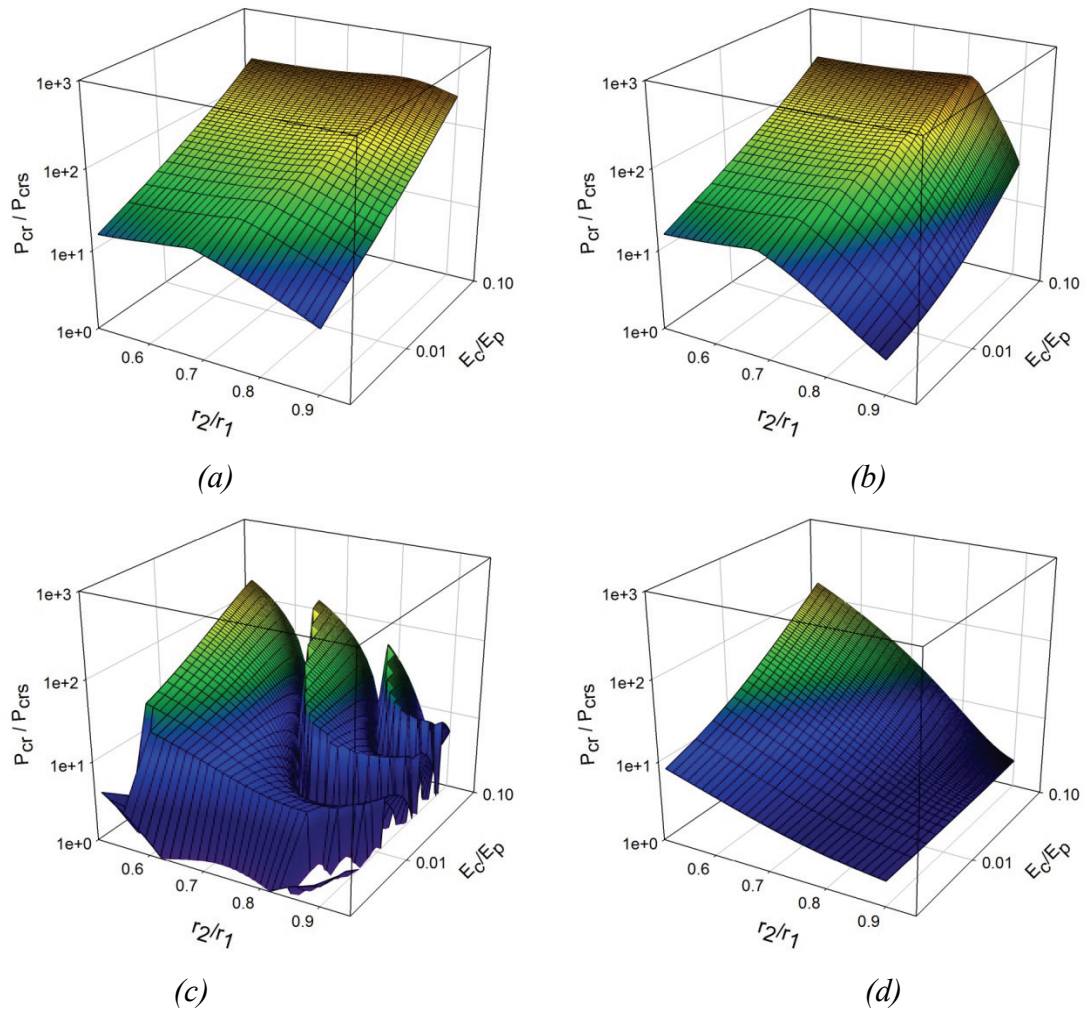

Figure 3.3. Ratio of the buckling capacity of the sandwich pipe to the external pipe as a function of geometric and material properties (a) Fully bonded (b) Core layer is disbonded from the external pipe (c) Core layer is disbonded from the internal pipe (d) Core layer is disbonded from both the internal and external pipes.

Figure 3.4 shows the variation of buckling pressure of the sandwich system as a function of internal pipe's geometry (t_1/r_1) and the pipeline material properties (E_c/E_p) within the practical range. In these figures, the $r_2/r_1$and t_2/r_2ratios have been taken as 0.8 and 0.05, respectively. These graphs show that the buckling pressure of the system is significantly influenced by t_1/r_1. Moreover, Figure 3.4.d shows that if the core layer is free to slide on both the internal and external pipes, then the increase in the core modulus of elasticity would not improve the structural performance of the pipe when subject to external pressure. For other configurations, however, the increase in the core's modulus of elasticity would increase the buckling pressure of the system.

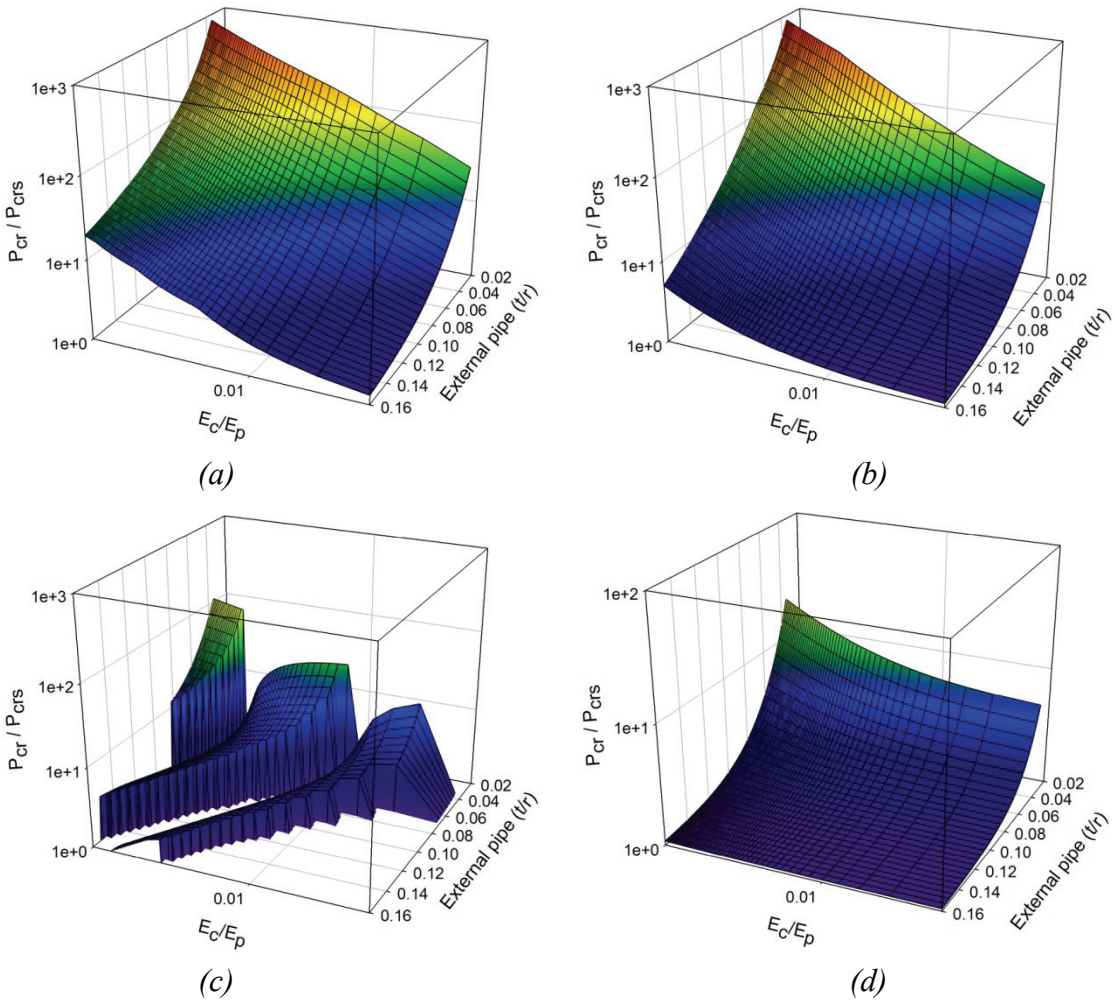

Figure 3.4. Ratio of the buckling capacity of the sandwich pipe to the external pipe as a function of geometric and material properties (a) Fully bonded (b) Core layer is disbonded from the external pipe (c) Core layer is disbonded from the internal pipe (d) Core layer is disbonded from both the internal and external pipes.

According to the results exhibited in Figures 3.3 and 3.4, in order to design an optimum sandwich pipe under external hydrostatic pressure, close attention should be paid to the bonding properties between the layers, as well as the geometrical and material related parameters like E_c/E_p, r_2/r_1 and t_1/r_1.

Figure 3.5 shows the mode number associated with the minimum buckling pressure of the SPs with various geometry and material properties. As illustrated in the figures, for the system under investigation, the buckling mode associated to the minimum buckling pressure of a sandwich pipe is not necessarily mode number 2. In fact, in most of the studied configurations, the buckling mode corresponding to the lowest capacity shifts upward as core's stiffness is increased. Figure 3.5.d shows that for the fully unbounded configuration, the corresponding buckling mode number is mode number 2 for all the studied parameters ranges. This conclusion would help to simplify the calculations significantly.

3.11. ACCURACY OF THE SIMPLIFIED EQUATIONS

In this section, both simplified solutions (i.e., Sato and Patel's and our proposed solutions) and are compared against the exact solution. The comparison is done for a sandwich system with core and pipes Poisson's ratio of 0.5 and 0.3, respectively. The percentile error is calculated by:

$$\%\,Error = \left|\frac{P_{cr(Exact)} - P_{cr(Simplified)}}{P_{cr(Exact)}}\right| \times 100 \tag{3.21}$$

Figure 3.6shows the error obtained using the SS solution (eqn. (3.16)). In this figure the buckling pressure calculated from equation (3.16) has been compared with the exact values calculated by solving equation (3.15). This graph has been generated for the first category boundary conditions (i.e., the sandwich pipes with fully bounded configuration). As seen in Figure 3.6.a, this simplified equation would produce error up to 180% for the illustrated range of parameters. Figure 3.6.b reports the margin of error for a sandwich pipe with $t_1/r_1 = 0.05$ and the internal to external pipe radius ratio of 0.8. This graph shows that the error produced by equation (3.15) for the sample pipe is at least 120% and can be as large as 200%. In conclusion, error produced by this equation increases as the core stiffness decreases and the external pipe thickness to radius ratio increases.

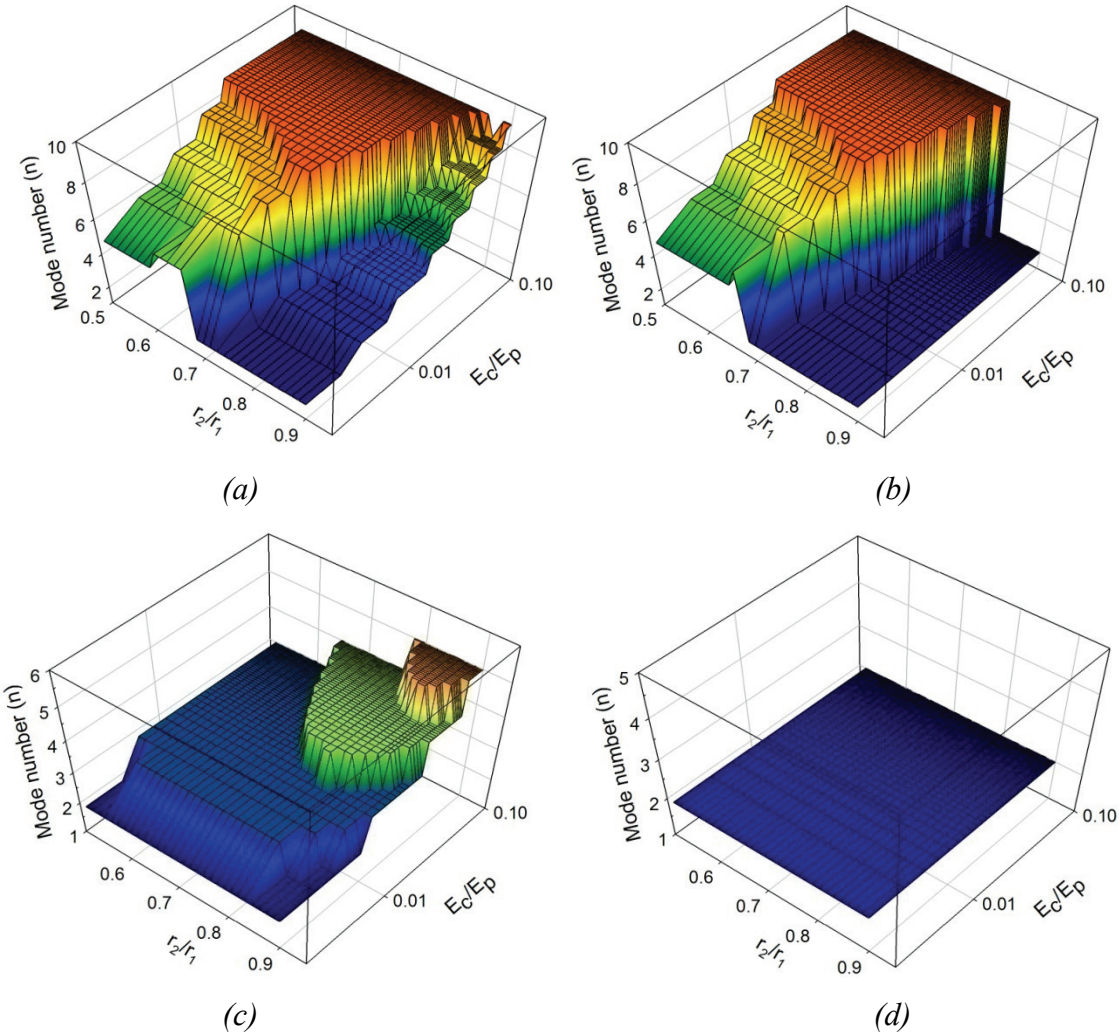

Figure 3.5. Sandwich pipe buckling mode numbers (a) Fully bonded (b) Core layer is disbonded from the external pipe (c) Core layer is disbonded from the internal pipe (d) Core layer is disbonded from both the internal and external pipes.

Figure 3.7 shows the error percentile resulting from equation (3.19) (the simplified solution developed in this study (ATS)), for the case of a fully bonded SP. As can be seen in this figure, the ATS yields more accurate results in comparison with the SS (i.e. eqn (3.16)). The SS produced a maximum error of 120%, where for the same pipe the ATS produces a maximum of 50% error in predicting the buckling pressure (the worst possible case).

Figure 3.8 shows the percentile error produced by our simplified solution in predicting the buckling pressure of the pipe with unbounded core layer to the external pipe configuration. In this figure, the exact results are obtained by solving equation

(3.15), using the second type of boundary condition (see description following eqn. (14)). As can be seen, the ATS produces very large errors for values of r_2/r_1 greater than 0.75. However, if the internal to external pipes radius ratio is smaller than 0.75, then the error would be less than 20%. In practice, most PIP systems use $r_2/r_1 < 0.75$. Therefore, the ATS (equation 3.19) would be admissible for use in practice. Figure 3.8.b shows the error percentile for a sandwich pipe with thickness to radius ratio of 0.05 and the internal to external pipe radius ratio of 0.8.

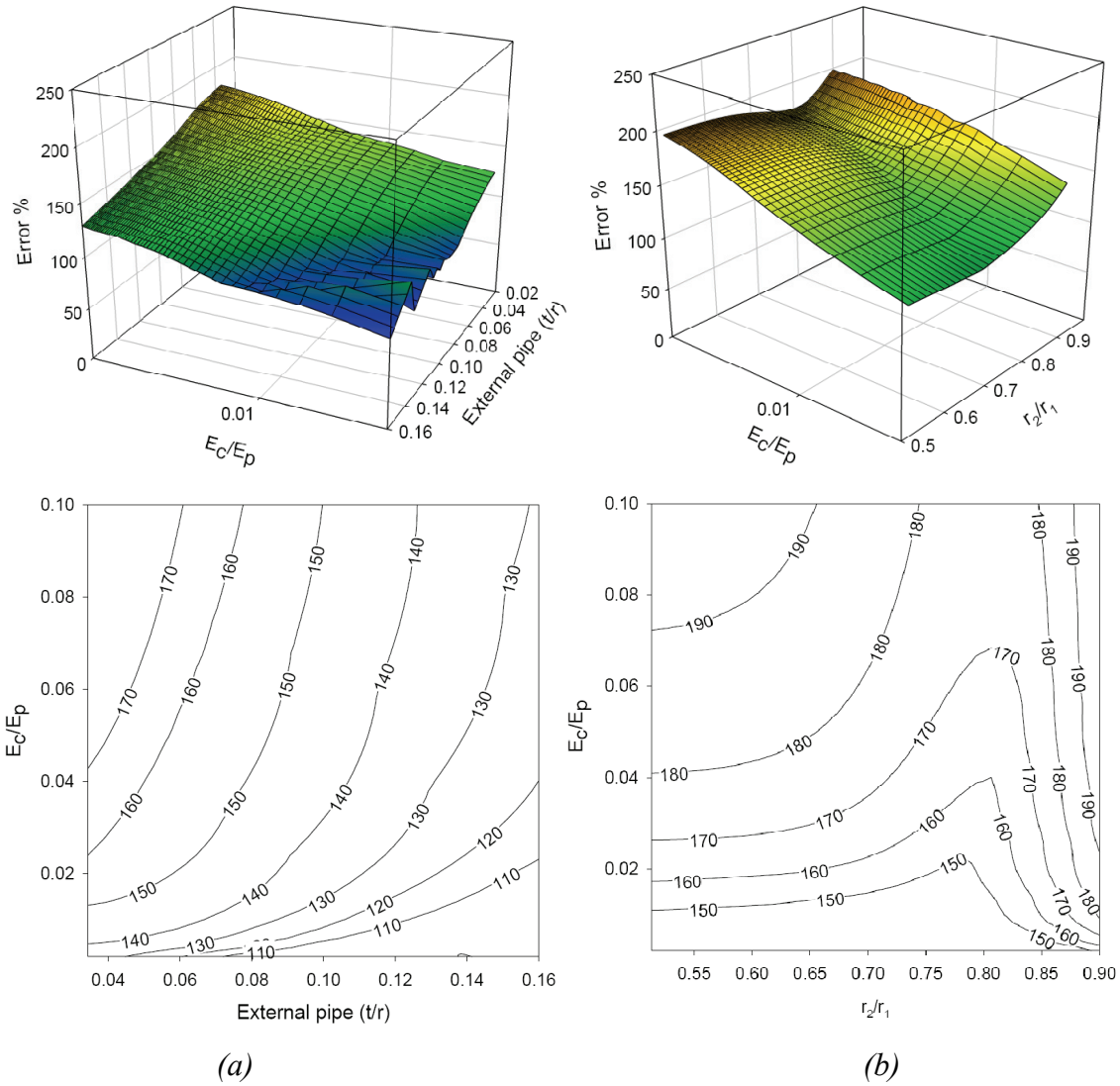

Figure 3.6. Error percentile resulting from the use of the SS [3.8,3.18] as a function of: (a) Ec/Ep and external pipe's t/r (b) Ec/Ep and r2/r1

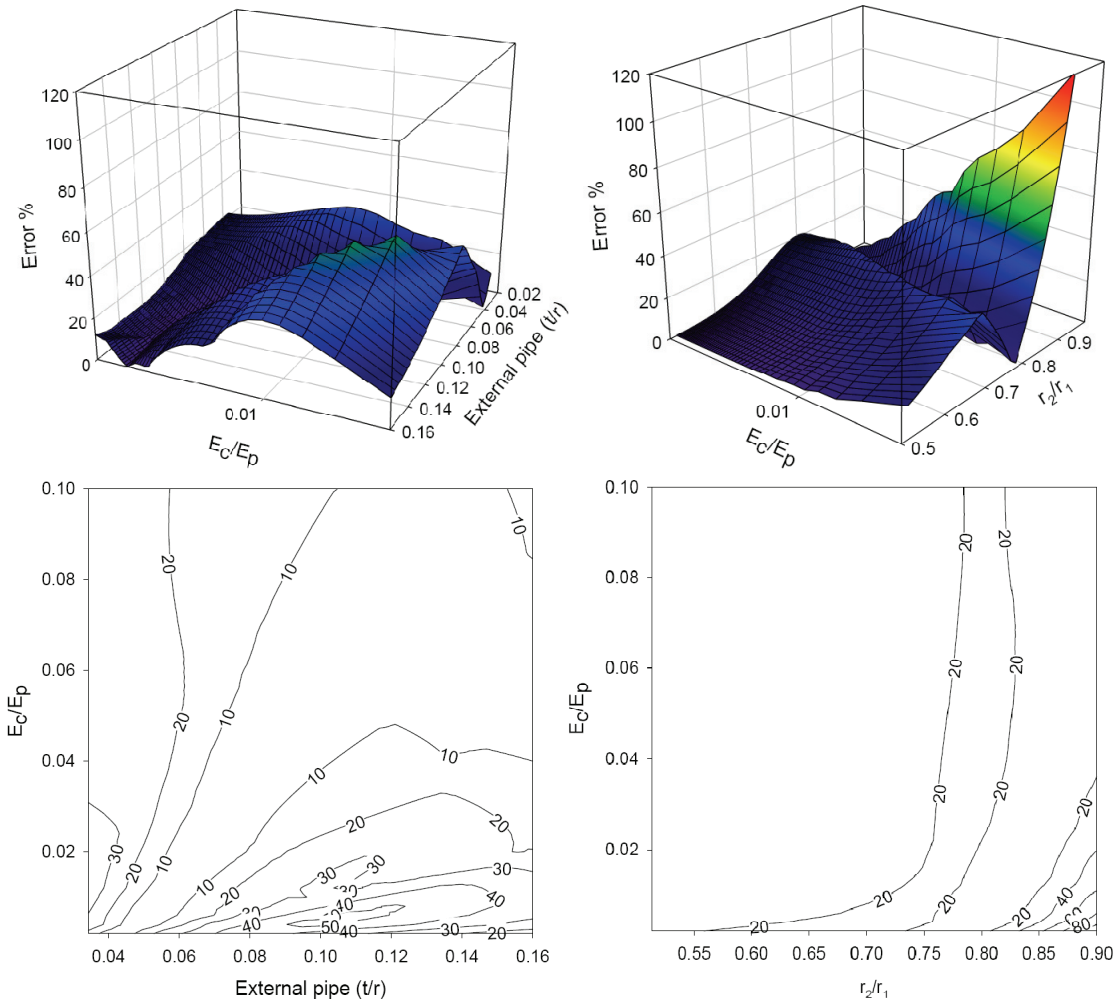

Figure 3.7. Error percentile produced by the ATS for the case of fully bonded configuration, as a function of (a) Ec/Ep and external pipe's t/r (b) Ec/Ep and r2/r1.

3.12. NUMERICAL RESULTS

In this section a series of Finite Element (FE) eigenvalue analysis are done to perform a parametric study to assess the accuracy of the proposed simplified solution. The FE software, ABAQUS standard [3.21], was used to construct and analyze the FE models. Due to the assumption of uniform structural properties and loading conditions along the length of a pipeline, a sandwich ring was modeled as the equivalent structure, to study the buckling characteristic of SP under hydrostatic pressure. The 20-node, reduced integration brick element (C3D20R) was used to construct the finite element model of the pipes. In this chapter, SP systems with incompressible core layers were

investigated to establish the margin of error produced by the solutions outlined earlier. Therefore, the core layer was modeled with the 20-node, reduced integration hybrid brick elements (C3D20RH), suited for modeling soft materials. Appropriate boundary conditions were applied to restrain the rigid body motions of the model; however, they were kept to a minimum so that the higher order buckling modes could be captured.

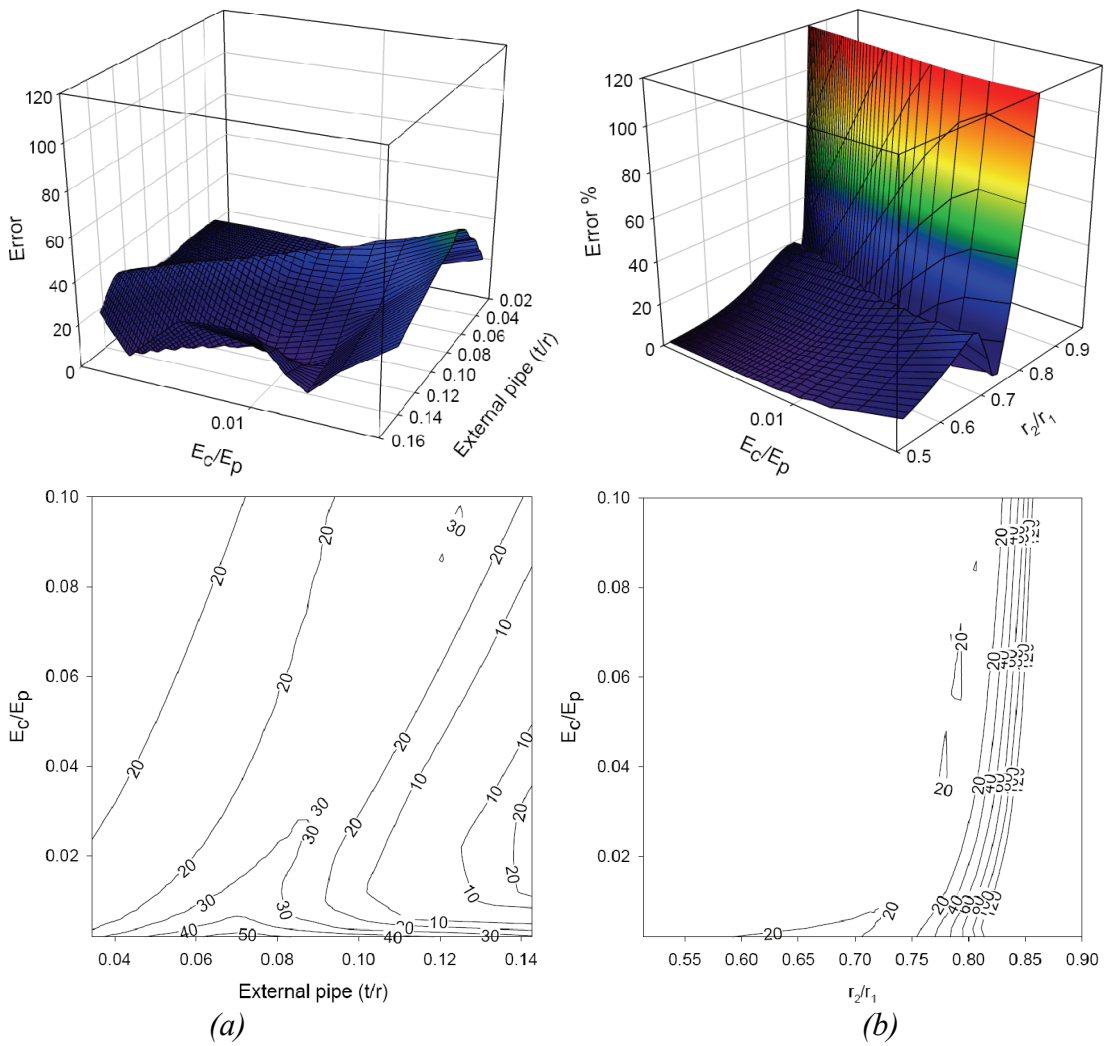

Figure 3.8. Error percentile produced by the ATS developed for the case of the external pipe sliding over the core as a function of (a) Ec/Ep and external pipe's t/r (b) Ec/Ep and r2/r1.

ABAQUS' "Tie" multipoint constraint option was used to model the fully bonded contacts between the core and internal or external pipes. However, in those

configurations in which the core layer was disbonded from the pipes, the contact mechanism was modeled using the linear two point constraint equations of the ABAQUS. With this approach, the radial displacement of the core on the contact surfaces is set to follow the radial displacement of the contacting surfaces of the pipes, but no constraint is imposed to the tangential displacements. This approach is prone to error, because the elements may intersect. To minimize this possibility, a fine mesh must be used. In this study a mesh convergence study was conducted to investigate the effect of the mesh density on the calculated buckling pressure. Figure 3.9 shows the buckling mode shapes of the four studied PIP configurations.

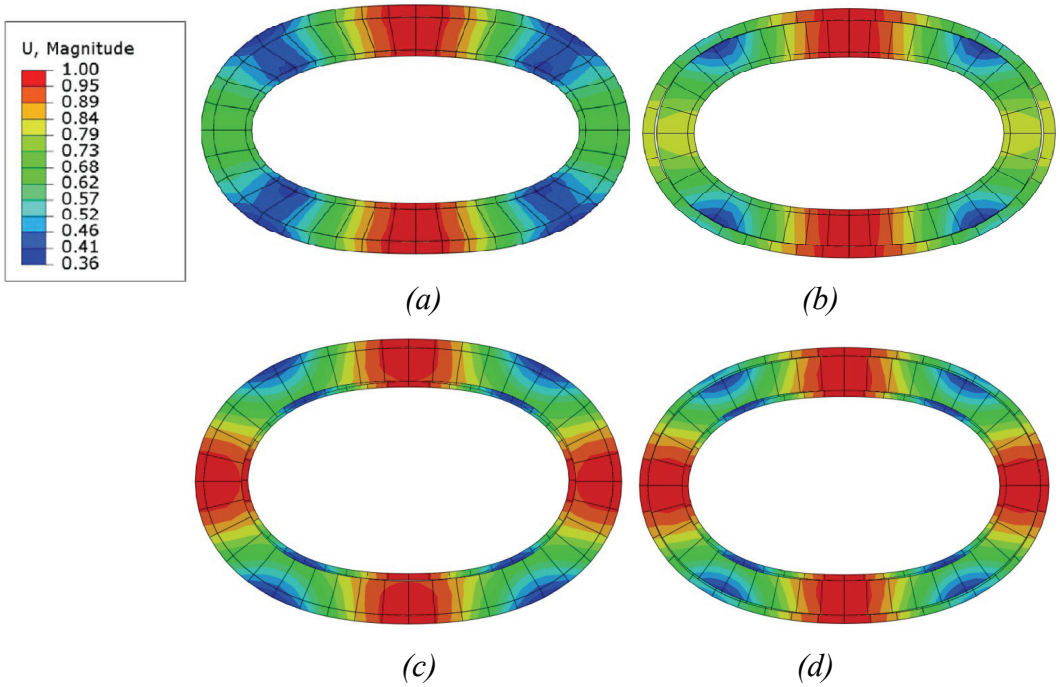

Figure 3.9. Buckling mode shape and deformation contours of the four studied PIP configurations. (a) Fully bonded (b) Core layer is disbonded from the external pipe (c) Core layer is disbonded from the internal pipe (d) Core layer is disbonded from both the internal and external pipes.

To test the integrity of the simplified solution, four sets of parametric studies were performed on the four analytically studied configurations. In each set, 1296 FE models were analyzed and the results were compared with those obtained using the simplified

solution. Figure 3.10.a presents the error percentile between the FE results and those obtained from the SS (i.e. eqn. (3.16)). As shown in this figure, the solution results in less than 50% errors for larger values of r_2/r_1. The comparison of the results obtained by the ATS simplified (eqn. 3.19) and FE is illustrated in Figure 3.10.b. As can be seen, the solution yields in a maximum error of slightly less than 50% for the smaller values of r_2/r_1. These graphs show that the either solution can predict the buckling pressure of a sandwich pipe, for a limited range of the parameters, with a reasonable accuracy.

Figure 3.10.c shows the error margins when using equation (3.18) for a SP system in which the core layer is disbonded from the external pipe. As illustrated in this figure, for E_c/E_p greater than 10^{-3}, this equation yields error greater than 60%. However, for the smaller values of E_c/E_p, which would pertain to most of the commonly used plastic materials, equation 18 would yield acceptable accuracy. It should be noted that the equations developed in this study have been found to slightly over predict the buckling pressure of the system.

Figure 3.11 shows the admissible parameter ranges for which one could use the simplified equations, expecting a margin of error to less than 50%. Also within a small range of parameters (i.e., r_2/r_1> 0.75 and E_c/E_p> 0.01), both solutions (Eqs (3.16) and (3.19)) would yield error margins greater than 50%. Therefore, in order to obtain reliable results in the noted ranges (i.e., the parameters ranges that fall within the cyan color region in Figure 3.11), it is recommended that a FE buckling analysis be conducted.

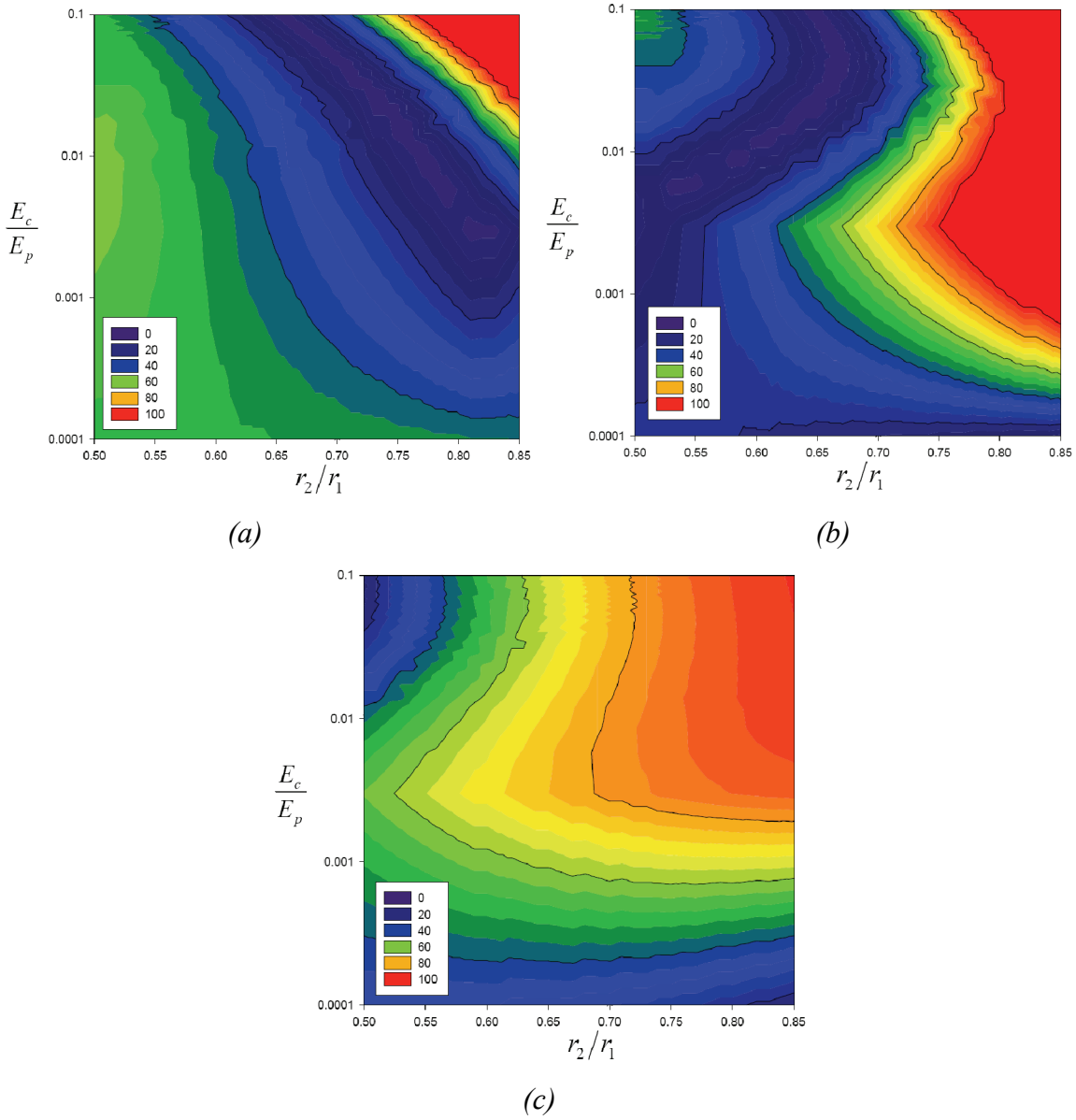

Figure 3.10. % Error produced by the simplified equations with respect to the FE results: (a) SS-Equation 3.16. (b) AST-Equation 3.19. (c) AST-Equation 3.18

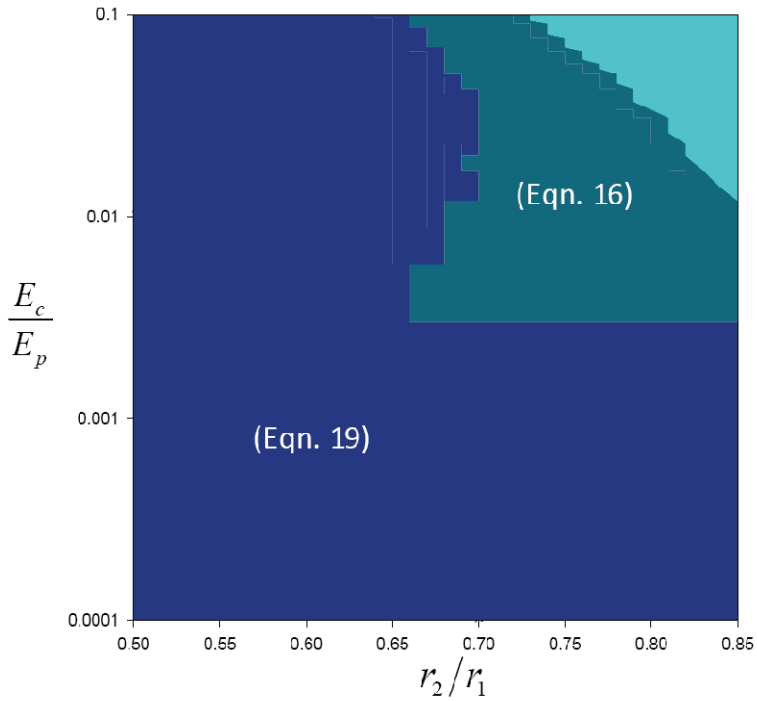

Figure 3.11. The admissible range of parameters for which each of the simplified equations can predict the buckling pressure with less than 50% errors

3.13. CONCLUSIONS

In this paper an analytical approach was used to develop the exact and simplified (approximate) solutions for evaluating the elastic buckling pressure of sandwich pipes under hydrostatic external pressure. The parameters that are required to describe the exact characteristic equation of the system were discussed in detail. Moreover, the integrity of the approximate solution produced by other researchers and that developed in this study was examined for ranges of physical and material related parameters. The practical and admissible ranges for the use of the simplified solutions were also established. Finally, the results were compared with the results obtained through an extensive series of FE parametric case studies and the accuracy of the equations was assessed. The conclusions made from this study can be summarized as:

- The contact mechanism between the core layer and the internal and external pipes would significantly affect the buckling capacity of the system.
- In contrast to a single pipe, for which the first buckling mode shape always corresponds to the second eigen mode (the 1st eigen mode would correspond to

the rigid-body mode), the same does not always hold in the case of a sandwich pipe . Therefore, to find the buckling capacity of a sandwich pipe, one should explore the higher eigenmodes.

- The results obtained from the exact solution were used to validate the assumptions made in developing the simplified solution and to establish the range applicability of the simplified solution.
- Comparison of the results obtained from the simplified solutions for the fully bonded system with those obtained from either the FE or exact analytical solutions indicated that the approximate solutions could produce reasonable accuracy for predicting the buckling capacity of the system, but for a limited range of the investigated parameters. It was shown that for stiffer core materials and greater ratios of internal to external pipe radii, the simplified solution of Sato and Patel [3.8] would yield more accurate results. However, for the other ranges, which would fall within a more practical domain for SPs with plastic core materials, the simplified solution presented in this study would predict the buckling capacity with a higher accuracy.
- The choice of any one of the simplified solutions is facilitated by the graph produced in this study. The graph can be used to gain a sense as what error margin one could expect when using the proposed simplified equation within a practical range.
- The Comparison of the results produced by the FE analyses and those obtained from the simplified solutions for the case where the core layer could slide on the external pipe demonstrated that the simplified equation (ATS) would produce large error margins within certain ranges; however, the solution would generate acceptable accuracy for SP systems with the conventionally used core materials.

3.14. REFERENCES

3.1. Kyriakides, S. and Netto, T. A. (2004). On the dynamic propagation and arrest of buckles in pipe-in-pipe systems. *International Journal of Solids and Structures, 41*(20), 5463-5482.

3.2. Kyriakides, S. (2002). Buckle propagation in pipe-in-pipe systems. Part I. Experiments. *International Journal of Solids and Structures, 39*(2), 351-366.

3.3. Kyriakides, S. and Netto, T. A. (2002). Dynamic propagation and arrest of buckles in pipe-in-pipe systems. *Proceedings of the International Conference on Offshore Mechanics and Arctic Engineering* – OMAE2002, 4, 199-205.

3.4. Kyriakides, S. and Vogler T.J. (2002). Buckle propagation in pipe-in-pipe systems. Part II. Analysis. *International Journal of Solids and Structures, 39*(2), 367-392.

3.5. Kardomateas, G. A. and Simitses, G. J. (2002). Buckling of long, sandwich cylindrical shells under pressure. *Proceedings of the International Conference on Computational Structures Technology*, 327-328.

3.6. Kardomateas, G. A. and Simitses, G. J. (2005). Buckling of long sandwich cylindrical shells under external pressure. *Journal of Applied Mechanics, 72*(4), 493-499.

3.7. Ohga, M., SanjeewaWijenayaka, A. and Croll, J. G. A. (2005). Reduced stiffness buckling of sandwich cylindrical shells under uniform external pressure. *Thin-Walled Structures, 43*(8), 1188-1201.

3.8. Sato, M. and Patel, M. H. (2007). Exact and simplified estimations for elastic buckling pressures of structural pipe-in-pipe cross sections under external hydrostatic pressure. *Journal of Marine Science and Technology, 12*(4), 251-262.

3.9. Sato, M., Patel, M. H., and Trarieux, F. (2008). Static displacement and elastic buckling characteristics of structural pipe-in-pipe cross-sections. *Structural Engineering Mechanics, 30*(3), 263-278.

3.10. Castello, X., and Estefen, S. F. (2008). Sandwich pipes for ultra deepwater applications. *Offshore Technology Conference,* Houston, Texas, USA.

3.11. Castello, X. and Estefen, S. F. (2006). Adhesion effect on the ultimate strength of sandwich pipes. *Proceedings of the 25th International Conference on Offshore Mechanics and Arctic Engineering,* OMAE2006-92481, Hamburg, Germany.

3.12. Estefen, S. F., Netto, T. A., and Pasqualino, I. P. (2005). Strength analyses of sandwich pipes for ultra deepwaters. *Journal of Applied Mechanics, 72*(4), 599-608.

3.13. Castello, X. and Estefen, S. F. (2006). Limit strength and reeling effects of sandwich pipes with bonded layers. *International Journal of Mechanical Sciences*, 49, 577–588.

3.14. Castello, X., Estefen, S. F., Leon H. R., Chad, L. C. and Souza, J. (2009). Design aspects and benefits of sandwich pipes for ultra deepwaters. *Proceedings of the 28th International Conference on Ocean, Offshore and Arctic Engineering,* OMAE2009 - 79528, Hawaii, USA.

3.15. Kyriakides, S. and Corona, E. (2007). *Mechanics of offshore pipelines* (1st ed.). Elsevier, Amsterdam.

3.16. Farshad, M. (1994). *Stability of structures*. ELSEVIER, Amsterdam.

3.17. Timoshenko, S., and Goodier, J. N. (1970). *Theory of elasticity* (3rd ed.). McGraw-Hill, New York; Toronto.

3.18. Brush DO. and Almroth, B. (1975). *Buckling of bars, plates and shells*. McGraw-Hill, New York.

3.19. Mathematica. (2008). Version 7. *Wolfram Research Inc,* IL, USA.

3.20. API SPECIFICATION 5L. (2000). *Specification for line pipe*. API Publishing Services, Washington, D.C.

3.21. ABAQUS User's and Theory Manual. (2008). Version 6.8, Dassault Systèmes, RI, USA.

CHAPTER 4
STABILITY AND POST-BUCKLING RESPONSE OF SANDWICH PIPES UNDER HYDROSTATIC EXTERNAL PRESSURE*

Kaveh Arjomandi and Farid Taheri
Department of Civil and Resource Engineering, Dalhousie University

4.1. ABSTRACT

Sandwich pipe systems can be considered as potentially optimum design configurations for overcoming the restrictions of single walled pipe being used in deep-water. This potential design alternative gained considerable attention in recent years. In this paper the stability of these systems was investigated. The possible equilibrium paths were evaluated and the effect of the various significant parameters on the characteristic behavior of the system was discussed. The Finite Element (FE) software package ABAQUS was used to construct more than 3000 FE models of the sandwich pipes with practical possible configurations. Four (4) design configurations were considered for the sandwich pipes with respect to the adhesion among the interfaces. The post-buckling behavior of each of these configurations was determined, with emphasis on a wide practical range of parameters. The behavior of these configurations is examined and the efficiency of each system is discussed. Finally, a simplified and fairly accurate equation is developed and recommended for calculating the limit pressure of sandwich pipes. The parameters of the proposed equation are also fully defined.

Keywords: Stability, Post-buckling, Pipe-in-pipe, Sandwich pipe, finite element analysis, hydrostatic pressure, simplified solution

---

* Submitted to the International Journal of Pressure Vessels and Piping.

4.2. NOMENCLATURE

imp	Imperfection magnitude
E_c	Core material elastic modulus
E_p	Pipes elastic modulus
n	Buckling mode number
P_{cr}	Sandwich pipe buckling pressure
P_{crs}	External pipe buckling pressure
r_1	Outer pipe nominal radius
r_2	Inner pipe nominal radius
r_1^o	Outer pipe initial nominal radius
r_2^o	Inner pipe initial nominal radius
t_1	Outer pipe wall thickness
t_2	Inner pipe wall thickness
Δ	Ovalization
Δr	Imperfection of the pipe radius as a function of θ
θ	Counterclockwise angle from the positive direction of X axis
v	Tangential deformation
ν_c	Core material Poisson's ratio
ν_p	Pipe material Poisson's ratio

4.3. INTRODUCTION

Day by day, the demand for various sources of energy is steadily increasing. Although new sources of energy are explored and several new energy power plants have been created, still one of the main sources of energy is the oil and gas. Having largely depleted shallow oil reserves, the extraction of deep-water oil reserves is being increasingly pursued for the world oil supply source required now and for the future. On the other hand, accessing deep-water reserves and extracting oil from there would not be possible unless effective and efficient oil transportation systems are developed. As a result, pipelines, as one of the main constituents of oil transportation systems, must be improved and new piping systems have to be developed. Single-walled steel pipe is a typical pipeline used to extract oil from typically shallow waters. However, this design configuration has a few restrictions for using in deep-water. Restrictions such as the limited external pressure capacity, high thermal conductivity and pipeline buoyancy issue during installation limit the water depth in which a single-wall pipe design configuration can be used. Sandwich pipes (SP), on the other hand, are clever design alternatives that can overcome these restrictions. In general, sandwich pipes consist of two stiffer pipes (usually steel) sandwiching a lighter weight core layer (usually a polymeric material). With such a configuration, SP can enjoy the structural and thermal insulation benefits provided by the two stiffer pipes sandwiching a core material with efficient thermal and structural properties. Moreover, the secondary containment provided by the external pipe improves the reliability of the system in case of product leakage.

SP systems can be categorized as Pipe in Pipe (PIP) systems in which the core layer has structural functionality as well as the thermal insulations role. Employing three layers in PIP systems, enables designers to design each part of the system for a specific purpose, as well as considering the whole system as an integrated structure. For example, the internal pipe (also referred to as the product pipe), can be designed based on the corrosion considerations and/or for facilitating the safe transport of the product. The core layer can have various functions; it can provide thermal insulation between the product and its surrounding environment, which is the main function of a general PIP system and/or serve as a support for internal or external pipe to resist against internal and external pressure (being the main function in a SP system). The core layer can also serve as a host

for a structural health monitoring system, as well as heating or cathodic protection systems. Based on the main function of the core layer, a wide range of materials such as plastics, gels, ceramics and composite materials can be selected as the core. The external pipe, also called the sleeve pipe, which would be in contact with the surrounding environment, must be able to resist corrosion and other structural requirements. Moreover, the secondary containment provided by the external pipe improves the reliability of the system in case of a product leak. Finally, all the three constituents can be designed as an integrated system to provide the required overall structural properties.

Designing an optimum sandwich pipe would not be possible, without a full understanding of the behavior of such a system is fully understood and the effect(s) of each part of the system on the response of the whole system. Several great works have been conducted in recent years from various perspectives to clarify the structural response of such systems under various loading and boundary conditions. The stability of a sandwich pipe can be compromised depending on the structural properties of the system and the environment under which the system is utilized. Most of the recent works investigating the structural behavior of PIPs have been conducted with the stability of the system. For example, buckle propagation phenomena is what could occurs in deep-water due to the water high external hydrostatic pressure. Many works in this area have been recently done by Kyriakides and his coworkers [4.1-4.4]. They studied the buckle propagation phenomena from analytical, numerical and experimental perspectives. Kardomateas and Simitses [4.5, 4.6] also studied the stability of long sandwich cylindrical shells under external pressure, analytically. Sato and Patel [4.7], Sato et al [4.8] and Arjomandi and Taheri [4.9] studied the buckling behavior of PIP systems under hydrostatic pressure and developed a simplified solution for estimating a PIP system's buckling capacity. Ohga et al. [4.10] studied the reduced stiffness buckling of sandwich cylindrical shells under uniform external pressure both numerically and analytically. Castello and Estefen [4.11, 4.12] and Estefen et al. [4.13] studied the feasibility of a sandwich system for deep water applications with both numerical and experimental approaches. In their investigations, they considered the behavior of sandwich pipes under various loading conditions. Furthermore, several other works have been done by other researchers in numerical modeling of a sandwich pipe considering various parameters,

and loading and boundary conditions, which for the sake of brevity, they are not been mentioned in here.

One of the main restrictions of the available analytical solutions is the use of shell theories for developing the characteristic equation. Even though shell theories yield less complicate equations, they are not however, practical for use in considering thick core layers. On the other hand, improving the analytical solution by adding more degrees of freedom to the equations is not feasible due to the complexity of the problem. In addition to the aforementioned restrictions, to reach simplified equations several assumptions must be made, which in turn would affect the accuracy of the final equations.

In this paper a practical solution is proposed through solving the problem with the Finite Element (FE) method. In summary, a series of finite element parametric studies were performed to study of effect of the parameters that would significantly influence the behavior of sandwich pipes under hydrostatic external pressure. Using the results of more than 3000 FE models, a set of simplified practical equations was established. The parameters used in the solution are defined for four different pipe configurations, accounting for the interaction properties between core layer and surrounding pipes.

4.4. MOTIVATION AND THE THEORY

Sandwich pipes used in oil and gas industry are long, circular cylindrical structures consisting of a core layer surrounding by two steel layers. Due to the structural configuration and uniform loading, studying the behavior of a sandwich pipe under hydrostatic external pressure can be considered as a 2-D problem in the polar coordinates. Figure 4.1shows the idealized geometry of such a system as well as the main geometric parameters.

Due to the interaction between the layers, understanding the behavior of a sandwich pipe under external hydrostatic pressure through an analytical solution is a complex task. Brush and Almroth [4.14] and Sato and Patel [4.7] proposed an analytical solution for this problem by simplifying the problem and finding the buckling pressure of a ring supported internally by an elastic foundation. They proposed the following equation:

$$P_{cr} = P_{crs} + \frac{1}{n^2 - 1} k \tag{4.1.a}$$

where:

$$k = E_c \frac{2n(\upsilon_c - 1) - 2\upsilon_c + 1}{4\upsilon_c^2 + \upsilon_c - 3} \tag{4.1.b}$$

$$P_{crs} = \left(\frac{t_1}{r_1}\right)^3 \frac{E_p(n^2 - 1)}{\left(1 - \upsilon_p^2\right)\left(\left(\frac{t_1}{r_1}\right)^2 + 12\right)} \tag{4.1.c}$$

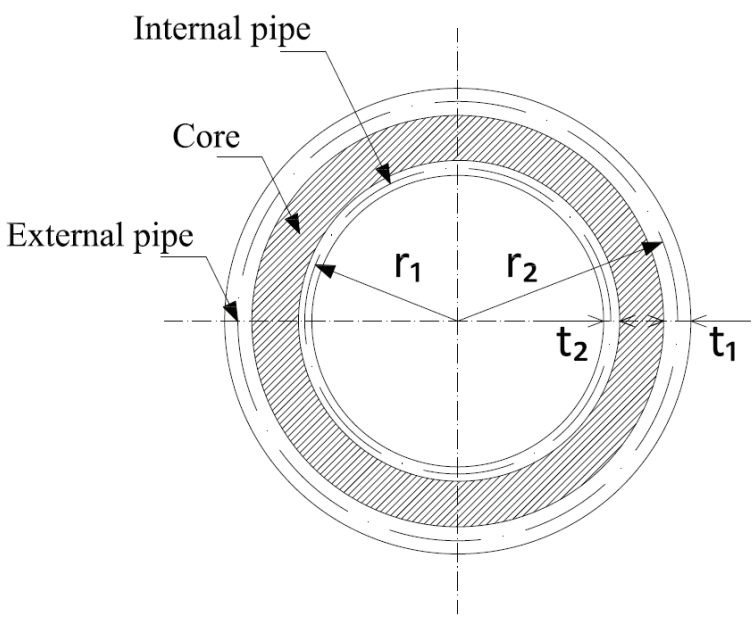

Figure 4.1. Idealized geometry of a sandwich pipe.

Subsequent studies have shown that the above solution would yield large error margins when applied to practical pipeline design. A study conducted by Arjomandi and Taheri [4.9] showed that the margin of error produced by the above equation for sandwich pipes with $E_c/E_p < 0.003$ or $r_2/r_1 < 0.65$ was greater than 50% in comparison to the buckling Eigen value results obtained through finite element analysis. It should be noted that the aforementioned range of parameters include a considerable range of design configurations. One reason for the discrepancy is due to the large number of simplifying assumption used in developing the equation. For instance, one of the main assumptions is replacing the core layer and internal pipe with an elastic foundation with equivalent stiffness. Other assumptions, such as the use of Sander's shell theory for

developing the characteristic equations of the system further reduces the accuracy of the results for some design cases.

To improve the accuracy Arjomandi and Taheri [4.9] developed a solution using fewer simplifying assumptions. In their solution the characteristic equation of the system was developed based on considering the effect of the external pipe, the internal pipe and core layer separately. Furthermore the adhesion behavior between the layers was also considered. Although the solution produces more accurate results for pipes with relatively soft or thick core materials, it cannot produce reasonable accuracy for all design cases. According to the proposed solution, for the design case where the core layer is bonded to the surrounding pipes, the buckling pressure of the sandwich system can be calculated using the following simplified equation [4.9]:

$$P_{cr} = \frac{\xi_1}{\xi_2} \tag{4.2.a}$$

where:

$$\begin{aligned}\xi_1 = {} & 192E_c^2 a_1 {r_1}^3 \left(\upsilon_p^2 - 1\right)^2 + E_p^2 {t_1}^4 n^2 \Lambda (n^2 - 1)(\Lambda + 7)^2 \\ & + 2E_c E_p r_1 t_1 \left(\upsilon_p^2 - 1\right)(\Lambda + 7)\{{t_1}^2 n^2 [n(\Lambda - 1) - \Lambda - 1] \\ & - 6t_1 r_1 [(n+1)^2 + (n-1)^2 \Lambda] - 12{r_1}^2 [n(\Lambda - 1) - \Lambda - 1]\}\end{aligned} \tag{4.2.b}$$

$$\begin{aligned}\xi_2 = {} & r_1 \left(\upsilon_p^2 - 1\right)(\Lambda + 7)\{-12E_c {r_1}^2 a_1 \left(\upsilon_p^2 - 1\right)[n(\Lambda - 1) - \Lambda - 1] \\ & + E_p t_1 n^2 \Lambda ({t_1}^2 + 12{r_1}^2)(\Lambda + 7)\}\end{aligned} \tag{4.2.c}$$

where $a_1 = r_1 - t_1/2$ and$a_2 = r_2 + t_2/2$ and parameter Λ is defined as:

$$\Lambda = 4\nu_c - 3 \tag{4.3}$$

Equation 4 shows another simplified equation proposed in that study for the cases where core layer can freely slide on the external pipe.

$$P_{cr} = P_{crs} + \frac{E_c}{[2n(1 - \nu_c) + 2\nu_c - 1](1 + \nu_c)} \tag{4.4}$$

As can be noted, the complexity and inaccuracy produced by the above-noted solutions still limit their application for all practical cases. In this paper, therefore, a new solution has been developed and proposed to further improve the accuracy. Using the FE method the characteristic equations of the system is solved by modeling a sandwich pipe consisting of all three layers; further, there exist no limitation on the thickness of the

pipes or core layer. Finally, a series of equations are proposed that can characterize stability of sandwich pipes having various bonding scenarios among their layers, fairly accurate.

4.5. BEHAVIOR OF A SANDWICH PIPE UNDER HYDROSTATIC EXTERNAL PRESSURE

The stability analysis of a structure can be analyzed by establishing the characteristic equations of the system and solving the equations to find the equilibrium paths of the system. If the equilibrium path of the structure is calculated based on the equilibrium of an undeformed geometry, it is referred to the "first-order theory". For the purpose of pipe stability analyzes under hydrostatic external pressure this theory is capable of predicting just the primary equilibrium path of the pipe. A more advanced theory considers the deformed geometry as well as the nonlinearities through a small deformation theory. This theory is called the "second-order theory" and is capable of predicting the bifurcation point of the equilibrium paths. Most of the analytical approaches proposed thus far for studying the stability problem of a pipe under hydrostatic external pressure use the later theory. Therefore, none of the former analytical approaches are capable of predicting the secondary equilibrium path of the pipe. However, primary and secondary equilibrium paths are just mathematical concepts and cannot be used to predict the post-buckling behavior of an imperfect pipe in real cases. The most advanced theory considers large deformations of a deformed geometry and is referred to the "third-order theory". This theory is capable of predicting both primary and secondary paths as well as the bifurcation point. Nonlinear FE analyzes of an imperfect pipe can be categorized within this theory. However, FE post-buckling analysis cannot calculate the mathematical primary and secondary equilibrium paths of a perfect pipe, but it can predict the equilibrium path of the pipe with a given small magnitude of imperfection which is generally fairly close to the perfect primary and secondary paths.

Figure 4.2 shows the typical schematic equilibrium paths of a sandwich pipe under hydrostatic external pressure. As mentioned above, the "first-order theory" can only predict the path OA shown in the figure. This is a similar result to that predicted by FE static analysis of a perfect pipe. Through the "second-order theory" one can establish

point A, which is the bifurcation point. This value is referred to as the buckling pressure of the pipe. Knowing this point, the behavior of the pipe can be divided into two parts, path OA which is the prebuckling regime and path AB which is the post-buckling regime. By this theory, a slight disturbance on a pipe being under buckling pressure would lead to a finite deformation of the pipe. The stability analysis of a system through the "second-order theory" yields a set of Eigenvalue equations; therefore, the buckling pressure calculated through this theory is referred to as the Eigenvalue buckling pressure of the system. As stated, the most accurate behavior can be captured through the "third-order theory". By this theory the pipe's response follows the primary equilibrium path (OA) up to the buckling pressure. Upon reaching the bifurcation point, the system would subscribe to the condition corresponding to its minimum total energy; therefore, the equilibrium state follows the secondary path (AC). In this study, the post-buckling behavior of imperfect pipes, following the path AD in the figure, is of interest. This secondary equilibrium path can be captured by static analysis of a pipe when the imperfection magnitude approaches zero.

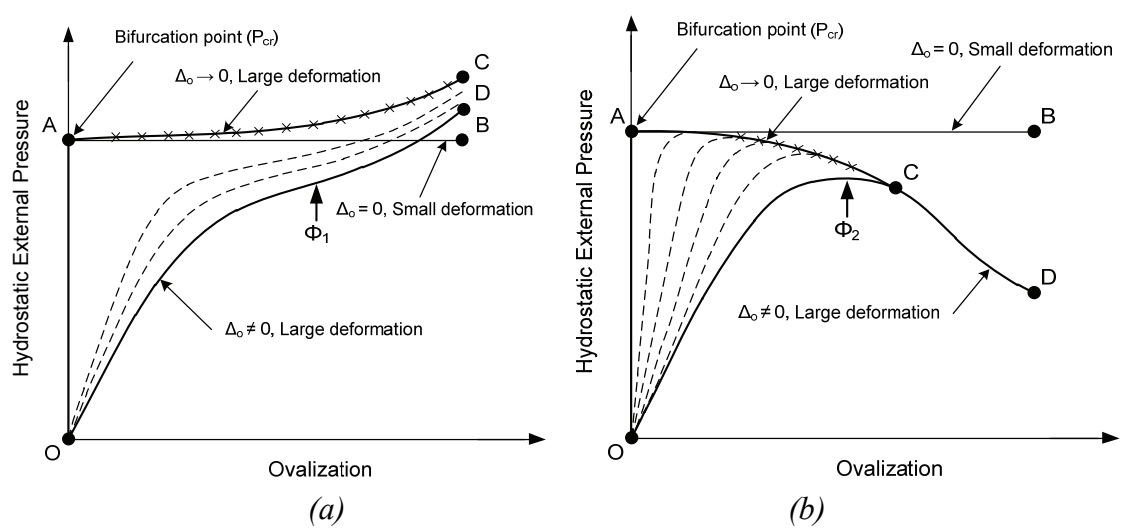

Figure 4.2. Schematic of sandwich pipe characteristic paths. (a) for pipes with stiffening response after buckling; (b) for pipes with softening response during their post-buckling.

As illustrated in Figure 4.2.a and 4.2.b, depending on geometrical and material properties, the behavior of sandwich pipes under hydrostatic external pressure would be classified into two categories.

i. The first category consists of pipes that no maximum value for their equilibrium paths can be established. In the other word, no maximum limit pressure can be calculated for this class of pipes. Typical characteristic path of this class of pipes is illustrated in Figure 4.2.a. The pressure capacity of this category of pipes increases after pipe ovalizes, and as the ovalization increases. Characteristic path of such pipes can be divided into three segments. First the pipe deforms with an almost constant stiffness up to a buckling limit point, after which larger deformations cause the decrease in the overall stiffness of the system. Afterward, the stiffness of the system keeps decreasing significantly up to a limit point of which the pipe gains additional stiffness. It is found that the magnitude of the external pressure at the inflection point of the characteristic path, in which the sign of the second derivative of the characteristic path changes, would be a good representation of the characteristic path of this class of pipes. Furthermore, this limit is close to the buckling pressure calculated using the Eigen value buckling analysis. It should be noted that the results are evaluated for elastic buckling cases. It is obvious that after the semi plateau regime, due to the large deformations, material's plasticity response will change the characteristic path and the plastic instability would ensue. Therefore, quantifying this plateau section would also help to study the plastic instability response of a sandwich pipe. This characteristic point is identified as Φ_1 in Figure 4.2.a and will be referred to as the Characteristic Path Inflection Point (CPIP), hereafter.

ii. The second class of sandwich pipes would behave practically like a single wall pipe [4.15]. The typical equilibrium paths of this category of pipes are shown in Figure 4.2.b. They would have a constant stiffness in the initial steps of the loading. As the load in increased further, stiffness would start decreasing up to a limit point; this point is labeled as Φ_2 in the figure. By reducing the imperfection magnitude of the pipe to zero, this limit point would tend to locate on the secondary equilibrium path which is identified by curve AC in the figure. After

the limit point, the rate of changing of stiffness of the pipe takes a negative trend and the system becomes unstable. It should be noted that by decreasing the magnitude of imperfection of the pipe, (i.e., structure's geometry approaching a perfect shape) the magnitude of Φ_2 would become closer to the buckling pressure obtained through an Eigen value analysis.

4.6. FINITE ELEMENT MODELS

In this study a series of Finite Element parametric models were developed and analyzed for simulating the behavior of sandwich pipes under external hydrostatic pressure. Because all the structural properties, loading and boundary conditions were assumed to be uniform along the pipe's length, this problem was considered as a quasi 2-D plane strain problem. A typical FE model created for this problem is presented in Figure 4.3.

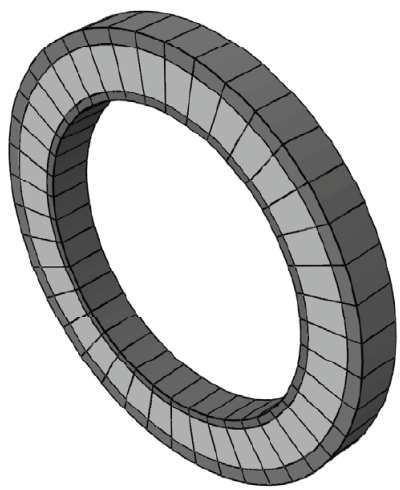

Figure 4.3. Geometry of the FE model.

The finite element software, ABAQUS standard, was used for creating and analyzing the FE models [4.16]. Element C3D20R, which is a 20 nodes quadratic brick element with reduced integration was used to build the FE models. The response of the elements modeling the core layer was improved by adopting the hybrid version of the same element (i.e. the case of an incompressible core material). Mesh convergence studies showed that the FE mesh with one through thickness element for each layer and 40 elements in circumferential direction was adequate for creating an effective mesh and obtaining accurate results for studied range of parameters.

To perform a post-buckling analysis, a geometric imperfection has to be included in the system. In reality no fully perfect system exists, and usually the structure suffers from a source of imperfection. Imperfection could exist in the form of imperfection in geometry, shape and magnitude of loading and/or boundary conditions. In this study geometrical imperfection has been considered of an initial ovality shape, which is one of the dominant types of imperfections in practice. In mathematical form this imperfection is defined as:

$$\Delta r_i = imp \times r_i^o \cos 2\theta \quad , \quad i = 1,2 \tag{4.5}$$

where imp is an arbitrary value signifying the amplitude of imperfection. By this equation the geometrical imperfection is applied to core layer, internal and external pipes, with the same magnitude and shape. Figure 4.4 illustrates the form of the geometrical imperfection that has been considered in this study. The imperfection magnitude in this figure is magnified by 30 times of that of typical models investigated in this study.

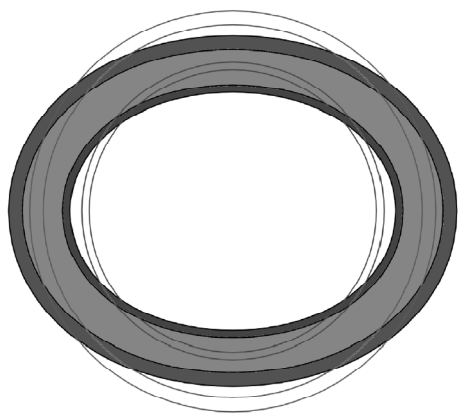

Figure 4.4. Geometrical imperfection applied to the FE model

Moreover, a minimum number of boundary conditions was defined to prevent the models' rigid body motions. It should be noted that the boundary conditions may restrict the deformation of the system for some higher buckling modes. The applied boundary conditions restrict any type of rigid body motions, but the pipe is free to deform into its preferred first buckling mode shape. However the form of the geometrical imperfection applied to the models is more similar to the expected first buckling mode, which is of practical interest in practical design. Therefore, the applied boundary conditions should not cause any inaccuracy.

Two techniques were adopted in modeling the interaction between the core layer and surrounding pipes. For those cases that the core layer was assumed to be bonded to the internal or external pipes, the nodes located at the interfacing surfaces were tied together using the Multi Point Constraint (MPC) function. In the second technique, the linear penalty method was used to model the interaction properties in those cases that the core layer was permitted to slide or separate from the internal or external pipes. The interface was therefore defined as surface to surface contact with finite sliding formulation. The penalty stiffness was set to 10 times of the representative underlying element stiffness.

4.7. CHARACTERISTIC PARAMETERS

The buckling pressure of sandwich pipes is a function of the pipeline geometrical and material properties. Equation 4.6 represents the characteristic parameters of a sandwich pipe.

$$P_{cr} = f\left(E_c, E_p, t_1, r_1, t_2, r_2, \upsilon_p, \upsilon_c, imp\right) \tag{4.6}$$

The analytical simplified equations (Eqn. 1, 2) and our earlier simplified closed form solutions [4.9] indicate that equation 4.6 can be rewritten in the following dimensionless equation:

$$\frac{P_{cr}}{E_p} = f\left(\frac{r_2}{r_1}, \frac{t_1}{r_1}, \frac{t_2}{r_2}, \frac{E_c}{E_p}, \upsilon_p, \upsilon_c, imp\right) \tag{4.7}$$

In this study the characteristic response of the sandwich pipe is defined on the basis of the ovalization of its external pipe. The following parameter is defined to capture the ovalization:

$$\Delta = \frac{r_1 - r_1^o}{r_1^o} \tag{4.8}$$

Figure 4.5 and 4.6show the influence of the variation of the selected parameters on the post-buckling behavior of a set of sandwich pipes used in practical design cases, in which the core layer is assumed to be bonded to both internal and external pipes. The imperfection magnitude in all cases was assumed to be $imp = 0.5\%$.

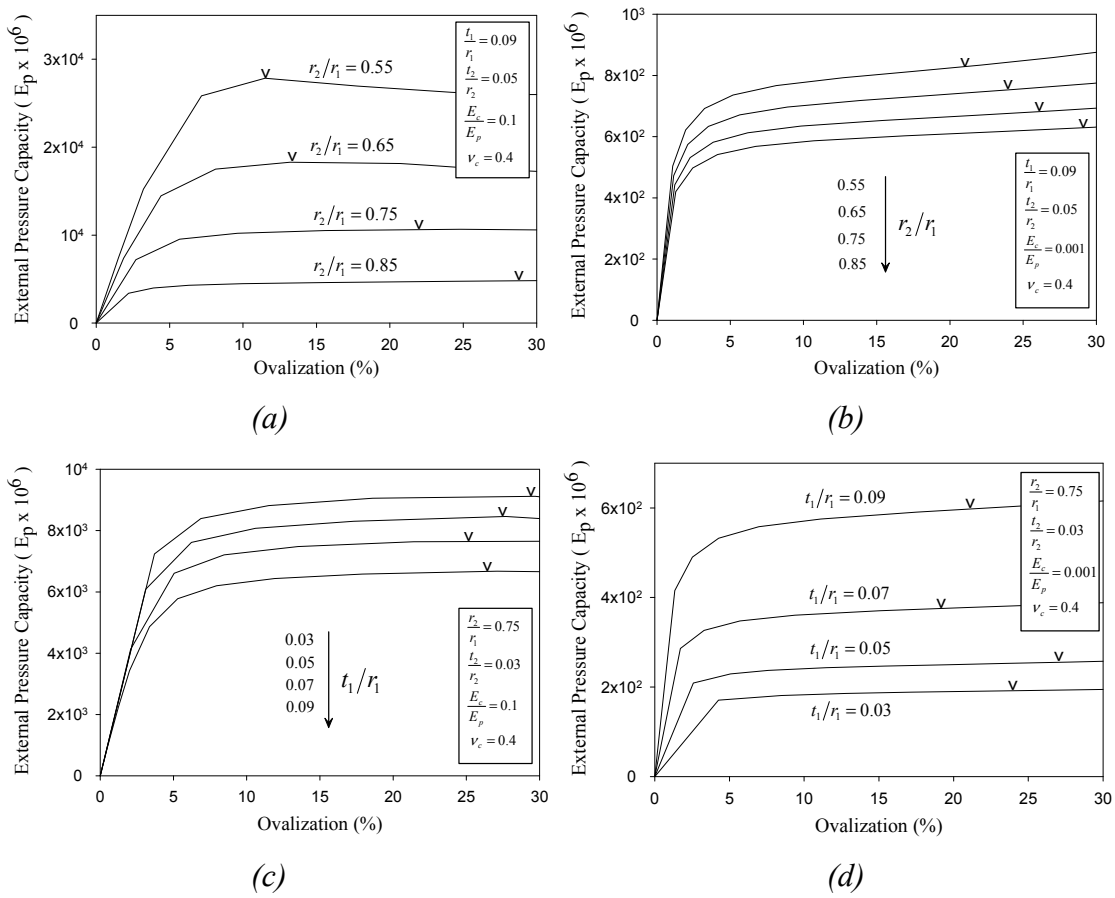

Figure 4.5. Effect of the characteristic parameters on the post-buckling behavior of sandwich pipes

Figures 4.5.a and 4.5.b show the influence of r_2/r_1 on the response of a set of sandwich pipes with two different core materials. Figure 4.5.a shows the characteristic equilibrium path for a set of sandwich pipes with a relatively stiff core material, while Figure 4.5.b shows the response of similar pipes but with a softer core. The limit of stability in the first category of pipes, or the CPIP point for the second category is identified in the figures by symbol 'V'. As expected, increasing the thickness of the core layer in sandwich pipes would significantly increase their buckling pressure capacity. Moreover, it is found that increasing the thickness of the core layer would decrease the ductility of the structure before reaching to buckling pressure. Comparison of the two series of pipes shows that the pipes with the Limit Equilibrium Instability (LEI) exhibit less ductility before reaching to the limit point. As a result, it can be concluded that the second category of sandwich pipes in this study are most likely to undergo linear type

buckling instability. On the other hand, the first series of pipes tend to undergo nonlinear buckling instability due to the plastic deformation.

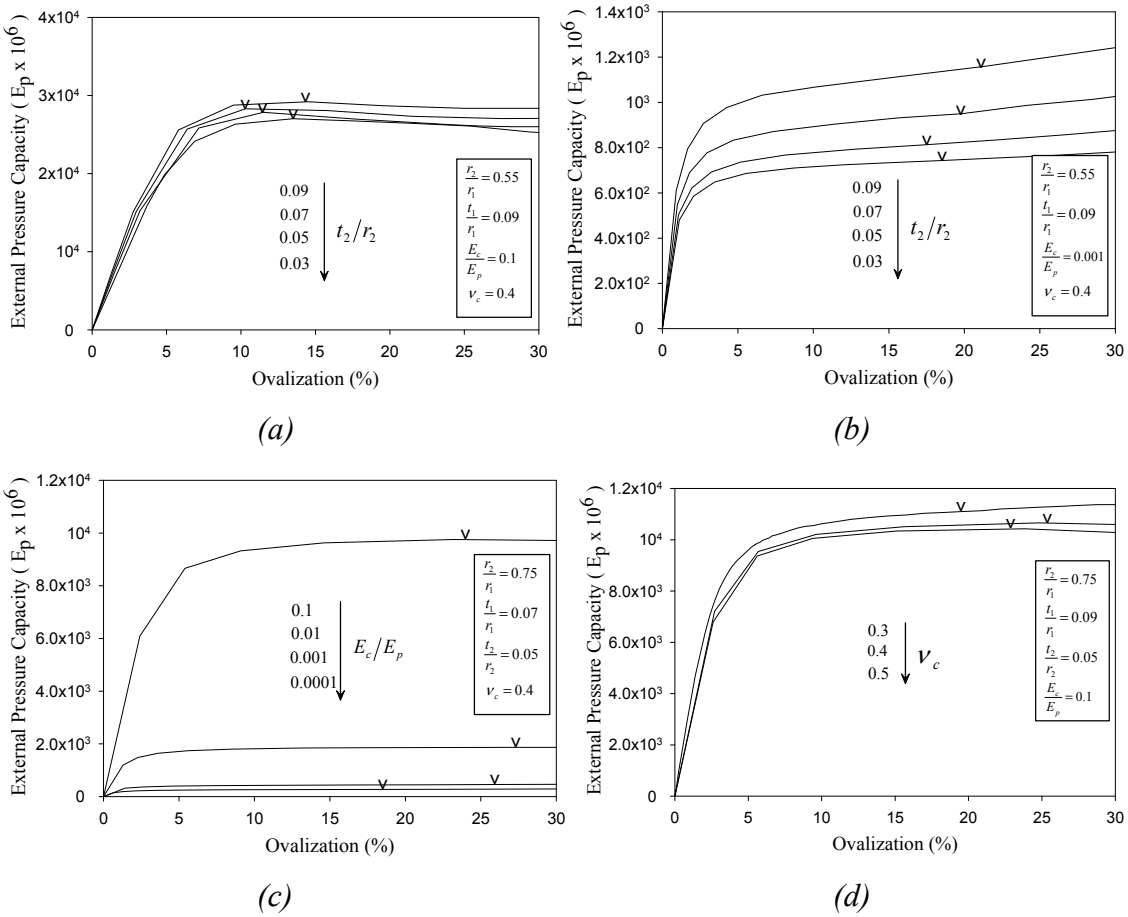

Figure 4.6. Effect of the characteristic parameters on the post-buckling behavior of sandwich pipes

Figures 4.5.c, 4.5.d, 4.6.a to 4.6.d illustrate the influence of t_1/r_1 and t_2/r_2 on the characteristic path of a set of sandwich pipes. As expected, by increasing the wall thickness of either internal or external pipes, the pressure capacity of both series of pipes increases. The magnitude of the increased capacity is dependent on the other properties of the pipe. In cases that the core material is stiffer, which exhibits limit equilibrium instability, the effect of change in t_1/r_1 and t_2/r_2 on the buckling capacity is less than those pipes with softer core materials. Figure 4.6.a shows the change in the characteristic trend in sandwich pipes with a relatively stiff core as a function of change in the internal pipe wall thickness. As can be seen in this figure, variation of t_2/r_2 does not have a

significant influence on the characteristic path. This fact has been used as an assumption in developing simplified analytical solutions by several researchers (see Brush and Almroth [4.14], Sato and Patel [4.7] and Arjomandi and Taheri [4.9]). Nevertheless, the results shown in Figure 4.6.b indicate that this assumption would not be admissible in pipes with a softer core material.

Finally, the influence of core stiffness and its Poisson's ratio are illustrated in Figures 4.6.c and 4.6.d As can be seen from the limit pressure points marked on the figures, the stiffer the core, the higher the pressure capacity. On the other hand the variation in Poisson's ration of the core material does not significantly alter the pressure capacity; in fact, a minor increase in the capacity could be observed as a function of the decrease in Poisson's ratio.

One of the characteristic parameters of a sandwich pipe is the magnitude and form of the imperfection of the pipe geometry. As stated earlier, in this study the geometric imperfection is considered as an initial ovality of the internal and external pipes, with both pipes' ovality mode being in the same direction. This form of imperfection is a typical mode of imperfection in pipelines. Moreover, this initial ovalization intensifies the first buckling mode shape in the system, which is the more probable buckling mode shape in reality.

API [4.17] restricts the maximum tolerance in diameter of pipe's with diameter in the range of 60.3 to 508 mm to 0.75% of the specified outside pipe diameter for either seamless or welded pipes. Considering this criterion, the effect of the initial ovality imperfection with the value up to 1.5% has been studied here.

Figure 4.7 illustrates the characteristic behavior of two sets of sandwich pipes, again with two different core materials. The variation in the core stiffness, in these two sets of designs influence the pipe's capacity and post-buckling response. Figure 4.7.a shows the characteristic path of a sandwich pipe in which the core material elastic modulus value is 0.001 of the pipe's material elastic modulus. In this case the pipe behaves stably for all the ovality amplitudes considered here. However, pipes with greater magnitude of imperfection behave more ductile before reaching to the CPIP pressure. Figure 4.7.b shows the characteristic path of the same set of pipes with a stiffer core material. As can be seen the response of this set of pipes is similar to the second set of sandwich pipes

which become instable after reaching the external pressure limit. The limit points are identified in the figure by symbol 'v'. Similar to the other pipe series, increasing the imperfection magnitude would enhance the ductile response of the pipes before reaching to the limit load. For this category of sandwich pipes, the variation in imperfection would influence the limit pressure more significantly in comparison to the first category. It is concluded that the considered range of imperfection (i.e., $0\% \leq \Delta_o \leq 1.5\%$) would not significantly alter the response of the pipes.

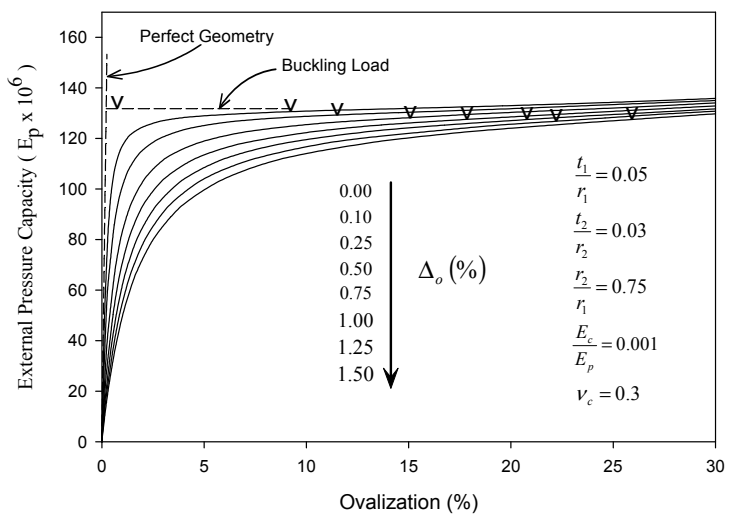

(a)

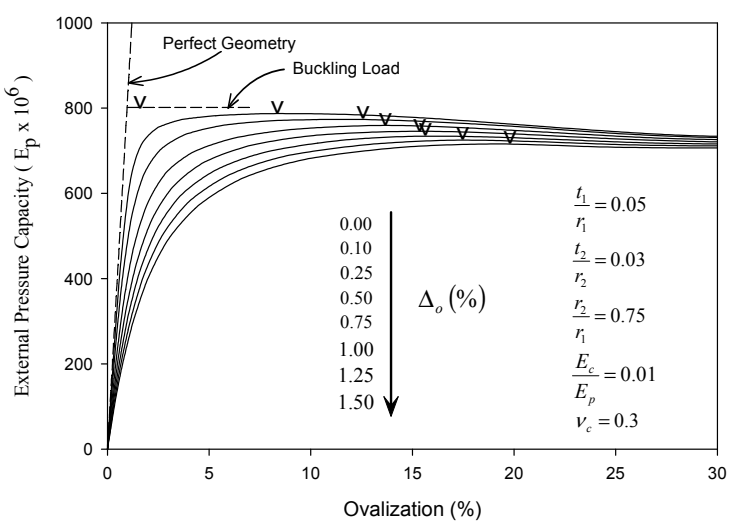

(b)

Figure 4.7. Pressure-Ovalization responses for sandwich pipes with various imperfections magnitude. (a) pipes with stiff core, (b) pipes with softer core.

4.8. PARAMETRIC STUDIES

In this investigation a series of finite element parametric studies was also conducted to study the influence of certain characteristic parameters on the response of the sandwich pipes under uniform hydrostatic external pressure. Table 4.1 shows the studied parameters and their range. The selection of the ranges is based on the practical engineering design cases.

Table 4.1.The parameters considered in the parametric study and their range

Parameter	r_2/r_1	t_1/r_1	t_2/r_2	E_c/E_p	ν_c
Range	0.55-0.85	0.03-0.09	0.03-0.09	0.0001-0.1	0.3-0.5

The pipe wall thickness to radius ratio parameter range has been chosen based on the API standard-wall threaded linepipe dimensions [4.17]. Imperfection magnitude and the surrounding pipes Poisson's ratio are kept constant, with the values of 0.5% and 0.3, respectively.

Four different design configurations, identifiable based on the interaction mechanism between the core layer and surrounding pipes, have been considered here. These configurations are:

i. The core is fully bonded to both the internal and external pipes. Figure 4.8.a shows the typical deformation of this type of pipes.
ii. The core is disbonded from the outer pipe in the tangential direction, but it is fully bonded to the inner pipe. In this case the outer pipe and core can separate from each other in the normal direction in case of tension, nevertheless in compression no inter-penetration exists. Figure 4.8.b shows the typical deformation form of this type of pipes.
iii. The core is disbonded from the internal pipe in the tangential direction, but is fully bonded to the external pipe. In this case the inner pipe and core can separate from each other in the normal direction in case of tension, nevertheless in compression they are not allowed to penetrate into one another. Figure 4.8.c shows the typical deformation form of this type of pipes.

iv. The core can slide freely on both the internal and external pipes in tangential direction. In the normal direction the core is restricted from penetration into the surrounding pipes, but it is free to separate from the boundaries under tension. Figure 4.8.d shows the typical deformation form of this type of pipes.

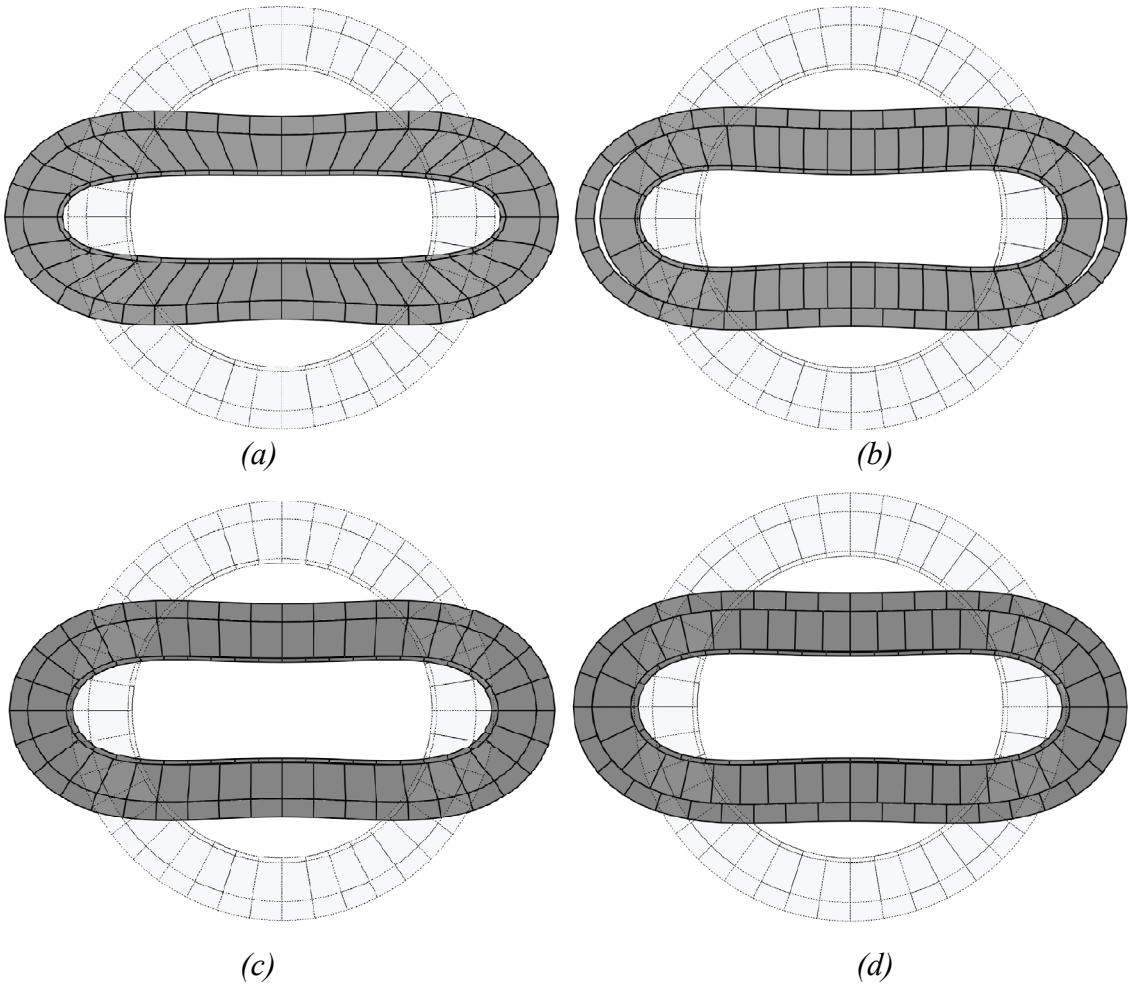

Figure 4.8. Typical deformation of sandwich pipes with various interface adhesion configurations of the core layer and surrounding pipes. (a) Fully bonded (b) Core layer is disbonded from the external pipe (c) Core layer is disbonded from the internal pipe (d) Core layer is disbonded from both internal and external pipes.

Considering all the studied parameters, a total of 768 FE models were constructed and analyzed for each of the design configurations. In summary, the simplified equations presented in the next section and the conclusions drawn in this paper are based on the analysis of more than 3000 FE models in the mentioned range of parameters.

4.9. DEVELOPMENT OF SIMPLIFIED PRACTICAL EQUATIONS

Considering the form of the analytical simplified equations and the physics of the problem, a simplified equation is proposed to present the FE analysis results. The equation is developed with its terms organized in separate groups, so that the influence of each group on the pressure capacity could be better appreciated. Equation 4.8 therefore presents the general form of the proposed equation. Parameters ψ_1 and ψ_2 in this equation represent the effect of core layer and internal pipe, respectively.

$$P_{cr} = \kappa P_{crs} + E_p(1 + \alpha_1 \nu_c^2)\left(\frac{t_1}{r_1}\right)^{\alpha_2}(\psi_1 + \psi_2) \tag{4.9}$$

where:

$$P_{crs} = \frac{E_p}{4\left(1 - \upsilon_p^2\right)}\left(\frac{t_1}{r_1}\right)^3 \tag{4.10}$$

$$\psi_1 = \gamma_1\left(\frac{E_c}{E_p}\right)^{\gamma_2}\left(1 - \frac{r_2}{r_1}\right)^{\gamma_3} \tag{4.11.a}$$

$$\psi_2 = \xi_1\left(\frac{E_c}{E_p}\right)^{\xi_2}\left(1 - \frac{r_2}{r_1}\right)^{\xi_3}\left(\frac{t_2}{r_2}\right)^{\xi_4} \tag{4.11.b}$$

Some MATLAB [4.18] code was developed to categorize pipes into one of the two main sandwich pipe categories. For each category, the corresponding characteristic limit pressure was calculated. Afterward, the SPSS statistical package [4.19] was used to fit equation 4.8 into the characteristic pressures so to obtain the constants. A constrained nonlinear regression algorithms recommended by Gill et al [4.20] with a sequential quadratic programming method was used for this purpose. The calculated constants for calculating the CPIP pressure for the first category of pipes with various design configurations are presented in Table 4.2. Table 4.3 shows the value of the constants that can be used to establish the limit equilibrium pressure of the pipe falling within the second category. As illustrated in these tables, the maximum expected error when using Equation 9 in comparison to the FE results is always less than 10% for any of the design configurations and pipe categories considered here.

Table 4.2. The value of constants to be used in Equation (4.9) for calculating CPIP pressure (Φ_1) for pipes in category 1

	κ	α_1	α_2	γ_1	γ_2	γ_3	ξ_1	ξ_2	ξ_3	ξ_4	$Error$ (%)
Fully bonded	0.9844	-0.5444	0.1	0.474	0.98	1.062	0.43	0.079	-0.1031	2.8	9.14
Outer unbonded	1.019	0.2461	-0.0904	0.816	0.982	3.146	0.1792	0.0329	-0.1062	2.929	9.79
Inner unbonded	0.9814	1.3922	0.083	0.712	0.962	2.827	0.202	0.041	-0.188	2.913	8.63
Core unbonded	0.9833	1.106	-0.0945	0.336	0.966	3.631	0.1589	0.0184	-0.0837	3.01	9.52

Table 4.3.The value of constants to be used in Equation (4.9) for calculating limit equilibrium pressure (Φ_2) for pipes in category 2

	κ	α_1	α_2	γ_1	γ_2	γ_3	ξ_1	ξ_2	ξ_3	ξ_4	$Error$ (%)
Fully bonded	1.0447	0.3259	0.1867	1.3043	1.153	2.289	0.1279	0.47	0.7295	0.5027	7.84
Outer unbonded	0.836	0.2461	-0.0904	0.816	0.982	3.146	0.0788	0.984	-1.1379	1.1799	8.96
Inner unbonded	-	-	-	-	-	-	-	-	-	-	-
Core unbonded	-	-	-	-	-	-	-	-	-	-	-

It is observed that the pipes in which their core layer is disbonded from their internal pipe would never undergo limit equilibrium instability. Therefore no constant values are proposed for these two configurations in Table 4.3.

4.10. RESULTS

The developed simplified equation can be used to study the influence of the characteristic parameters on pipes response. Figure 4.9 shows the influence of variation in the core thickness and stiffness on the external pressure capacity of the pipes in the

range of practical values described earlier. The figures correspond to various design configurations with respect to the interaction properties between the layers.

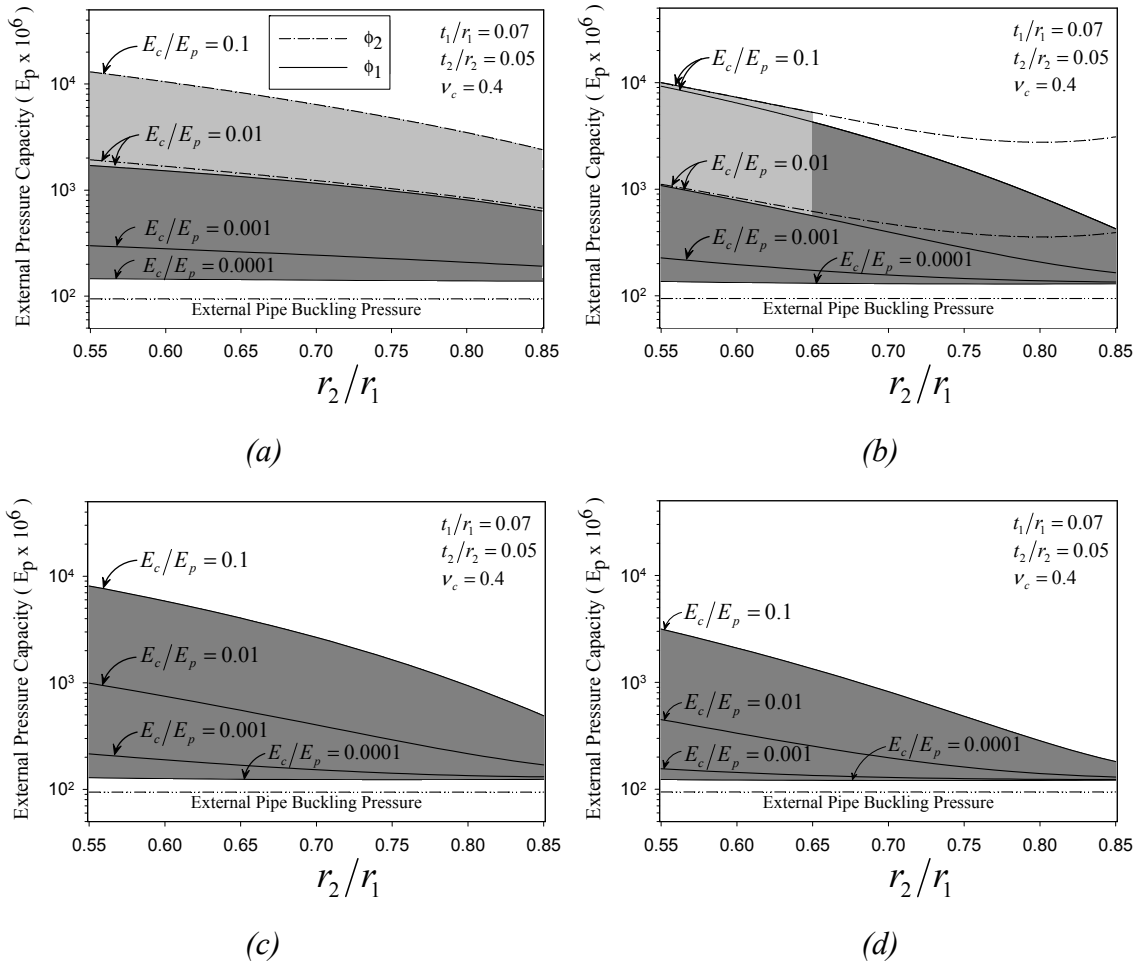

Figure 4.9. Influence of the variation of the core thickness and stiffness and interface properties between the layers on the external pressure capacity of the pipe for a sandwich pipe with $t_1/r_1 = 0.07$, $t_2/r_2 = 0.05$ and $\nu_c = 0.4$. (a) Fully bonded (b) Core layer is disbonded from the external pipe (c) Core layer is disbonded from the internal pipe (d) Core layer is disbonded from both internal and external pipes.

Figure 4.9.a shows the variation in CPIP pressure and limit equilibrium pressures for the first and second categories of pipes, respectively. These curves correspond to the pipes whose core layer and surrounding pipes are bonded together. The light gray area in this figure relates to the second category pipes that undergo Limit Equilibrium Instability

(LEI); the dark gray area corresponds to the range of parameters considered for the first category pipes. It is found that pipes with $E_c/E_p = 0.01$ could exhibit both a stable or unstable behavior depending on the range of the other characteristic parameters. However, despite the pipe parameters, the predicted characteristic pressures for pipes with either the first or second category of characteristic behaviors are very close to one another. In figure 4.9.a the solid lines depict the value of CPIP pressure and the dotted-lines depict the limit equilibrium pressure. As seen in the figure, the difference in the values identified by the lines for $E_c/E_p = 0.01$ is almost indistinguishable. The slight difference between the results is believed to be due to the regression error involved in the proposed equations. Furthermore, the figure also indicates that increasing the stiffness of the core layer would significantly increase the pressure capacity of the sandwich pipes. However, this phenomenon is more apparent in the sandwich pipes with thick core layers.

Figure 4.9.b shows the variation in the external pressure capacity of sandwich pipes with $t_1/r_1 = 0.07$, $t_2/r_2 = 0.05$ and $\nu_c = 0.4$ as a function of E_c/E_p and r_2/r_1. These curves have been generated for a design configuration in which the core layer is disbonded from the external pipe, but it is bonded to the inner pipe. As can be seen, pipes with this type of interface configuration respond stably for a wider range of the characteristic parameters. As shown in the figure, the investigated pipes are stable for all values of the parameters, except for $E_c/E_p > 0.01$ and $r_2/r_1 < 0.65$. It should be noted that due to the influence of various parameters, development of a general unified criterion that could predict the response of such sandwich pipes is not practically possible. However, it is noted that sandwich pipes with $E_c/E_p < 0.01$ would never exhibit instability under an applied external pressure. Moreover, when E_c/E_p is greater than 0.01, the lowest value obtained through Equation (4.9) would define the pressure capacity of the pipe.

Figures 4.9.c and 4.9.d illustrate the pressure capacity of sandwich pipes with different layers interface properties. The curves in Figure 4.9.c are generated for a sandwich pipes in whose the core layer is disbonded from its internal pipe and Figure 4.9.d shows the same curves for a sandwich pipe in which the core layer is completely disbonded from both surrounding pipes. As mentioned above in those configurations that the internal pipe is disbonded from the core layer, the pipe would not become unstable

regardless of the magnitude of the external pressure, and thus, would always fall within category 1 pipes.

Comparison of the results reveals that as expected, pipes having similar characteristic parameters, with fully bonded interlayer configuration, would always exhibit the greatest buckling pressure. The next best configuration would be sandwich pipes in which the external pipe is disbonded from the core layer, but the core is still bonded to the internal pipe. It should be noted, however that the difference in the pressure capacities of the two configurations would be considerable, especially in the design cases when a thin core layer is used. Among the studied configurations, as also expected, the pipes whose core is disbonded from both internal and external pipes exhibit the least capacity. In conclusion, the comparison of the results indicate the pressure capacity of a sandwich pipe with fully bonded interlayer properties could be more than 10 orders of magnitude than whose core/pipe interface interaction are not fully bonded.

4.11. CONCLUSIONS

In this paper, the finite element method has been used to study the stability response of sandwich pipes under external pressure. The structural parameters, used in the investigation were selected to cover a practical range of parameters. Using the results, the behavior of sandwich pipes was categorized into two classes, depending on their secondary equilibrium paths in their load-deformation response. A new value in the equilibrium path was also defined as the corresponding value to the limit equilibrium pressure, referred to as the Characteristic Path Inflection Point (CPIP). It should be noted that, this study was performed with this main assumption that the pipes would undergo linear buckling. Depending on the bonding properties between core layer and surrounding pipes, the sandwich pipes were classified into four categories. The structural parameters most significantly affecting the characteristic behavior of the pipe were established and the influence of each of the parameters on the limit pressure was established. Finally, a simplified practical equation was proposed for calculating the characteristic limit pressure of the system. The value of the constants required for establishing the equation for each of the design configurations were also defined. The summary and conclusions are as follows:

- Unlike the practical single wall steel pipes, sandwich pipes would exhibit two different stability behaviors, depending on their structural properties. The main difference between these two categories is the form of the secondary equilibrium path. Therefore, understanding these behaviors are important for (i) distinguishing between linear and nonlinear buckling behaviors, (ii) appropriately analyzing the buckle and buckle propagating phenomena in sandwich pipes, and (iii) properly consideration of the ductility of the pipeline before reaching to the limit pressure. In brief, the equilibrium path of a pipe, in the vicinity or after reaching to the limit pressure, can be established by categorizing the pipes based on their characteristic behavior is pipe classified in.
- More accurate predictions can be made through solving the problem with the finite element method in comparison to the available analytical approaches. The results of the finite element analysis can be used to establish simplified equations, thereby reducing the margin of error produced by the current analytical solutions.
- The post-buckling analysis results indicated the assumption of neglecting the influence of the inner pipe would be admissible only in sandwich pipes having a relatively stiff core material. This assumption, which is one of the main assumptions made in the development of the previous analytical solutions, would not hold for the case of sandwich pipes with a soft (e.g. insulative) core.
- It was found that one of the most significant parameters affecting the limit pressure is the core material stiffness. Increasing the stiffness of the core material would significantly increase the limit pressure. However, Poisson's ratio of the core material does not have a significant influence on the buckling pressure. It can be concluded from the results that the use of less compressible core materials would slightly decrease the limit pressure.
- Core layer thickness would have a significant effect on both limit pressure and ductility of the system before reaching to the limit pressure. It can be concluded from this study that increasing the thickness of the core would decrease the ductility of the system, but would increase the limit pressure of the pipe. Therefore, in a sandwich pipe, the core thickness should be optimized for

ensuring adequate pressure resistance as well as appropriate ductility required for the system.

- For the range of the studied parameters, it is proposed that the CPIP equilibrium pressure value established in this study could be considered as an appropriate value for establishing the limit buckling pressure of the pipe for the first category of pipes. Interestingly, results indicated that the geometrical imperfection of the pipe had less influence on the limit pressure of the pipes in the first category compared to the limit stability pressure of the second category of sandwich pipes.
- Comparison of the limit pressure established for the different design configurations indicated that the pipes with fully bonded constituent showed the most efficient design configuration. On the other hand the design configurations in which the core was disbonded from both internal and external pipes exhibited the worst limit pressure value.
- The results also revealed that the pipes with a stiffer core layer would more likely exhibit a declining secondary equilibrium path, while the pipes with a softer core layers showed increasing secondary path. Therefore, it can be concluded that sandwich pipes having a stiff core layer would be prone to linear buckling whereas those with a softer core would undergo nonlinear buckling.

4.12. ACKNOWLEDGMENTS

The financial support of the Atlantic Innovation Fund, through C-CORE Canada, is gratefully appreciated.

4.13. REFERENCES

4.1. Kyriakides, S. and Netto, T. A. (2004). On the dynamic propagation and arrest of buckles in pipe-in-pipe systems. *International Journal of Solids and Structures, 41*(20), 5463-5482.

4.2. Kyriakides, S. (2002). Buckle propagation in pipe-in-pipe systems. Part I. Experiments. *International Journal of Solids and Structures, 39*(2), 351-366.

4.3. Kyriakides, S. and Netto, T. A. (2002). Dynamic propagation and arrest of buckles in pipe-in-pipe systems. *Proceedings of the International Conference on Offshore Mechanics and Arctic Engineering* - OMAE, 4, 199-205.

4.4. Kyriakides, S. and Vogler T.J. (2002). Buckle propagation in pipe-in-pipe systems. Part II. Analysis. *International Journal of Solids and Structures, 39*(2), 367-392.

4.5. Kardomateas, G. A. and Simitses, G. J. (2002). Buckling of long, sandwich cylindrical shells under pressure. Proceedings of the International Conference on Computational Structures Technology, 327-328.

4.6. Kardomateas, G. A. and Simitses, G. J. (2005). Buckling of long sandwich cylindrical shells under external pressure. *Journal of Applied Mechanics, 72*(4), 493-499.

4.7. Sato, M. and Patel, M. H. (2007). Exact and simplified estimations for elastic buckling pressures of structural pipe-in-pipe cross sections under external hydrostatic pressure. *Journal of Marine Science and Technology, 12*(4), 251-262.

4.8. Sato, M., Patel, M. H., and Trarieux, F. (2008). Static displacement and elastic buckling characteristics of structural pipe-in-pipe cross-sections. *Structural Engineering Mechanics, 30*(3), 263-278.

4.9. Arjomandi, K. and Taheri F. (2009). Elastic buckling capacity of bonded and unbonded sandwich pipes under external hydrostatic pressure. *Submitted to the Journal of Mechanics of Materials and Structure.*(First revision was submitted)

4.10. Ohga, M. , SanjeewaWijenayaka, A. and Croll, J. G. A. (2005). Reduced stiffness buckling of sandwich cylindrical shells under uniform external pressure. *Thin-Walled Structures, 43*(8), 1188-1201.

4.11. Castello, X., and Estefen, S. F. (2008). Sandwich pipes for ultra deep-water applications. *Offshore Technology Conference,* OTC 197041*,* Houston, Texas, USA.

4.12. Castello, X. and Estefen, S. F. (2006). Adhesion effect on the ultimate strength of sandwich pipes. *International Conference on Offshore Mechanics and Arctic Engineering, OMAE2006-92481,* Hamburg, Germany.

4.13. Estefen, S. F., Netto, T. A., and Pasqualino, I. P. (2005). Strength analyses of sandwich pipes for ultra deep-waters. *Journal of Applied Mechanics, 72*(4), 599-608.

4.14. Brush DO. and Almroth, B. (1975). *Buckling of bars, plates and shells*. McGraw-Hill, New York.

4.15. Timoshenko, S., and Goodier, J. N. (1970). *Theory of elasticity* (3rd ed.). McGraw-Hill, New York; Toronto.

4.16. ABAQUS User's and Theory Manual. (2008). Version 6.8, Dassault Systèmes, RI, USA.

4.17. API SPECIFICATION 5L. (2000). *Specification for line pipe*. API Publishing Services, Washington, D.C.

4.18. MATLAB (2008). Version 7, The MathWorks Inc., MA, USA.

4.19. SPSS (2008). Version 17, SPSS Inc., IL, USA.

4.20. Gill, P. E., Murray W. M., Saunders M. A. and Wright. M. H. (1986). User's guide for NPSOL (version 4.0): A FORTRAN package for nonlinear programming. Technical Report SOL 86-2. Stanford University: Department of Operations Research.

CHAPTER 5
INFLUENCE OF THE MATERIAL PLASTICITY ON THE CHARACTERISTIC BEHAVIOR OF SANDWICH PIPES*

Kaveh Arjomandi and Farid Taheri
Department of Civil and Resource Engineering, Dalhousie University

5.1. ABSTRACT

Sandwich Pipes (SP) can be considered as an enhanced design configuration for Pipe in Pipe (PIP) systems. By improving the structural properties of the core layer and the components' interface adhesion, SP systems can be an effective design alternative for deepwater applications. However, designing such a hybrid structure demands more knowledge of the response of the system under the governing loading and environmental conditions. A SP system would be a suitable design alternative for offshore pipelines that are subjected to very large hydrostatic pressure in deepwater. Therefore, full understanding of the behavior of such systems under the external hydrostatic pressure is a prerequisite for designing optimum SPs.

In this paper a set of parametric models are generated based on practical design configurations. The Finite Element (FE) software package, ABAQUS, is used to create the models and analyze them. The FE models are analyzed through eigenvalue buckling and post-buckling analyses with the assumptions of linear and nonlinear buckling. Appropriate initial imperfections and FE parameters are administered. Moreover, the integrity of FE models is investigated through a mesh convergence study and also by considering various types of element locking mechanism. The results of these three methods of analysis are compared and the discrepancy between the results obtained through the linear analysis in comparison to the nonlinear post-buckling analysis is highlighted. Moreover, the influence of using various material plasticity models on the buckling and post-buckling responses is also investigated. Different models describing the materials stress-strain curves in the form of the elastic perfectly plastic, elastic followed by plastic exponential hardening, as well as the existence of the Lüder's bands

---

* *8th International Pipeline Conference proceeding*. *IPC 2010-31518*, Alberta, Canada.

are also considered. Furthermore, the effect of core material's stiffness on the buckling and post-buckling response of the system is also examined. Based on the equivalent plastic strain, it will be shown that in order to ensure system's effective composite sandwich action, the core must have a certain minimal stiffness. Finally, the influence of the enhancement in the steel grade used to form either the internal or external pipe on the stability response of both PIP and SP systems will be illustrated.

5.2. NOMENCLATURE

imp	Imperfection magnitude
E_s	Steel pipes elastic modulus
K	Strength index
n	Strain hardening index
r_1	Outer pipe nominal radius
r_1^o	Outer pipe initial nominal radius
r_2	Inner pipe nominal radius
Δr	Imperfection of the pipe radius as a function of θ
$\Delta\varepsilon_L$	Lüder's strain
ε	True strain
σ	True stress

5.3. INTRODUCTION

The depletion of the world's shallow oil reserves has increased the demand for the oil left in the remote, deep water reserves. However, oil extraction from these deep and harsh water reserves is only possible when special attention is paid to oil transportation facilities. One of the main parts of oil transportation systems are pipelines; therefore, due to more complex issues involved with the installation and operation of pipelines in deepwater, the design concerns for achieving optimum transportation pipelines are amplified. More specifically, these issues are pipeline buoyancy, thermal insulation between the oil and the surrounding environment while transportation, high external pressure and corrosion. These restrictions limit the traditional single walled steel pipes to a limited water depth and specific environmental conditions. The idea of employing two

pipes in a Pipe in Pipe (PIP) configuration has been mainly employed in the case of offshore pipelines in order to overcome the thermal insulation issues. In addition to insulation purposes, in those cases where a leak would induce a great risk to the ambient environment, the external pipe may be designed to provide secondary containment. A modification which can be made to PIP systems to improve the structural properties of the pipeline is the introduction of a sandwich system. Sandwich Pipes (SP) can be considered as a PIP system in which the structural integrity of the system has been improved by using the sandwich system. Consequently, in comparison to PIP systems, sandwich pipes can provide both the thermal insulation and the secondary containment features of PIP systems as well as enhanced structural properties. Therefore, SP systems can offer a smart design alternative for oil transportation pipelines. However, very few industrial projects have taken advantage of the structural improvements that are possible through use of sandwich pipes.

Figure 5.1 is a schematic of a typical SP system. As can be seen in the figure, a SP system consists of an internal pipe, a relatively thick lightweight core layer, and an external pipe. Depending on the design target parameters, each part of this system can be designed for a specific purpose. The internal pipe, also referred to as the product pipe, is usually designed to endure a specified internal pressure and to facilitate the safe transportation of the product. One of the main core layer's functions is to provide thermal insulation between the oil product and the ambient environment in order to keep the product viscosity sufficiently low, thus allowing the oil to flow easily. Moreover, the core can improve the structural properties of the system by providing a proper containment for the external pipe and a proper load transferring structure between the surrounding pipes. The annulus area between the pipes can also be a host for monitoring, heating or cathodic protection systems. A wide range of core materials such as plastics, gels, ceramics and composite materials may be used to achieve the system's thermal and structural requirements. The external pipe, also called the sleeve pipe, is employed to protect the internal and core layers from the surrounding environment. In PIP systems, the external pipe carries the external pressure individually or in the case of SP systems it works as the main part of the sandwich system. Therefore, thinner external pipes are specified for SP systems when compared to PIP systems designed for the same water depth. Furthermore,

the external pipe can be designed to provide a secondary containment for the product, in case of leakage through the inner pipe and core layer.

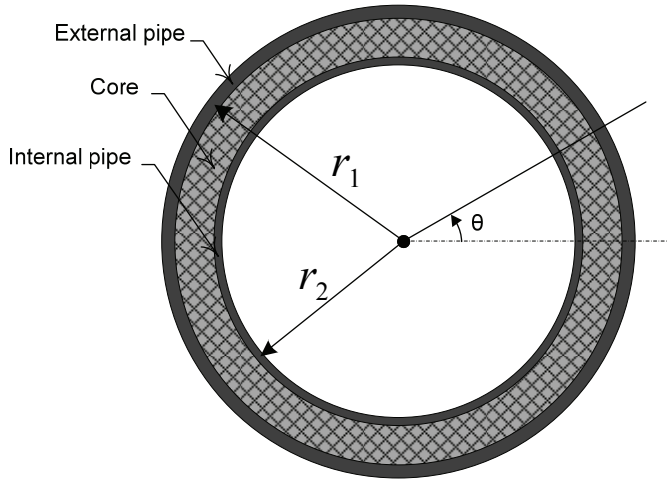

Figure 5.1. Idealized geometry of a sandwich pipe.

Recently, a great deal of research has been done on characterizing the behavior of SP and PIP systems. Most of the recent work has involved investigation into the structural stability behavior of these systems. For example, deep water pipelines may undergo buckle propagation phenomena due to high external hydrostatic pressure. Many works in this area have been recently performed by Kyriakides and his coworkers [5.1-5.4] who studied the buckle propagation phenomena from analytical, numerical and experimental perspectives. Kardomateas and Simitses [5.5, 5.6] analytically studied the stability of long sandwich cylindrical shells under external pressure. Sato and Patel [5.7], Sato *et al*.[5.8] and Arjomandi and Taheri [5.9] studied the buckling behavior of SP systems under hydrostatic pressure and developed a simplified solution for estimating the PIP system's pressure capacity. Ohga et al. [5.10] studied the reduced stiffness buckling of sandwich cylindrical shells under uniform external pressure both numerically and analytically. In another study Castello and Estefen [5.11, 5.12] and Estefen et al. [5.13] investigated the feasibility of a sandwich system for deep water applications with both numerical and experimental approaches. In their investigations, they considered the behavior of sandwich pipes under various loading conditions. Furthermore, additional

research involving the numerical modeling of sandwich pipes has been completed by other researchers, which for the sake of brevity are not been mentioned here.

Former studies, which investigated the structural characteristics of SP systems, can be divided into two main categories based on their methodology used to determine the capacity of sandwich system. These two categories are numerical and analytical methods. The main restriction of the analytical solutions is that the final equations would become extremely complex if the material nonlinearity is included in the models. Consequently, all of the proposed analytical solutions use a linear material model for both the internal and external pipes as well as the core layer. On the other hand, no comprehensive numerical study has been found in the literature that investigates the stability of sandwich pipes under external hydrostatic pressure while also considering material nonlinearity. In this study, the effect of the material nonlinearity on the characteristic response of the system has been investigated and it is found that taking the material nonlinearity into account has a significant effect on the characteristic behavior.

In the current paper, a set of parametric studies was performed in order to investigate the influence of material plasticity on the buckling and post-buckling response of a possible design set of PIP and SP. A practical design geometry was used and the influence of the core stiffness in the response of PIP and SP systems were investigated. Furthermore, the calculated response of the PIP and SP systems were compared to each other. To study the influence of the plastic profile in the stress-strain curve of the material, several possible practical material properties were considered. The calculated response of the system based on each of the chosen material behaviors was compared and conclusions subsequently drawn. Moreover, by adopting steel materials with various yield stresses, the influence of upgrading the steel grade in either the internal or external pipes in both pipe systems was investigated.

5.4. FINITE ELEMENT MODEL

In this paper, a set of Finite Element (FE) parametric study models have been created using the FE software ABAQUS/Standard [5.14]. It was found that in case of employing polymeric incompressible core materials the created FE models were highly susceptible to volumetric locking. In order to select the most efficient FE model, the accuracy of

various FE mesh configurations employing various element types was investigated. Figure 5.2 illustrates the results of a mesh convergence and element sensitivity study on a sandwich pipe having an almost incompressible core material (ν=0.49) with an intermediate core stiffness. In this figure the convergence of five mesh configurations are investigated. A mesh configuration (C3D8R+H) was created by using the Abaqus linear element with reduced integration (C3D8R) for the internal and external pipes and employing the Abaqus linear hybrid element (C3D8RH) as the core layer.

Three other mesh configurations were created using the Abaqus quadratic brick elements. In C3D20 and C3D20R mesh configurations, the Abaqus 20 nodes brick elements with respectively regular (C3D20) and reduced (C3D20R) integrations were used to create the model. In order to study the efficiency of the quadratic hybrid elements, also a mesh configuration (C3D20+H) which combines a quadratic element (C3D20) for modeling the steel pipes and a quadratic hybrid element (C3D20H) for modeling the core layer was included in this convergence study. It should be mentioned that in the four above-mentioned configurations, one through thickness layer of elements was used for creating the core layer. Finally in C3D20+3xH configuration, the influence of the number of through thickness elements in the core layer was investigated by considering a mesh configuration in which the core layer has three through thickness hybrid elements and the steel pipes have a layer of regular integration elements.

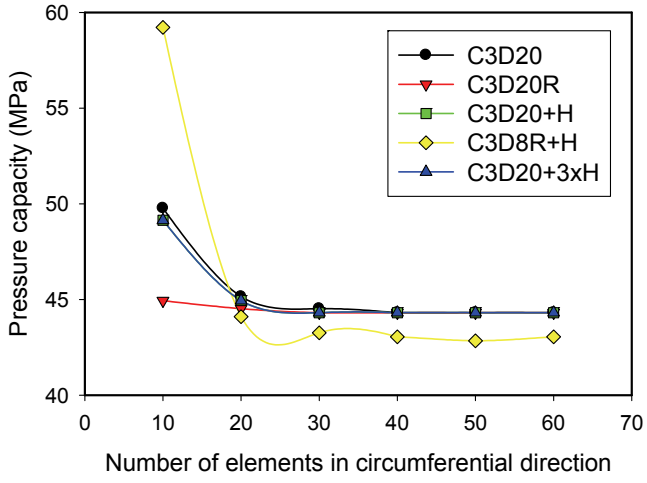

Figure 5.2. Mesh convergence study

In summary the convergence study results demonstrate that using reduced integration elements would release the volumetric locking proving that the use of hybrid elements is unnecessary. Moreover, considering both the accuracy of the results and the analysis cost of FE models the C3D20R mesh configuration in which the ABAQUS finite element, C3D20R, a quadratic reduced integration brick element, was used to create a quasi-2D model of the pipe system.

Furthermore, from the mesh convergence study, it was determined that a finite element mesh with one through thickness element for each layer and 40 elements in the circumferential direction would create a sufficiently accurate mesh. Figure 5.3 illustrates the geometry and mesh configuration of the FE model. The boundary conditions of the model in the longitudinal direction were applied in such a way to create a plane strain condition.

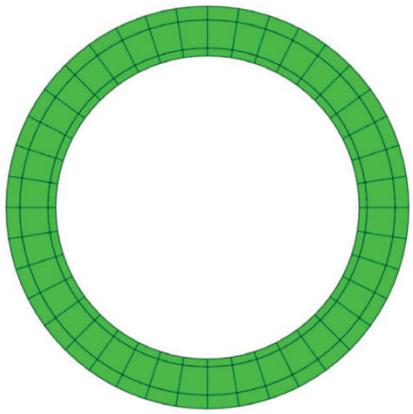

Figure 5.3. Geometry and mesh configuration of the FE model

During the plastic post-buckling analysis of a pipe system with plane strain boundary conditions, non proportional stresses would be applied in the event of large strains. Therefore, deformation plasticity theory was used to model the material behavior in the plastic regime. The current study is mainly based on using the polymeric materials as the core layer; therefore the elastic strain limit of the core material was considered to be much larger in comparison to the surrounding steel pipes. As a result, the core layer was modeled using an elastic material model. Moreover, it should be mentioned that the interaction of the interface between the surrounding pipes and the core layer would have a significant influence on the characteristic response and pressure capacity of the pipe. However, in this study for the sake of simplicity it was assumed that the core layer is

fully bonded to both external and internal pipes. To model this behavior in ABAQUS the Tie option was used.

To simulate the post-buckling response of the pipe, which would occur in reality, imperfections should be considered in the pipe geometry, in the boundary conditions and/or in the applied loadings. In this study, a geometrical imperfection was considered as the main source of imperfection within the pipe system. The geometrical imperfection applied to the internal and external pipes can be defined by Equation 5.1. The imp parameter in this equation was taken as 0.0005.

$$\Delta r_i = imp \times r_i^o \cos 2\theta \quad , \quad i = 1,2 \tag{5.1}$$

The parametric study models were generated based on a practical design configuration. In those models the internal and external pipe diameter to thickness ratio were respectively considered as 40 and 28.6. These values were extracted from the API standard [5.15]. The main focus of this study is the investigation of the influence of material plasticity on the buckling and post-buckling response of the pipe system. As a result, the assumed diameter to thickness ratios was determined such that the pipe system would undergo plastic buckling. While maintaining these geometrical properties constant, the influence of changing the other structural parameters such as the core stiffness and the surrounding pipes material properties were studied.

5.5. BUCKLING AND POST-BUCKLING RESPONSE

In this section, the influence of the steel material grade and plastic stress-strain profile on the buckling and post-buckling response of the system is investigated using the FE parametric study results. In this study the ovality of the external pipe, which can be calculated by Equation 5.2, is considered as the characteristic behavior of the pipe.

$$\Delta = \frac{r_1 - r_1^o}{r_1^o} \tag{5.2}$$

Three possible core materials were considered to cover the material range which may be used in the construction of PIP and SP systems. Softer materials are more economical when the thermal insulation rule of the core layer is more imperative such as in PIP

configurations. On the other hand, in SP systems employing stiffer core layers would increase the integrity of the pipeline structure besides increasing of the cost of the core layer. The range of the core layer stiffness studied here covers polymers, advanced composites and possible ceramic materials which may be employed in PIP systems with relatively stiff core layers as well as practical SP systems.

5.5.1. Influence of the Lüder's banding

Depending on the manufacturing process, steel pipes exhibit different material behavior in the circumferential direction. Due to cold working during the UOE manufacturing process, some of the high grade steel pipes do not have any Lüder's banding after reaching the yield point. This is in contrast to some other grades of steel pipes such as those which are made from low carbon and hot finished steels, which exhibit considerable Lüder's banding in the circumferential direction [5.16].

It should be mentioned that the Lüder's bands phenomenon is the plastic instability in the material and is classified as propagative and transient instabilities. In this phenomenon the instability in the material would propagate at a level of constant stress. Therefore the dynamic influence of the Lüder's bands is more significant when a considerable region in the structure is under uniform stress conditions. However, investigating the stress contour of SPs under hydrostatic external pressure shows that the gradient of the stress condition in the steel pipes is significant. Therefore, in this study the influence of the Lüder's bands is investigated by analyzing the system statically and the effect of the dynamic propagation of material instabilities was neglected.

In this study, a general steel material model, which is capable of generating both of these behaviors, is used as the material model in the circumferential direction. This general model is graphically demonstrated in Figure 5.4.

In this figure, path OABE represents the stress-strain curve with the following segments:

- OA: The material in this regime behaves elastically up to a yield point corresponding to point A.
- AB: This regime is related to the Lüder's banding behavior. Lüder's banding behavior represents material instability which occurs in the transition from elastic

to plastic deformation. Material in this regime has a plastic behavior. Here, a zero hardening has been assumed for this segment.

- BE: After reaching point B, the material deforms in a homogeneously plastic manner with a considerable hardening in comparison with the Lüder's Banding regime. The stress-strain behavior of the material follows an exponential equation in this regime. In reality, this path ends up with a failure point which corresponds to large strains with a magnitude of greater than 10%. Because this study is mainly focused on the post-buckling behavior of the pipe after buckling and before reaching to such large strains, failure of the material was not considered in the FE models.

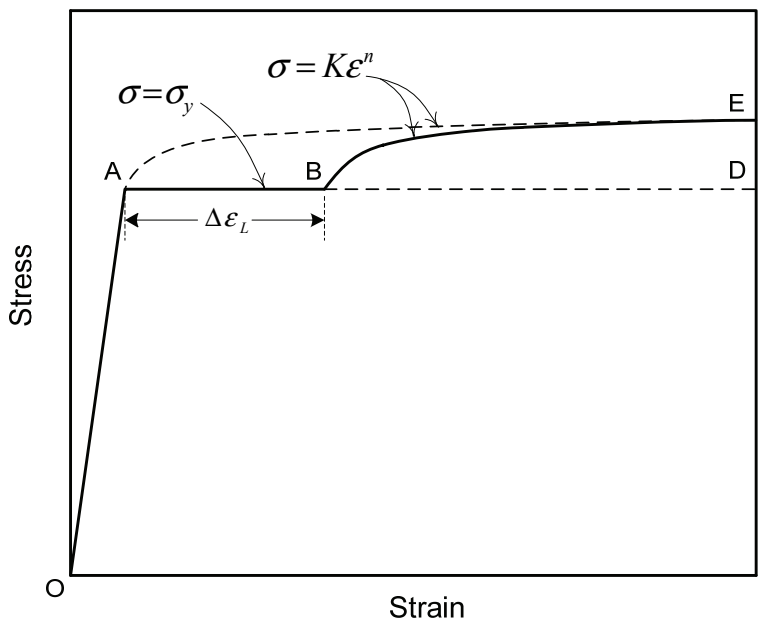

Figure 5.4. General steel stress-strain curve

The material behavior can be described mathematically as:

$$\sigma = \begin{cases} E_s\varepsilon & 0 \le \varepsilon < \varepsilon_e \\ \sigma_y & \varepsilon_e \le \varepsilon < \varepsilon_e + \Delta\varepsilon_L \\ K\varepsilon^n & \varepsilon_e + \Delta\varepsilon_L \le \varepsilon \end{cases} \tag{5.3}$$

where $\varepsilon_e = \sigma_y / E_s$.

By changing the material constants in the above mentioned general material model the following material behaviors are investigated in this work:

- Elastic plastic material with hardening and Lüder's banding which is represented by path OABE. This material behavior consists of all three parts of the stress-strain curve. After reaching to the yield point (A), the material becomes unstable during the Lüder's banding response (AB) which ends up with a hardened plastic response (BE). A typical range for the Lüder's strain in steel pipes is $0.01 - 0.05$.
- Elastic Perfectly Plastic (EPP) behavior (path OAD). This behavior can be modeled by assuming a large Lüder's band. Mathematically it can be written as$(\Delta\varepsilon_L + \varepsilon_e) > \varepsilon_{max}$, where ε_{max} in this equation is the maximum strain which would occur in the pipe system within the post-buckling analysis.
- Elastic plastic material without Lüder's banding behavior which is shown by path OAE. Steel pipes which do not exhibit a Lüder's band response have this type of behavior. To model this behavior with the assumed general material model the Lüder's strain is taken zero.

Figure 5.5 illustrates the response of the studied pipes analyzed with various material plastic stress-strain regime behaviors in the circumferential direction. In this figure, it is assumed that the internal and external pipes are made from X100 grade steel, having the same plastic response. The stiffness of the core material is assumed to be 1% of the steel's stiffness which is a practical stiffness for polymer materials. To provide a more practical sense, the right vertical axis is scaled as the water depth that the pipe system can tolerate without any internal pressure. As can be seen in this figure, there is not a significant difference in the elastic response and the buckling pressure between the studied pipes. Although using steel grades having hardening behavior right after the yield point would slightly increase the buckling pressure, the existence of a small Lüder's band between the hardening regime and the yield point eliminates the influence of the hardening regime on the buckling pressure.

A comparison of the post-buckling responses demonstrates that the characteristic response of the pipes always falls between two boundaries. As can be seen in Figure 5.5, the pipes with EPP material properties exhibit the lower bound response. Even though the

response of the system can be improved by decreasing the Lüder's strain, in the large magnitude of ovality all the hardened models approach to the same value.

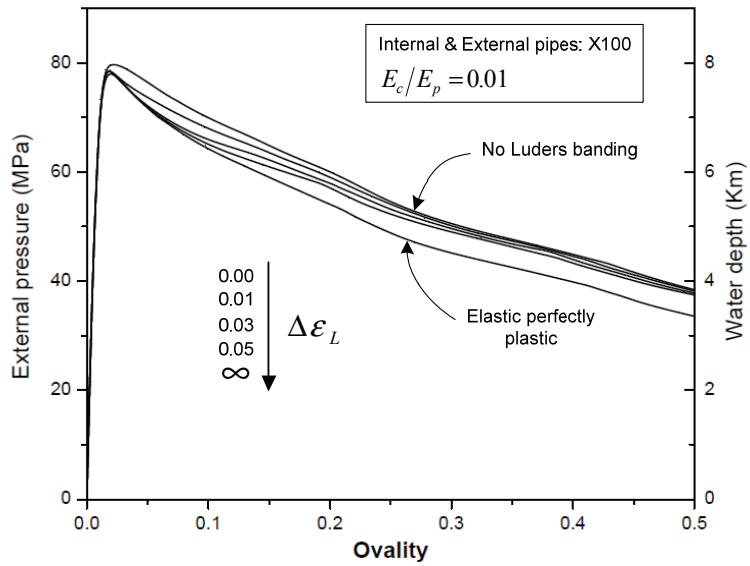

Figure 5.5. Influence of the material plastic response on the buckling and post-buckling response of the pipe

5.5.2. Influence of the core stiffness

The influence of the core stiffness on the response of the pipe system was investigated by assuming three magnitudes of stiffness for the core layer. These magnitudes were chosen based on the range of the materials which can be used as the core layer in real applications. The lowest core stiffness, which is 0.1% of the steel stiffness, can be used in a potential PIP design. On the other hand, the greatest studied stiffness, which is 10% of the steel stiffness, can be a potential SP design configuration.

Figure 5.6 illustrates the buckling and post-buckling response of the studied configurations when the internal and external pipes are constructed from X100 grade steel. In these figures the results of three different analysis methods are shown. The analysis methods used here are the eigenvalue buckling analysis and the elastic and plastic post-buckling analysis. Moreover, the curves labeled "plastic post-buckling analysis" correspond to the various values of Lüder's strain adopted in this investigation.

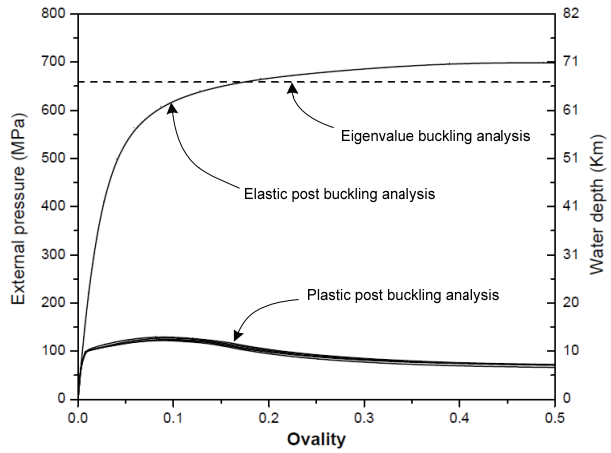

(a)

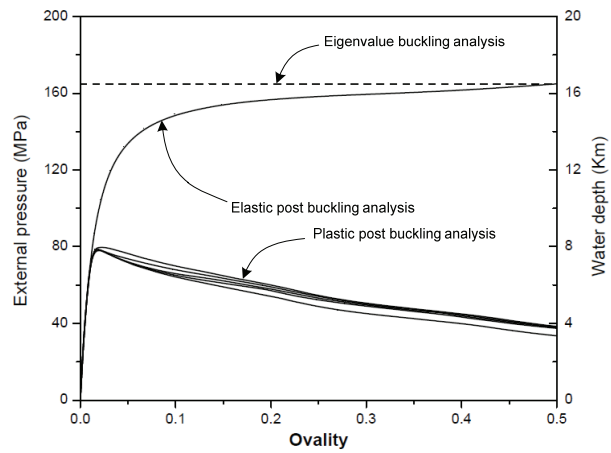

(b)

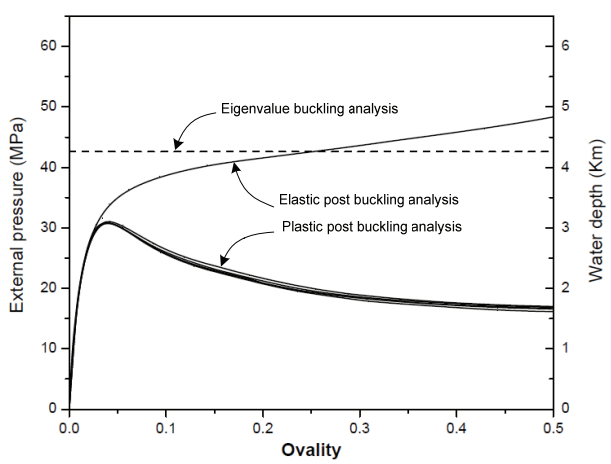

(c)

Figure 5.6. Influence of the core stiffness on the buckling and post-buckling response. (a) $E_c/E_p = 0.1$*(b)* $E_c/E_p = 0.01$ *(c)* $E_c/E_p = 0.001$.

As can be seen in Figure 5.6, the core stiffness has less effect on the pressure capacity of the pipes obtained through a plastic post-buckling analysis in comparison with the eigenvalue or the elastic post-buckling methods. The results from the eigenvalue buckling analysis illustrate that the corresponding buckling pressure of pipes having a core layer stiffness ratio of 0.1%, 1% and 10%, respectively, have a 42.6, 164.8 and 658.3 MPa pressure capacity. That is, if the material plasticity is not considered in the models, an increase of 100% in the core stiffness ratio magnitude would increase the capacity of the pipe system up to 1500%. Whereas, if the plasticity of the steel material is taken into account, for the same magnitude of core stiffness improvement the capacity of the SP system would only increased by 395%.

The plastic post-buckling analyzes results in Figure 6 demonstrate that using a relatively stiff polymer core layer with a stiffness ratio of 0.01 can extend the pipeline operating depth from 3,166 meters to 7,979 meters in comparison with the PIP system made from a softer core layer with a stiffness ratio of 0.001.

5.5.3. Influence of yield strength

In this section, the influence of employing the higher grade steel pipes on the characteristic response of the aforementioned SP and PIP systems will be discussed. As mentioned before, the only difference between the studied SP and PIP systems is the stiffness of the core. The chosen design configuration for the SP system had a core/steel stiffness ratio of 10%. Figures 5.7 and 5.8 demonstrate the characteristic behavior of this SP system as well as the equivalent plastic strain contour of the pipe at the greatest external pressure magnitude. In Figure 5.7, the change in the characteristic response of the system, employing various steel grade external pipes, is illustrated. In this figure the internal pipe steel's grade is X60 while the external pipe grade changes from X60 to X120. Figure 5.8 shows the effect of using various steel grade pipes as the internal pipe. By comparing Figures 5.7 and 5.8, it can be concluded that using a higher grade of steel for the external pipe improves the pressure capacity of the pipe system more than those design configurations in which the internal pipe's steel grade was enhanced. However, employing higher grade steel pipes as the internal pipe would still improve the pressure capacity of the system significantly.

The plastic strain contours demonstrated in Figures 5.7 and 5.8 show that in these SP configurations, both the internal and external pipes undergo plastic deformations. However, the equivalent plastic strain magnitude occurring in the internal pipe is greater than that which occurs in the external pipe.

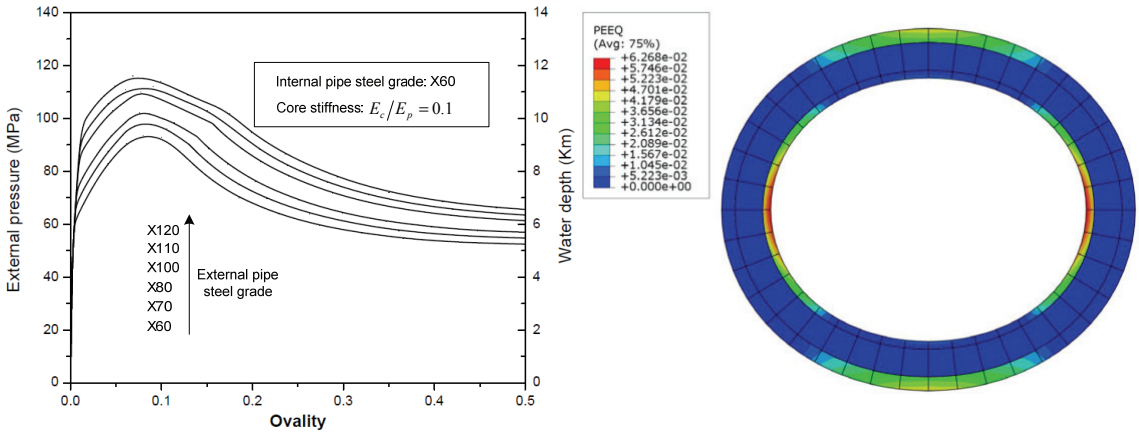

Figure 5.7. Influence of the external pipe steel grade on the buckling, post-buckling and plastic strain contour response for the studied SP configuration.

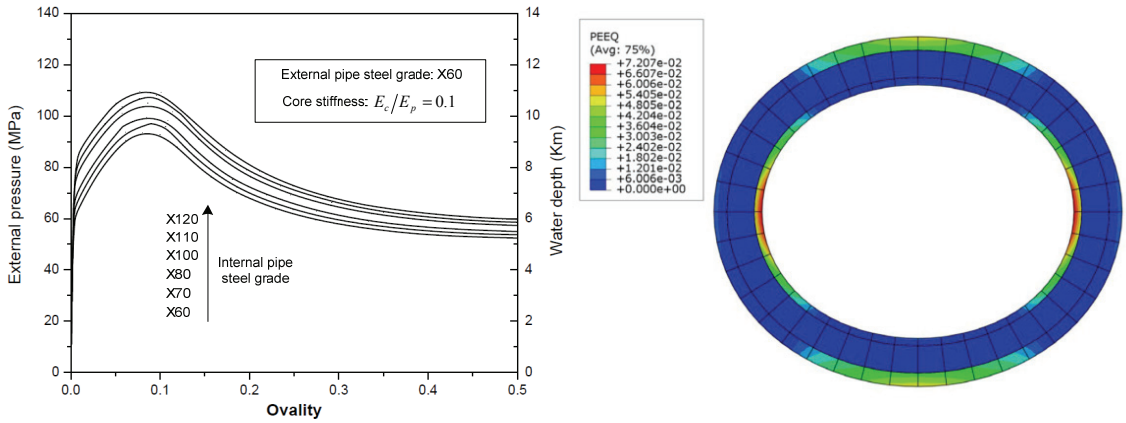

Figure 5.8. Influence of the internal pipe steel grade on the buckling, post-buckling and plastic strain contour response for the studied SP configuration.

Figures 5.9 and 5.10 illustrate the response of the PIP configuration made from a core material with stiffness ratio of 0.1%. Figure 5.9 and 5.10 respectively illustrate the influence of employing various grades of steel for the external and internal pipes. Comparing these figures shows that using a higher grade steel for the external pipe improves the capacity of the pipe system significantly. On the other hand, improving the

steel grade of the internal pipes does not have any significant effect on the capacity of the pipe system. However, improving the internal pipe's steel grade in PIP configurations improves the ductility of the system under external pressure. Comparison between the equivalent plastic strain contours in Figure 5.7, 5.8, 5.9 and 5.10 shows that in the studied PIP configuration, only the external pipe undergoes plastic strains.

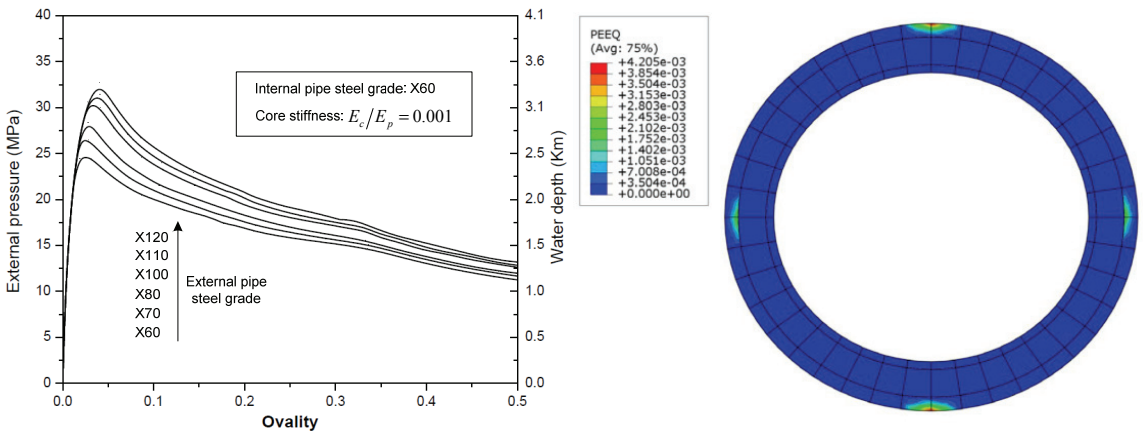

Figure 5.9.Influence of the external pipe steel grade on the buckling, post-buckling and plastic strain contour response for the studied SP configuration.

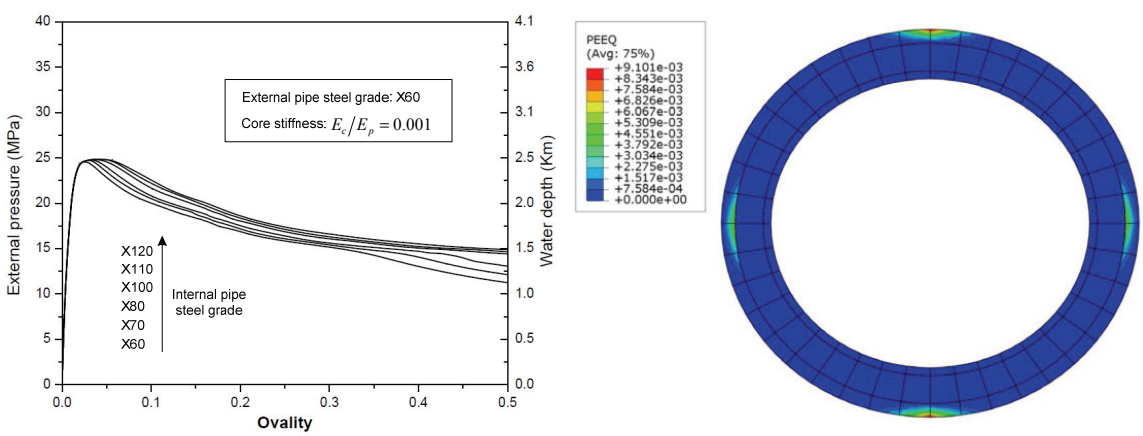

Figure 5.10.Influence of the internal pipe steel grade on the buckling, post-buckling and plastic strain contour response for the studied SP configuration.

5.6. CONCLUSIONS

In this paper, the influence of the plastic behavior of the steel pipes on the buckling and post-buckling response of PIP and SP systems was studied. Moreover, the

consequence of employing various grades of steel pipes with various plastic properties has been compared. A summary of the conclusions are as follows:

- Comparison of the EPP and elastic-plastic materials with Lüder's banding indicates that the stress-strain profile of the material after yielding does not have a significant effect on the buckling capacity of the studied pipes.
- Steel materials having Lüder's banding or exponential hardening after reaching yield strength may be modeled with an elastic-perfectly plastic model without significant loss in the accuracy of the calculated pipe characteristic response.
- Although the core stiffness has a significant influence on the plastic post-buckling pressure, its effect is much greater when considering the results obtained through the eigenvalue buckling and elastic post-buckling analyses.
- Employing high grade steel pipes as either the external or internal pipe in SP configurations would improve the capacity of the system considerably. The improvement would be greater when the external pipe's steel grade was enhanced (as oppose to when the internal pipe's grade is improved).
- In PIP systems, although employing high grade steel pipes as the external pipe improves the capacity of the system, using high grade internal pipes would not have a significant influence on the external pressure capacity of the pipe.
- Comparison of the PIP and SP equivalent stress and plastic strain contours revealed that adopting a core with a 10% stiffness ratio would be sufficient for creating an effective SP structure in which the internal pipe, core layer and the external pipe work as an integral unit. Whereas in the PIP design configuration (usually with 0.1% core stiffness ratio), only the external pipe would be resisting the external pressure.

5.7. ACKNOWLEDGMENTS

The financial supports from the Atlantic Innovation Fund and The Natural Sciences and Engineering Research Council of Canada (NSERC), are gratefully appreciated.

5.8. REFERENCES

5.1. Kyriakides, S. and Netto, T. A. (2004). On the dynamic propagation and arrest of buckles in pipe-in-pipe systems. *International Journal of Solids and Structures, 41*(20), 5463-5482.

5.2. Kyriakides, S. (2002). Buckle propagation in pipe-in-pipe systems. Part I. Experiments. *International Journal of Solids and Structures, 39*(2), 351-366.

5.3. Kyriakides, S. and Netto, T. A. (2002). Dynamic propagation and arrest of buckles in pipe-in-pipe systems. *Proceedings of the International Conference on Offshore Mechanics and Arctic Engineering* - OMAE, 4, 199-205.

5.4. Kyriakides, S. and Vogler T.J. (2002). Buckle propagation in pipe-in-pipe systems. Part II. Analysis. *International Journal of Solids and Structures, 39*(2), 367-392.

5.5. Kardomateas, G. A. and Simitses, G. J. (2002). Buckling of long, sandwich cylindrical shells under pressure. Proceedings of the International Conference on Computational Structures Technology, 327-328.

5.6. Kardomateas, G. A. and Simitses, G. J. (2005). Buckling of long sandwich cylindrical shells under external pressure. *Journal of Applied Mechanics, 72*(4), 493-499.

5.7. Sato, M. and Patel, M. H. (2007). Exact and simplified estimations for elastic buckling pressures of structural pipe-in-pipe cross sections under external hydrostatic pressure. *Journal of Marine Science and Technology, 12*(4), 251-262.

5.8. Sato, M., Patel, M. H., and Trarieux, F. (2008). Static displacement and elastic buckling characteristics of structural pipe-in-pipe cross-sections. *Structural Engineering Mechanics, 30*(3), 263-278.

5.9. Arjomandi, K. and Taheri F. (2009). Elastic buckling capacity of bonded and unbonded sandwich pipes under external hydrostatic pressure. To appear in *the Journal of Mechanics of Materials and Structure*.

5.10. Ohga, M. , SanjeewaWijenayaka, A. and Croll, J. G. A. (2005). Reduced stiffness buckling of sandwich cylindrical shells under uniform external pressure. *Thin-Walled Structures, 43*(8), 1188-1201.

5.11. Castello, X., and Estefen, S. F. (2008). Sandwich pipes for ultra deep-water applications. *Offshore Technology Conference,* OTC 197041*,* Houston, Texas, USA.

5.12. Castello, X. and Estefen, S. F. (2006). Adhesion effect on the ultimate strength of sandwich pipes. *International Conference on Offshore Mechanics and Arctic Engineering, OMAE2006-92481,* Hamburg, Germany.

5.13. Estefen, S. F., Netto, T. A., and Pasqualino, I. P. (2005). Strength analyses of sandwich pipes for ultra deep-waters. *Journal of Applied Mechanics, 72*(4), 599-608.

5.14. ABAQUS User's and Theory Manual. (2008). Version 6.8, Dassault Systèmes, RI, USA.

5.15. API SPECIFICATION 5L. (2000). *Specification for line pipe*. API Publishing Services, Washington, D.C.

5.16. Kyriakides, S. and Corona, E. (2007). *Mechanics of offshore pipelines* (1st ed.). Elsevier, Amsterdam.

CHAPTER 6
A NEW LOOK AT THE EXTERNAL PRESSURE CAPACITY OF SANDWICH PIPES*

Kaveh Arjomandi and Farid Taheri
Department of Civil and Resource Engineering, Dalhousie University

6.1. ABSTRACT

Sandwich Pipes (SPs) have been developed to overcome the required flow assurance and pressure capacity issues in deep and ultra-deep waters. This research aims at studying the influence of certain structural parameters on the pressure capacity (also referred to as the plastic buckling pressure) of Sandwich pipelines. The use of high grade steel pipes, as the internal or external pipes, has also been considered as one of the design parameters in this study. Moreover, a comprehensive parametric study, considering a practical range of the parameters that influence the response of SPs (and considering 3840 SP configurations) was conducted. The results from this large array of pipes were used to formulate a practical equation, capable of estimating the plastic buckling pressure of SPs. The accuracy of the proposed equation was evaluated by comparing the results with the experimental and numerical results available in the literature. The comparative results demonstrated that the proposed equation could predict the buckling capacity of such pipes with a reasonable accuracy. Furthermore, the proposed equation was used, along with a general optimization procedure, to establish the most optimum and cost-effective combination of structural parameters for SPs suitable for use in various water depths.

Keywords: Sandwich pipes, buckling capacity, finite element analysis, analytical solution, influence of materials properties, optimized design, cost function.

---

* Submitted to the Journal of Marine Structures.

6.2. NOMENCLATURES

A_{s1}	Cross section area of the external pipe
A_{s2}	Cross section area of the internal pipe
A_c	Cross section area of the core
C_{Man-SP}	Manufacturing and material cost of the sandwich pipe
C_{Man-P1}	Manufacturing and material cost of the external pipe
C_{Man-P2}	Manufacturing and material cost of the internal pipe
C_{Man-C}	Manufacturing and material cost of the core
E_c	Core material elastic modulus
E_p	Internal and external pipes' elastic modulus
P_{cr}	Sandwich pipe buckling pressure
P_{crs}	External pipe buckling pressure
imp	Imperfection magnitude
n	Buckling mode number
r_1	Outer pipe nominal radius
r_2	Inner pipe nominal radius
r_1^o	Outer pipe initial nominal radius
r_2^o	Inner pipe initial nominal radius
r_1^{max}	Maximum external pipe radius measured
r_1^{min}	Minimum external pipe radius measured
t_1	Outer pipe wall thickness
t_2	Inner pipe wall thickness
t_c	Core layer thickness
σ_{y1}	Yield stress of the external pipe's steel
σ_{y2}	Yield stress of the internal pipe's steel
σ_{y-X60}	Yield stress of X60 grade steel
Δ	Ovalization parameter
Δr	Imperfection of the pipe radius as a function of θ
ν_c	Core material Poisson's ratio
ν_p	Pipe material Poisson's ratio

6.3. INTRODUCTION

Day by day, world's demand for oil and gas is increasing, even as world's accessible reserves are depleting. Although many governments are concentrating effort on the extraction of energy from alternative sources, it is an irrefutable fact that oil and gas are the most significant sources of our world's energy. As a result, engineers are facing new challenges concerning the extraction of oil and gas from offshore, mostly in remote areas in deep waters. One of the challenging problems facing oil extraction from remote reserves is the development of new transportation pipeline systems to overcome the limitations of the traditionally used pipes. It is a known fact that both the installation and operation of single-walled steel pipes are restricted to a certain depth, because of the excessive buoyancy weight and very thick wall thicknesses required to tolerate the external hydrostatic pressure at such high depths. Moreover, the thermal installation properties required to ensure the flow of the products demand a design configuration that includes an enhanced thermal insulation system as part of the pipeline.

Sandwich Pipes (SPs) are viewed as a clever design alternative that combine the structural attribute of a circular cylindrical sandwich structure along with the required thermal insulation features. In general, SPs consist of two thin-wall steel pipes sandwiching a relatively thicker and softer core. In its first application in the offshore oil and gas industry, this configuration was employed in the so called "Pipe in Pipe" (PIP) configuration, in order to improve the thermal insulation properties of the pipeline. However in PIPs, the core layer does not have any structural attribute; therefore, in the case of deepwater fields, the PIP systems would become excessively heavy in order to offer the required structural integrity. Alternatively, in a SP configuration, the structural properties of the core layer and the interaction between the core layer and surrounding pipes are improved. Therefore, the whole sandwich structure is designed to carry the applied loads. In this system, the internal pipe, also referred to as the product pipe, facilitates the safe transportation of the oil and gas product. The middle layer (i.e. the core layer) is designed based on both structural and thermal insulation perspectives. However, materials with superior thermal insulation properties usually possess inferior structural properties. Therefore, the choice of a proper core material with an optimum thickness requires an optimized design philosophy. A wide range of plastics, gels,

ceramics and composite materials can be considered to form the core layer. The core layer can also be considered as a host for various monitoring sensors, cathodic protection and/or heating system. The exterior layer of the system is the external pipe, also referred to as the carrier pipe, which separates the surrounding environment from the carrying product. Moreover, the secondary containment provided by the external pipe improves the reliability of the system in case of leakage of pipe's fluid.

Designing an optimum pipeline is not possible, unless the behavior of the system under the governing loading conditions is fully characterized. In SPs, the structural response of the system is a function of the structural properties of each individual constituent of the system, as well as their interaction properties. Therefore, due to the large number of parameters involved, understanding the structural behavior of SP systems becomes a complex problem, which has drawn considerable attention in the recent years. Most of the recent works investigating the structural behavior of SPs have considered system's stability. Stability of SPs under external hydrostatic pressure is one of the governing design scenarios in deep waters.

Sato and Patel [6.1], Sato et al. [6.2] and Arjomandi and Taheri [6.3] studied the buckling behavior of SP systems under hydrostatic external pressure and developed simplified solutions for estimating the SP system's buckling capacity through analytical approaches. In another study, Kardomateas and Simitses [6.4, 6.5] analytically studied the stability of long sandwich cylindrical shells, which can be considered as the general configuration of SPs, under uniform external pressure. Ohga et al. [6.6] also studied the reduced stiffness buckling of sandwich cylindrical shells under uniform external pressure, both numerically and analytically.

A vital structural parameter in SP systems is the adhesion properties between the core layer and its surrounding pipes. Castello and Estefen [6.7, 6.8], investigated the ultimate strength of sandwich pipes under combined external pressure and bending, for several degrees of adhesion between the core layer and external pipe. Moreover, Castello and Estefen investigated the effect of cyclic loads, applied during the reeling installation method, on the collapse pressure. In another series of studies, Arjomandi and Taheri [6.3, 6.9] analytically and numerically investigated the influence of various scenarios of bonding between the core layer and both external and internal pipes on the elastic

buckling pressure. The Propagation of local buckling along a pipeline under steady state buckle propagation pressure is a phenomenon that can occur in oil and gas pipelines in deep waters. Several investigations have also been conducted to study this phenomenon. A series of remarkable works by Kyriakides and his coworkers [6.10-6.13] have also considered the buckle propagation phenomena in such pipes from experimental, analytical and numerical perspectives.

Estefen et al. [6.14] also conducted one of the initial feasibility studies on employing sandwich pipes for deep and ultra deep waters; they studied the behaviour of SPs under various loading scenarios, using numerical and experimental approaches. Finally, through a comparative study, Estefen et al. concluded that SP systems can be a viable design alternative for applications in water depths up to 3,000 meters. In another study, Castello et al. [6.15] compared PIP with SP systems designed for hypothetical oil filed with several core materials. Furthermore, several other researchers have performed numerical modeling of a sandwich pipe considering various parameters, and loading and boundary conditions

Arjomandi and Taheri [6.16] demonstrated that although the pressure capacity calculated based on the elastic assumptions could provide a good understanding of the system's response, it cannot be used for most practical designs. In that study, the authors investigated the influence of selected structural parameters on the margin of error when comparing the elastic buckling capacity to the plastic buckling capacities. Their study showed that the magnitude of the error could be excessively large, especially in the case of SPs with a relatively stiff core layer.

In the study presented here, the Finite Element (FE) method is used to build the numerical models which could capture the real response of sandwich pipes. Appropriate forms of initial imperfection, material models, boundary conditions and FE parameters were considered. A comprehensive parametric study on more than 3800 SP configurations with practical design parameters was performed. By accounting for both geometry and material nonlinearities, the characteristic response of the system was captured and the influence of each design parameter was discussed. A wide range of structural design parameters was considered. These included: various grades of steel

pipes (in the range of X60 to X120), various core layer stiffnesses and thicknesses and a range of steel pipe dimensions per API 5L specifications [6.17].

Former studies have revealed that developing a closed form equation for calculating the plastic buckling pressure of sandwich pipes is unfeasible. As the main objective of this study, therefore, an attempt has been made to develop a practical and simplified equation for evaluating the plastic capacity of SPs, based on the finite element approach. It will be demonstrated that the developed equation would be capable of calculating the pressure capacity of SPs with practical design configurations with an error margin less than 10%. Finally, through an optimization procedure, the material and geometry of the sandwich pipe system will be optimized for water depths up to 10,000 meters.

6.4. THEORY AND MOTIVATION

Sandwich pipes used in the oil and gas industry are generally long circular cylindrical structures consisting of two concentric steel pipes sandwiching a softer core layer. In such a configuration, the structural properties of the system, boundary conditions and applied load along the pipeline longitudinal axis are uniform; therefore, it would be admissible to consider the behavior of such a system, subject to hydrostatic external pressure, as a 2-D problem in the polar coordinates, as shown in Figure 6.1.

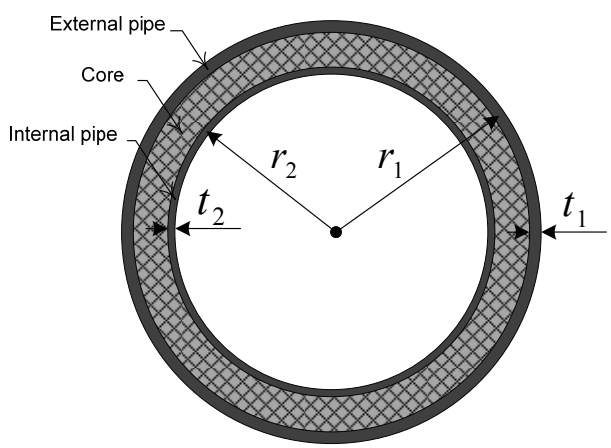

Figure 6.1. Idealized geometry of the sandwich pipes.

In the case of elastic structures, the elastic buckling pressure of the system represents the pressure capacity of the system. Brush and Almroth [6.18] and Sato and Patel [6.1] proposed an analytical solution for calculating the buckling capacity (designated as P_{cr}-

BASP, hereafter), by simplifying the problem and determining the buckling pressure of a ring internally supported by an elastic foundation. They proposed the following equation:

$$P_{cr-BASP} = P_{crs} + \frac{1}{n^2 - 1} k \tag{6.1}$$

where:

$$k = E_c \frac{2n(\upsilon_c - 1) - 2\upsilon_c + 1}{4\upsilon_c^2 + \upsilon_c - 3} \tag{6.2}$$

and P_{crs} is the buckling pressure of the external pipe, obtained by:

$$P_{crs} = \left(\frac{t_1}{r_1}\right)^3 \frac{E_p(n^2 - 1)}{\left(1 - \upsilon_p^2\right)\left(\left(\frac{t_1}{r_1}\right)^2 + 12\right)} \tag{6.3}$$

The investigation by Arjomandi and Taheri [6.3] illustrated that above equation's prediction of the buckling pressure involves relatively very large margins, especially for those SPs with thick and soft core. It was hypothesized that the large margin of error was caused by the large number of simplifying assumptions made in developing the final equations. For instance, in deriving Equation (6.1), it was assumed that internal pipe's geometry and core layer's geometry would not influence the buckling pressure. However, our former studies have revealed that these parameters can significantly influence both the characteristic response and the pressure capacity of the pipe [6.9, 6.16]. Another assumption that limits the applicability of this equation is the preselected pattern of the buckling mode. A same sinusoidal pattern in the polar coordinates was also assumed for all three layers of the pipe. This assumption introduces a large error margin to the final equation in some design configurations.

In order to improve the accuracy of the equation, Arjomandi and Taheri [6.3] developed a modified solution; moreover, in developing their equation, they considered a larger number of effective structural parameters than the earlier solutions; moreover, the influence of the external pipe, the internal pipe and the core layer was considered separately. Furthermore, the adhesion between the layers was included in their solution. Although the proposed solution can predict the buckling pressure of SPs having relatively soft or thick core materials with improved accuracy, it does not produce reasonable accuracy for all design configurations. According to the proposed solution, for the design configurations where the core layer is bonded to the surrounding pipes, the buckling

pressure of the sandwich system can be calculated using the following simplified equation [6.9]:

$$P_{cr-AT} = \frac{\xi_1}{\xi_2} \tag{6.4}$$

where P_{cr-AT} signifies the critical buckling capacity based on Arjomandi and Taheri's solution, and

$$\begin{aligned}\xi_1 = 192E_c^2 a_1 {r_1}^3\left(\upsilon_p^2 - 1\right)^2 + E_p^2 {t_1}^4 n^2 \Lambda (n^2 - 1)(\Lambda + 7)^2 \\ + 2E_c E_p r_1 t_1\left(\upsilon_p^2 - 1\right)(\Lambda + 7)\{{t_1}^2 n^2[n(\Lambda - 1) - \Lambda - 1] \\ - 6t_1 r_1[(n+1)^2 + (n-1)^2\Lambda] - 12{r_1}^2[n(\Lambda - 1) - \Lambda - 1]\}\end{aligned} \tag{6.5}$$

$$\begin{aligned}\xi_2 = r_1\left(\upsilon_p^2 - 1\right)(\Lambda + 7)\{-12E_c {r_1}^2 a_1\left(\upsilon_p^2 - 1\right)[n(\Lambda - 1) - \Lambda - 1] \\ + E_p t_1 n^2 \Lambda ({t_1}^2 + 12{r_1}^2)(\Lambda + 7)\}\end{aligned} \tag{6.6}$$

where parameter Λ is defined as:

$$\Lambda = 4\nu_c - 3 \tag{6.7}$$

As mentioned above, all of the proposed analytical closed form solutions developed thus far for predicting the elastic pressure capacity of the system have not considered material nonlinearity. However, a previous work of Arjomandi and Taheri [6.16] revealed that the consideration of material plasticity leads to a significantly reduced pressure capacity for the system. Figure6.2 illustrates the results comparing the external pressure capacities calculated using the mentioned approaches, with elastic and plastic material behavior assumptions. In this figure, a practical sandwich pipe configuration has been considered and the effect of altering the external pipe thickness to radius ratio is studied. This study shows that Equation (6.1) significantly over predicts the elastic buckling pressure in comparison with the FE linear perturbation analysis results; the error margin produced by this equation is larger for SPs with a relatively thick core layer or with a relatively thin-wall external pipe. It can be seen in Figure 6.2 that within the considered parameter range, the above simplifying equation developed by the authors can predict the elastic buckling pressure capacity with improved accuracy. However, both of the simplified equations developed through analytical approaches still produce results with considerably large error margins when compared with the linear perturbation FE results.

Figure 6.2 also illustrates a comparison between the pressure capacity of the system calculated from models with elastic and plastic materials. As can be seen in the figure, by

increasing the thickness of the external pipe, the influence of material plasticity becomes more significant. It should be mentioned that besides the geometrical parameters, whose effects are accounted for in both the elastic and plastic models, some material parameters (such as the yield strength) would have more influence on the pressure capacity. In summary, it was found that with the exception of a limited number of design configurations, which are considered mostly impractical, plastic buckling would be the predominant failure mode. Therefore, for most practical design configurations, the use of the abovementioned simplified solutions or FE linear perturbation methods for calculating the pressure capacity of SPs would be erroneous and impractical.

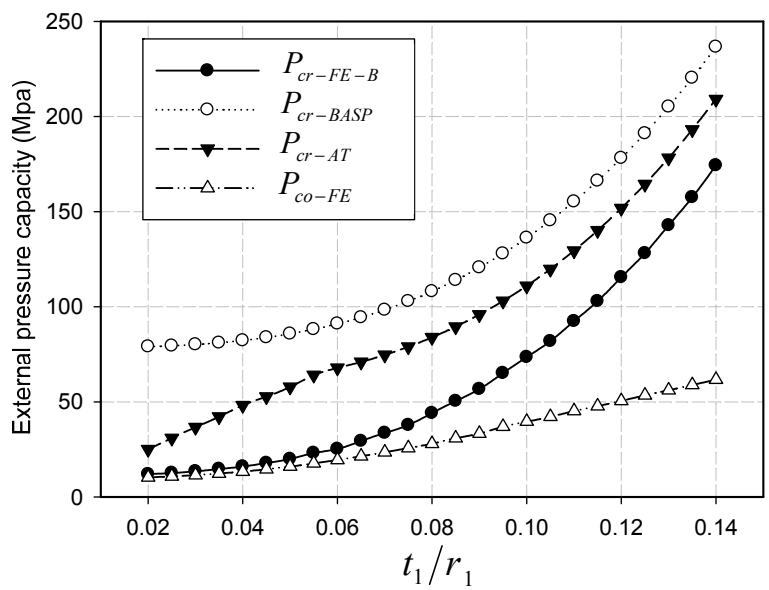

Figure 6.2. Comparison of the pressure capacity calculated through different approaches for a sandwich pipe with $t_2/r_2 = 0.03$, $r_2/r_1 = 0.85$ *and X60 grade steel internal and external pipes.*

6.5. PARAMETRIC STUDY

In general, Equation (6.8) represents the relationship between the pipe's external pressure capacity as a function of the influencing parameters.

$$P_{cr} = f\left(E_c, E_p, t_1, r_1, t_2, r_2, \upsilon_p, \upsilon_c, \sigma_{y1}, \sigma_{y2}, imp\right) \tag{6.8}$$

The aim of this study is the investigation of the behavior of a series of SPs with practical SP with practical configurations, subject to hydrostatic external pressure.

Therefore, those parameters which are not variables in practical designs, or have less influence on the pressure capacity of the system, have been taken as constants. These parameters areυ_p, υ_c and imp, which are taken as 0.3, 0.4 and 0.005, respectively. Furthermore, to improve the efficiency of the results, the pipeline parameters are nondimensionalized and the final equations and conclusions are drawn based on the nondimensionalized parameters. Inspired by the analytical closed-form solutions proposed in the literature for the elastic buckling pressure, the structural parameters are nondimensionalized as listed in Equation (6.9). Moreover, the studies related to the elastic buckling analytical solutions have shown that the elastic buckling pressure can be nondimensionalized with respect to the steel pipes elastic modulus. As will be seen, in the case of plastic buckling of SPs, similar nondimensionalized parameters can be used without significant loss in accuracy.

$$\frac{P_{cr}}{E_p} = f\left(\frac{r_2}{r_1}, \frac{t_1}{r_1}, \frac{t_2}{r_2}, \frac{E_c}{E_p}, \frac{\sigma_{y1}}{E_p}, \frac{\sigma_{y2}}{E_p}\right) \tag{6.9}$$

In our parametric studies the selected range of the nondimensionalized parameters cover the more practical range of SP design. Steel pipes' *t/r* ratio range has been chosen based on the API 5L standard wall pipelines. Figure 6.3 illustrates the distribution of API standard wall pipes with respect to t/r. This histogram only includes pipes with specified outer diameters greater than 5 inches. As can be seen in the figure, the variation of the t/r ratio in the steel pipes, which are practically applicable in SP systems, is 0.03 to 0.09, which is the studied range in this paper.

Moreover, the parameters r_2/r_1 and E_c/E_p are selected based on a practical thickness range and practical materials suitable for the core layer. Other design parameters for SPs are the internal and external steel pipes' grades. In the numerical models, different steel grades for the internal and external pipes are considered; here, a range of grades consisting of X60, X80, X100 and X120 are studied. Table 6.1 summarizes the selected range for each parameter. The combination of these parameters generates 3,840 SP configurations, which covers a wide range of practical SP designs.

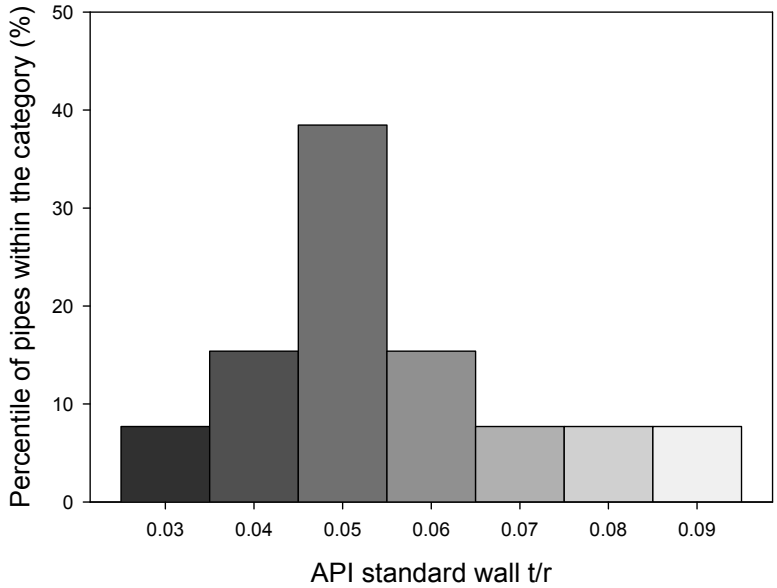

Figure 6.3. Distribution of API steel pipes with respect to the pipe thickness to radius ratio.

Table 6.1. Range of the parameters used in the parametric study.

r_2/r_1	t_1/r_1	t_2/r_2	E_c/E_p	σ_{y1}/E_p	σ_{y2}/E_p
0.70	0.03	0.03	0.001	0.001998 (X60)	0.001998 (X60)
0.75	0.05	0.05	0.01	0.002665 (X80)	0.002665 (X80)
0.80	0.07	0.07	0.1	0.003331 (X100)	0.003331 (X100)
0.85	0.09	0.09		0.003997 (X120)	0.003997 (X120)
0.90					

6.6. FINITE ELEMENT MODELS

The Finite Element (FE) method has been adopted to build a set of quasi 2D models, representing the cross section of a sandwich pipe having an infinite length. Figure 6.4 illustrates the general geometry and FE mesh of the models. The FE package, Abaqus/CAE [6.19], was employed for creating and analyzing the models. Python, the

programming language within the ABAQUS, was used to create and manage the parametric study's files. Moreover, a MATLAB [6.20] code was developed for extracting and processing the desired results from the Abaqus output files.

In order to allow the FE models to deform into nonsymmetrical patterns, or to capture the higher buckling modes, a full circular section with a minimum number of boundary conditions was modeled. By mesh convergence studies, it was determined that an FE mesh consisting of 40 elements in the circumferential direction and one row of elements for modeling each layer would be adequate for creating an efficient mesh to capture the characteristic behavior with reasonable accuracy. The Abaqus element C3D20R, a 20 nodes reduced integration brick element, was chosen for meshing both the steel pipes and core layer. This element type was selected based on a comparative study between various types of elements, which took into account the accuracy of the results, computation efficiency and avoidance of shear and volumetric locking. Furthermore, for this study, it was assumed that the core layer is fully bonded to both the internal and the external pipes. Therefore, the interaction between the layers was modeled by bonding together all the active degrees of freedom of the nodes located on the interfacing surfaces. The Multi Point Constraint (MPC) function in Abaqus was used for this aspect of the modeling.

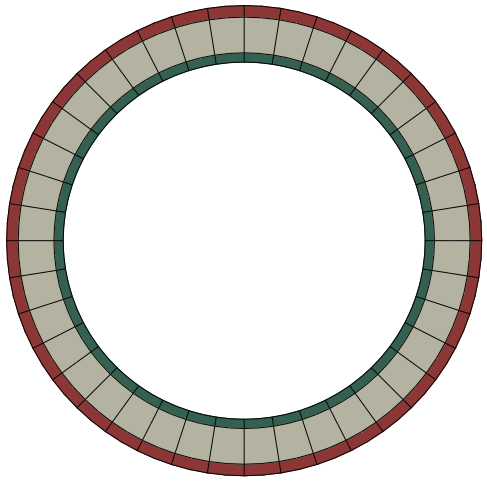

Figure 6.4. General geometry and FE mesh.

One of our previous studies [6.16] illustrated that material stress-strain curve's profile, after the yield point, would not exert a significant influence on the pressure

capacity of the sandwich pipes. The influence of steel's behavior was further examined by considering three different stress-strain profiles: an Elastic Perfectly Plastic (EPP) profile, an elastic regime followed by an exponentially hardening behavior and lastly, a material model consisting of an elastic regime followed by Lüder's banding and an exponentially hardening response. Their study showed that models created with the EPP steel materials could effectively capture the characteristic behavior and pressure capacity of the system without a significant loss of accuracy. Therefore, in this study, the external and internal pipes were modeled using the EPP material model with various yield stresses. The steel material properties were extracted from API 5L [6.17]. Furthermore, for simplicity and because most polymeric materials have a greater yield strain in comparison to steel, the core layer was modeled using an elastic material model.

In the real world, no perfect system exists and all structural systems suffer from some type of imperfections, which could be embedded in the geometry, boundary condition and/or applied loads. Therefore, in order to enable the numerical models to capture the real response of the system, some form of imperfection should be applied to the system. In this study a geometrical imperfection, in the form of an initial ovality, was applied to the pipeline cross section. This imperfection can be defined by Equation (6.10) for each layer of the system.

$$\Delta r_i = imp \times r_i^o \cos 2\theta \quad , \quad i = 1,2 \tag{6.10}$$

In this equation imp is the imperfection magnitude which is taken as 0.005 for all three layers.

Considering the nature of the problem, the external pressure should be applied in a load controlled fashion. Moreover, due to the resulting numerical instability in such modeling, attention must be paid to the magnitude of the applied pressure, the initial step size and the minimum allowable step increment related to the nonlinear solver module. In this study, in order to streamline the numerical models, the applied pressure is set as the buckling pressure calculated by Equation (6.4) Another numerical issue which can be encountered is the susceptibility of the models in responding as if they were under external traction, which can be due to the very small magnitude of the imperfection, combined with the effect of the Arc-Length method used for solving the nonlinear

equations. To avoid this problem, it would be necessary to set the first increment size and the minimum size of the remaining increments to a sufficiently small value, so to facilitate the solution. In summary, in order to build efficient FE models, which are both computationally efficient and capable of capturing the response accurately, the FE solvers' parameters must be selected carefully.

6.7. PARAMETRIC STUDY RESULTS

In this section the characteristic behavior of the system is captured by monitoring the ovality magnitude of the external pipe. The ovality magnitude is established by the following equation:

$$\Delta = \frac{r_1^{max} - r_1^{min}}{r_1^{max} + r_1^{min}} \tag{6.11}$$

Moreover, the influence of the significant structural parameters on the characteristic response and the pressure capacity of the system is demonstrated. The influence of structural parameters such as the steel pipes t/r ratio, core thickness and the grade of steel pipes will be studied for individual parameter. Furthermore, because the effect of the structural parameters may be different when core materials with different stiffness are used, all other parameters' effects are illustrated as a function of the core stiffness. Moreover, the effect of changing the parameters is also shown by illustrating the plastic contours of the system under the capacity pressure.

*6.7.1. Influence of the steel pipes thickness to radius (*t/r*) ratio*

The thickness to radius ratios of the external to internal pipes are two of the main design parameters that affect the buoyancy weight of the pipeline, its cost and the pressure capacity. Figure 6.5 illustrates the influence of changing the thickness of either the internal or external pipes on the characteristic behavior of SP configurations. Two different values of core stiffness are examined. Figure 6.5.a shows the characteristic response of a pipe with a r_2/r_1 value of 0.8 and an E_c/E_p value of 0.01 for various internal and external pipes' t/r. The solid curves illustrate the response of pipes with varying t_1/r_1 ratios in the range of 0.03 through 0.09, while the dashed lines show the effect of changing the internal pipe thickness for varying t_2/r_2. As can be seen in the

figure, as expected, increasing the thickness of either the external or internal pipes improves the capacity of the system; however, this improvement is slightly greater than that seen in the case when external pipe's thickness is increased.

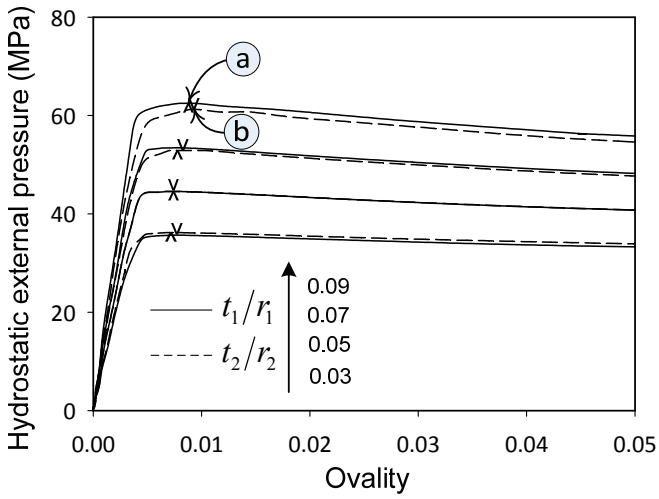

(a)

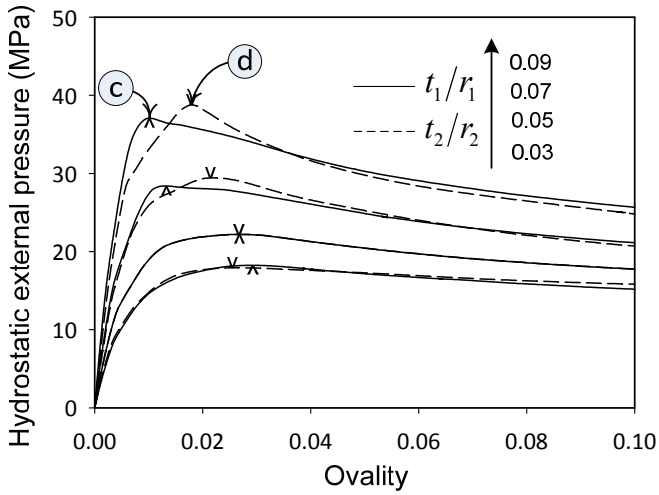

(b)

Figure 6.5. Influence of the steel pipe's thickness to radius ratio on the characteristic behavior of sandwich pipe with $r_2/r_1 = 0.8$ *and X60 internal and external pipes (a)*$E_c/E_p = 0.01$ *(b)* $E_c/E_p = 0.001$.

Figure 6.5.b shows the response for similar sandwich pipes, but with softer core material. For this case, it is interesting to note that an increase in the internal pipe's

thickness improves the pressure capacity of the system more than that observed in the previous case. This phenomenon is in complete contrast to the design philosophy of PIP systems. In PIP systems it is assumed that the external pipe's contribution in controlling the pressure capacity is larger than that of the internal pipe. Therefore, in the design of a PIP, the external pipe is designed to carry the external pressure and the capacities of the core layer and internal pipe are completely ignored. As can be seen in the figure, both the internal and external pipes in SP systems do indeed contribute to carrying the external pressure, and in the case of softer cores, which are customarily used more often in PIP systems, the internal pipe would contribute even more if proper adhesion is provided between the layers.

This phenomenon of the internal pipe having a greater contribution on the pressure capacity than the external pipe can be explained by considering the characteristic path of the system and the distribution of the equivalent plastic strain under the ultimate pressure. By comparing the characteristic paths of the abovementioned SPs, it can be concluded that SPs with softer core are more deformable before reaching to the buckling pressure. Moreover, as can be seen in Figure 6.5, increasing the thickness of the external pipe would decreases the deformability of the system while increasing the thickness of the internal pipe does not significantly change the deformability of the system before reaching to the buckling pressure. Therefore, employing thicker external pipes improves the pressure capacity of the system and also decreases the deformability of the system. In contrast, using thicker internal pipes would improve the pressure capacity, but would not change the deformability significantly.

Figure 6.6 shows the equivalent plastic strain contours for four of the SP configurations at the ultimate capacity. A comparison between the plastic strain contours shows that in the sample SPs with stiffer cores, the internal pipe undergoes plastic strains. For the case of SPs with softer cores, no plastic strain occurs in the internal pipe. A study of the plastic strain contours for either of the configurations having thicker wall external pipes illustrates that employing thick-walled external pipes would increase the compressive stress concentration, which in turn would cause in external pipe's instability, and consequently the collapse of the whole system. Therefore, it can be concluded that in

designing structurally optimum SP systems, both system's stiffness and ductility must be considered.

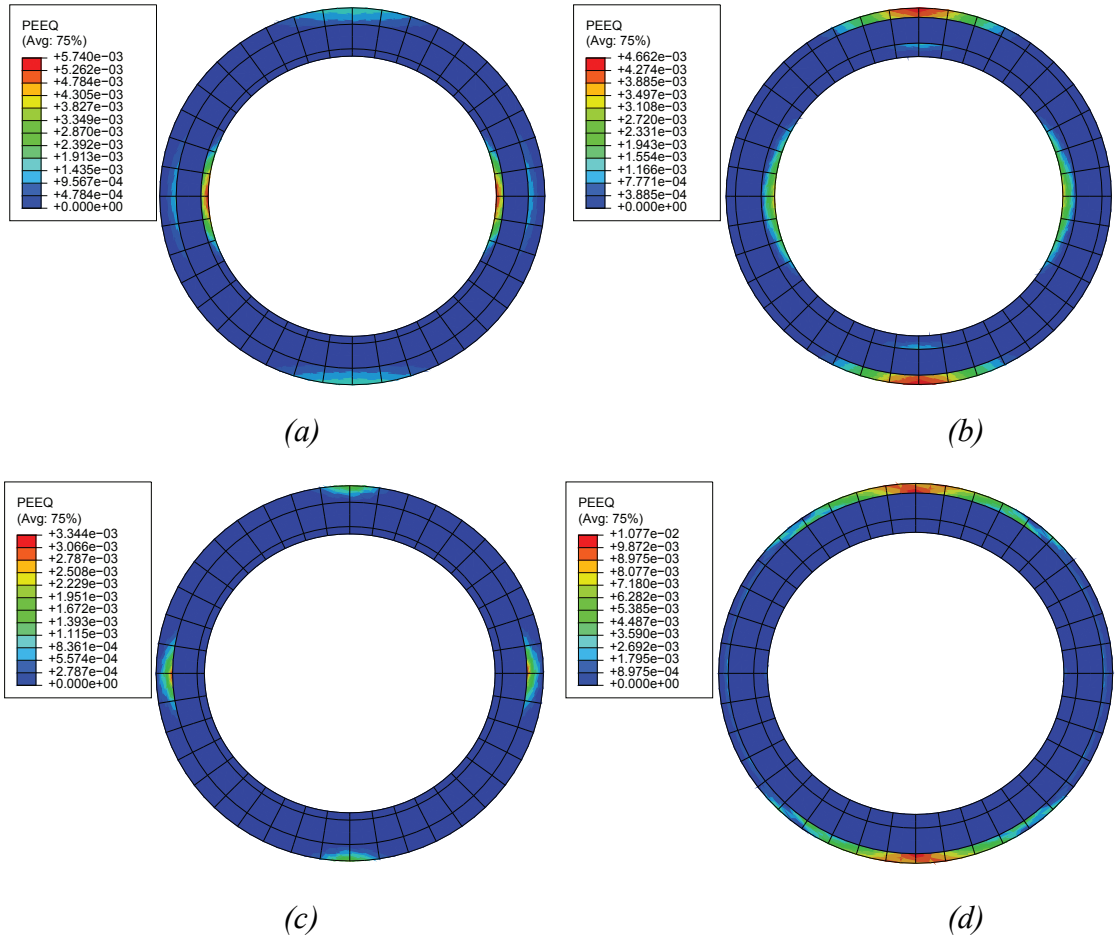

Figure 6.6. Equivalent plastic strain contours for the selected SP configurations. (a) $t_1/r_1 = 0.09$ *(b)* $t_1/r_1 = 0.05$*, both with* $E_c/E_p = 0.01$*. (c)* $t_1/r_1 = 0.09$ *(d)* $t_1/r_1 = 0.05$*, both with* $E_c/E_p = 0.001$*.*

As mentioned earlier, the influence of t/r ratios (of the internal and external pipes) on the pressure capacity of SP systems is also dependent on the other parameters. The results of a study on the effect of steel pipes' dimensions for a set of SP configurations having various internal and external pipe steel grades and core stiffnesses are demonstrated in Figure 6.7. In this figure, the change in the pressure capacity of SPs with core stiffness ratios ranging from 0.001 through 0.1 is illustrated as a function of the internal and external pipes' t/r ratios for various grades of steel. The solid lines in the figure illustrate the pressure capacity of SPs with an internal pipe steel grade of X60 and external pipe

with steel grades ranging from X60 through X120. The dashed lines show the effect of changing the internal pipe's steel grade (from X60 to X120) by maintaining the external pipe's steel grade constant (i.e., X60).

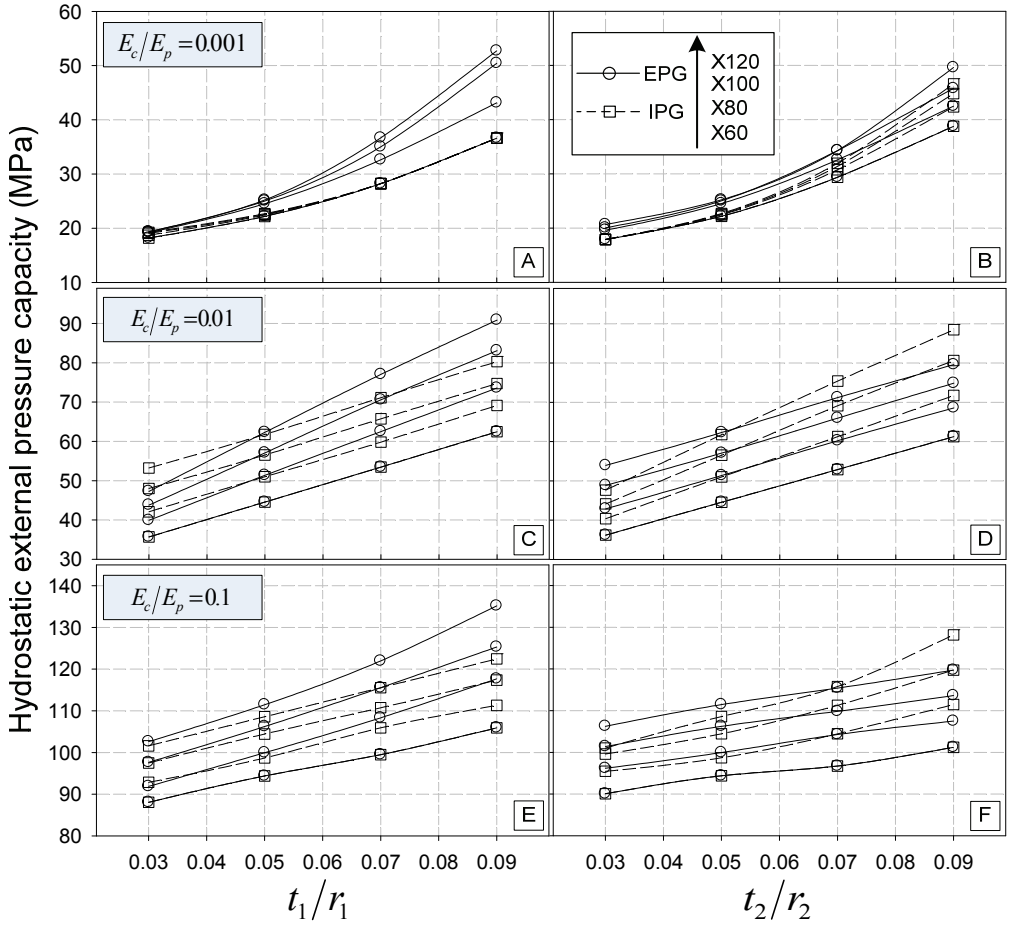

Figure 6.7. Influence of steel pipe's thickness to radius ratio on the pressure capacity of SPs with various core stiffness ratios and $r_2/r_1 = 0.8$.

The analysis of the results reveals that increasing either the t_1/r_1 or t_2/r_2 parameter improves the pressure capacity significantly; however, this improvement is more significant for the SPs with stiffer cores. Additionally, the comparison of the results further indicates that increasing either the internal or external pipe's steel grade would enhance the capacity significantly. However, the degree of enhancement is inter-dependent on the internal and external pipes' t/r ratio. It is obvious that enhancing the internal pipe's steel grade would have a greater influence on the pressure capacity of the SP configurations in which more robust internal pipes are employed rather than the same

system, but with thicker wall external pipes. Similarly, enhancing the external pipe's steel grade would have a greater capacity enhancement in the SP systems with thicker wall external pipes than the systems with thicker wall internal pipes. Another interesting conclusion is that upgrading the internal pipe's steel grade would not improve the external pressure capacity of the system when the relatively stiffer core (i.e. $E_c/E_p = 0.1$) is used. Moreover, in the case of such stiff core SPs, even upgrading the external pipe's steel grade would not increase the pressure capacity significantly for pipes with smaller t/r ratios.

It should be mentioned that as the results presented in Figure 6.7 reveals, the contribution of upgrading either the external or internal pipe's steel grade in improving the capacity would be more than that obtained by increasing the t/r ratio of the steel pipes. For instance, Figure 6.7.E shows that an SP with a t_1/r_1 of 0.05 and an external pipe steel grade of X80 would have a greater capacity in comparison with the same SP with a t_1/r_1 of 0.07 and an external pipe steel grade of X60. As a result, one can use a SP with a relatively thinner, but higher grade steel pipes, as a more feasible alternative to pipelines with large diameter. However, when considering such an alternative, one should pay special attention to the welding procedure.

In conclusion, designing SPs necessitates a tradeoff between pipes' steel grade and their geometrical properties. Therefore, designing an optimum SP would not be possible, unless the interaction of the mentioned parameters is taken into consideration.

6.7.2. Influence of the Core thickness

The thickness of the core layer in SP systems should be determined based on the required structural and thermal demands. From a structural point of view, changing the thickness of the core layer can change both the pressure capacity and the stability characteristic path of the system. Figure 6.8.a and b show the characteristic behavior of a sandwich pipe with t_1/r_1 and t_2/r_2parameters equal to 0.05 and a core stiffness ratio of 0.01 up to the ovality magnitude, Δ (Eqn. 11), of 0.3 and 0.02, respectively. In this case study, both the internal and external pipes' steel grades are taken as X60. As can be seen in the figure, the thin core SP behaves like a typical single wall pipe. In this category of SP, the magnitude of the ovality increases by increasing the magnitude of the applied

pressure in a linear fashion, up to the buckling pressure. After reaching this point, the pipe becomes unstable and collapses. On the other hand, the thick SP has a different characteristic behavior.

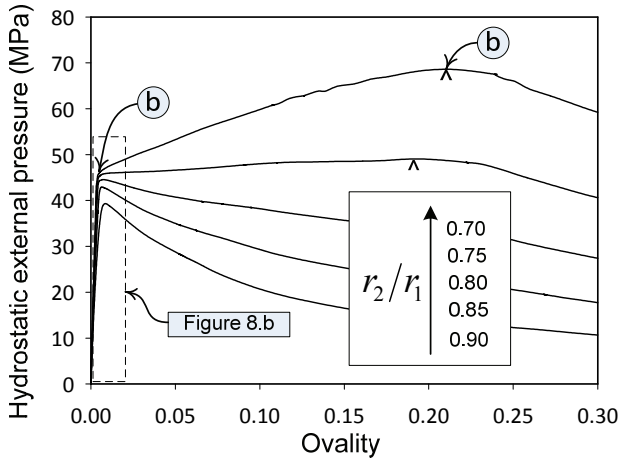

(a)

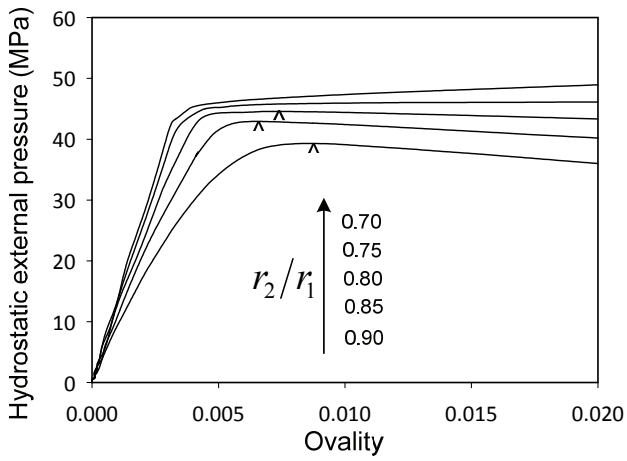

(b)

Figure 6.8. Influence of the core thickness on the characteristic behavior of SPs with $t_1/r_1 = t_2/r_2 = 0.05$ *,* $E_c/E_p = 0.01$ *and X60 grade steel internal and external pipes. Characteristic paths are shown up to the ovality magnitude of (a) 0.3. (b) 0.02.*

As also seen in Figure 6.8.a, for the pipes with core thickness ratios of 0.75 and 0.7, the ovality of the pipe linearly increases as the magnitude of the applied pressure reaches to the first proportional limit, and keeps increasing until it reaches a limiting value. As can be seen in the figures, in configurations with relatively thick cores ($r_2/r_1 = 0.75$ and

$r_2/r_1 = 0.70$), the SPs would become unstable, with much larger ovality magnitudes than those configurations with relatively thin core layers.

The plastic strain contour of the sample SP under the first pressure limit is illustrated in Figure 6.9.a. After reaching to this first limit state, the material and geometrical nonlinearities change the stiffness of the system despite the fact that the whole system remains stable. The second stable path is the path between point a and b in Figure 6.8, where point b represents the pressure capacity of the system. The plastic strain contours of the SP configuration with r_2/r_1 of 0.7 at the first proportional limit, and at the ultimate pressure are illustrated in Figure 6.9.b. In summary, the core thickness parameter is an important parameter, not only for designing a SP under external pressure, but also when the deformability of pipe's cross section is of concern.

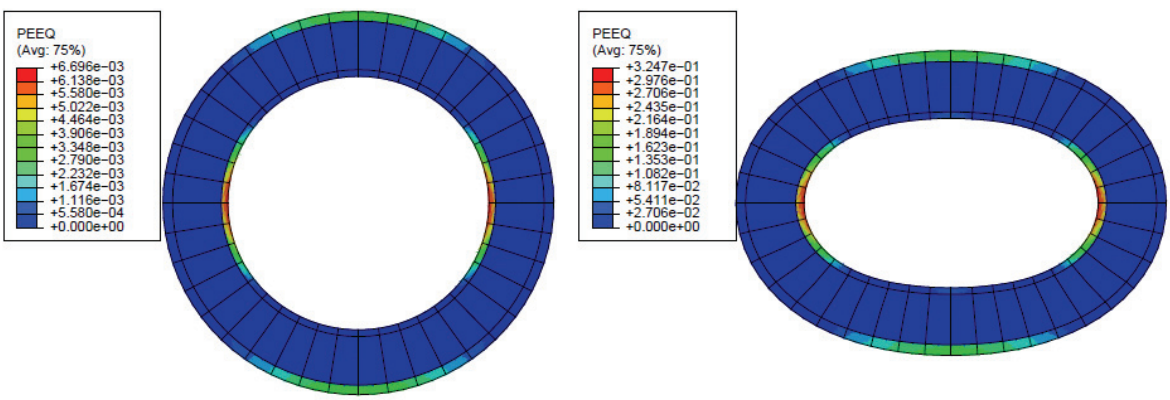

Figure 6.9.Equivalent plastic strain contours at (a) the first proportional limit of the external pressure capacity (b) the ultimate external pressure capacity.

In order to further demonstrate the influence of the core thickness, the pressure capacities of two sets of SPs with various steel pipes' t/r are illustrated in Figure 6.10. The left column figures show the effect of core thickness in SPs with a t_1/r_1 ratio of 0.07 and at_2/r_2 ratio of 0.03 for various steel grades for the internal and external pipes. The figures on the right column present the variation of the same quantities but for SP systems with t_1/r_1 and t_2/r_2ratios equal to 0.05. As can be seen in all of the configurations, increasing the core thickness increases the pressure capacity of the system. However, the magnitude of this enhancement is highly dependent on the stiffness of the core material. For a core material with a greater stiffness, the enhancement due to

the core thickness is greater. The other significant parameters are the internal and external pipes' steel grades. The influence of these parameters on the magnitude of the pressure capacity is more complicated than can be described by a simple and unified relationship. However, it can be said that upgrading the external pipe's steel would always improve the pressure capacity of the system; nonetheless, the influence of the internal pipe's steel grade is dependent on the other SP configuration parameters.

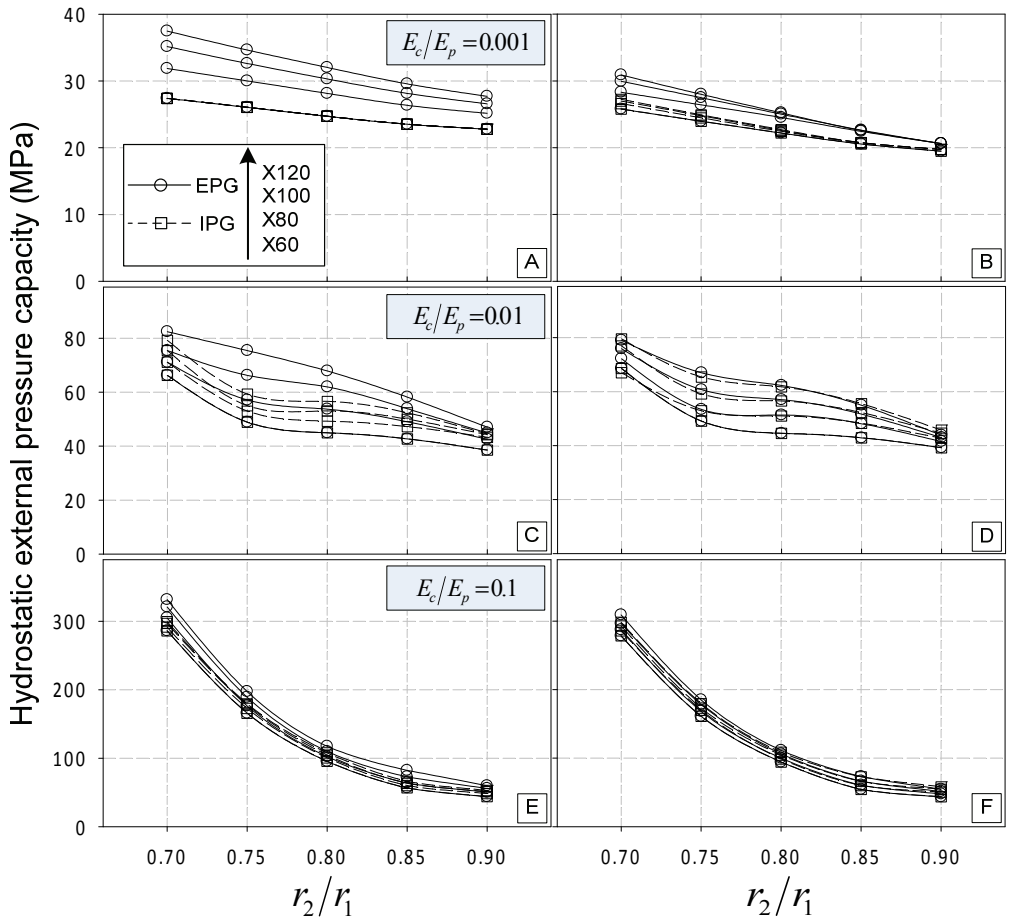

Figure 6.10. Influence of the core thickness on the pressure capacity of sandwich pipes with various core stiffness ratios and X60 internal and external pipes. (Left column) pipes with $t_1/r_1 = 0.07, t_2/r_2 = 0.03$. (Right column) pipes with $t_1/r_1 = t_2/r_2 = 0.05$.

6.7.3. Influence of the Steel pipes grade

The influence of the internal and external pipes steel grades on the pressure capacity of SPs was discussed above, including the influence of other interacting parameters. In summary, no general conclusion can be made in regards to whether an improvement to

the internal or external pipes' grade would result in a significant improvement to the system's capacity. Figure 6.11 further supports our conclusion; it illustrates the characteristic path of a sample set of SPs with a r_2/r_1 ratio and core stiffness ratio of 0.8 and 0.01, respectively. As can be seen, the influence of upgrading the external pipe's steel from X60 to X80 on the external pressure capacity is considerable; however, upgrading the external pipe's steel to higher grade than X80 does not improve the pressure capacity by a significant margin. Likewise, improving internal pipe's grade beyond X60 produces insignificant improvement to SP's pressure capacity. It should be noted that, upgrading pipes' steel would enhance the cross section deformability in the pre-buckling regime.

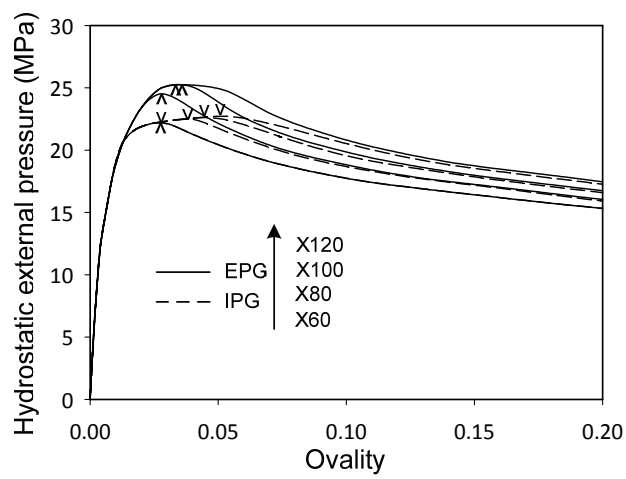

Figure 6.11. Influence of the steel pipe's grade on the characteristic behavior of a sandwich pipe with $r_2/r_1 = 0.8$ and $E_c/E_p = 0.01$.

6.8. A SIMPLIFIED AND PRACTICAL EQUATION

Due to the relatively wide range of parameters involved in the analysis of SPs, one cannot feasibly develop a simple equation by which one could determine the pressure capacity of SPs with all the possible configurations, with a reasonable degree of accuracy. Therefore, Equation (6.9) has been reconfigured, in the following form:

$$\frac{P_{CO}}{E_p} = a\left(\frac{t_1}{r_1}\right)^b \left(\frac{t_c}{r_1}\right)^c \left(\frac{\sigma_{ye}}{E_p}\right)^d + e\left(\frac{t_1}{r_1}\right)^f \left(\frac{t_2}{r_2}\right)^g \left(\frac{t_c}{r_1}\right)^h \left(\frac{\sigma_{yi}}{E_p}\right)^i + j\left(\frac{t_1}{r_1}\right)^k \left(\frac{t_2}{r_2}\right)^l \left(\frac{t_c}{r_1}\right)^m \tag{6.12}$$

Note that In order to employ the above design equation, the 13 constants (*a, b, . . . , m*) should be established for each core stiffness magnitude. In this study, constants' values were established for three core stiffness ratios (i.e., 0.001, 0.01 and 0.1), which cover most of the cores used in practice. These values are tabulated in Table 6.2. Therefore, Equation (6.12) can be effectively used to estimate the pressure capacity of most SPs used in the industry. In order to calculate the constants, a MATLAB [6.20] code was developed to extract the pressure capacities from the characteristic paths of the SPs analyzed by the Abaqus. A total of 1280 models were developed and analyzed for each core stiffness ratio; therefore, the results obtained from the analysis of a total of 3840 models were used to establish the constants. The SPSS statistical package [6.21] was used to fit Equation (6.12) to the FE results, and the value of constants were established. A constrained nonlinear regression algorithms recommended by Gill et al [6.22], with a sequential quadratic programming method was used for this purpose. Subsequently, another MATLAB code was generated to further improve the accuracy of the equation, by seeking the constants values in the vicinity of the values calculated by the SPSS. As can be seen in Table 6.2, the maximum error produced by Equation (6.12) with respect to the predicted capacity of SP systems with core stiffness ratios of 0.001, 0.01 and 0.1 are respectively 9%, 15% and 19%. It should be noted that indeed the error margins are in general much smaller than those noted above. The relatively larger error margins are associated with a few SP configurations; those consisted of relatively very thick internal and very thin external pipes, or those with either very thin or very thick core layer. For example, if SPs having r_2/r_1 ratio of 0.9 and t_1/r_1 ratio of 0.03 are excluded from the design configurations, Equation (6.12) is capable of predicting the pressure capacity with less than 10% margin of error for all the core stiffness ratios.

It should be mentioned that Equation (6.12) was developed for calculating the pressure capacity of the system with a reasonable accuracy. However, if the intention is to design a SP system, the above equation should be modified using the appropriate statistical methods, so the predictions would be more con the conservative side.

Table 6.2. Values of the constants appearing in Equation (6.12) for calculating the pressure capacity of SPs

E_c/E_p	a	b	c	d	e	f	g	h	i	j	k	l	m	**Max error %**
0.1	2.032	0.909	0.377	1.055	0.759	0.152	0.884	-0.224	1.021	7.250E-02	-0.067	-0.094	3.833	9.58
0.01	0.765	1.068	0.253	0.890	0.422	0.148	0.947	0.112	0.777	6.020E-05	-0.943	-0.689	3.871	15.08
0.001	1.406	2.102	-0.134	0.747	0.231	-0.016	2.742	-0.515	0.317	2.457E-04	-0.244	0.206	1.133	19.31

Moreover, our findings indicate that a linear relationship exists between SPs' capacity and the logarithmic value of the core stiffness ratio. As a result, Equation (6.12) can also be used for predicting the pressure capacity of the SPs whose core stiffness falls within the range noted in Table 6.2.

6.8.1. Comparison with the experimental results

There have been only a few experimental studies documented in public domain in reference to characterization of the external pressure capacity of SP systems. One of the notable one is that by Estefen et al. [6.14], who conducted an experimental study on small scale specimens. Estefen and his coworkers investigated the pressure capacity of SPs consisting of inner and outer aluminum tubes sandwiching a polypropylene core layer. Two sets of pipe configurations, with two pipes in each set, were experimentally investigated. Table 6.3 shows their pipes' configurations and experimental results, as well as the pipes pressure capacity calculated using Equation (6.12). The comparison between the predicted values obtained using Equation (6.12) and the experimental results shows good agreement. In fact, for the SPs with thicker core layer, the proposed equation in this study can calculate the pressure capacity with an error margin of only 8.22%. However, the error produced by Equation (6.12) in calculating the capacity of the SP with the thinner core is as great as 26.91%.

Table 6.3. Comparison of the experimental and numerical results produced by Estefen et al. [6.14] with the pressure capacities calculated by Equation (6.12).

Specimen	r_2 (mm)	t_2 (mm)	t_c (mm)	t_1 (mm)	P_{CO} Experiment (MPa)	P_{CO} Numerical (MPa)	P_{CO} Eq. 12 (MPa)	% error Exp.vs Eq.12	% error Exp.vsNum.
PIP.M2.G1.I02	23.14	1.68	11.26	1.62	37.64	39.56	37.62	8.22	14.00
PIP.M2.G1.I03	23.26	1.62	11.10	1.61	31.14	38.27	36.24		
PIP.M2.G2.I01	23.27	1.70	4.62	1.46	20.31	20.84	23.51	26.91	16.75
PIP.M2.G2.I02	23.33	1.69	4.69	1.49	17.13	22.42	23.65		

The comparison between the experimental results of Estefen et al. [6.14] with their own numerical results shows that the average errors for the thicker and thinner cases are respectively 14.00% and 16.75%. This comparison indicates that even the use of sophisticated finite element modeling would still produce a relatively large error margin

for some configurations. It should be noted that the error margins noted in the table should not be all attributed to the developed equations. Indeed there could be error due to the manufacturing related anomalies when preparing the test articles, the test procedure and the configuration of the numerical models developed by Estefen *et al*. Therefore, the error margins noted above would not necessary indicate the margin of inaccuracy of the developed equations in this study. It should be noted that if one ignores the predicted result of Equation (6.12) for the PIP.M2.G2.I02 specimen, then the maximum error produced by Equation (6.12) would be 15.75% for the SPs with thicker core layers. It can be therefore concluded that the proposed equation in this study could predicts the pressure capacity of the experimentally tested SPs with acceptable accuracy.

6.9. OPTIMIZATION OF THE SYSTEM PARAMETERS

The main purpose of any design procedure in calculating the design parameters is to minimize an objective function. The main optimization objective in designing offshore pipelines is the overall cost of the pipeline, including the installation, fabrication and maintenance costs. However, estimation of these costs through a simple equation is not possible; therefore, cost estimation of offshore pipeline requires a comprehensive procedure. The intention of the optimization procedure presented in this section is to present a general procedure, which can be adopted to minimize a desired cost function. It should be noted that for the real applications, a more comprehensive method for estimating the cost should be employed. To simplify the cost function in this study, only the manufacturing cost has been considered. Therefore, the cost for the SPs considered here is estimated as a function of the material and manufacturing costs associated with each of the consistent layers of a SP. It should be noted that beside the materials' costs, there are other parameters that affect the overall cost of manufacturing of such systems. For instance, the actual welding cost and the cost of the adhesive that is used in some design cases to adhere the core to the pipes have not been considered in our cost estimation routine. For the sake of simplicity, therefore, only the material and welding costs (welding cost has been included implicitly in the cost of the inner and outer steel pipes), have been taken into account in this study. However, it is believed that the

formulated cost function includes the majority of the costs associated with formation of such systems. Therefore, the cost function is defined as:

$$C_{Man-SP} = C_{Man-P1} + C_{Man-P2} + C_{Man-C} \tag{6.13}$$

where C_{Man-P1} ,C_{Man-P2} and C_{Man-C} are respectively the internal pipe, external pipe and core layer manufacturing costs. Moreover, it is assumed that the manufacturing cost of the steel pipes is a function of the steel grade, which can be calculated through the following equation:

$$C_{Man-Pi} = \alpha A_{si}\left[1 + 0.3\left(\frac{\sigma_{yi}}{\sigma_{y(X60)}}\right)^2\right] \qquad i = 1,2(\text{or inner and outer}) \tag{6.14}$$

In this equation, α is the relative cost of the steel grade used in the internal and external pipes in relation to core material's cost. According to this equation, if the steel grade of the external or internal pipe is increased from X60 to X80, X100 or X120, then the manufacturing cost (including the material and welding cost), would be increased by 18%, 41% or 69%, respectively. Moreover, Equation (6.15) has been adopted as the cost function for the core layer. In this equation, it is assumed that the manufacturing cost of the core layer is a function of its elastic modulus.

$$C_{Man-C} = A_c\left[1 + 0.1\left(\frac{E_c}{E_p}\right)\right] \tag{6.15}$$

It should be noted that Equations (6.14) and (6.15) were developed based on information gathered through a market survey conducted by the author by considering the approximate costs of the materials in the market.

Having the cost functions, the optimization problem can be defined by the following statement:

$$\begin{cases} Minimize: & C_{Man-SP} \\ Subject\ to: & P_{CO} = \rho \times g \times (Water\ depth) \end{cases} \tag{6.16}$$

where P_{CO} is the constraint function, which can be calculated by Equation (6.12). By solving this optimization problem, the pipe's optimized configuration with respect to the cost function can be established. Several optimization procedures can be adopted for this purpose. Here, a "minimum-seeking" MATLAB code was developed to search for the

structural parameters, within a practical range, such that the cost function is minimized. The algorithm of this optimization procedure is presented in Figure 6.12. In this research the practical ranges for t_1/r_1 and t_2/r_2 are taken as 0.03-0.11 and 0.01-0.10, respectively. Moreover, the steel grade ranges from X60 to X120.

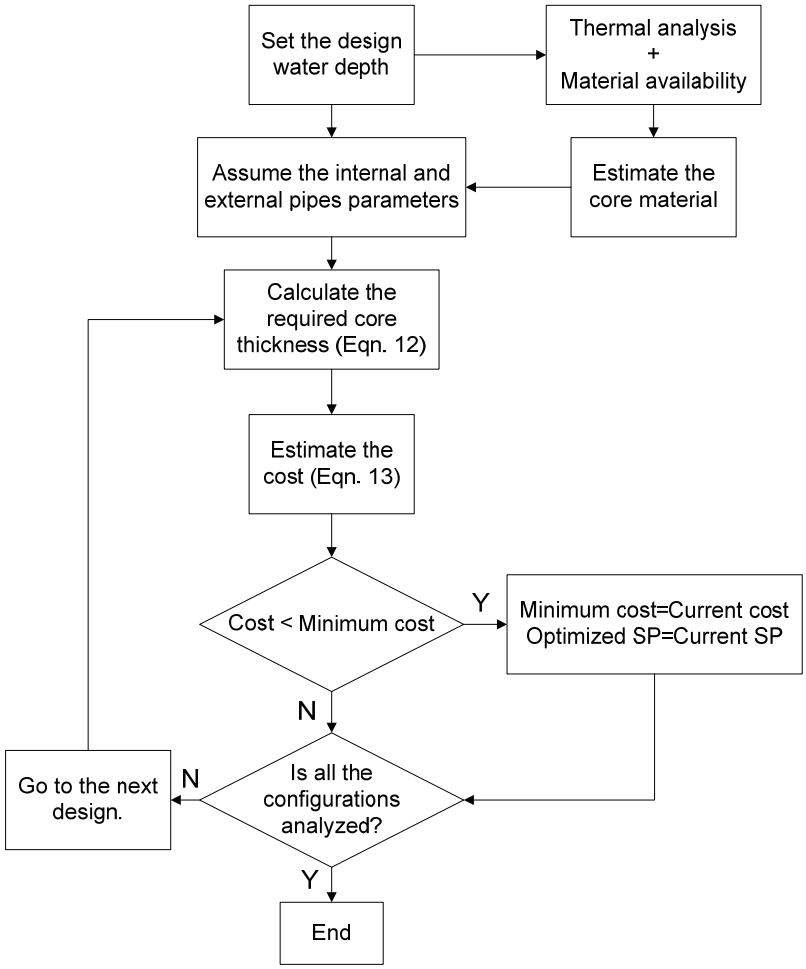

Figure 6.12. The optimization algorithm used for optimizing SP configurations at a given water depth and core material.

Figure 6.13 presents the results obtained from the solution of Equation (6.16) for the case of $\alpha = 10$. Figures 13.a and 13.b show the optimized values of $t_1/r_1$and t_2/r_2ratios with respect to the operational water depth. As can be seen in the figure, more robust internal and external pipes are required in deep water applications. The results demonstrate that employing stiffer core materials would allow the designer to opt for thinner internal and external pipes, and would therefore help to decrease the buoyancy weight of the pipeline. However, it should be noted that in addition to the structural

requirements, the thermal requirements also play a significant role in the core material and its thickness.

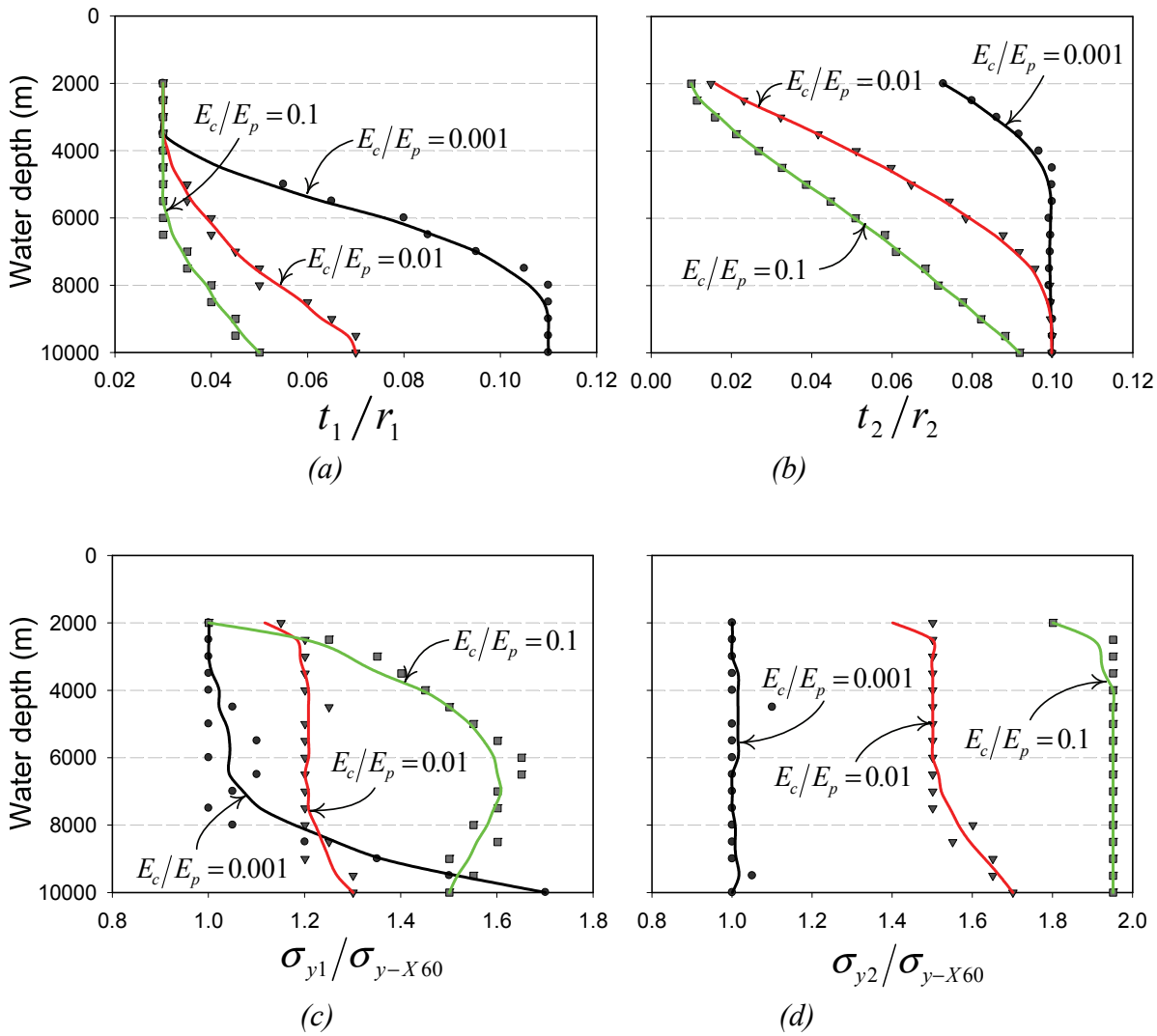

Figure 6.13. Optimization results of Equation (6.16) for α = 10 (a)t_1/r_1 (b) t_2/r_2 (c)$\sigma_{y1}/\sigma_{y-X60}$ (d)$\sigma_{y2}/\sigma_{y-X60}$.

Figures 13.c and 13.d illustrate that for most water depths, the steel grades of the internal and external pipe would be higher for the systems with stiffer core materials. In other words, employing stiffer core materials would improve the cost efficiency of the system, so long as relatively high grade steel pipes are used. It should be mentioned that these results are highly dependent on the cost function; therefore changing the cost function would alter the optimized values markedly.

6.10. CONCLUSION

A numerical finite element (FE) approach was employed in this study to investigate the pressure capacity (also referred to as the plastic buckling pressure) of sandwich pipes. Both material and geometrical nonlinearity were considered in the FE models; therefore, the real response of the system could be captured. Using the results obtained from the parametric study conducted through the analysis of a very large number of SP models, the influence of various structural parameters could be investigated. One of the major achievements of this study is the development of a practical equation with the capability to predict the pressure capacity of SP systems with a reasonable accuracy, when compared with the results obtained from earlier research involved experimental and advanced numerical models, as reported by other investigators. Finally, by defining a simplified manufacturing cost function and using the pressure capacity equation developed in this study, a minimum-seeking algorithm was used to establish the optimized parameters for water depths ranging from 2000 through 10000 meters. The summary of our findings are:

- Our computational investigation, which accounted for the material and geometrical nonlinearities, revealed that the methods which do not consider material nonlinearity produce large error in evaluating the external pressure capacity of SPs. This conclusion was validated by comparing the computational results with the results obtained through our earlier linear perturbation FE buckling analysis, as well as using the simplified equations proposed by other investigators.
- The parametric study results presented here revealed that increasing the t/r ratio of either the internal or external pipes could significantly improve the pressure capacity of the system. However, the comparison of the characteristic paths of the studied SPs revealed that even though increasing the t/r ratio of the external pipe would improve the pressure capacity of the system, it would decrease the deformability of the system before reaching to the buckling pressure. On the other

hand, employing an internal pipe with greater t/r ratio would improve both the pressure capacity and ductility of the system.

- A comparison of the characteristic paths of SPs with various core thickness and stiffness values indicated that the core layer influenced the profile of the characteristic path. It can be concluded that there would be two categories of SPs, depending on their characteristic paths - SPs with a relatively thin core layer would more likely follow a linear regime leading to their buckling capacity; on the other hand, SPs consisting of a relatively thick core would more likely follow a bilinear characteristic path up to their plastic buckling limit.
- The parametric study results indicated that increasing the thickness of the core would improve the pressure capacity of the system, but the magnitude of this enhancement would be dependent on the other pipeline parameters. However, it can be said that the improvement in the pressure capacity is greater for SPs with stiffer core materials.
- In this study the influence of using high grade steel as the internal and/or external pipes was investigated. It was found that upgrading the steel grade of either the internal or external pipes would significantly improve the pressure capacity. However, the influence of the internal pipe's steel grade would also be dependent on the structural properties of the core. That is, for SPs configurations with lower grade of core layer, for which an improvement in the internal pipe's steel grade would not improve the external pressure capacity of the pipe markedly.
- A comparison between the pressure capacity calculated by the proposed equation and the FE results showed a maximum error margin of 10% for practical SP configurations. Moreover, the results obtained through the proposed equation were compared with some pertinent experimental results found in the literature. The comparison showed that the proposed equation was capable of predicting the pressure capacity of SPs with reasonable accuracy.
- In order to present an algorithm for the structural optimization of SPs and to also demonstrate how the optimized structural parameters would have to be adjusted to ensure SP's stability at a given water depth, a simple manufacturing cost function was proposed. Using the cost function and the developed pressure capacity

equation, the optimum structural parameters for various water depths, ranging from 2000 through 10,000 meters, were established. It was found that for most water depths, the use of a stiffer core material in SP system would be cost effective only if higher grade steel pipes are employed.

6.11. ACKNOWLEDGEMENT

The financial support of the Natural Sciences and Engineering Council of Canada (NSERC) in support of this work is gratefully acknowledged.

6.12. REFERENCES

6.1. Sato, M. and Patel, M. H. (2007). Exact and simplified estimations for elastic buckling pressures of structural pipe-in-pipe cross sections under external hydrostatic pressure. *Journal of Marine Science and Technology, 12*(4), 251-262.

6.2. Sato, M., Patel, M. H., and Trarieux, F. (2008). Static displacement and elastic buckling characteristics of structural pipe-in-pipe cross-sections. *Structural Engineering Mechanics, 30*(3), 263-278.

6.3. Arjomandi, K. and Taheri F. (2009). Elastic buckling capacity of bonded and unbounded sandwich pipes under external hydrostatic pressure. To appear in the *Journal of Mechanics of Materials and Structure*.

6.4. Kardomateas, G. A. and Simitses, G. J. (2002). Buckling of long, sandwich cylindrical shells under pressure. *Proceedings of the International Conference on Computational Structures Technology*, 327-328.

6.5. Kardomateas, G. A. and Simitses, G. J. (2005). Buckling of long sandwich cylindrical shells under external pressure. *Journal of Applied Mechanics, 72*(4), 493-499.

6.6. Ohga, M. , SanjeewaWijenayaka, A. and Croll, J. G. A. (2005). Reduced stiffness buckling of sandwich cylindrical shells under uniform external pressure. *Thin-Walled Structures, 43*(8), 1188-1201.

6.7. Castello, X. and Estefen, S. F. (2006). Adhesion effect on the ultimate strength of sandwich pipes. *International Conference on Offshore Mechanics and Arctic Engineering, OMAE2006-92481,* Hamburg, Germany.

6.8. Castello, X., and Estefen, S. F. (2008). Sandwich pipes for ultra deep-water applications. *Offshore Technology Conference,* OTC 197041*,* Houston, Texas, USA.

6.9. Arjomandi, K. and Taheri F. (2009). Stability and Post Buckling Response of sandwich pipes under hydrostatic external pressure. Submitted to the *International Journal of Pressure Vessels and Piping*.

6.10. Kyriakides, S. and Netto, T. A. (2004). On the dynamic propagation and arrest of buckles in pipe-in-pipe systems. *International Journal of Solids and Structures, 41*(20), 5463-5482.

6.11. Kyriakides, S. (2002). Buckle propagation in pipe-in-pipe systems. Part I. Experiments. *International Journal of Solids and Structures, 39*(2), 351-366.

6.12. Kyriakides, S. and Netto, T. A. (2002). Dynamic propagation and arrest of buckles in pipe-in-pipe systems. *Proceedings of the International Conference on Offshore Mechanics and Arctic Engineering* - OMAE, 4, 199-205.

6.13. Kyriakides, S. and Vogler T.J. (2002). Buckle propagation in pipe-in-pipe systems. Part II. Analysis. *International Journal of Solids and Structures, 39*(2), 367-392.

6.14. Estefen, S. F., Netto, T. A., and Pasqualino, I. P. (2005). Strength analyses of sandwich pipes for ultra deep-waters. *Journal of Applied Mechanics, 72*(4), 599-608.

6.15. Castello, X., Estefen, S. F., Leon H. R., Chad L. C. and Souza J. (2009). Design Aspect and Benefits of Sandwich Pipes for Ultra Deepwaters. *International Conference on Offshore Mechanics and Arctic Engineering, OMAE2009-79528,* Hawaii, USA.

6.16. Arjomandi, K. and Taheri F. (2010). Influence of the Material Plasticity on the Characteristic Behavior of Sandwich Pipes. Submitted to the *8th International Pipeline Conference*. *IPC2010-31518*, Alberta, Canada.

6.17. API SPECIFICATION 5L. (2000). *Specification for line pipe*. API Publishing Services, Washington, D.C.

6.18. Brush DO. and Almroth, B. (1975). *Buckling of bars, plates and shells*. McGraw-Hill, New York.

6.19. ABAQUS User's and Theory Manuals. (2008). Version 6.8, Dassault Systèmes, RI, USA.

6.20. MATLAB (2008). Version 7, The MathWorks Inc., MA, USA.

6.21. SPSS (2008). Version 17, SPSS Inc., IL, USA.

6.22. Gill, P. E., Murray W. M., Saunders M. A. and Wright. M. H. (1986). User's guide for NPSOL (version 4.0): A FORTRAN package for nonlinear programming. Technical Report SOL 86-2. Stanford University: Department of Operations Research.

CHAPTER 7

THE INFLUENCE OF INTRA-LAYER ADHESION CONFIGURATION ON THE PRESSURE CAPACITY AND OPTIMIZED CONFIGURATION OF SANDWICH PIPES*

Kaveh Arjomandi and Farid Taheri
Department of Civil and Resource Engineering, Dalhousie University
Halifax, Nova Scotia, Canada

7.1. ABSTRACT

Sandwich pipes (SPs) offer sensible and cost-effective design alternative for extraction of oil and gas in deep and harsh waters. By employing the potential thermal insulation properties offered by the core material used in SPs, and the structural integrity provided by the sandwich mechanics, SPs can be optimally designed to provide safe transportation system for oil and gas under specific loading and environmental conditions.

In this paper, the influence of the structural parameters that would significantly impact the characteristic behavior and pressure capacity of SP systems, having various intra-layer adhesion properties, are investigated. SPs response is simulated by the Finite Element (FE) numerical method, accounting for the material and geometrical nonlinearities, and considering the intra-layer condition. Finally, the results of more than 12,000 nonlinear FE models are used to develop three simplified practical equations, capable of evaluating the pressure capacity of SPs having various intra-layer mechanisms and material configurations, with an acceptable accuracy.

As one of the main objectives of this study, the influence of the intra-layer adhesion configuration on the optimal design of such pipes at various water depths is also investigated. The optimization procedure previously recommended by the authors is extended to establish the optimal structural configurations.

Keywords: Sandwich pipes, core, buckling, post-buckling, intra-layer, interface, adhesion properties, cost optimization, finite element, analytical solution.

---

* Submitted to the Journal of Ocean Engineering.

7.2. NOMENCLATURE

A_{s1}	Cross section area of the external pipe
A_{s2}	Cross section area of the internal pipe
A_c	Cross section area of the core
C_{Man-SP}	Manufacturing cost of the sandwich pipe
C_{Man-P1}	Manufacturing cost of the external pipe
C_{Man-P2}	Manufacturing cost of the internal pipe
C_{Man-C}	Manufacturing cost of the core
EPG	External pipe's steel grade
E_c	Core material's elastic modulus
E_p	Internal and external pipes' elastic modulus
IPG	Internal pipe's steel grade
P_{crs}	External pipe buckling pressure
imp	Imperfection magnitude
n	Buckling mode number
r_1	Outer pipe nominal radius
r_2	Inner pipe nominal radius
r_1^o	Outer pipe initial nominal radius
r_2^o	Inner pipe initial nominal radius
r_1^{max}	Maximum measured external pipe radius
r_1^{mn}	Minimum measured external pipe radius
t_1	Outer pipe wall thickness
t_2	Inner pipe wall thickness
t_c	Core layer thickness
σ_{y1}	Yield stress of the external pipe material
σ_{y2}	Yield stress of the internal pipe material
σ_{y-X60}	Yield stress of X60 grade steel
Δ	Ovalization magnitude
Δr	Imperfection of the pipe radius as a function of θ
ν_c	Core material Poisson's ratio

ν_p Pipe material Poisson's ratio

7.3. INTRODUCTION

Modern harvesting of our world's limited oil and gas resources has been ongoing since the 18th century. Since then, day by day, the increase in world's demands for more energy and raw material resources has accelerated the oil and gas production. As a result, the access to current oil and gas reserves is diminishing; as a result, demands for deep water resources are increasing. On the other hand, the oil and gas production and transportation facilities and techniques used for shallow and accessible reserves are not feasible for deeper reservoirs located in harsh and remote areas. Consequently, engineers are facing new challenges for improving the traditionally used systems and developing new systems. Pipelines as one of the key component of the transportation system; therefore, their configurations and performance must be improved in order to effectively respond to the new requirements. Employing the traditional steel single walled pipes is limited to a specific operational depth. Moreover, the oil product must be kept adequately warm to flow; therefore the oil product should be thermally isolated from the ambient cooler environment.

In order to improve the thermal insulation properties of the traditional single wall steel pipes, the idea of Pipe in Pipe (PIP) design configuration was developed. PIP systems are composed of three concentric cylindrical elements. The internal pipe, also called the product pipe, is in contact with the product and facilitates the oil product flow. The core layer can be selected such that it would act as a proper thermal insulator surrounding the internal pipe. Moreover, the core layer can be a host for structural and health monitoring systems, the cathodic protection systems and/or the heating facilities. The outermost layer of the system, the external pipe (also called the sleeve pipe), separates the core layer and internal pipe from the surrounding environment. Moreover, the secondary containment provided by the external pipe would improve the assurance of the system in case of oil product leaking from the internal pipe.

Because PIP systems can be designed to fit the required thermal insulation properties, these systems have been employed in many practical offshore applications. However, in most of the PIP projects, the potential sandwich structure has been ignored

and each component of the system has been individually designed based on its governing loads. However, previous studies reveal that if the whole system is considered as a sandwich structure, a considerably lighter and a more cost-effective pipeline could be designed for a specific loading condition. As a result, the idea of sandwich pipe has been developed. In SP systems a relatively soft core layer is sandwiched by relatively stiff internal and external pipes. The core layer in SP systems provides the required thermal insulation properties as well as the appropriate structural properties to transfer loads between the internal and external pipes. Therefore, in SP systems the core layer must include both structural and thermal properties.

One of the initial feasibility studies on employing SP systems for offshore deep and ultra deep waters was conducted by Estefen et al. [7.1]. They conducted small scale laboratory tests as well as the corresponding Finite Element (FE) numerical analysis to investigate the behavior of SP systems under various loading scenarios. Finally, through the numerical and experimental studies, they concluded that SP systems having polypropylene or cement core layers can be efficient design alternatives for offshore pipelines. However, they have mentioned that the design of such systems must be tailored for the specific demands of each pipeline project due to the large number of design parameters to be specified. In another study, Castello et al. [7.2] investigated the influence of the core layer properties on the external pressure capacity of SP systems through the FE numerical approach. Moreover, they compared PIP with SP design alternatives for a hypothetical oil field and also investigated the effect of the relative direction between the inner and outer pipes maximum diameters on the external pressure capacity of the system.

Other research has been conducted with the aim of developing closed form analytical solutions for predicting the external pressure capacity of SP systems. One of the initial studies on developing the characteristic equations of the system was performed by Brush and Almroth [7.3]. They developed the characteristic equation of a SP system by simplifying the system to a plane-strain 2D problem of a ring on an elastic foundation. Recently, Sato and Patel [7.4] and Sato et al. [7.5] improved Brush and Almroth's solutions and recommended a simplified equation for calculating the core stiffness parameter. In another study, Arjomandi and Taheri [7.6] studied the stability problem of

the buckling of SP systems under hydrostatic external pressure and developed simplified solutions for estimating SPs' buckling capacity. This study considered the influence of the intra-layer adhesion properties between the core layer and the surrounding pipes and developed four sets of equations for evaluating the elastic buckling pressure. Moreover, it proposed simplified equations for SPs having various intra-layer adhesion properties.

In order to analyze the stability of an SP system under uniform hydrostatic external pressure, the system can generally be considered as a long sandwich cylindrical shell structure having an infinite length. A few other research projects have been conducted to study the behavior of such systems. Kardomateas and Simitses [7.7, 7.8] analytically studied the stability of long sandwich cylindrical shells under uniform external pressure. Ohga et al. [7.9] also studied the reduced stiffness buckling of sandwich cylindrical shells under uniform external pressure, both numerically and analytically.

Former studies have shown that the intra-layer adhesion properties would have a significant influence on both the characteristic behavior and the pressure capacity of the system. Investigating the effect of the degree of adhesion between the core layer and either internal or external pipes was the subject of a study conducted by Castello and Estefen [7.10, 7.11]. Moreover, they studied the influence of the applied cyclic loads during the reeling installation method on the collapse pressure of the system. Arjomandi and Taheri [7.6, 7.12] in a series of works, analytically and numerically investigated the influence of various scenarios of bonding between the structural layers on the elastic buckling pressure of the pipe.

Previous investigations have revealed that under a steady state buckle propagation pressure, which might be lower than external buckling pressure, local buckling could be propagated along the pipeline. Several investigations have been conducted to study this phenomenon from different aspects. A series of remarkable works by Kyriakides and his coworkers [7.13-7.16] investigated buckle propagation phenomena from experimental, analytical and numerical perspectives.

A former numerical study of the authors [7.17], investigating the behavior of a set of practical SP cases revealed that practical SP configurations are highly susceptible to losing their stability through plastic buckling. Comparison between the elastic and plastic buckling pressures of such pipes shows that the difference between these two values can

be excessively large, especially in the case of SPs having a relatively stiff core layer. Therefore, it was concluded that employing the equations developed based on the elastic material assumptions would interject a large margin of error into the design procedure.

In another study, Arjomandi and Taheri [7.18] conducted a set of comprehensive numerical FE parametric studies to investigate the behaviour of SPs under hydrostatic external pressure considering the material and geometrical nonlinearities. They investigated the structural parameters that would have significant influence on the characteristic behaviour and also the capacity of the system. However, they only focused on the SP configuration in which the core layer was bonded to both the internal and external pipes. Using the parametric study results, they developed a simplified practical equation for calculating the pressure capacity of the system. Finally, using the pressure capacity equations and a recommended manufacturing cost function also developed by them, they proposed an optimization procedure for establishing the optimized SP's structural parameters for various water depths.

In this paper, the influence of the structural properties that could significantly influence the characteristic behaviour and pressure capacity of SPs having four intra-layer adhesion mechanisms is numerically investigated. The investigation included more than 12,000 FE models developed to study the characteristic behaviour and pressure capacity of the systems. The general equation previously developed and proposed by the authors was calibrated for applications to alternative SP configurations, in which the core layer could slide on the internal and/or external pipes. The accuracy of the developed equations was examined by comparing the pressure capacity calculated from the proposed equations with the FE and experimental results from the literature. Using the developed equations and a manufacturing cost function recommended by the authors in their previous study, the optimized structural parameters were evaluated for SPs having various intra-layer configurations and core stiffnesses, for various operational water depths.

7.4. THEORY AND MOTIVATION

As stated earlier, sandwich pipes used in the oil and gas industry are generally long cylindrical structures consisting of two concentric steel pipes sandwiching a relatively

softer core layer. Because of the uniform structural properties, boundary conditions and applied loads along the pipeline, the problem can be considered as a 2D plain strain problem of a multilayer ring consisting of three concentric circular layers. The general SP's geometrical and material parameters are illustrated in Figure 7.1.

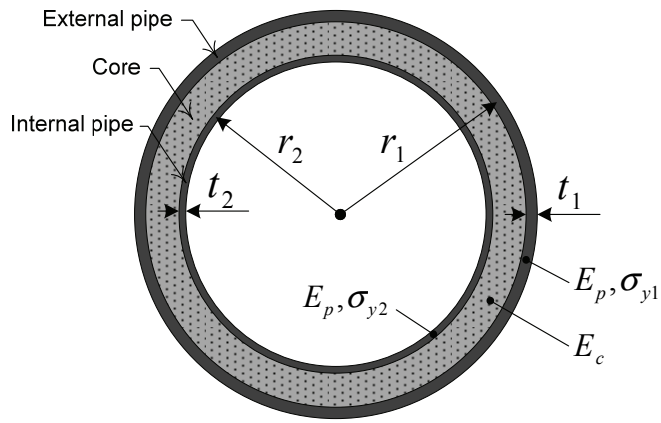

Figure 7.1. Geometrical and material configuration of the SP system

For a SP whose materials are assumed to follow an elastic regime, the elastic buckling pressure of the system would constitute the pressure capacity of the system. Brush and Almroth [7.3] proposed an analytical solution for calculating the elastic buckling pressure ($P_{cr-BASP}$) of such a system by simplifying the problem and finding the buckling pressure of a ring internally supported by an elastic foundation. Sato and Patel [7.4] improved Bruch as Almroth's solution and recommended a simplified equation for calculating the core layer stiffness. Finally they proposed the following equations:

$$P_{cr-BASP} = P_{crs} + \frac{1}{n^2 - 1} k \tag{7.1}$$

where:

$$k = E_c \frac{2n(\upsilon_c - 1) - 2\upsilon_c + 1}{4\upsilon_c^2 + \upsilon_c - 3} \tag{7.2}$$

and $P_{crs}$is the buckling pressure of the external pipe obtained by:

$$P_{crs} = \left(\frac{t_1}{r_1}\right)^3 \frac{E_p(n^2 - 1)}{\left(1 - \upsilon_p^2\right)\left(\left(\frac{t_1}{r_1}\right)^2 + 12\right)} \tag{7.3}$$

Arjomandi and Taheri [7.6] conducted a comparative study between the elastic buckling pressure calculated from the FE numerical approach and Equation (7.1) and found that the above equation's prediction of the buckling pressure of the system could

include very large margins of error, especially for those SPs having thick and soft core layers. It was hypothesized that the large margin of error was initiated from the large number of simplifying assumptions used in developing the equations. For instance, in deriving Equation (7.1), it was assumed that the geometrical properties of the internal pipe and core layer would not affect the buckling pressure. However, these former studies illustrate that these parameters can significantly change both the characteristic response and the pressure capacity of the pipe [7.12]. Another assumption that limits the applicability of this equation is the preselected pattern of the buckling mode. To simplify the calculations a similar sinusoidal pattern for all three layers of a sandwich pipe was assumed in the polar coordinates. This assumption would introduce a large margin of error to the final equation in some design configurations depending on the real SP buckling mode.

Arjomandi and Taheri [7.6] conducted a study to improve the accuracy of the analytical solutions. To do so, they included the effect of the internal pipe's structural parameters and the core thickness. They developed the characteristic equation of the system by considering the influence of the external pipe, the internal pipe and the core layer separately. Furthermore, a parameter accounting for the adhesion between the layers was included in their solution. Finally, the proposed equation was successful in evaluating the pressure capacity of SP configurations having relatively soft or thick core layers with a better accuracy than the former equations; however it still could not produce reasonable accuracy for all design configurations. Equation (7.4) demonstrates their solution for calculating the elastic buckling pressure of sandwich pipes in which the core layer is bonded to both the internal and external pipes:

$$P_{cr-AT} = \frac{\xi_1}{\xi_2} \tag{7.4}$$

where P_{cr-AT} signifies the critical buckling capacity based on Arjomandi and Taheri's solution, and

$$\begin{aligned}\xi_1 = {} & 192E_c^2 a_1 {r_1}^3 \left(v_p^2 - 1\right)^2 + E_p^2 {t_1}^4 n^2 \Lambda (n^2 - 1)(\Lambda + 7)^2 \\ & + 2E_c E_p r_1 t_1 \left(v_p^2 - 1\right)(\Lambda + 7)\{{t_1}^2 n^2 [n(\Lambda - 1) - \Lambda - 1] \\ & - 6t_1 r_1 [(n+1)^2 + (n-1)^2 \Lambda] - 12{r_1}^2 [n(\Lambda - 1) - \Lambda - 1]\}\end{aligned} \tag{7.5}$$

$$\xi_2 = r_1\left(v_p^2 - 1\right)(\Lambda + 7)\left\{-12E_c{r_1}^2 a_1\left(v_p^2 - 1\right)[n(\Lambda - 1) - \Lambda - 1] + E_p t_1 n^2 \Lambda({t_1}^2 + 12{r_1}^2)(\Lambda + 7)\right\} \tag{7.6}$$

where parameter Λ is defined as:

$$\Lambda = 4v_c - 3 \tag{7.7}$$

The analytical equations for evaluating the external buckling capacity of SPs recommended by most of the pipeline design codes, such as API RP-1111 [7.19] and DNV-OS-F101 [7.20] are based on the linear assumption, and the existence of a potential imperfection in a pipeline. Moreover, many other analysis methods employed in practice, such as the FE eigenvalue buckling analysis or the post buckling analysis, are developed based on the assumption that the materials behave linear elastically. However, previous studies of the authors have demonstrated that within a wide range of practical design configurations, SP systems could undergo plastic deformations before actually buckling (i.e., they undergo plastic buckling) [7.17]. In other words, the materials forming the pipeline undergo plastic deformation before reaching the collapse pressure. Therefore, designing safe SPs demands consideration of materials' nonlinearity. In a comprehensive FE parametric study, Arjomandi and Taheri [7.18] investigated the behavior of a sandwich pipe configuration in which the core layer was fully bonded to both the internal and external pipes. They used the pressure capacity values calculated by the FE and suggested a general form semi-empirical equation suitable for calculating the plastic buckling pressure of SPs. Equation (7.8) illustrates the general form of the proposed equation. The equation includes 13 constants which were calibrated based on the FE results for SPs having the fully bonded configuration.

$$\frac{P_{CO}}{E_p} = a\left(\frac{t_1}{r_1}\right)^b\left(\frac{t_c}{r_1}\right)^c\left(\frac{\sigma_{y1}}{E_p}\right)^d + e\left(\frac{t_1}{r_1}\right)^f\left(\frac{t_2}{r_2}\right)^g\left(\frac{t_c}{r_1}\right)^h\left(\frac{\sigma_{y2}}{E_p}\right)^i + j\left(\frac{t_1}{r_1}\right)^k\left(\frac{t_2}{r_2}\right)^l\left(\frac{t_c}{r_1}\right)^m \tag{7.8}$$

Former studies on the influence of the adhesion properties between the layers in linear models have revealed that SP systems having similar structural properties but different intra-layer adhesion properties would exhibit significantly different pressure capacities. To the authors' knowledge, there has been no comprehensive parametric study investigating the intra-layer adhesion properties effect on the pressure capacity of SP

systems by taking the material nonlinearities into consideration. Moreover, there exist no equations in the literature whether simplified or complex, for evaluating both the elastic and plastic buckling pressure capacity of SPs.

In this study, the influence of the structural parameters that affect the characteristic behavior of SPs having various interface layer adhesion is investigated. Moreover, the general equation, previously proposed by the authors, for evaluating the pressure capacity of SPs having fully bonded intra-layer adhesion properties is further calibrated to accommodate the other three possible SP configurations with alternative intra-layer adhesion configurations. The results of 3072 FE models constructed for each SP configuration (i.e. in total more than 12,000 models), were employed for calibrating the simplified practical equations. These equations account for the effects of the material and geometrical nonlinearities, as well as the intra-layer adhesion properties.

It should be noted that due to the regression related errors, the exclusive use of the proposed equations for design purpose is not recommended; however, the proposed equations could be effectively used for the purpose of preliminary design approximations, and in optimization procedures, with a reasonable degree of confidence. Finally, to demonstrate the use of the pressure capacity equations within an optimization procedure to establish the optimal material and geometrical parameters, a minimum seeking optimization algorithm would be used to optimize a series of SPs having various possible intra-layer adhesion configurations. Moreover, in order to develop the optimization procedure, a simple manufacturing cost function previously proposed by the authors was employed. Using the optimization algorithm, the SP configurations were optimized for a range of water depths between 1,000 and 10,000 meters. The results of this study were illustrated and the influences of the water depth, intra-layer adhesion properties and core stiffness were discussed.

7.5. PARAMETRIC STUDY

In this study, a range of structural parameters was selected such to cover all the possible practical SP configurations. Table 7.1 illustrates the selected structural parameters and their studied ranges. The ranges of the core thickness ratio (r_2/r_1) and the core stiffness ratio (E_c/E_p) were selected based on the required thermal insulation

properties used in practice and the practical range of the possible core material properties. The thickness to the radius ratio of the internal and external pipes was chosen in consideration of the API standard steel pipes' geometries [7.19]. Moreover, the influences of the steel grades of the internal and external pipes were investigated in the range of X60 to X120. However, the parametric study models were created based on the ratio of the yield stress to the Young's modulus of the internal and external pipes' material. Therefore, the results of this study can be used for any system having materials with the yield stress to Young modulus ratios listed in Table 7.1.

Table 7.1. Range of the parameters used in the parametric study.

r_2/r_1	t_1/r_1	t_2/r_2	E_c/E_p	σ_{y1}/E_p	σ_{y2}/E_p
0.70	0.03	0.03	0.001	0.001998 (X60)	0.001998 (X60)
0.75	0.05	0.05	0.01	0.002665 (X80)	0.002665 (X80)
0.80	0.07	0.07	0.1	0.003331 (X100)	0.003331 (X100)
0.85	0.09	0.09		0.003997 (X120)	0.003997 (X120)
0.90					

As stated earlier, in addition to the pipeline geometrical and material parameters, the influence of the intra-layer interaction mechanism between the core layer and the surrounding pipes on the response of SPs was also investigated. The possible intra-layer configurations considered are as follows:

a) Fully Bonded (FB): In which the core layer and the surrounding pipes are fully bonded together.
b) Inner Unbonded (IU): In which the core layer is bonded to the external pipe but it can slide on or separate from the internal pipe.
c) Outer Unbonded (OU): In which the core layer is bonded to the internal pipe but it can slide on or separate from the external pipe.
d) Both Unbonded (BU): In which the core is free to slide on or separate from either the external or internal pipes.

7.6. FINITE ELEMENT MODELS

The FE package, Abaqus/CAE was used for creating and analyzing the models and post processing the results [7.21]. The parametric study models were created and run by the Python, the programming language within Abaqus. Finally, a MATLAB [7.22] code was developed to extract the characteristic paths, analyze the results and establish the pressure capacity of the pipes.

An SP system lying on the seabed can be considered as a structure having uniform structural properties and boundary conditions under uniform external pressure along the pipeline axis; therefore the system was modeled as a 2D problem. The mesh convergence study results show that employing 40 circumferential elements and one through the thickness element for each layer produce a mesh that could produce results with acceptable accuracy. In consideration of the shear and volumetric locking issues and the accuracy and numerical efficiency, several element types were evaluated and the Abaqus 3D brick element, C3D20R, was chosen as the most efficient element for generating the FE semi-2D models.

It should be mentioned that, despite the symmetry, using a half circle model would not allow computation of all the possible deformation models associated with the non-symmetrical and higher modes. Therefore, a full circular FE model was used to simulate system's cross section. Moreover, proper boundary conditions were applied to enforce the plane strain condition and also to prevent rigid body motions. In summary, in modeling such systems over-constraining the system must be avoided, so the FE model can mimic the actual response of the system.

Selecting of an appropriate material model is one of the most important aspects of accurate finite element analysis. A former study by the authors revealed that the inclusion of material plasticity in the models would significantly reduce the linear buckling pressure of the system [7.17]; in other words, employing a linear material model would not produce a safe design. However, in the same study it was shown that the profile of the stress-strain curve after the yield point would not have a significant influence on the characteristic response of SP systems subject to external hydrostatic pressure. In this study the material behavior of the external and internal pipes is modeled using the Elastic Perfectly Plastic (EPP) model. Based on the former study, it was observed that employing

the EPP material model would yield a lower bound characteristic path compared to the results when other nonlinear material models were used to model the internal and external pipes. The steel material properties were extracted from API 5L [7.19]. Moreover, most of the polymeric materials practically used to form the core layer would have relatively greater yield strains in comparison to steel. Therefore, for the sake of simplicity the core layer was modeled with a linear material model.

The interaction properties between the layers were modeled using two approaches. The first approach was employed when the interfacing surfaces of the contacting layers were fully bonded together, that is the corresponding nodes located on the interfacing surfaces had similar active degrees of freedom. This condition was modeled using the Multi Point Constraint (MPC) function in Abaqus [7.21]. The second interaction condition would occur when the interfacing surfaces are allowed to slide on or separate from each other, but the intercourse between the surfaces is prohibited. To model this condition, the Abaqus surface to surface contact model with a frictionless tangential property was employed. Moreover, the interaction in the normal direction was modeled using the linear penalty method in which the penalty stiffness was set to 10 times the representative underlying element stiffness.

In order to capture the post buckling behavior of SPs, a similar geometrical imperfection in the form of ovality was applied to all three layers of the pipe. The imperfection was generated using the following equation:

$$\Delta r_i = imp \times r_i^o \cos 2\theta \quad , \quad i = 1,2 \tag{7.9}$$

Using this equation, the imperfection was applied to the nominal radius of the pipe, while the thickness of the pipe was kept perfectly constant. The imp in the equation is the imperfection magnitude which was taken as 0.005.

More details about creating and analyzing the FE models can be found in Arjomandi and Taheri (2010d).

7.7. PARAMETRIC STUDY RESULTS

The characteristic behavior of a SP system is influenced by the structural properties of its constituents. Having three structural layers and various interaction mechanisms between the layers, a SP's characteristic behavior cannot be generalized as it can for a

single walled pipe. The characteristic behavior of the system is a function of the chosen characteristic response. In this study the ovality of the external pipe was taken as the characteristic response, calculated by:

$$\Delta = \frac{r_1^{max} - r_1}{r_1^{max} + r_1^{min}} \tag{7.10}$$

By employing this characteristic response, it is assumed that the system will collapse if the external pipe becomes unstable, which is an applicable assumption for the practical range of SP configurations.

7.7.1. Characteristic paths categories

Investigation of the parametric study's results revealed that in general, SPs could exhibit three distinct characteristic paths.

a) In the first path SPs could behave like a single walled steel pipe. The pipes would deform almost linearly up to a limit point corresponding to pipes' pressure capacity, also called the plastic buckling pressure. After reaching this pressure capacity, the system would become unstable and collapse. Most of the studied pipes in the following sections exhibit this type behavior.

b) SPs in the second category would have bilinear characteristic paths before reaching the pressure capacity. This category of pipes would exhibit a linear characteristic behavior up to the first proportional limit pressure, followed by another stable and almost linear path. Finally, the second stable path would end up at the collapse pressure. Mostly, SPs having thick core layers with intermediate core material stiffness and FB intra-layer adhesion properties fall into this category. In pipes having this category of behavior, formation of initial plastic hinges would not cause the structure's instability; therefore, the pipe would continue to deform till more plastic hinges are formed.

c) SPs following within the third category would never become unstable under hydrostatic external pressure. That is, the ovality would increase by increasing the magnitude of the external pressure, and for any magnitude of ovality the characteristic path would maintain a positive slope. Within the studied range of

parameters, SP configurations having relatively stiff core layers ($E_c/E_p = 0.1$) may fit this category.

Figure 7.2 illustrates the characteristic path and the maximum Equivalent Plastic Strain (PEEQ) of a typical SP system falling within the above category. The pipe in this figure has BU intra-layer adhesion properties, and a relatively stiff core layer. As can be seen in Figure 7.2.a, the system is stable for any magnitude of the characteristic response. Moreover, the maximum PEEQ values in the system and the location of the maximums under the four ovality magnitudes of 5, 15, 35 and 50%, are illustrated in Figure 7.2.b. In the studied system, the maximum PEEQ magnitude varies between zero at zero external pressure and 10%, which would occur when internal pipe's internal surfaces touch each other. Core layer's contribution in this category is more significant in comparison with the other two configurations. Therefore, forming major plastic regions in the internal and external pipes could not eliminate all the constraints and the pipe would remain stable even after substantial plastic hinges appear in the steel pipes.

In the following sections, the influence of the significant structural parameters on both the characteristic behavior and the pressure capacity of the SP systems are discussed.

7.7.2. Influence of the core thickness ratio

In this paper, the (r_2/r_1) parameter represents a measure of the core thickness and is referred to as the core thickness ratio. Equation (7.11), demonstrates the relation between this parameter and the core thickness of the pipe as a dimensionless parameter. Therefore, SPs having thick core layers have smaller values of the core thickness ratios in comparison with the SPs having thin core layers.

$$\frac{r_2}{r_1} = 1 - \frac{t_c}{r_1} \tag{7.11}$$

The results of the parametric studies show that increasing the thickness of the core layer enhances the pressure capacity of the pipeline in all the configurations having any intra-layer adhesion properties. Figure 7.3 shows the characteristic behavior of a set of SP configurations with various core thickness ratios. As can be seen in Figure 7.3.a, changing the core thickness would change the characteristic profile of the pipeline. The

pipes having the core thickness ratios between 0.75 and 0.9 have the first category of characteristic behavior, while the SP case having a core thickness ratio of 0.7 exhibits the second category of behavior. The pipe having $r_2/r_1 = 0.7$, after reaching the first proportional limit at an ovality magnitude of 0.8%, is still stable and after having more stable deformation on the second stable path becomes unstable at the collapse pressure corresponding to an ovality magnitude of 23%.

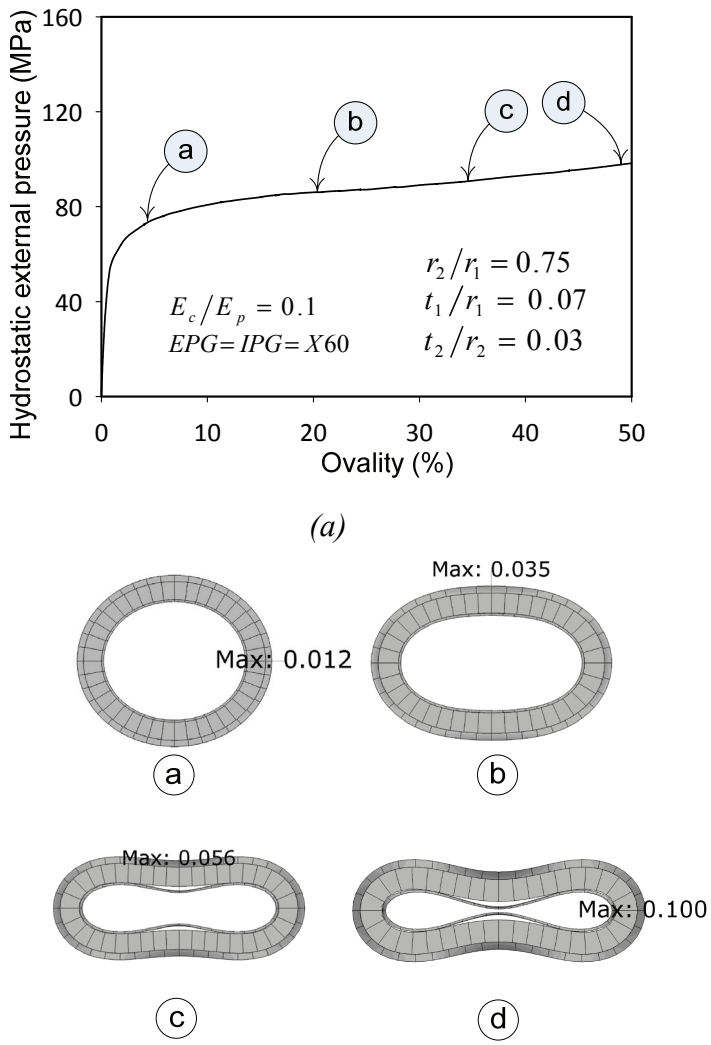

Figure 7.2. (a) Characteristic behavior and (b) Maximum Equivalent Plastic Strain (PEEQ) of an SP configuration having the third category of characteristic path.

The core thickness ratio also affects the deformability of the system before reaching the collapse pressure. As can be seen in Figure 7.3.a and 7.3.b, those SP systems having a

bilinear characteristic path before reaching to the collapse pressure are much more deformable than the SPs having a linear characteristic path. However, the influence of the core thickness on the deformability of the system is also dependent on the other structural properties.

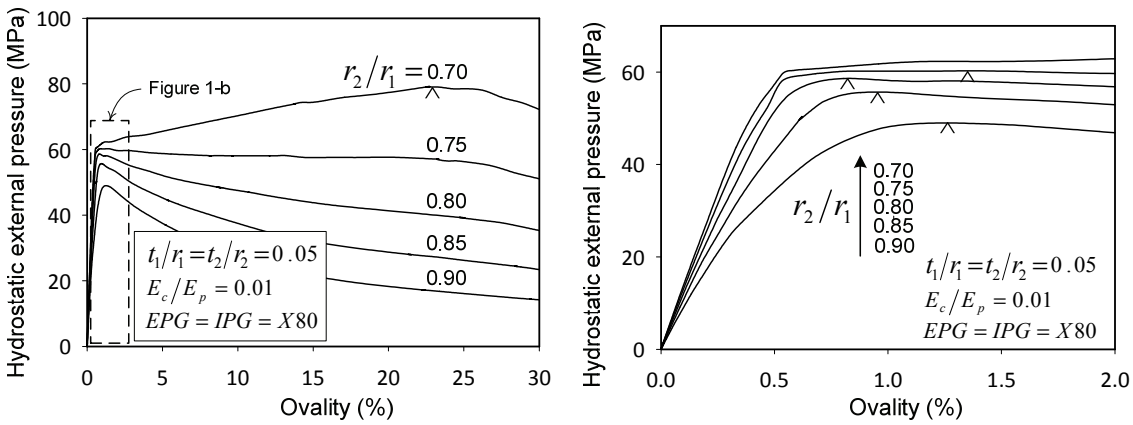

(a) *(b)*

Figure 7.3. Influence of the core thickness on the characteristic behavior of SPs with fully bonded configuration. (a) Up to ovality magnitude of 30% (b) up to ovality magnitude of 2%.

The parametric study results show that releasing either the internal pipe or the external pipe from the core layer would have almost the same influence on the pressure capacity of the system. Figure 7.4 shows the influence of the thickness of the core layer on the characteristic behavior of a set of SPs having IU and OU intra-layer configurations. This figure illustrates that the pressure capacities of systems having alternative OU or IU configurations are almost similar. However, our study shows that the IU configurations would represent a larger deformation before reaching the collapse pressure in comparison with the OU configurations having similar other structural properties.

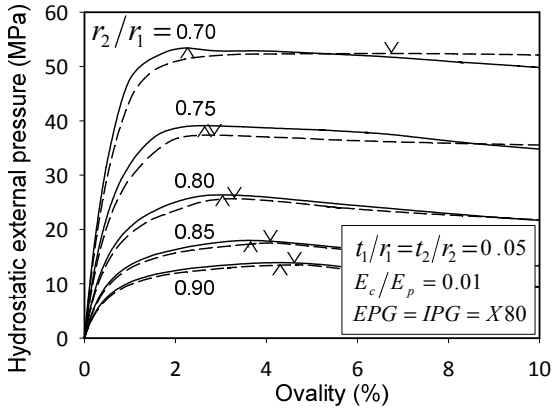

Figure 7.4.Influence of the core thickness on the characteristic behavior of SPs having OU and IU configurations. Solid lines show the characteristic behavior of OU configurations and dashed lines illustrate the characteristic behavior of IU configurations. Symbol (^) represent the collapse point for OU configuration and symbol (v) shows the collapse point for the IU configuration.

Figure 7.5 illustrates the characteristic paths of the same set of SPs having the BU intra-layer configuration. Investigating the characteristic behavior of this category of SPs showed that in the pipes having this configuration, increasing the core thickness ratio improves the pressure capacity of the system and decreases the deformability of the pipe before reaching the collapse pressure.

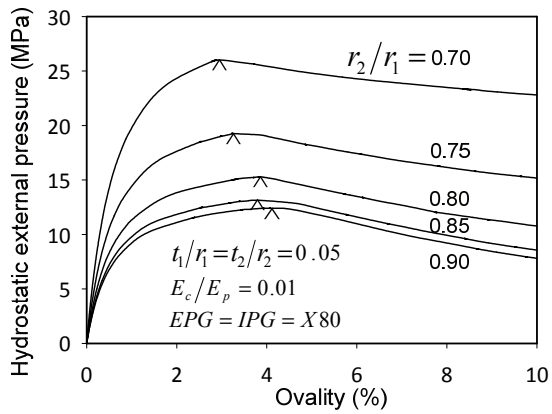

Figure 7.5.Influence of the core thickness on the characteristic behaviorof SPs with BU configuration.

In summary, Figure 7.6 illustrates the influence of the intra-layer interaction properties on the collapse pressure of the above-mentioned SP configurations. As can be seen in the figure, and also concluding from our parametric study results, those SPs having the FB configuration have the largest pressure capacity for any core thickness ratio. On the other hand, SPs having the BU configuration always have the minimum capacity in comparison with the other three configurations. The OU and IU configurations would create SPs with intermediate pressure capacities falling between the capacity of FB and BU configurations. However, SPs having relatively thin core layers have almost the same capacities in all of the OU, IU or BU configurations. While, in the case of SPs having relatively thick core layers, bonding the core layer to either the internal or external pipe would improve the capacity of the system significantly.

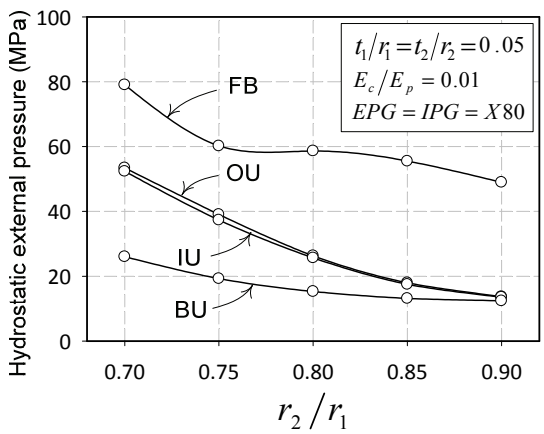

Figure 7.6.Influence of the core thickness on the pressure capacity of SPs with BU configuration.

7.7.3. Influence of the external pipe's thickness to the radius ratio

It is expected that increasing the external pipe's wall thickness enhances the pressure capacity of SPs, regardless of the intra-layer adhesion configuration. However, the magnitude of this improvement is highly dependent on the intra-layer adhesion properties. Figure 7.7.a and 7.7.b illustrate the characteristic paths of a set of SPs with FB and BU configurations. As can be seen in Figure 7.7.a, in the case of the FB configuration, increasing the external pipe's wall thickness from 0.03 to 0.09 enhances the capacity of the system from 47 to 82 MPa, which is a 75% improvement. Whereas, as Figure 7.7.b illustrates, the same magnitude of enhancement in the t_1/r_1 value, in pipes

with the same properties but having the BU configuration, improves the capacity from 11 to 39 MP, which is a 254% improvement. The parametric study results reveal that for the studied range of parameters, improving the t_1/r_1value in a pipe having the BU configuration would improve the capacity more in comparison with a similar system but having the FB intra-layer configuration. Moreover, it should be mentioned that the deformability of the FB configurations before reaching the collapse pressure is significantly smaller than the BU configurations.

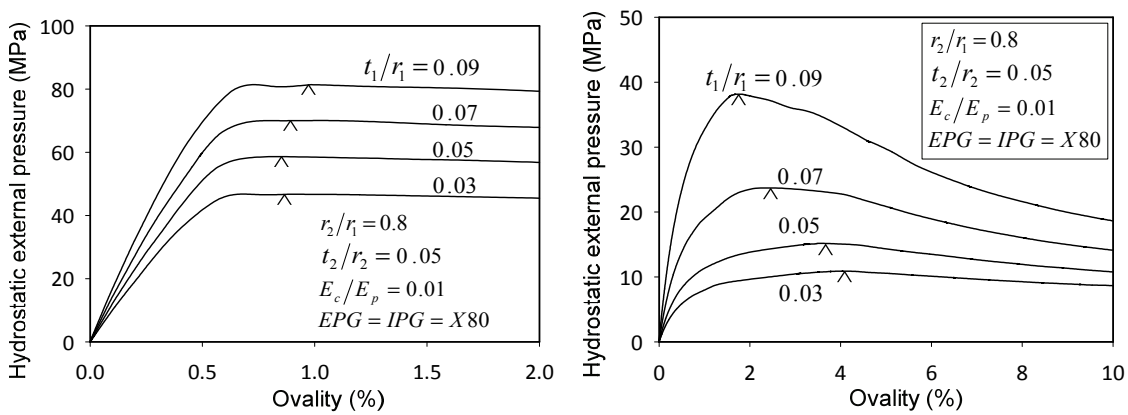

Figure 7.7.Influence of external pipe's thickness to radius ratio on the characteristic behavior of SPs with (a) FB configuration (b) BU configuration.

Figure 7.8 shows the characteristic paths of another set of SPs with OU and IU configurations. As can be seen in the figure, the OU configuration in the SPs with the external pipe's wall thickness of 0.03 and 0.05 yields a greater capacity than the IU configuration, while for the greater t_1/r_1 values the IU configuration is more efficient. In other words, if employing relatively thick-wall external pipes are intended, the IU configurations in which the core layer is bonded to the external pipe, but is unbonded from the internal pipe would have a greater capacity than the OU configuration. But in the case of SPs having relatively thin external pipes, using the OU configuration would be more efficient. Furthermore, it should be mentioned that in OU and IU configurations the stable deformability of the pipe would decrease when the pressure capacity increases.

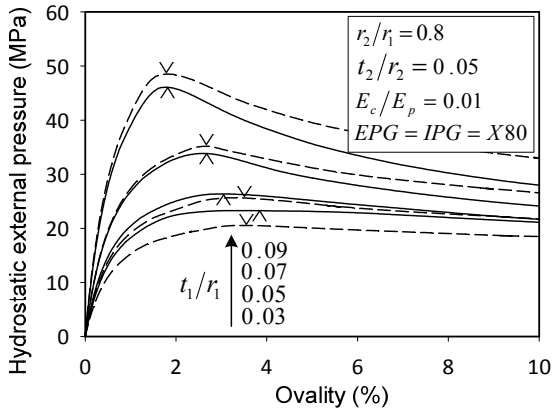

Figure 7.8.Influence of external pipe's thickness to radius ratio on the characteristic behavior of SPs having OU and IU configurations. Solid lines show the characteristic behavior of OU configurations and dashed lines illustrate the characteristic behavior of IU configurations. Symbol (^) represent the collapse point for OU configuration and symbol (v) shows the collapse point for the IU configuration.

Figure 7.9 shows the variation of the pressure capacity in a practical SP case having various external pipes' wall thicknesses, and various intra-layer configurations. As can be seen in the figure, for any value of t_1/r_1 the FB configuration has the greatest pressure capacity, and the BU configuration has the smallest capacity. Moreover, the OU and IU configurations can be considered as an enhancement to the BU configuration; but, they have considerably smaller capacities in comparison with the FB configuration.

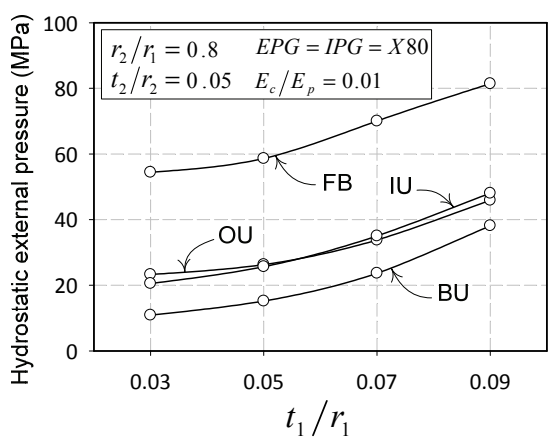

Figure 7.9. Influence of external pipe's thickness to radius ratio on the pressure capacity of SPs.

7.7.4. Influence of the internal pipe's thickness to radius ratio

Most of the analytical solutions and pipeline design guidelines ignore the contribution of the capacity of the internal pipe on the whole system. However, the results of our studies have shown that the internal pipe could provide considerable enhancement on the capacity of the system, and even in some cases, it has a greater effect than the external pipe. Figure 7.10 shows the change in the characteristic paths of two SP sets having FB and BU configurations with respect to the t_2/r_2 value. A comparison between Figures 7.7 and 7.10 reveals that the increase in the value of t_2/r_2would produce almost the same influence as would the increase int_1/r_1.

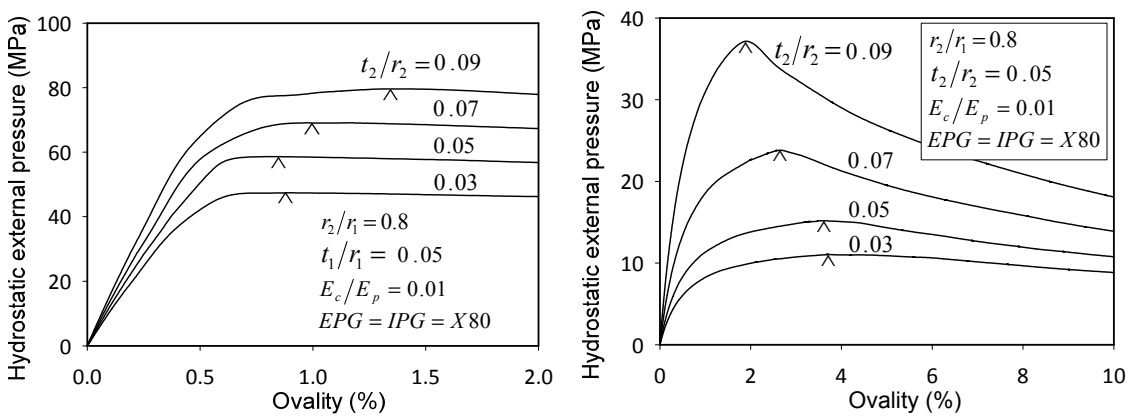

(a) *(b)*

Figure 7.10. Influence of internal pipe's thickness to radius ratio on the characteristic behavior of SPs with (a) fully bonded configuration (b) BU configuration.

Figure 7.11 represents the change in the behavior of SPs having IU and OU configurations with respect to the t_2/r_2value. As can be seen in this figure, increasing the thickness of the internal pipe increases the capacity of the system and decreases the deformability of the system. Moreover, similar to what was found for the t_1/r_1 value, the efficiency of IU and OU configurations is dependent on the t_2/r_2 value. That is, for SPs having relatively thin walled internal pipes, the IU configuration results in a greater capacity, while for SPs with relatively thick walled internal pipes, the OU configuration would provide a better efficiency than the IU configuration.

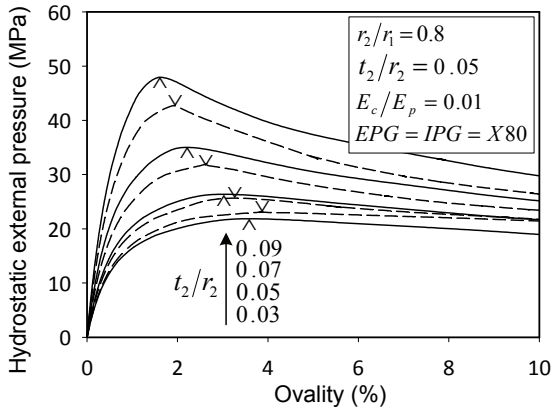

Figure 7.11.Influence of internal pipe's thickness to radius ratio on the characteristic behavior of SPs having OU and IU configurations. Solid lines show the characteristic behavior of OU configurations and dashed lines illustrate the characteristic behavior of IU configurations. Symbol (^) represent the collapse point for OU configuration and symbol (v) shows the collapse point for the IU configuration.

In conclusion, if a relatively robust internal pipe is employed, the OU configuration in which the internal pipe is bonded to the core would result in a better pressure capacity; while for SPs having external pipes with relatively greater wall thicknesses, the IU configuration is more efficient.

Figure 7.12 summarizes the pressure capacity of SPs presented in Figures 7.10 and 7.11. As can be seen in this figure, the efficiency of the intra-layer mechanism in IU and OU is dependent on the t_2/r_2 values. The results of this case study show that for the SP case with t_2/r_2 of 0.03, upgrading the BU configuration to either IU or OU configurations would enhance the capacity of the system by 109%. While in the SP system with t_2/r_2 of 0.09, upgrading the BU configuration to OU and IU configurations would improve the capacity of the system by 16% and 30%, respectively. The results of our parametric studies show that the influence of the internal pipe's thickness on the pressure capacity is more dependent on the intra-layer configuration in comparison with the effect of the external pipe's thickness.

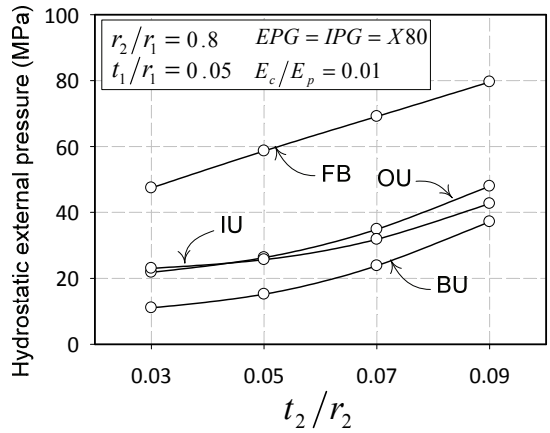

Figure 7.12. Influence of internal pipe's thickness to radius ratio on the pressure capacity of SPs.

7.7.5. Influence of the core stiffness ratio

In general, increasing the core stiffness improves the pressure capacity of the system. However, the magnitude of the capacity enhancement is highly dependent on the intra-layer adhesion properties. Moreover, changing the core layer stiffness ratio would influence the characteristic path profile and would even change the path category. Figure 7.13 illustrates the influence of the core stiffness ratio on the characteristic paths of two sets of SPs having FB and BU configurations. As can be seen in Figure 7.13.a, the characteristic path of the SP system having E_c/E_p of 0.1 is a bilinear path before reaching the collapse pressure. While, those sandwich pipes having relatively soft core layers follow the first category of the above-mentioned characteristic paths. Consequently, the core stiffness would significantly influence the stable deformability of the system.

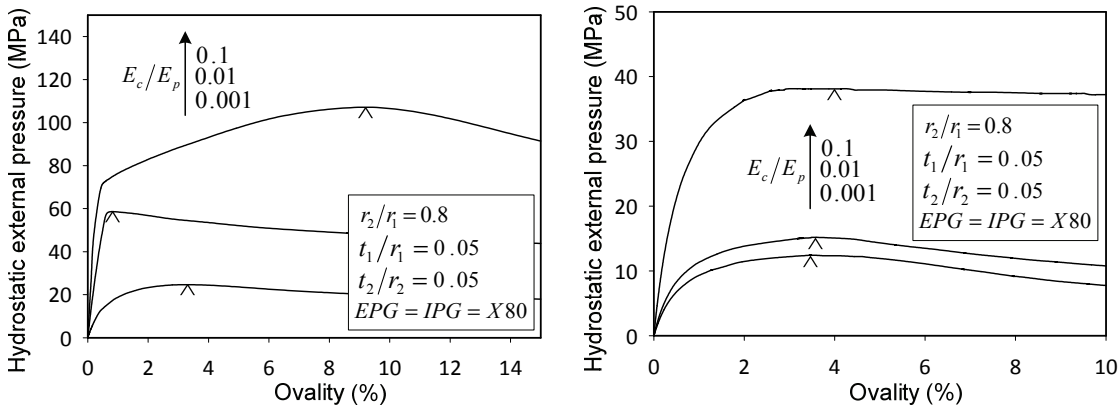

(a) *(b)*

Figure 7.13. Influence of the core stiffness on the characteristic behavior of SPs with (a) fully bonded configuration (b) BU configuration.

As illustrated in Figure 7.14, IU and OU configurations represent the same pressure capacities for relatively soft core materials ($E_c/E_p = 0.001, E_c/E_p = 0.01$), but in the case of relatively stiff core layers, the IU configuration in which the core layer is bonded to the external pipe is more efficient. Moreover, for all core stiffness ratios the IU configuration has a greater stable deformability.

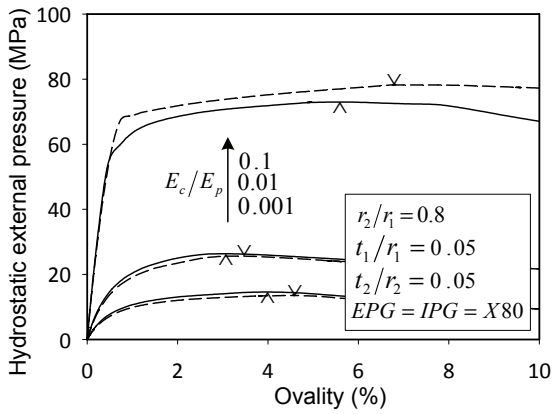

Figure 7.14. Influence of the core stiffness on the characteristic behavior of SPs with OU and IU configurations. Solid lines show the characteristic behavior of OU configurations and dashed lines illustrate the characteristic behavior of IU configurations. Symbol (^) represents the collapse point for OU configuration and symbol (v) shows the collapse point for the IU configuration.

Figure 7.15 illustrates the change in the pressure capacity of the cases studied in Figures 7.13 and 7.14 with respect to the core stiffness ratio. As can be seen in this figure, the BU, IU and OU configurations provide almost similar pressure capacities for the SP case with$E_c/E_p = 0.001$. Therefore, it can be concluded that in SPs with relatively soft cores bonding the core layer to either the external or internal pipes cannot improve the capacity of the system, unless the core layer is bonded to both of the surrounding pipes.

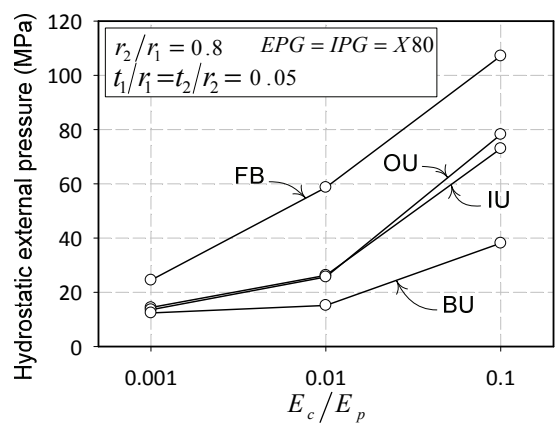

Figure 7.15. Influence of the core stiffness on the pressure capacity of SPs.

It should be mentioned that in most of the practical PIP systems in which the core layer is designed to offer thermal insulation properties, the core stiffness ratio would be less than 0.001. Therefore, the so-called practical PIP systems can be analyzed and designed without modeling the bond between the layers unless a special bonding layer is considered between the core layer and both internal and external pipes to provide the FB configuration. Furthermore, a comparison study shows that in the case of relatively soft core layers there is not a significant difference between the pressure capacities of the OU and IU configurations. However, for SPs having relatively stiff core layers, the OU configuration shows a slightly greater capacity.

7.7.6. Influence of the internal and external pipes' steel grade

Figure 7.16 illustrates the effect of steel's grades on the characteristic paths of a set of SPs having various intra-layer configurations. As can be seen in this figure, an enhancement of internal or external pipes' steel grades would improve the pressure

capacity of the system. However, the magnitudes of the capacity enhancement in OU, IU and BU configurations are less than in the FB configurations. Furthermore, the parametric study results show that upgrading the steel grade of the internal and/or external pipes improves the stable deformability of the system.

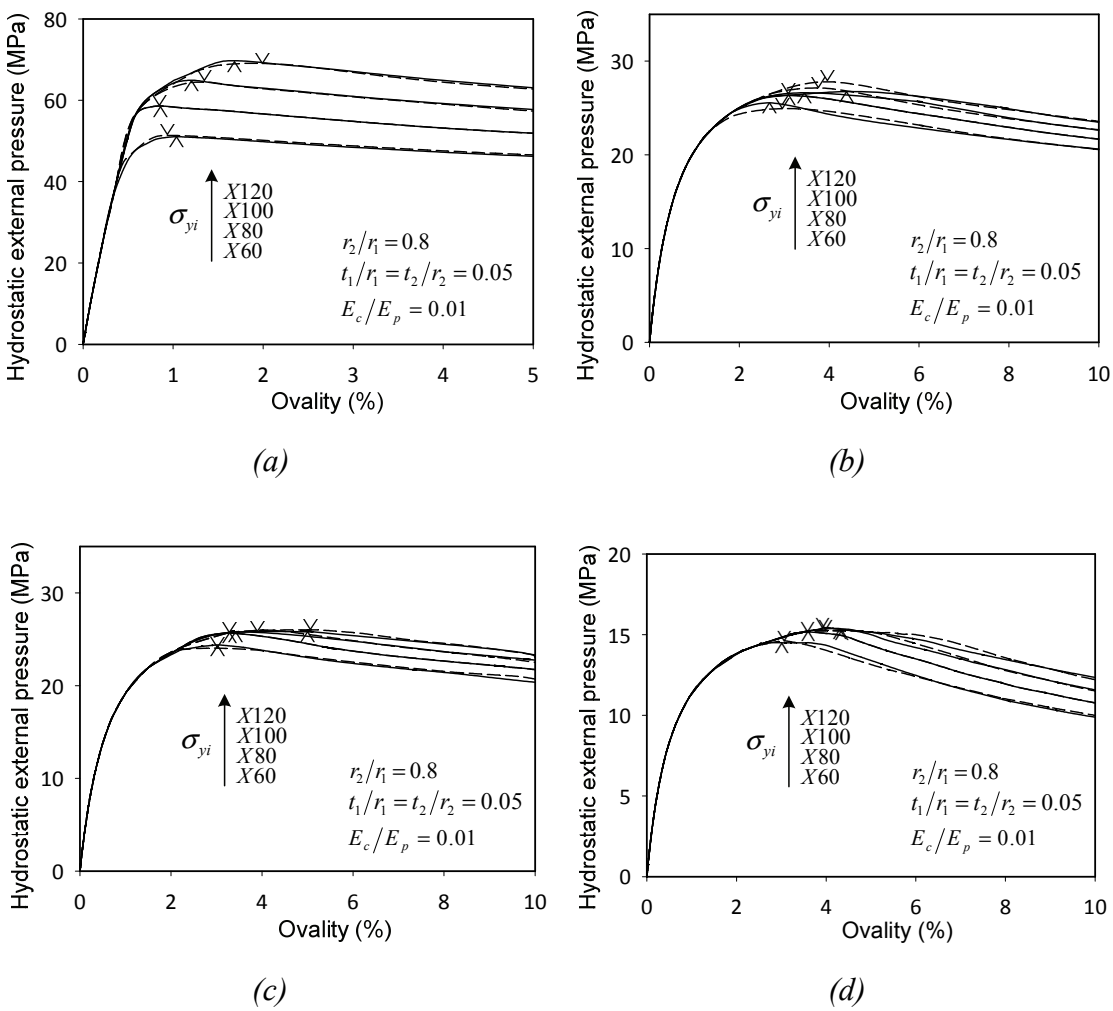

Figure 7.16. Influence of internal and external pipes' steel grade on the characteristic behavior of SPs having FB configuration. (a) FB configuration. (b) OU configuration. (c) IU configuration. (d) BU configuration. Solid lines show the influence of changing in the steel grade of the external pipe on the characteristic behavior and dashed lines illustrate the effect of changing in the internal pipe steel grade on the characteristic behavior of pipes. Symbol (^) represent the collapse point for solid lines and symbol (v) shows the collapse point for dashed lines.

In the case of the OU configuration, it is observed that improving the internal pipe's steel grade is more efficient than upgrading the external pipe's steel grade. Moreover, for the SP sets illustrated in Figure 7.14.b, improving the external pipe's steel grade to more than X80 would not have any significant effect on the pressure capacity of the system, and would only improve the deformability of the system before reaching the collapse pressure. Figures 7.16.c and 7.16.d show the characteristic behaviors for the IU and BU configurations, respectively. As can be seen in these figures, improving the steel grades of the external and internal pipes has a similar effect on the characteristic path. Moreover, in these configurations upgrading the steel pipes to steel grades greater than X80 would not significantly improve the capacity of the system. It should be noted that the effect of the steel pipes' grade is highly dependent on the other parameters of the pipeline; however the parametric study results show that upgrading the steel grades of the internal and/or external pipes is more efficient in the FB configuration than in the other three configurations.

Figure 7.17 summarizes the influence of internal or external pipes' steel grade on the pressure capacity of the system for a practical set of design configurations. As can be seen in the figure, for all the intra-layer configurations, upgrading the internal and external pipes' steel grades have the same influence on the pressure capacity. Moreover, our parametric study results show that the BU, IU and OU configurations would not significantly benefit from employing pipes having steel grades higher than X80 in comparison with the FB configuration. In other words, in order to enhance the external pressure capacity of the sandwich pipes by employing high grade steel pipes as either internal or external pipes, the core layer should be bonded to the surrounding pipes.

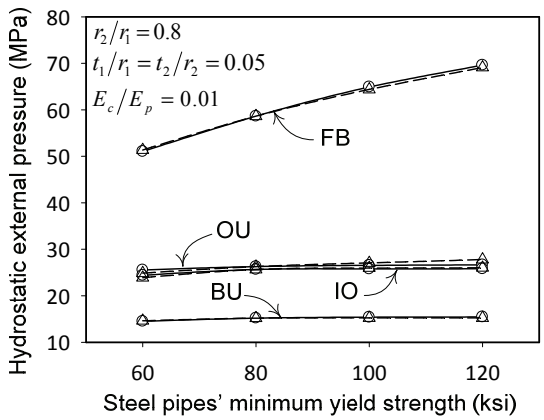

Figure 7.17. Influences of the internal and external pipes' steel grade on the pressure capacity of SPs. The solid lines with circular symbols demonstrate SP designs with internal pipe's steel grade of X80 and various external pipes' steel grades. Moreover the dashed lines with triangular symbols shows SP designs with external pipe's steel grade of X80 and various external pipes' steel grades.

7.8. SIMPLIFIED PRACTICAL EQUATIONS

Former studies by the authors have shown that Equation (7.8) can only be used for evaluating the pressure capacity of SPs having the FB intra-layer configuration with a reasonable accuracy. Table 7.2 demonstrates the calculated set of constants from fitting Equation (7.8) on the SPs' pressure capacities evaluated from the parametric study results as well as the maximum error of the equation in comparison with the FE results. Moreover, Arjomandi and Taheri [7.18] evaluated the error margin produced by the above equation for more practical design cases in which the SP configurations having $r_2/r_1$of 0.9 and t_1/r_1 of 0.03 were excluded from the study. As a result, they found that Equation (7.8) was capable of evaluating the pressure capacity of practical SPs having an FB configuration with less than 10% error margin.

In this study, Equation (7.8) was used for evaluating the pressure capacity of SPs having the alternative intra-layer configurations (i.e., IU, OU and BU). The SPSS [7.23] statistical package was used to fit Equation (7.8) into the calculated pressure capacities of SPs having OU, IU and BU configurations using the FE approach. The pressure capacities calculated from 3072 sandwich pipe FE models for each intra-layer

configuration were used to find the equation's constants. SP configurations having the parameters ranges presented in Table 7.1, excluding the SPs having r_2/r_1 of 0.9, were used for each intra-layer design configurations. In order to improve the accuracy of the equations, the values of the constants appearing in Equation (7.8) were calculated for three core stiffness ratios of 0.001, 0.01 and 0.1. Tables 7.3 to 7.5 illustrate the calculated constants' values for SPs having OU, IU and BU configurations, respectively.

However, special attention must be paid in using Table 7.6, in which the constants' values for the BU configuration are provided. This is because as discussed earlier, the BU SP configurations having stiffness ratios of 0.1, and as such, are highly susceptible to having the third type of characteristic path, which would be stable for any magnitude of ovality. Therefore, the use of nonlinear FE analysis for characterizing the response of a SP having a stiffen ratio of 0.1, and BU configuration is highly recommended.

Moreover, the maximum error margins produced by Equation (7.8) for evaluating the pressure capacity of SPs in the studied range of parameters are also shown in Tables 7.3 to 7.5. As can be seen in these tables, the maximum error of the equation is dependent on the SP's intra-layer configuration and also the core stiffness ratio. However, it can be said that the error of the equation would be less than 20% for all the possible configurations. This error margin is reasonable, considering the fact that the relatively simple equation can be used to establish the buckling capacity of a wide range of SP configurations having complex intra-layer mechanism and material plasticity.

Table 7.2. The value of constants of Equation (7.8) for calculating the pressure capacity of the FB SPs

E_c/E_p	*a*	*b*	*c*	*d*	*e*	*f*	*g*	*h*	*i*	*j*	*k*	*l*	*m*	**Max error %**
0.1	2.032	0.909	0.377	1.055	0.759	0.152	0.884	-0.224	1.021	7.250E-02	-0.067	-0.094	3.833	9.58
0.01	0.765	1.068	0.253	0.890	0.422	0.148	0.947	0.112	0.777	6.020E-05	-0.943	-0.689	3.871	15.08
0.001	1.406	2.102	-0.134	0.747	0.231	-0.016	2.742	-0.515	0.317	2.457E-04	-0.244	0.206	1.133	19.31

Table 7.3. The value of constants of Equation (7.8) for calculating the pressure capacity of the OU SPs

E_c/E_p	*a*	*b*	*c*	*d*	*e*	*f*	*g*	*h*	*i*	*j*	*k*	*l*	*m*	**Max error %**
0.1	0.773	1.757	-1.018	1.148	0.182	-0.032	0.648	0.964	0.586	3.40E-02	-0.341	-0.198	4.444	11.56
0.01	5.210	2.552	-0.083	0.795	3.029	0.026	2.391	-0.039	0.741	2.42E-03	-0.153	-0.033	2.622	17.04
0.001	3.071	2.617	-0.111	0.662	0.102	-0.234	2.695	-0.093	0.176	1.59E-03	-0.043	0.033	3.272	16.10

Table 7.4. The value of constants of Equation (7.8) for calculating the pressure capacity of the IU SPs.

E_c/E_p	*a*	*b*	*c*	*d*	*e*	*f*	*g*	*h*	*i*	*j*	*k*	*l*	*m*	**Max error %**
0.1	1.26	0.63	1.54	0.81	0.01	0.52	0.48	-1.25	0.75	4.02E-02	-0.06	-0.29	3.95	16.91
0.01	1.45	2.14	0.14	0.66	4.85	-0.01	2.71	-0.17	0.77	1.74E-03	-0.12	-0.21	2.80	15.88
0.001	1.29	2.33	0.03	0.60	0.01	-0.47	0.69	2.27	0.45	3.66E-02	-0.25	3.11	-0.46	19.97

Table 7.5. The value of constants of Equation (7.8) for calculating the pressure capacity of the BU SPs.

E_c/E_p	*a*	*b*	*c*	*d*	*e*	*f*	*g*	*h*	*i*	*j*	*k*	*l*	*m*	**Max error %**
0.1	3.42	3.26	-0.50	0.59	0.06	-0.15	-0.12	3.12	0.30	6.97E-03	0.07	2.87	-1.53	13.59
0.01	0.77	2.63	-0.21	0.47	0.02	-0.04	-0.12	3.21	0.40	7.66E-02	-0.03	2.91	-0.27	15.62
0.001	2.14	2.70	-0.04	0.54	0.19	-0.06	0.27	4.48	0.60	6.75E-02	-0.20	3.03	-0.21	15.92

7.8.1. Verification with the experimental results

One of the experimental studies on the behavior of SPs under hydrostatic external pressure has been conducted by Stefen et al. [7.1], who performed a set of experimental studies on small scale laboratory samples of SPs to investigate their behavior under the hydrostatic external pressure. They tested SP samples having concrete and polypropylene core materials sandwiched by aluminum tubes, and studied the influence of different core thickness ratios for each type of core material. Two specimens were tested for each configuration and the characteristic behaviors and collapse pressures of the pipes were monitored. The stiffness ratio between the concrete core layer and the aluminum pipes used in Stefen et al.'s research was relatively large in comparison with the practical SP configurations made by steel pipes. Therefore, in this study, only the results from their tests on SPs having a polypropylene core layer are used for the verification of the integrity of the proposed equations.

Table 7.6 presents the pressure capacity of the pipes evaluated experimentally by Stefen et al [7.1], as well as the pressure capacity evaluated by Equation (7.8) of this paper for various intra-layer configurations. In order to use Equation (7.8) for a SP having core stiffness ratio that fall in between the values of the calibrated constants, a linear interpolation was used to establish the pressure capacity as a function of the logarithm of the corresponding core stiffness.

Table 7.6. Correlation of Stefen et al.[7.18] experimental results with the pressure capacity calculated from Equation (7.8) using constants for various intra layer properties.

Specimen	r_2 (mm)	t_2 (mm)	t_c (mm)	t_1 (mm)	P_{CO} Experiment (Mpa)	P_{CO} FB (Mpa)	P_{CO} OU (Mpa)	P_{CO} IU (Mpa)	P_{CO} BU (Mpa)
PIP.M2.G1.I02	23.14	1.68	11.26	1.62	37.64	37.62	22.68	25.79	12.83
PIP.M2.G1.I03	23.26	1.62	11.10	1.61	31.14	36.24	21.90	24.63	12.12
PIP.M2.G2.I01	23.27	1.70	4.62	1.46	20.31	23.51	13.23	13.24	8.51
PIP.M2.G2.I02	23.33	1.69	4.69	1.49	17.13	23.65	13.24	13.24	8.50

As mentioned above, the adhesion between the layers would significantly influence the pressure capacity of SPs. On the other hand, because in practice the interface condition between the layers may fall between the fully bonded and unbonded cases, none of the above-mentioned configurations can exactly represent the real SP configuration. Nonetheless, it can be stated that the pressure capacity of a SP system having an intermediate intra-layer bond condition would be a pressure capacity with its value falling between the pressure capacity of an unbonded and a fully bonded configuration (as the lower and upper bounds), respectively. In the experiments conducted by Stefen et al. the polypropylene core layer was first mounted on the internal pipe and then the combined system was slipped into the external pipe, and finally an epoxy resin was used to create a strong bond between the core layer and both the internal and external pipes. As a result, the pressure capacities of their systems are closer to the capacities calculated for the FB configurations. As seen, the use of the equation derived for the BU configuration significantly under predicted the capacity of the system.

7.9. OPTIMIZATION OF THE SYSTEM

One of the main purposes of developing the above-mentioned simplified equations was to find an equation which could be used to optimize SP configurations. Establishing an optimized SP configuration through a nonlinear FE analysis would be an extremely time–consuming endeavor, thereby rendering the approach impractical. However, the use of the relatively simple equations proposed in this study could be viewed as a reasonable alternative to the complex FE approach, thus assisting the offshore pipeline designers to establish the optimum design configurations in practice.

The objective function used in designing the offshore pipelines usually involves the minimization of the construction and maintenance costs of the pipeline. These costs constitute a majority of the overall cost of a SP. It should be noted that estimation of all the expenses (i.e., theses associated with the manufacturing, installation and operation and other related environmental costs), with a simple equation, would not be feasible. However, with the aim of presenting a simple practical optimization procedure and also to illustrate the influence of the adhesion between layers on the optimized configuration, the simple manufacturing cost function proposed by Arjomandi and Taheri [7.18] was

used in this research. The cost function assumes that the manufacturing cost of the pipeline is the sum of the manufacturing cost of each layer as depicted by Equation (7.12).

$$C_{Man-SP} = C_{Man-P1} + C_{Man-P2} + C_{Man-C} \tag{7.12}$$

where C_{Man-P1} ,C_{Man-P2} and C_{Man-C} are respectively the manufacturing costs of the internal pipe, external pipe and the core layer which can be calculated by:

$$C_{Man-Pi} = \alpha A_{si}\left[1 + 0.3\left(\frac{\sigma_{yi}}{\sigma_{y-X60}}\right)\right] \qquad i = 1,2 \tag{7.13}$$

and

$$C_{Man-C} = A_c\left[1 + 0.1\left(\frac{E_c}{E_p}\right)\right] \tag{7.14}$$

where α is the calibration constant, which represents the relative cost between the core material and steel. In this study, α has been taken as 5, which was calculated based on the average cost of the studied core materials and the steel.

Several mathematical approaches could be used to solve SP's geometrical and material optimization problem. In this paper a minimum seeking algorithm was used within a finite range of the practical SP configurations. However, in order to find an optimum configuration for a specific water depth, the studied SP configurations must have the potential to tolerate the required hydrostatic external pressure. Our observation of the results indicates that there would be a limit for the pressure capacity of each SP configuration. For example, the operational water depths of SPs having core stiffness of 0.01 are 5000, 8000 and 8500 meters, respectively, for BU, IU and OU configurations.

As mentioned above, the SPs having the BU configuration and core stiffness ratio of 0.1 mainly exhibit a stable characteristic path; therefore, they were excluded from the optimization study. However, their interesting characteristic behavior might help the installation and maintenance of the pipeline in real applications. Therefore, they should be considered as a design alternative offering special stability features for use in relatively shallow waters.

Figure 7.18 illustrates the optimum external pipe's thickness to radius ratio evaluated for water depths between 1,000 and 10,000 meters. The results show that for any specific water depth, the optimum t_1/r_1value decreases by increasing the stiffness of the core, for

any intra-layer configuration. Moreover, the core stiffness ratio would establish which configuration would yield the largest and smallest optimized external pipe's thickness to radius ratio. As can be seen in the figure, in the case of SPs having core stiffness ratios of 0.001 and 0.01, the smallest and largest optimum external pipe's thickness to radius ratios belong, respectively, to the FB and BU configurations. Whereas, in the SP cases having E_c/E_p of 0.1, for a specific water depth the OU configuration in which the external pipe is free to slide or separate from the core layer would have the smallest optimizedt_1/r_1 values, while the IU configuration would exhibit the largest. Comparison of the optimized t_1/r_1values for OU and IU configurations indicates that except for the SP configurations having relatively stiff core layers, the OU and IU configurations would have almost the same optimum external pipe's thickness to radius ratios. However, the OU configuration has a slightly greater operational water depth than the IU configuration.

Figure 7.19 demonstrates the optimum internal pipe thickness to radius ratios with respect to the water depth for the four studied intra-layer configurations. As can be seen in the figure, similar to the t_1/r_1 parameter, the optimum t_2/r_2value is also dependent on the core stiffness ratio. However, it can be said that for the relatively soft cores ($E_c/E_p = 0.001, 0.01$) the BU configuration yields the smallest optimum t_2/r_2 values, while for SPs having relatively stiff core layers the IU configurations have the minimum t_2/r_2values. Furthermore, in the case of stiff core SPs, the pipes having FB and OU configurations in which the core layer is bonded to the internal pipe would have the largest internal pipe's thickness to radius ratios.

Figure 7.20 illustrates the optimum r_2/r_1values for SPs having core stiffness ratios of 0.1. The optimum r_2/r_1values for other core stiffness values are mostly 0.9. Whereas, as can be seen in Figure 7.19, in the case of SPs having relatively stiff core layers and IU or OU configurations, ther_2/r_1 value decreases by increasing the operational water depth.

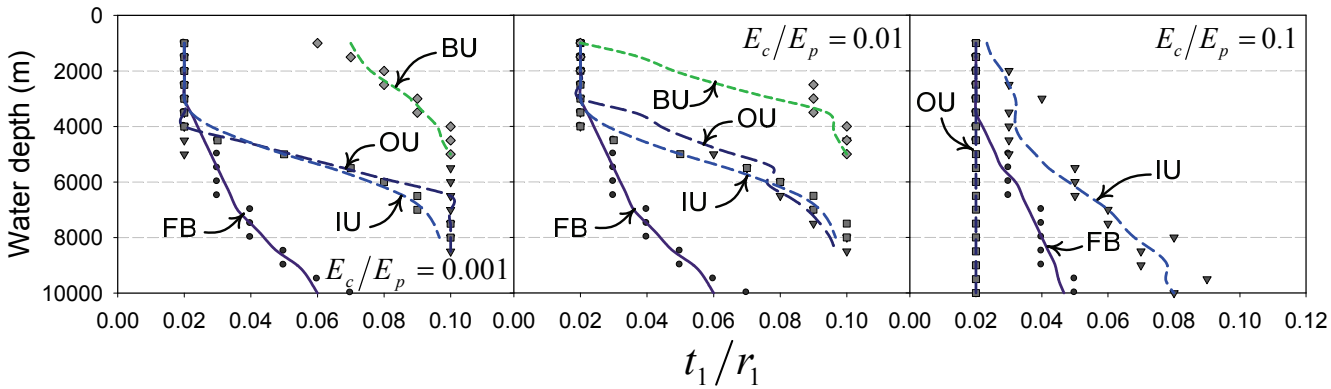

Figure 7.18. Optimized external pipe's thickness to radius ratios for the water depth range between 1000 and 10000 meters considering various intra layer interaction properties.

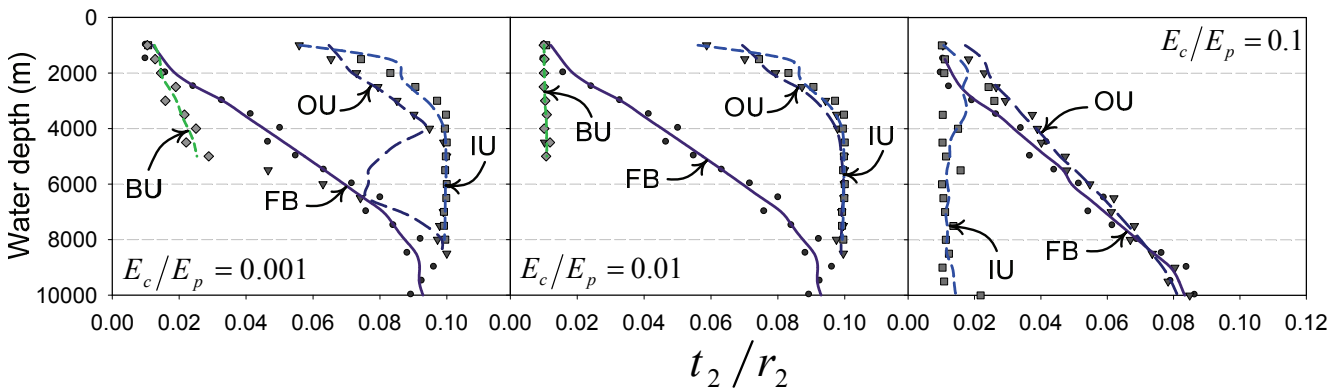

Figure 7.19.Optimized internal pipe's thickness to radius ratios for the water depth range between 1000 and 10000 meters considering various intra layer interaction properties.

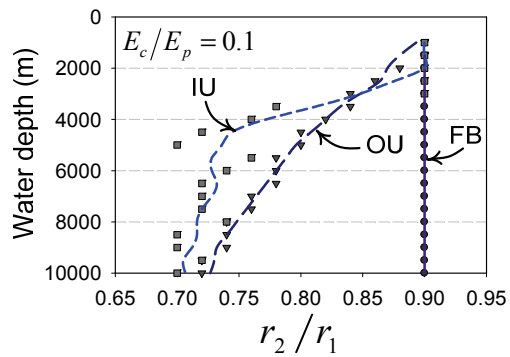

Figure 7.20. Optimized internal pipe to the external pipe's radius ratio for the SP configurations with $\boldsymbol{E_c/E_p}$ of 0.1.

An SP system employs two steel pipes as the internal and external pipes which might have different steel grades. Therefore, the steel grade of the internal and external pipes can be considered as design parameters which would have significant effects on the pressure capacity and stable deformability of the pipeline. One of the objectives of this study is investigating the effect of upgrading the internal and/or external pipe's steel grades on designing an efficient SP system. Therefore, the optimized internal and external pipes steel grades were calculated for various water depths and intra-layer configurations. The results of this study were demonstrated in Figure 7.21 and 7.22 which illustrate the external pipe and internal pipes' optimum steel grades, respectively. The results of this study indicate that by increasing the operational water depth, higher steel grades are required for both the internal and external pipes in most of the SP configurations.

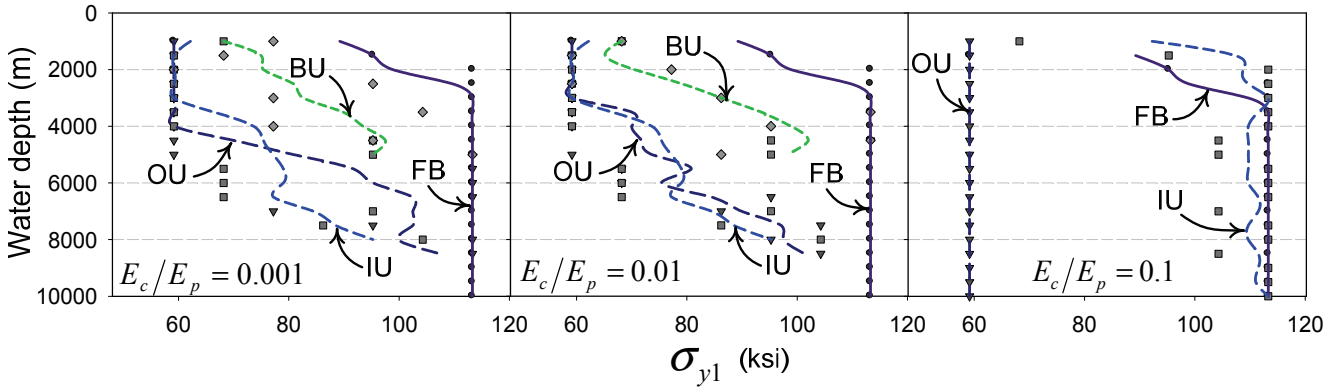

Figure 7.21. External pipe's optimized steel grade.

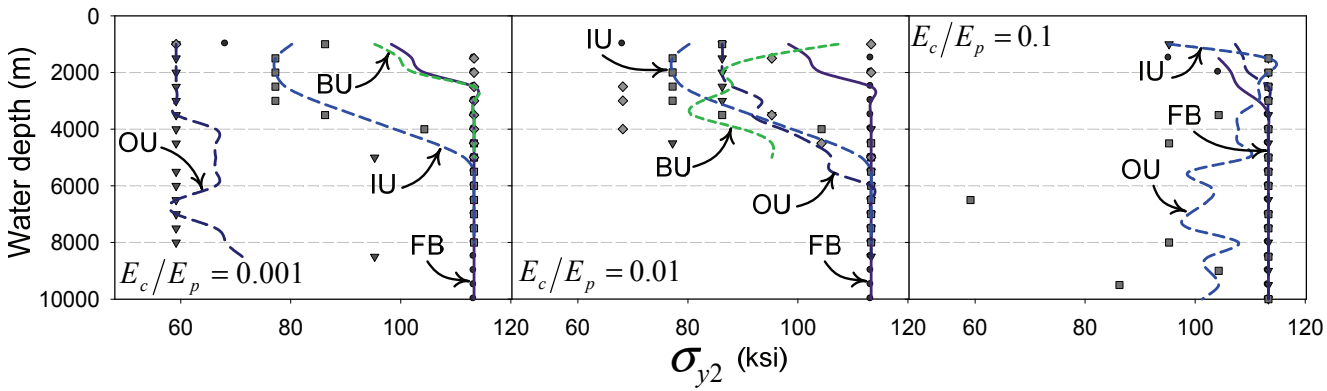

Figure 7.22. Internal pipe's optimized steel grade.

As can be seen from the figures, upgrading the steel grades of either the external pipe or the internal pipe would generate the most influence on the efficiency of the FB configuration. In other words, it can be said that the efficiency of FB configurations can be significantly improved by employing higher grade steel. Moreover, the comparison between the results of OU and IU configurations in Figure 7.21 also illustrates that by increasing the stiffness of the core, the optimum steel grade of the external pipe would decrease the capacity of the OU configurations, but would increase the capacity in the IU configuration. In other words, improving the external pipe's steel grade would be more effective if adequate intra-layer adhesion exists. The comparison of the results of the optimum internal and external pipes' steel grade also reveals that except for a few cases, the influence of the grade of the internal would be greater than that used in the external pipe. This is because larger magnitude of stress and plastic strain concentrations would develop in the smaller diameter internal pipe at the collapse pressure.

Figure 7.23 illustrates the cost comparison between the studied optimum configurations for various water depths. The relative optimized cost in this figure is the ratio between the optimized cost of the studied SP with respect to the optimized cost for the SP having an FB configuration and a 0.1 core stiffness ratio for the operational water depth of 1000 meters. As can be seen in the figure, for all the values of core stiffness, the FB would produce the most optimum intra-layer configuration. After the FB configuration, SPs having OU, IU and BU, respectively are the most efficient. Moreover, SPs having OU and IU configurations with intermediate core stiffness ($E_c/E_p = 0.01$) yield the same optimum costs for a specific water depth, while in the case of relatively soft or stiff core layers ($E_c/E_p = 0.001$ and $E_c/E_p = 0.1$) the OU configuration is significantly more efficient. Furthermore, studying the BU configuration shows that increasing the stiffness of the core layer in the BU configuration would significantly improve the efficiency of the system.

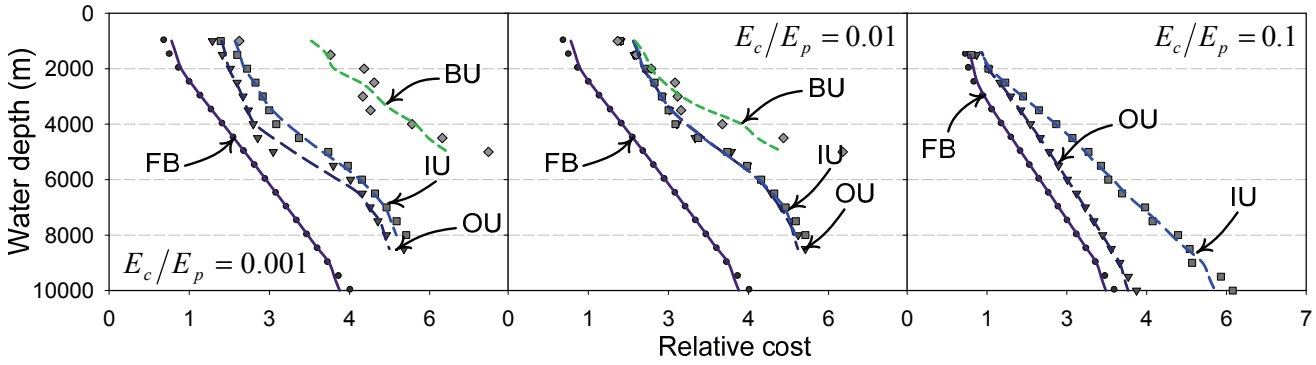

Figure 7.23. Optimized manufacturing cost of various SP configurations.

7.10. SUMMARY AND CONCLUSIONS

In this paper, the influence of the intra-layer adhesion properties on the systems' characteristic behavior and pressure capacity of sandwich pipes having a wide range of design parameters was investigated. In addition, the influence of the design parameters such as the external and internal pipes' thickness to radius ratios, core thickness and stiffness and the internal and external pipes' steel grades were also investigated. Accurate FE models were developed and a comprehensive parametric study was conducted using more than 12,000 FE models. Using the FE results, a simplified equation which was developed previously by the authors for evaluating the buckling capacity of SPs falling within the FB configuration, was calibrated for the other configurations. The calibrated equations enable one to evaluate the buckling capacity of all other possible SP configurations, including the category in which the core layer may slides on the internal and/or external pipes, or even separate from the pipes. The developed equations were used along with an approximate manufacturing cost function to establish the optimum design parameters of SP systems suited for various water depths. Using the optimization study results, the variation of the optimum design parameters and the relative cost of each configuration with respect to the operational water depth were illustrated. The summary and conclusions of this research can be summarized as:

- Depending on the pipe properties, SPs would exhibit three categories of characteristic behavior. Most of the SP configurations fall in the first and second categories, which would respectively exhibit linear and bilinear characteristic paths before reaching their ultimate pressure capacity. However, the third category of SPs would never become unstable under an external pressure. As an example, a SP with a relatively stiff core layer, with unbonded core from both the internal and external pipes, would fall in the third category.
- The results of the parametric studies revealed that the FB configuration would offer the greatest pressure capacity, and the BU configuration would yield the smallest capacity for a SP with similar configuration. Moreover, comparison between the capacities of OU and IU configurations reveals that SPs having OU

and IU configurations with similar other parameters would exhibit almost similar pressure capacities.

- Changing the thickness or stiffness of the core layer would significantly influence the capacity of the system and would even change the pipe's characteristic behavior category. It was found that increasing the thickness and/or stiffness of the core layer improved the pressure capacity of the system; however, the magnitude of the improvement was dependent on the other structural properties, especially onto the condition of the intra-layer bond interface. The parametric study results showed that perfect bond between the core layer and either of the external or internal pipes would improve the influence of core layer's parameters significantly.
- Improving the thickness to radius ratio of either the internal or external pipes increased the pressure capacity of the system. Despite the fact that some approaches ignore the contribution of the internal pipe on the capacity of the system under external pressure, the results illustrated that the internal pipe would have a significant influence on the pressure capacity.
- An important question in any designer's mind is the level of enhancement one could obtain by upgrading the internal and/or external pipes' steel grades in SP systems. The parametric study results revealed that employing high grade steel pipes in SP systems would exhibit the highest attribute in the FB configuration. For other configurations, the influence of the steel grade would be affected by the other parameters; in fact, in some cases enhancing the steel grades of either the internal and/or external pipes would not improve the pressure capacity of the system.
- The simplified equation suggested by the authors in one of their previous works (applicable to the FB configuration only) was calibrated for applicability to the other configurations in this research. The calculated errors in comparison to the FE analysis results and the experimental results extracted from the literature indicated that the proposed equations could produce reasonably accurate outcomes when used for practical applications and optimization procedures.

- A former cost function suggested by the authors and the equations developed in this study were further used to establish the most optimum SP design configurations for various water depths, in consideration of various intra-layer configurations. The optimization study results reveal that, for the considered cost function, the optimum intra-layer configurations would be, respectively FB, OU, IU and BU. However, no general rule could be established for accounting the other structural parameters.

7.11. REFERENCES

7.1. Estefen, S. F., Netto, T. A., and Pasqualino, I. P., (2005). Strength analyses of sandwich pipes for ultra deep-waters. *Journal of Applied Mechanics, 72*(4), 599-608.

7.2. Castello, X., Estefen, S. F., Leon H. R., Chad L. C. and Souza J., (2009). Design Aspect and Benefits of Sandwich Pipes for Ultra Deepwaters. *International Conference on Offshore Mechanics and Arctic Engineering, OMAE2009-79528,* Hawaii, USA.

7.3. Brush DO. and Almroth, B., (1975). *Buckling of bars, plates and shells*. McGraw-Hill, New York.

7.4. Sato, M. and Patel, M. H., (2007).Exact and simplified estimations for elastic buckling pressures of structural pipe-in-pipe cross sections under external hydrostatic pressure. *Journal of Marine Science and Technology, 12*(4), 251-262.

7.5. Sato, M., Patel, M. H., and Trarieux, F., (2008).Static displacement and elastic buckling characteristics of structural pipe-in-pipe cross-sections. *Structural Engineering Mechanics, 30*(3), 263-278.

7.6. Arjomandi, K. and Taheri F., (2010).Elastic buckling capacity of bonded and unbounded sandwich pipes under external hydrostatic pressure. To appear in the *Journal of Mechanics of Materials and Structure*.

7.7. Kardomateas, G. A. and Simitses, G. J., (2002).Buckling of long, sandwich cylindrical shells under pressure. *Proceedings of the International Conference on Computational Structures Technology*, 327-328.

7.8. Kardomateas, G. A. and Simitses, G. J., (2005).Buckling of long sandwich cylindrical shells under external pressure. *Journal of Applied Mechanics, 72*(4), 493-499.

7.9. Ohga, M. , Sanjeewa Wijenayaka, A. and Croll, J. G. A., (2005). Reduced stiffness buckling of sandwich cylindrical shells under uniform external pressure. *Thin-Walled Structures, 43*(8), 1188-1201.

7.10. Castello, X. and Estefen, S. F., (2006). Adhesion effect on the ultimate strength of sandwich pipes. *International Conference on Offshore Mechanics and Arctic Engineering, OMAE2006-92481,* Hamburg, Germany.

7.11. Castello, X., and Estefen, S. F., (2008). Sandwich pipes for ultra deep-water applications. *Offshore Technology Conference,* OTC 197041*,* Houston, Texas, USA.

7.12. Arjomandi, K. and Taheri F., (2010).Stability and Post Buckling Response of sandwich pipes under hydrostatic external pressure. Submitted to the *International Journal of Pressure Vessels and Piping*.

7.13. Kyriakides, S., (2002). Buckle propagation in pipe-in-pipe systems. Part I. Experiments. *International Journal of Solids and Structures, 39*(2), 351-366.

7.14. Kyriakides, S. and Netto, T. A., (2002). Dynamic propagation and arrest of buckles in pipe-in-pipe systems. *Proceedings of the International Conference on Offshore Mechanics and Arctic Engineering* - OMAE, 4, 199-205.

7.15. Kyriakides, S. and Vogler T.J., (2002). Buckle propagation in pipe-in-pipe systems. Part II. Analysis. *International Journal of Solids and Structures, 39*(2), 367-392.

7.16. Kyriakides, S. and Netto, T. A., (2004). On the dynamic propagation and arrest of buckles in pipe-in-pipe systems. *International Journal of Solids and Structures, 41*(20), 5463-5482.

7.17. Arjomandi, K. and Taheri F., (2010).Influence of the Material Plasticity on the Characteristic Behavior of Sandwich Pipes.*8th International Pipeline Conference.IPC2010-31518*, Alberta, Canada.

7.18. Arjomandi, K. and Taheri F., (2010).External Pressure Capacity of Sandwich Pipes. Submitted to the journal of *Marine Structures*.

7.19. API SPECIFICATION 5L., (2000). *Specification for line pipe*.API Publishing Services, Washington, D.C.

7.20. DNV Offshore Standard Det Norske Veritas, (2000). *Dnv-Os-F101, Submarine Pipeline Systems*. GCS AS, Norway.

7.21. ABAQUS User's and Theory Manuals., 2008.Version 6.8, Dassault Systèmes, RI, USA.

7.22. MATLAB, 2008. Version 7, The MathWorks Inc., MA, USA.

7.23. SPSS, 2008.Version 17, SPSS Inc., IL, USA.

CHAPTER 8
BENDING CAPACITY OF SANDWICH PIPES*

Kaveh Arjomandi and Farid Taheri
Department of Civil and Resource Engineering, Dalhousie University
Halifax, Nova Scotia, Canada

8.1. ABSTRACT

A Sandwich Pipe (SP) is an effective design alternative that can accommodate load and thermal insulation requirements set for pipelines used in deep and ultra-deep water applications. However, the design and development of a reliable SP requires an in depth understanding of the behavior of such a system under various loading conditions. In this paper, the behavior of SPs subject to pure bending, which is one of the governing loading conditions for offshore pipelines, is investigated.

In order to perform this investigation, a series of numerical parametric models, using the Finite Element (FE) method, was developed. The linear eigenvalue buckling analysis and the nonlinear post-buckling analysis were conducted to explore the systems' response. The influence of several significant structural parameters (i.e., in the context of various combinations of the geometrical and material properties, as well as the consideration of various possible intra-layer adhesion mechanisms), on the pre-buckling, buckling and post-buckling responses of SPs was investigated.

Moreover, the yield property of cold-formed pipes composed of high-grade steel is dependent on the material's extrusion orientation. With the increased use of such pipes in the oil and gas industry, it is crucial to understand the effect of material's yield anisotropy on the system response. In this research, the influence of steel's yield anisotropy was considered in numerical models using Hill's anisotropic material model. As well, the effect of anisotropic parameters on a system's bending capacity system was also investigated.

---

* Submitted to the Journal of Ocean Engineering.

8.2. NOMENCLATURE

D_1	Outer pipe specified outside diameter
D_2	Inner pipe specified outside diameter
E_c	Core material's elastic modulus
E_p	Internal and external pipes' elastic modulus
K	Pipeline curvature
M_{cr}^1	Buckling moment of the external pipe calculated from Equation (8.2)
M_{cr}^{SP}	Buckling moment of the SP system
N	Number of axisymmetric imperfection waves
R_i	Radius of pipe at node i
a_o, a_1	Imperfection magnitude parameters
l	Pipeline length
r_1	Outer pipe nominal radius
r_2	Inner pipe nominal radius
t_1	Outer pipe wall thickness
t_2	Inner pipe wall thickness
t_c	Core layer thickness
x	The longitudinal coordinate along the pipeline axis
x_i	The longitudinal coordinate of the ith node
θ_i	The polar coordinate of the ith node in the deformed shape
σ_{rr}	Stress in the radial direction
$\sigma_{\theta\theta}$	Stress in the tangential direction
σ_{zz}	Stress in the longitudinal direction
σ_{rr-y}	Yield stress in the radial direction
$\sigma_{\theta\theta-y}$	Yield stress in the tangential direction
σ_{zz-y}	Yield stress in the longitudinal direction
σ_{y1}	Yield stress of the external pipe material
σ_{y2}	Yield stress of the internal pipe material
σ_{ij}	Stress component in the corresponding direction
Δr_i	Imperfection of the pipe radius at node i

Λ	Pipeline non-dimensional length calculated from Equation (8.4)
λ	Half wavelength of the axisymmetric initial imperfection
ν_c	Core material Poisson's ratio
ν_p	Pipe material Poisson's ratio

8.3. INTRODUCTION

Bending is a primary loading condition applied to both onshore and offshore pipelines during installation and service life. In all major offshore pipeline installation methods, extreme bending is applied to pipelines during their installation. In the reeling method, the installation process of a pipeline begins with the spooling of a pipeline onto a reel, a process which applies excessive bending and incurs the corresponding plastic deformations. The pipeline would undergo further plastic bending deformations during the unspooling process. In another installation technique known as the S-lay method, excessive bending loads in the presence of a tensile load are applied to the pipeline while in contact with the stringer. Indeed, in all major offshore installation techniques, such as the reeling, the S-lay and the J-lay, combined bending loads and hydrostatic external pressure are experienced by the pipeline in the sagbend regime during the installation process.

An offshore pipeline might also be subjected to severe bending loads during its service life. Free spanning is a prime example of a condition where the contact between a pipeline and seabed is lost over a large span. This condition can occur over a rough seabed or on one subjected to scouring, such as the Strudel scouring in the Arctic. An Arctic offshore pipeline may also be subjected to bending loads due to ice keel gouging. A pipeline must therefore be able to withstand the bending loads, whether caused by seabed soil movements, gouging, or other natural or man-made phenomena.

Bending loads would also be applied to both onshore and offshore pipelines due to the subsidence of the foundation. In cases where offshore pipelines are installed in shallow waters or onshore pipelines are located in Arctic environments, the foundation of the pipeline may contain permafrost. Consequently, as the pipeline warms up due to its conveying fluid, it could develop a "thaw bulb" around the pipe. Another example of

onshore pipelines under bending loads is when the pipeline is pulled through an underground borehole in the directional drilling method.

Pipe-in-Pipe (PIP) systems were developed to improve the thermal insulation properties of traditional single-walled steel pipes. PIP systems are composed of three concentric cylindrical elements. The internal pipe, also called the product pipe, is in contact with the product and facilitates the product flow. The external pipe, or sleeve pipe, is in contact with the surrounding environment and separates the core layer and internal pipe from the outside. The secondary boundary provided by the external pipe ensures containment of the product should the oil leak from the internal pipe. An idealized model of an SP system and the corresponding cylindrical coordinate system is presented in Figure 8.1.

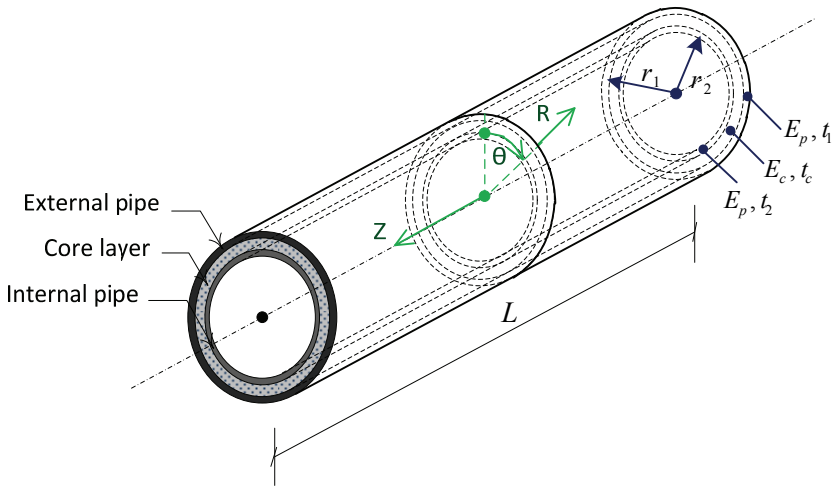

Figure 8.1. Idealized geometry and material properties of a SP system in the polar coordinate system.

The main function of the core layer in a PIP system is to provide appropriate thermal insulation to minimize thermal loss of the oil product in the flowline and thus facilitate product flow. However, the structural properties of the core layer and its interaction with the internal and external pipes would have a significant influence on the structural properties of the pipeline. In an SP system, the use of a more resilient structural core material improves the structural properties of the system and strengthens the potential sandwich structure. Therefore, using an SP system instead of a PIP system would be more economical, as well as being more environmentally friendly. It should also be

mentioned that combining the requisite thermal insulation and structural properties in a material to be used as the core layer would increase the cost of the core material. Nonetheless, using such a core layer would allow the designer to choose lighter internal and external pipes and consequently reduce the overall cost of the system.

SP systems can be effectively used for forming deep and ultra-deep offshore oil transportation flowlines, especially in Arctic regions, where thermal insulation, resistance to excessive external pressure and reduction of buoyancy weight during the installation process are required. Arctic oil pipelines must have sufficient thermal installation properties to keep the product warm and insulated from the ambient cold temperature and reduce the formation of hydrates. Moreover, pipeline systems intended for use in deep and ultra-deep waters must be able to endure the resulting extreme hydrostatic pressure. A persistent challenge affecting the use of traditional steel pipes in deep water and limiting their usage to a specific depth is their immense weight that adversely affects the installation process.

While sandwich pipes have been investigated by other researchers from various perspectives, most investigations have mainly examined their response under various loading conditions. The behavior of SPs under hydrostatic external pressure has been delineated through experimental, numerical and analytical methods, with much research having being devoted to the development of characteristic equations of the system used for calculating the buckling pressure via the eigenvalue linear perturbation method. One initial study was performed by Brush and Almroth in 1975 [8.1], who developed the characteristic equation of a cylindrical sandwich shell by simplifying the system to a plane-strain 2D problem of a ring resting on an elastic foundation. More recently, Sato and Patel [8.2] and Sato et al. [8.3] improved Brush and Almroth's solution and also recommended a simplified equation for calculating the stiffness of the equivalent spring system. In another study, Arjomandi and Taheri [8.4] developed a more accurate solution for calculating the buckling pressure of SPs under hydrostatic external pressure. One of the most significant improvements in their solution was the consideration of intra-layer adhesion condition contact between the core layer and the surrounding pipes.

The Finite Element (FE) numerical method and experimental laboratory tests have also been employed in characterizing the behavior of SPs under various loading

conditions. One of the initial studies was conducted by Estefen et al. [8.5] to investigate the behavior of SP systems under combined external pressure and bending loads. They studied the behavior of small-scale laboratory specimens made from aluminum pipes and polypropylene or cement core layers. Through both numerical and experimental investigations, they concluded that the studied SP systems are efficient design alternatives for offshore pipelines. In another study by Castello et al. [8.6], the influence of the core layer properties on the external pressure capacity was investigated using the FE numerical method. They also compared PIP with SP design alternatives for a hypothetical oil field and investigated the effect of the relative direction between the inner and outer pipes' maximum diameters on the external pressure capacity of the system.

Earlier studies have demonstrated that intra-layer adhesion properties have a significant influence on both the characteristic behavior and the pressure capacity of the system. In a series of research investigations undertaken by Castello and Estefen [8.7, 8.8], a numerical parametric study was developed to investigate the influence of intra-layer adhesion properties on the characteristic behavior of the system. The adhesion properties used in their numerical models were calculated through a series of experimental tests. In all of the above-mentioned studies by Estefen and his coworkers, a 2D FE model was used to examine the influence of the geometrical and material properties on the behavior of a set of SP systems under combined bending and external pressure. However, the 2D FE models were only capable of addressing the stability of the cross-section of the system. As a result, their results are valid only for pipes whose instability is governed by the Brazier effect (i.e., cross-section instability). This limitation arises from the inability of 2D models to capture the longitudinal wrinkles that could occur along a pipeline's axis. In another series of research by the authors [8.4, 8.9], the influence of various scenarios of interface bonding between the structural layers on the elastic buckling pressure of the pipe was analytically and numerically investigated.

Previous investigations have revealed that under a steady-state pressure, local buckling could be propagated along the pipeline; this phenomenon is also known as buckle propagation. It should be mentioned that buckle propagation pressure can be lower than external buckling pressure capacity. Several investigations have been

conducted to examine this phenomenon from different aspects. A series of remarkable studies by Kyriakides and his coworkers [8.10-8.13] has investigated buckle propagation phenomena from experimental, analytical and numerical perspectives.

Additional numerical parametric studies were subsequently conducted by the authors to investigate the behavior of SPs under hydrostatic external pressure. In one of our studies [8.14], the plastic buckling of SPs was characterized. It was established that the eigenvalue buckling analysis method would yield a wide margin of error in predicting the pressure capacity of SPs. In another series of studies by the authors [8.15, 8.16], the buckling and post-buckling behavior of SPs was investigated through a set of parametric models. A large number of FE models representing SPs with various intra-layer adhesion properties as well as several material models were developed. Using the parametric study results, a set of simplified practical equations was developed to calculate the pressure capacity of the system. Finally, by combining the pressure capacity equations with a recommended manufacturing cost function [8.16], an optimization procedure was developed to establish the optimized SP's structural parameters for a given depth.

The bending capacity and response function of the Penguins pipeline, a 60km PIP system developed in the northern North Sea, was investigated by Carr et al. [8.17]. They experimentally tested the prototype scale of the pipe and captured the pipe's response as having a field joint. Due to the existence of field joints in the FE models, there was no need to consider any type of imperfection in analyzing the post-buckling behavior. However, they only captured the bending capacity limit corresponding to the extreme cross-section ovality, which is the most likely governing class of instability for pipes with field joints. It should be mentioned that, in their study, the core layer was bonded to both internal and external pipes. They concluded that instability occurred because of the formation of inward bulges in both the internal and external pipes.

Due to the increased manufacturing of steel pipelines through the cold-forming process, the characterization of the behavior of such pipes is becoming more important. The yield capacity of cold-formed pipelines is anisotropic depending on the material's orientation with respect to the pipeline axis. Corona et al. [8.18] investigated the influence of material yield anisotropy in single-walled aluminum tubes numerically. They found that the bifurcation curvature of aluminum tubes with a diameter-to-thickness ratio

of 36.13 was significantly influenced by material anisotropy parameters. In another study, Suzuki and Kondo [8.19] studied the behavior of X80 steel pipelines under pure bending through a set of full-scale experimental and numerical investigations. The diameter-to-thickness ratio of the studied specimens was 49. In the numerical studies, Suzuki and Kondo used an isotropic material model to evaluate the characteristic behavior of the specimens. Their numerical models showed a strong correlation to the experimental results in pre-buckling and buckling regimes, but not to post-buckling behavior.

In this research, the behavior of sandwich pipe systems under pure bending is characterized. A series of 3D FE models incorporating geometrical, material and contact nonlinearities was created using the commercial FE package, Abaqus. To perform the investigation, both the linear perturbation eigenvalue buckling analysis and nonlinear post-buckling analysis were conducted. Using the buckling analysis, the influence of pipeline length, core thickness and stiffness was examined on both the buckling moment and longitudinal wrinkle wavelength. Structural parameters that could significantly affect the buckling mode shape of the system were also investigated.

An appropriate geometrical imperfection was included in the models developed for the post- buckling analysis. The imperfection was applied to the pipe in such a way that the FE models were capable of capturing the ovalization of the cross-section as well as the growth of the short wavelength wrinkles along the pipeline axis. Using the FE models, the influence of the geometrical and material parameters that would significantly influence the pre-buckling, buckling and post-buckling behavior of a series of practical configurations was investigated. Furthermore, various possibilities of the intra-layer adhesion bonding were included in the FE models and the resultant responses were characterized and compared. Finally, the influence of steel's yield anisotropy on the characteristic behavior of an SP system was examined and the potential improvement gained by the use of high grade steel pipes is discussed.

8.4. THEORY AND MOTIVATION

Investigating the behavior of pipes under pure bending came to the attention of several researchers already at the beginning of the 20th century. The general behavior of a

pipe under bending can be classified into three categories depending on the geometrical and material properties.

The main distinguishing characteristic behavior of pipes under pure bending is that the applied bending induces ovalization in pipe's cross-section. Known as the Brazier's effect, this ovalization reduces the stiffness of the system. By increasing the bending magnitude, the ovalization localizes in a zone, causing the collapse of the pipe at a certain point. This category of pipes is referred to as Class I in this paper. The stability problem of such systems was studied first by Brazier in 1927 [8.20]. He found that this category of cylinders collapsed when the radially inward deflection reached 2/9 of the cylinder radius. The bending moment corresponding to this deformation can be calculated by [8.21]:

$$M_{cr-B} = \frac{2\sqrt{2}}{9}\frac{E\pi r t^2}{\sqrt{1-\upsilon^2}} \tag{8.1}$$

In the case of short pipes having large D/t parameters subject to bending, short wavelength wrinkles form in the longitudinal direction. By increasing the applied moment, the deformation amplitude of the ripples increases, followed by a catastrophic collapse at a limit load. This category of pipes is classified as Class II in this text. Investigating the bifurcation buckling of cylindrical shells, including the longitudinal wrinkles, was initially considered by Flugge in 1932 [8.22]. However, his study was impeded by the inadequacy of the computational capabilities of the time. In 1961, Seide and Weingarten found that the critical buckling stress for this class of cylindrical shells is essentially equal to the critical stress of the system under uniform axial compression [8.23]. Therefore, they recommended the following equation:

$$M_{cr} = S\sigma_{cr} = \pi r^2 t \sigma_{cr} \tag{8.2}$$

In this equation, σ_{cr} is the critical uniaxial compression stress which can be calculated by [8.21]:

$$\sigma_{cr} = \frac{Et}{r\sqrt{3(1-\upsilon^2)}} \tag{8.3}$$

Kyriakides and Ju [8.24] and Ju and Kyriakides [8.25], through a series of experimental and numerical studies, developed a set of characteristic equations to describe both Class I and Class II types of behaviors. They defined deformation equations

as incorporating three main features. First, the equations were capable of capturing the ovalization in the pipe's cross-section; second, the ovalization along the pipeline axis could be locally developed and; third, the equations are capable of simulating the wrinkle growth along the pipeline axis. They found that by employing this formulation, the characteristic behavior and buckling moment of cylindrical shells falling in the first and second classes of pipes can be accurately calculated.

Pipes with intermediate length and D/t values fall in the third category of pipes, here referred to as Class III. In this category, the instability modes consist of an interaction between the first and second class modes, and thus the method used to evaluate the instability limit moment should be capable of addressing this interaction. The instability of such cylinders was first investigated by Axelrad in 1965 [8.26], who found that the moment capacity of these systems is a function of the ratios of the pipe's thickness and length to the radius. Calladine [8.27] suggested a non-dimensionalized geometrical parameter be used to classify the behavior category of cylindrical shells as:

$$\Lambda \sim \sqrt{\frac{l^2 t}{r^3}} \tag{8.4}$$

It should be mentioned that, in contrast to the other two classes of pipes, the length parameter has a significant influence on the behavior of this category of pipes. Ju and Kyriakides (25) proposed a more complex series expansion to describe the deformation of such systems in comparison to the deformation equations used to describe the first and second classes. Generally, most of the studies developed to characterize the behavior of cylindrical shells are related to the first and the second categories of cylinders. As a result, and due to the complex behavior of the intermediate class, they are less discussed in the literature; nevertheless, advances in computational capabilities and numerical methods have made the investigation of the behavior of such systems more feasible.

A summary of the various classes of behaviors and the influence of the geometrical properties (represented by parameter Λ) on the classification of those behaviors are presented in Figure 8.2. As can be seen in this figure, the second class of pipes exhibits maximum bending capacity and minimum deformability prior to reaching the buckling moment. The pre-buckling, buckling limit and post-buckling regimes in Figure 8.2.b are indicated by the solid lines, solid circular symbols and dashed lines, respectively. The

first class of pipes, which collapse due to excessive section ovality, would have the lowest bending capacity but maximum deformability before buckling. $M_1$and M_2 in these figures represent the minimum and maximum bending capacities, respectively, of a system which can be consequently calculated by Equations (8.2) and (8.1) for a single-walled pipe. Previous studies have revealed that, for metallic pipes made of regular metals, the magnitude of M_1 is nearly twice that of M_2 [Fuchs et al. 8.22].

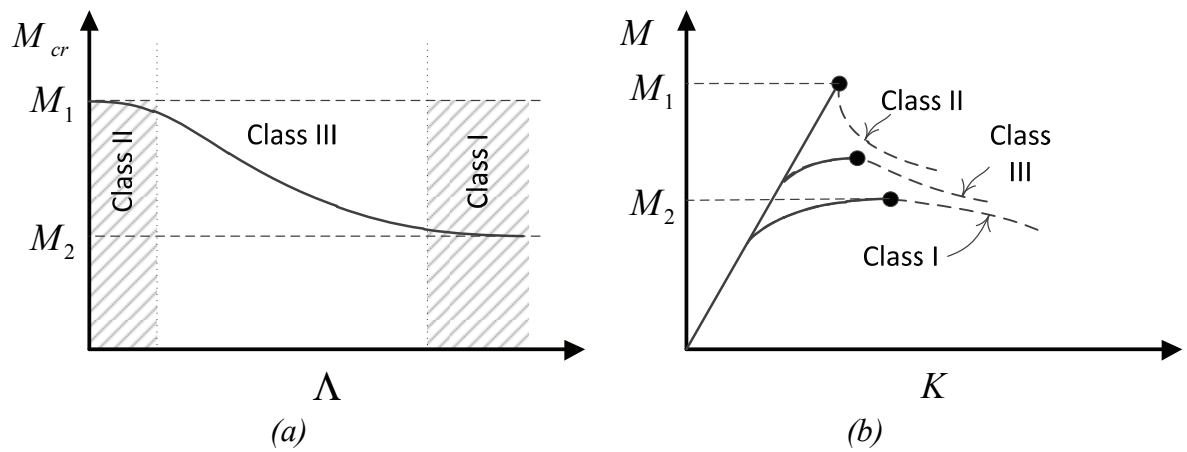

Figure 8.2. General stability behavior of different classes of cylindrical shells under pure bending. (After [8.22])

The behavior of multi-layered cylindrical shells made from anisotropic layers was investigated by several researchers. Fuchs et al. reported a state-of-the-art review in 1993 regarding analytical approaches developed to investigate the behavior of laminated anisotropic circular cylinders under bending. They studied the systems' behavior using a numerical method, discovering that the deformation pattern of the system changed significantly depending on layer configuration. Many investigations were conducted to study the behavior of cylindrical laminate shells in response to the wide application of such structures in various industries. However, due to the brevity of this chapter, this body of research is not discussed here.

Although Cylindrical Laminated Shells (CLS) and sandwich pipes are both multi-layered cylindrical structures, theories developed to characterize the behavior of CLSs are not applicable to SPs, as the total thickness of sandwich pipes is at least 15% of the average radius, which makes the prediction of the response of such systems inadmissible by the first-order theories of laminated shells. To the authors' knowledge, there is no

analytical solution in the literature that can be applied to SP systems under bending due to the extreme complexity of the characteristic equations involved in such systems. However, as cited, the behavior of SPs under bending has been investigated by several researchers using numerical methods.

The numerous limitations of the previous studies motivated the authors to carry out this investigation. Moreover, to the authors' knowledge, no study to date has investigated the influence of yield anisotropy on high-grade steel's stability response. Recent advancements in the manufacturing of high-grade steel pipes, together with the industry's demands for the application of these pipes, have made their use a feasible option for oil and gas pipelines. Yet, in order to make the transportation of oil and gas products in deep waters more economical, a thorough understanding of the behavior of SPs made of high-grade steel pipes is essential. In this study, the response of SP systems made of steel with yield anisotropy is considered and the results compared with conventional SP systems. Additional novel contributions of this research include the characterization of the influence of the intra-layer adhesion configuration on the three-dimensional stability response of SPs and the evaluation of their bending capacities.

8.5. BUCKLING BEHAVIOR OF SPS UNDER BENDING

8.5.1. Finite element models

Using the finite element software, Abaqus, a set of 3D FE models was developed to investigate the buckling behavior of SPs. Python (the programming language within Abaqus) was used to generate efficient mesh variations and also manage the parametric study files. In this section, the results of the buckling linear eigenvalue perturbation method employed to evaluate the buckling moment and the corresponding mode shape of SP systems are presented. The most significant structural parameters were selected and the influences of each parameter on the buckling moment, the buckling mode shape, and the longitudinal wavelength were investigated.

It should be mentioned that, due to the existence of large magnitudes of nonlinearities at the instability point, the application of linear buckling analysis would not be an admissible means for establishing the actual buckling behavior of pipes. Various sources of nonlinearities, such as the material, geometrical and the nonlinearities

resulting from the possible interaction mechanism between the layers' interface could exist in SP systems. However, the eigenvalue buckling analysis method is a valuable analysis tool for the preliminary analysis of such systems and for streamlining the subsequently required nonlinear analysis.

The FE mesh was generated using Abaqus's C3D20R, a 20-node reduced integration 3D brick element [8.28]. An element sensitivity study was performed to eliminate any possible mesh locking or zero energy modes. In addition, a mesh convergence study was performed to determine the most efficient mesh size. Figure 8.3 illustrates the results of the mesh convergence study. The mesh size was chosen so that the change in the buckling moment was less than 0.1% in comparison to the incremental coarser mesh. The results of this study show that employing 44 elements in the circumferential direction would yield the required accuracy. The number of elements in the longitudinal and through-thickness directions was automatically adjusted by a developed Python script in this study, ensuing that the aspect ratio of the elements was kept as close as possible to unity.

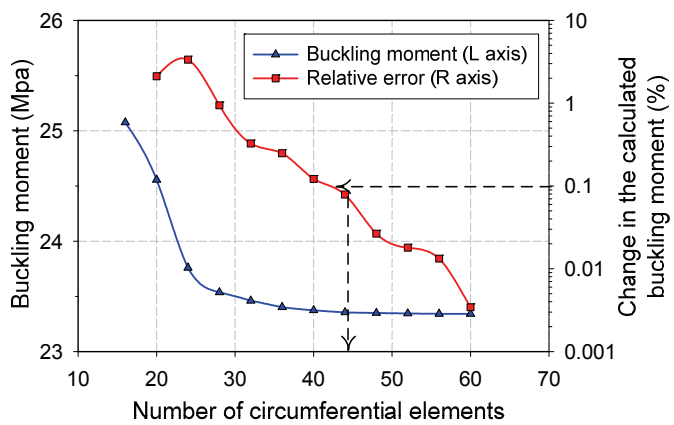

Figure 8.3. Mesh convergence study results for the SP system .

The boundary conditions in the finite element models were created such that the cross-section of the pipe at the ends could deform freely in the plane perpendicular to the pipeline axis. In other words, the radial displacements of the nodes forming the pipe ends were permitted to translate freely (i.e., they were not constrained). Equation (8.5) was used to define the multipoint constraint at the pipe's ends with respect to a reference point located on the axisymmetric axis, at the planes corresponding to the pipe's ends.

$$\tan\theta_R = \frac{Z_i^{ref} - Z_i}{\left(R_i^{ref}\cos\theta_i^{ref} - R_i\cos\theta_i\right)} \tag{8.5}$$

where θ_R is the pipe's end rotation at the reference point.

8.5.2. Analysis results

Inspired by the non-dimensional parameter introduced by Equation (8.4), three significant structural parameters were chosen to investigate the buckling behavior of SPs. According to Equation (8.4), the behavior of a single-walled pipe is a function of the ratio of the pipeline's length and wall thickness to its radius. In this study, a practical configuration of an SP system with an API size 14 internal pipe was chosen. It was assumed that the equivalent thickness of SP systems can be represented by core's thickness and stiffness. In addition to core's thickness and stiffness, the effect of pipe's length is also discussed.

<u>*Pipeline length effect*</u>

Similar to single-walled pipes, the buckling mode shapes of SP systems are influenced by pipeline length. The buckling mode shapes of three similar SP systems with various lengths are illustrated in Figure 8.4. The pipeline presented in the figure consists of API size 14 ($D_2 = 0.3556m$) and 16 ($D_1 = 0.4064m$) as the internal and external pipes, respectively [8.29]. Moreover, a relatively stiff core material with a stiffness ratio (E_c/E_p) of 0.01 was assumed.

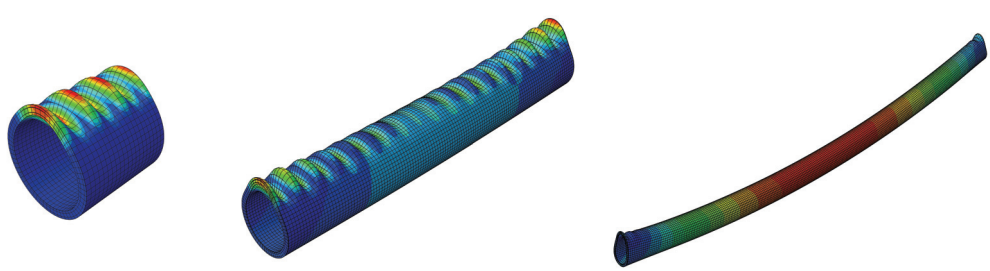

(a) *(b)* *(c)*

Figure 8.4. Influence of the pipeline length on the buckling mode shapes of SP systems.

(a)$L/D = 1$. *(b)*$L/D = 6$. *(c)*$L/D = 20$.

As can be seen in the figure, the relatively short SP system buckles due to forming short wavelength ripples perpendicular to the longitudinal axis. Conversely, the buckling mode shape of the relatively long SP system does not show any wrinkles along the pipe and can be described as a buckling mode type governed by the Brazier effect. Similar to single-walled pipes, the SP systems with an intermediate length of $L/D = 6$ in the studied case have a mixed-mode buckling shape.

Figure 8.5 illustrates the influence of the pipeline length on the buckling moment of the above-mentioned system with a length ranging from 1 to 180 times the external pipe's outer diameter. It should be mentioned that due to computational hardware limitations, a relatively coarser mesh was used for pipes with L/D parameters greater than 20. As can be seen in the figure, pipes having shorter lengths are significantly influenced by the prescribed boundary conditions. In this class of pipes, the first buckling mode shape includes short wavelength wrinkles along pipe's length. The buckling modes on the compressive side of both the internal and external pipes are similar to the buckling mode of a short pipe subjected to axial load only. However, the maximum deformation value of the external pipe is greater than the internal pipe's maximum deformation, which is in turn dependent on core thickness and stiffness.

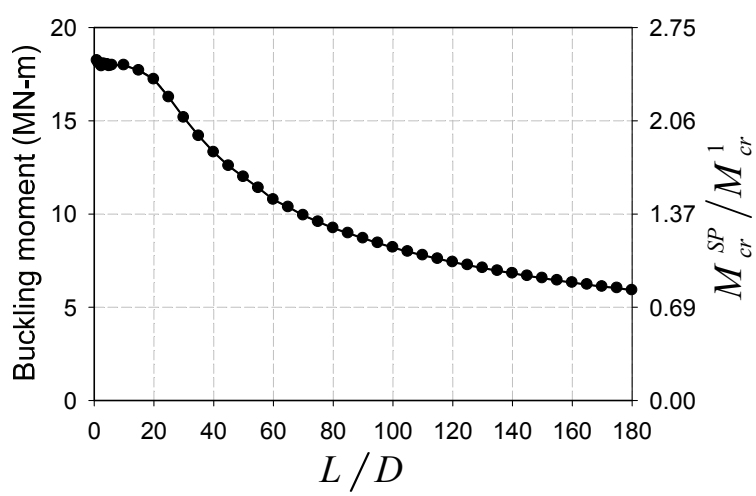

Figure 8.5. Influence of the L/D parameter on the buckling moment capacity of the SP systems.

Figure 8.6 illustrates the variation of the number of wrinkles along the pipeline axis by increasing the pipeline length. These graphs are developed for an SP with,

respectively, API size 14 and 16 internal and external pipes. The core stiffness ratio in the studied case was 0.01. Figure 8.6.a shows the deformation profile of the axis undergoing maximum compressive stress, which is located at the top of the external pipe. As can be seen in this figure, the buckling mode shape of short pipes includes short wavelength wrinkles with a uniform magnitude along the pipeline axis. In the studied case, by increasing the pipeline length to six times the external pipe's diameter, the significant influence of the Brazier effect can be captured. Furthermore, in the longer pipes, the extreme ovalization of the pipe section causes pipeline instability and wrinkles not being formed uniformly all along the pipe.

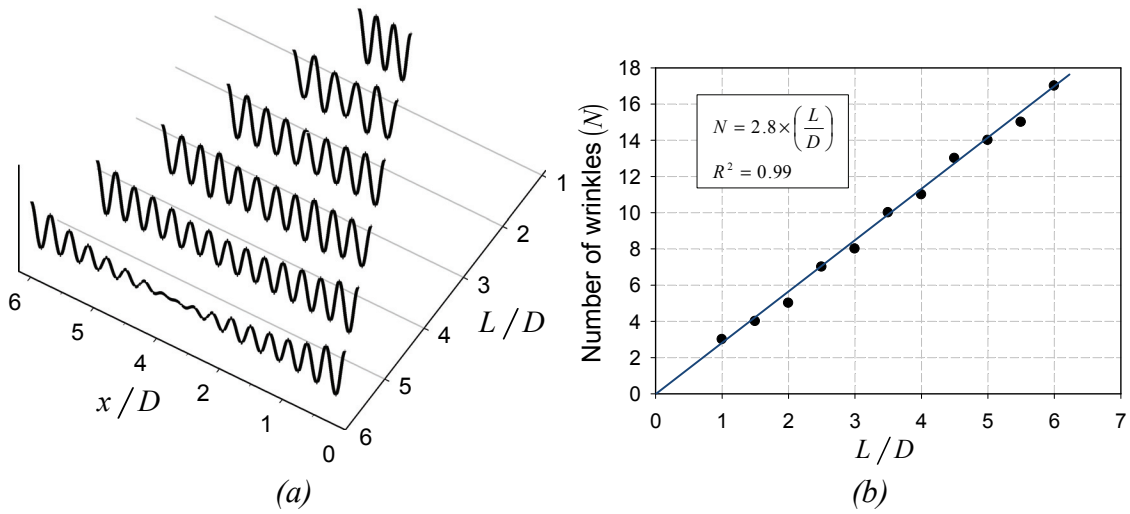

*Figure 8.6. The response of a practical range of SP configuration. (a) Deformation profile of the compression side of the pipes, along the pipeline axis, (b) Variation of the number of wrinkles along the pipeline axis, as a function of (**L/D**).*

Figure 8.6.b presents the variation of the number of waves (wrinkles) along the pipeline axis as a function of the pipe-length-to-diameter ratio. As can be seen in this figure, the number of wavelengths is changed linearly with respect to pipeline length. Our study shows that for all the practical short lengths SP configurations, the wavelength is independent of pipeline length. It should be mentioned that after a specific length – which is $L/D = 6$ in the studied case – the wrinkles would not form linearly along the pipe and consequently the number of wrinkles is no longer considered a linear function of the pipeline length.

Core thickness effect

The core-thickness in a sandwich structure is one of the main structural parameters which could increase the bending stiffness of the structure significantly. Figure 8.7 illustrates the influence of the core thickness on the buckling mode shape of a practical SP case. In this figure, the buckling modes of an SP system having an API size 14 internal pipe, a core stiffness ratio of 0.01 and various external pipes diameters are presented. As can be seen in Figure 8.7.a, the wavelength of the wrinkles along the pipe would not be significantly affected by core thickness. However, as Figure 8.7.b shows, in SP systems with thicker core layers the deformation magnitude in the external pipe in considerably larger than the internal pipe's deformations. As can be seen in Figure 8.7.b, the deformation profile of the internal pipe is similar to the external pipe, but with smaller magnitude.

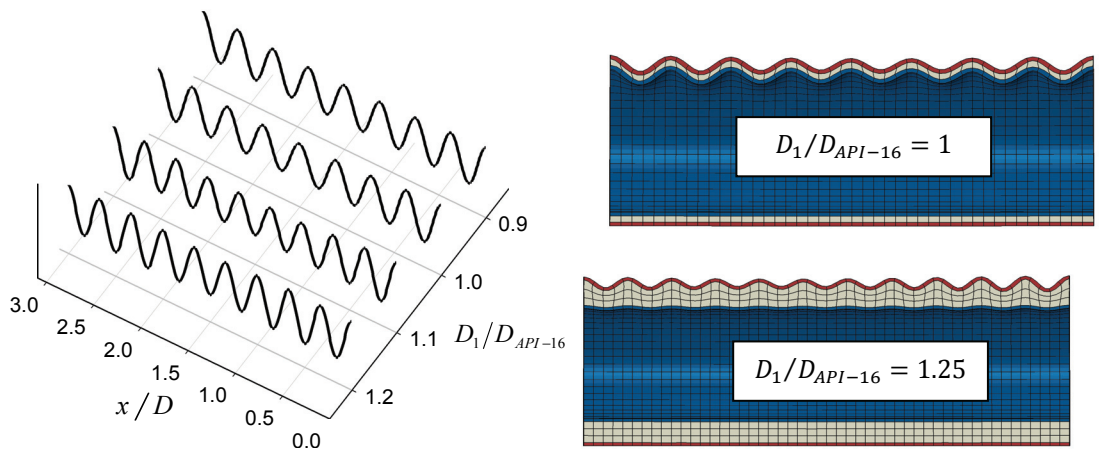

(a) *(b)*

Figure 8.7. Influence of the core thickness on the buckling mode shape of the system. (a) Deformation profile of the compression side of the pipe. (b) Buckling mode shape of the system.

Figure 8.8.a shows the effect of the core thickness on the buckling moment of the same set of SPs. For the presented cases, increasing the external pipe's size from API size 16 ($D_1 = 0.4064m$) to 20 ($D_1 = 0.5080m$), which increases the weight and cost of the steel by 32%, would increase the number of waves from 8 to 9 and the buckling moment of the system by 26%.

The core thickness is one of the main structural and thermal parameters which should be carefully considered in the design of an SP system. In practice, this parameter should be selected based on both thermal and structural considerations. However, if the design of the core layer is based solely on the structural properties, an optimum core thickness can be calculated for an SP system by optimizing the capacity and cost of the system. Figure 8.8.b illustrates the normalized buckling-moment-to-steel-cost ratio of the above-mentioned set of SP systems and the consequent optimum configuration. The buckling capacity and the steel cost are normalized with respect to an SP system having an API size 16 external pipe.

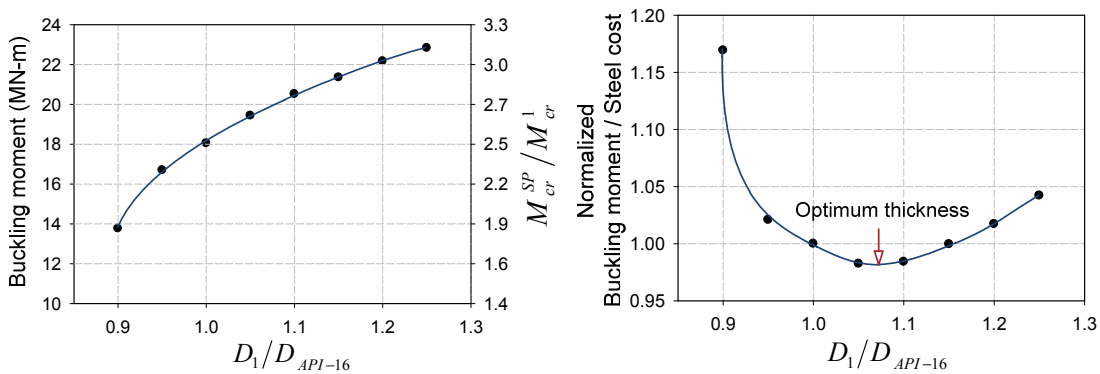

(a) *(b)*

Figure 8.8. The influence of the core thickness on the buckling moment of the system.

<u>*Core stiffness effect*</u>

The stiffness ratio between the core and the sandwiching elements (E_c/E_p) is also a significant structural parameter in a sandwich structure that can considerably influence the bending stiffness and stability response of a system. In SP systems under pure bending, the external pipe undergoes larger compressive stresses and is more susceptible to forming local instabilities. The core layer in an SP system is designed to provide a proper support for the external pipe and also to transfer loads between the sandwiching pipes. The success of the load transfer mechanism is highly dependent on the core stiffness ratio parameter.

Figure 8.9 illustrates the influence of the core stiffness ratio parameter on the buckling mode shape of an SP system with, respectively, API size 14 and 16 internal and

external pipes. As can be seen in Figure 8.9.a, the SP system with a soft core ($E_c/E_p = 0.0001$) becomes unstable due to the formation of local instabilities in the external pipe. In this system, the internal pipe does not have a significant role in carrying the bending load. However, in cases of SPs with stiffer core layers ($E_c/E_p = 0.001,\ 0.01$), a stronger sandwich load transferring mechanism exists and thus the internal and external pipes carry the bending moment together. As a result, such pipes become unstable when local instability waves form in both the internal and external pipes. Figure 8.9.d illustrates the buckling mode shape of an SP system with a relatively stiff core material ($E_c/E_p = 0.1$). As can be seen in the figure, in such a case the effect of higher modes would become more significant and therefore the pipe would buckle in higher buckling modes.

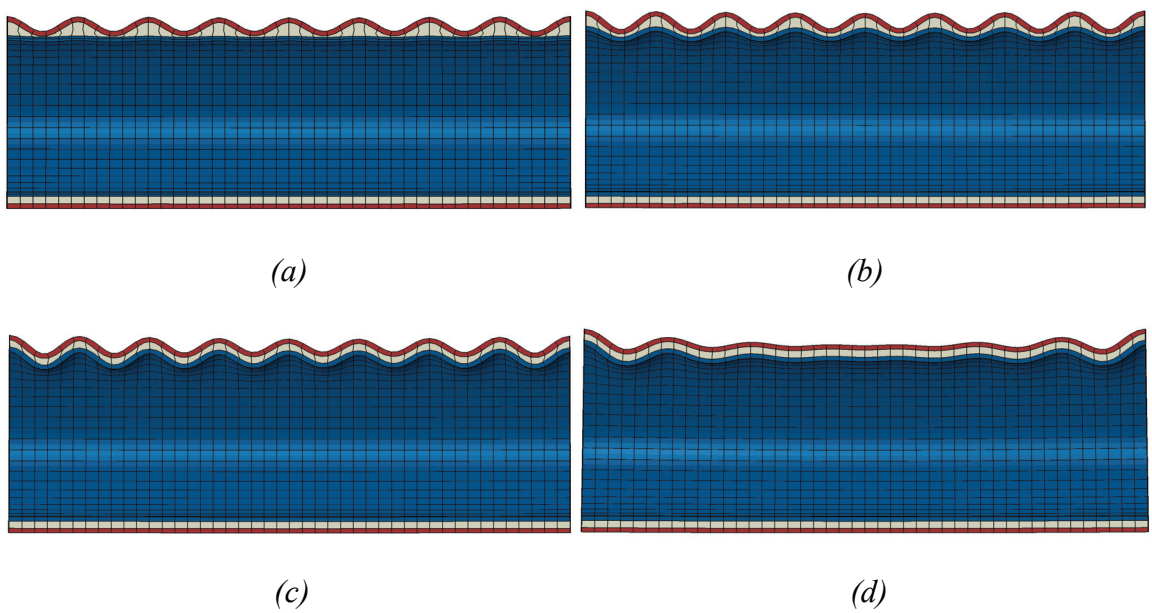

Figure 8.9. Buckling mode shapes of the SP systems with core stiffness ratio of: (a) 0.0001. (b) 0.001. (c) 0.01. (d) 0.1.

Moreover, the core stiffness ratio significantly affects the buckling moment of SPs as well as the buckling mode shape. Figure 8.10 shows the influence of the core stiffness ratio on the buckling moment of the abovementioned system in a log-normal graph. As can be seen in the figure, the influence of the core stiffness parameter is greater if a stiffer range of core materials is considered as a design option. For the studied case, if the stiffness ratio parameter were increased from 0.0001 to 0.001, the buckling moment

would improve only 10%, while if the stiffness ratio parameter were increased from 0.01 to 0.1, the buckling moment would be enhanced by 140%.

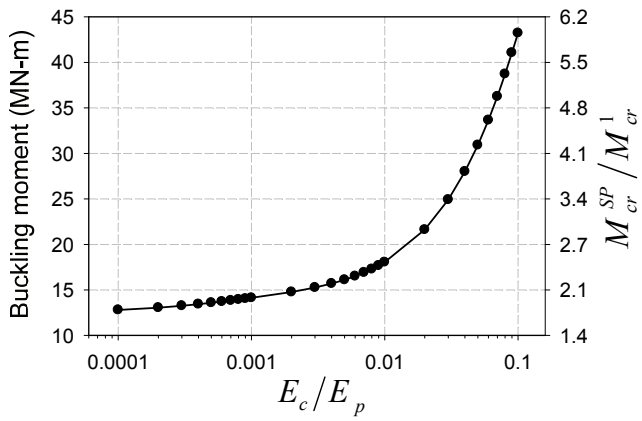

Figure 8.10. Influence of the core stiffness ratio on the buckling moment of a sample SP system.

8.6. POST-BUCKLING BEHAVIOR OF SPS UNDER PURE BENDING

The linear eigenvalue buckling analysis method can accurately evaluate the stability behavior of a linear system and could also be used in nonlinear systems for initial stability analysis calculations. However, to analyze the stability behavior of structural systems suffering from any type of nonlinearities, more advanced numerical methods should be used. In this study, the nonlinear post-buckling analysis was employed to investigate the influence of various structural parameters on the characteristic response of SP systems. The SP system's geometrical properties, the core layer's stiffness and the interaction mechanism between the layers were chosen as significant structural parameters. In addition, the influence of the internal and external pipes' materials yield anisotropy was studied in this research.

8.6.1. Finite element models

The post-buckling behavior of an SP system can be simulated using the nonlinear Finite Element (FE) method. In this research, Abaqus CAE and its programming language, Python, were used to create and manage the FE and parametric study models and also to post-process the results. The Abaqus/standard, which is the implicit solver

engine of the Abaqus, was used to analyze the FE numerical models. As well, a few MATLAB codes were developed to pre-process the numerical models and to extract and process the desired results from the Abaqus output files [8.30].

This research was conducted to investigate the local buckling behavior of SP systems; as discussed above, the pipeline length would significantly influence the stability behavior of SP systems. In the case of long pipes, stability behavior and buckling mode shapes are similar to the global buckling behavior of long pipes under axial load, while for short pipes, the SP system buckles due to the formation of short wavelength wrinkles along the pipeline axis. In order to capture the cross-section instabilities due to either the forming of wrinkles or the Brazier effect, a set of 3D FE models was developed. By comparing the SPs with various lengths, it was found that models with $L/D = 3$ would be capable of capturing local instability behaviors and were also numerically efficient.

This study revealed that pipeline's length had a significant influence on the accuracy of numerical solutions. In a long pipe, the end rotations are much larger compared to short pipes. As a result, when modeling pipes, pipe end sections distort more in longer pipes than in shorter pipes, and thus numerical models of long pipes experience larger magnitudes of nonlinearity and larger residual stresses. However, capturing the limit instability capacity of a pipe is a highly sensitive numerical problem. The existence of both the large magnitude of residual stresses and high numerical sensitivity significantly affects the accuracy of the results. Consequently, in order to overcome the numerical inaccuracy problems, in the post-buckling analysis of SPs, as short a length as possible was selected, while appropriate imperfection modes were applied to the system to account for various buckling modes.

An appropriate type of imperfection could be in the form of an applied load or in a variation in the boundary condition or geometry. In this study, an axisymmetric initial imperfection with a wavelength of 2λ was assigned to the model geometry (the value of λ should be established through an appropriate eigenvalue analysis). Using this wavelength ensures that the linear system would buckle in a mode shape associated with the minimum total potential energy of the system. A small bias toward the center of the pipeline was applied to the amplitude of the waves so to shift the instability away from

the pipe ends (see Figure 8.11). The imperfection magnitude applied to each node of the FE model was calculated by [8.31]:

$$\Delta r_i = R_i \left[a_o - a_1 \cos\left(\frac{\pi x_i}{N\lambda}\right)\right] \cos\left(\frac{\pi x_i}{\lambda}\right), \qquad 0 \le x_i \le L \tag{8.6}$$

Parameters N and λ are, respectively, the number of waves and the wavelength of the wrinkles along the pipeline axis; these should be calculated through an appropriate eigenvalue buckling analysis for the given pipe. Moreover, a_o and a_1 in this equation control the maximum imperfection and also the bias magnitude. API 5L [8.29] recommends that the maximum diameter tolerance (or the bias magnitude) for pipe sizes with a diameter between $2\,{}^{3}/_{8}$" and 20"(which is the studied range in this paper) be less than 0.75% of the specified outer diameter of the pipe. Therefore, in this study, a_o and a_1 are, respectively, taken as 0.3% and 0.075% (which after substituting in Eq. (8.6) would yield the mentioned 0.75% criterion). As a result, the magnitude of the harmonic imperfection varies between 0.45% at the pipe ends and 0.75% at the middle of the pipe. Figure 8.11 illustrates a largely magnified view of such imperfection along the length of an SP, cut along its longitudinal axis.

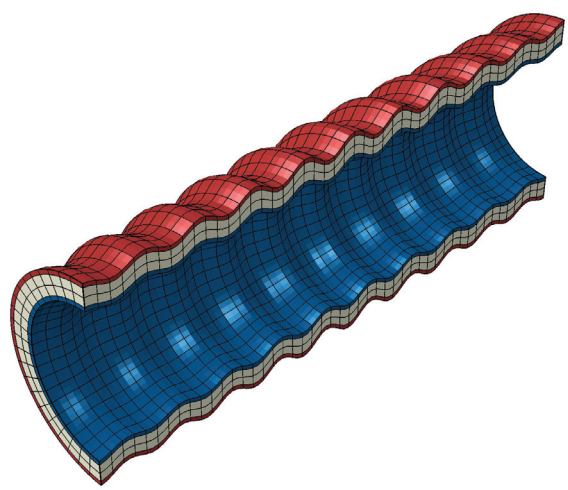

Figure 8.11. A SP system with its geometrical imperfection magnified 20 times

The same 3D finite element mesh which was used in the eigenvalue buckling analysis was used for simulating the post-buckling behavior. The bending loads were applied as deformation controlled rotations at the reference points located at the pipe's

ends. The general Newton-Raphson method was used to analyze the systems exhibiting a relatively smooth characteristic path. However, for pipes with a more abrupt characteristic path near their instability limit, the use of the Riks method was necessary. Thus, to keep the analysis cost-effective, the Newton-Raphson method was employed as the default nonlinear solution method unless the use of Riks method was essential.

In the post-buckling regime, a pipeline would experience large magnitudes of strain and the consideration of a material's plastic response would be necessary. In this study, the material behavior of the external and internal pipes is modeled using the Elastic Perfectly Plastic (EPP) material model. The steel material properties were extracted from API 5L (2000). The yield strain of the polymeric materials used to form the core is much larger than the yield strain of steel. For example, the yield strain of the polypropylene material is about ten times larger than that of steel. As a result, the plastic material behavior of the core does not have a significant effect on the pre-buckling and buckling behavior of SP systems. It should be noted that in some cases this assumption would enter error due to forming of large strains in the core layer at the buckling curvature. However, for the sake of simplicity, the core layer was modeled as a linearly elastic material.

An important structural parameter in SP systems is the intra-layer interaction mechanism between the steel pipes and the core layer. Depending on the intra-layer adhesion configurations, SP systems can be classified into four categories, as follows:

i. The core is fully bonded to both the internal and external pipes. This configuration is referred to as FB hereafter.
ii. The core can slide on or separate from the external pipe but is bonded to the internal pipe. This configuration is referred to as OU hereafter.
iii. The core is bonded to the external pipe but can slide on or separate from the internal pipe. This configuration is referred to as IU hereafter.
iv. The core layer can freely separate from or slide on the both internal and external pipes. This configuration is referred to as BU hereafter.

In order to simulate the above-mentioned interface configurations, two interaction models were used in this research. The bonded interface was modeled by applying the Multi-Point Constraint (MPC) to the nodes located at the interaction surfaces using the

Tie option of the Abaqus. MPCs are imposed by replacing the degrees of freedom of the slave node with those of the master node. The interface property, in which the two contact surfaces are free to slide on or separate from one another, was modeled by a surface-to-surface contact model of the Abaqus. In this model, a frictionless contact property was assumed for the tangential direction and the linear penalty method was used to define the normal behavior of the contact. In the numerical models, the penalty stiffness parameter was set to ten times the representative underlying element stiffness.

8.6.2. Analysis results

The main structural parameters of an SP system were classified into three categories in this research. The three categories are: (i) the geometrical properties, (ii) material properties and (iii) the intra-layer interaction mechanisms. In the following sections, the influence of the parameters in each category will be discussed. Due to the significant influence of core stiffness on the characteristic behavior of SPs, all the above-mentioned parameters will be considered in SPs with two different core stiffnesses: (i) relatively soft and (ii) hard.

In order to present the results in a more interpretable format, the characteristic responses are normalized with respect to the external pipe's capacity. Therefore, the moment and curvature response of SP systems are normalized with respect to the fully plastic moment and curvature capacity of the external pipe calculated by [8.31]:

$$M_o = \sigma_{y1} D_1^2 t_1 \tag{8.7.a}$$

$$K_1 = \frac{t_1}{D_1^2} \tag{8.7.b}$$

In the case of SP systems made from external pipes with material yield anisotropy, σ_{y1} is referred to as the yield stress of the external pipe's material along the pipeline axis.

<u>*Geometrical properties*</u>

Figure 8.12 illustrates the influence of core thickness on the characteristic path of an SP system with internal pipe API size 14 and an FB intra-layer adhesion configuration. Comparison of Figures 12.a and 12.b shows that SP systems with different core

stiffnesses would exhibit two different stability behaviors. As can be seen in Figure 8.12.a, SP systems with a relatively soft core have a linear characteristic path in the pre-buckling regime followed by a nonlinear regime which ends up at the limit state instability point. After the limit point (which is marked in the figure by the symbol ^), the pipe becomes unstable and collapses. In this text, the SP systems that follow this type of instability behavior are classified as the first category.

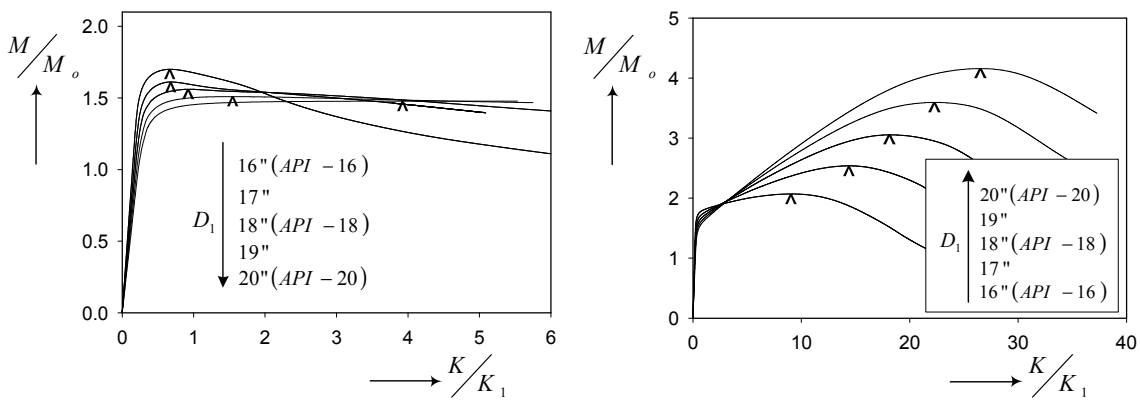

(a) *(b)*

Figure 8.12. Influence of the core thickness on the characteristic behavior of a SP system having core stiffness ratio of (a) 0.001. (b) 0.01.

Figure 8.12.b illustrates the characteristic behavior of a set of SP systems with a relatively stiff core layer and various core thicknesses. As can be seen in the figure, the characteristic behavior has an idealized bilinear pattern prior to reaching the limit stability point marked by ^. In this category, referred here to as the second category, the initial linear proportional pre-buckling path is followed by a secondary stable path with significantly less stiffness prior to reaching the limit state instability point. As a result, before becoming unstable, pipes in this category are more deformable than the pipes in the first category. In other words, the strain capacity of pipes in the second category is much greater than for pipes in the first category.

The efficiency of the external pipe in an SP system is dependent on the core stiffness. For SPs with relatively soft core layers, as illustrated in Figure 8.12.a, employing larger diameter external pipes would degrade the efficiency of the SP system. In other words, although increasing the core thickness improves the moment capacity of

the system, the ratio of the system's capacity to the external pipe's capacity decreases. However, as shown in Figure 8.12.b, in SPs with stiffer core layers, the effect of the sandwich structure is more significant and therefore employing larger diameter external pipes (i.e., thicker core layers) would improve both the efficiency of the sandwich structure and the moment capacity of the system. By comparing the characteristic behavior of SPs with various core thicknesses, we can see that increasing the core thickness improves the deformability of the system before reaching the limit state instability point.

In comparing the graphs of the external pipes with similar diameter but different core stiffnesses, Figure 8.12 shows that increasing core stiffness would have a significant effect on increasing the curvature capacity of the SP system. For example, for an SP system with an API size 16 external pipe, improving the core stiffness ratio from 0.001 to 0.01 would boost the curvature capacity of the system by more than 13 times.

Figures 13 and 14 illustrate the deformed shape and the maximum equivalent plastic strain distribution of the systems for the two core stiffness ratios (considered in Figure 8.12), at the limit instability state. As can be seen, improving the core stiffness ratio would significantly improve the strain capacity of the system. However, the magnitude of the critical strain improvement is more significant in SP systems with thicker core layers. This study also shows that, for a practical range of SPs with a relatively soft core, the maximum plastic strain at the limit instability point occurs in the internal pipe, while in SPs having relatively stiff cores, it occurs in the external pipe.

As discussed in the previous sections, the pipeline length plays a significant role in the stability response of a pipeline. To capture all the possible buckling modes, it is imperative from a numerical modeling prospective to model a pipeline that is sufficiently long. Figure 8.15 illustrates the influence of pipeline length on the characteristic behavior of SP systems with, respectively, API size 14 and 16 internal and external pipes. As can be seen in this figure, for SPs with either soft or stiff cores, the pipeline length does not have a significant effect on either the moment or curvature capacity of the system.

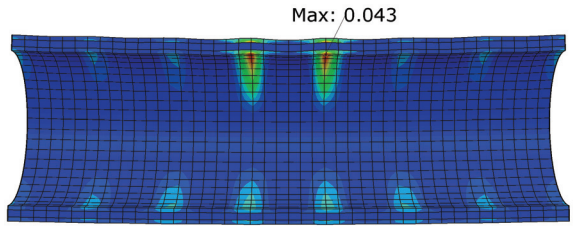

(a)

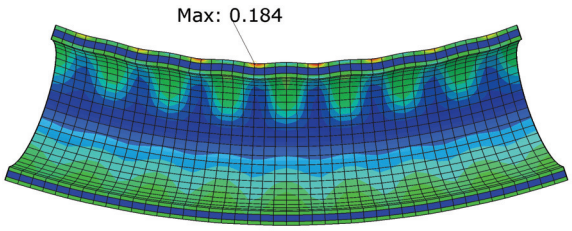

(b)

Figure 8.13. The deformed shape and plastic strain of a SP system at the maximum bending capacity. (a) SP with core stiffness ratio is 0.001. (b) SP with core stiffness ratio is 0.01.

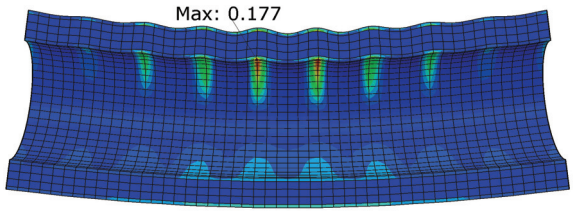

(a)

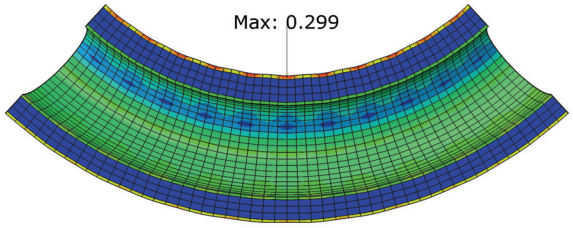

(b)

Figure 8.14. The deformed shape and maximum plastic strain of a sandwich pipe having FB intra-layer configuration at maximum bending capacity in SPs with two different size external pipe: (a) API size 16 (b) API size 20.

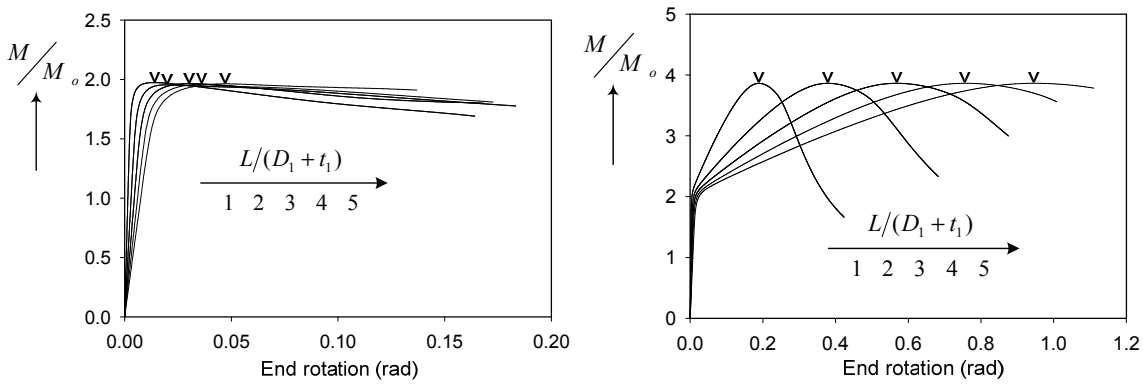

(a) *(b)*

Figure 8.15. Influence of the pipeline length on the characteristic behavior of a SP system having core stiffness ratio of (a) 0.001. (b) 0.01.

<u>*Intra-layer adhesion configuration*</u>

The interface adhesion condition between the constitutive layers in an SP system is a significant structural parameter, which can considerably influence both the deformation and load capacity of a system. Figure 8.16 illustrates the deformed shape of the four described possible configurations at the critical limit state for an SP system with API sizes 14 and 16 internal and external pipes, respectively. In this figure, the deformed shapes are magnified five times. This study shows that the interface condition also influences the deformation mode of the system at the instability limit state. As can be seen in Figure 8.16.a, (i.e., in the FB configuration), the SP system becomes unstable primarily due to the Brazier effect. Consequently, SP systems with FB configurations would exhibit a large curvature capacity compared to the other configurations.

Figure 8.16.b shows the deformed shape of an SP system with an OU configuration. The deformation mode of a such system includes outward bulges in the external pipe, which is less constrained in comparison to the FB configuration. In contrast, in the case of IU configuration, the instability deformed shape (Figure 8.16.c) includes more pronounced inward bulges in the internal pipe. These results also indicate that no general trend can be extracted for the deformed shape at the limit state for the BU configuration. Depending on the other structural parameters, SPs with the BU configuration would

exhibit either inward bulges in the internal pipe or outward bulges in the external pipe, or a combination of these two deformation patterns at the limit instability state.

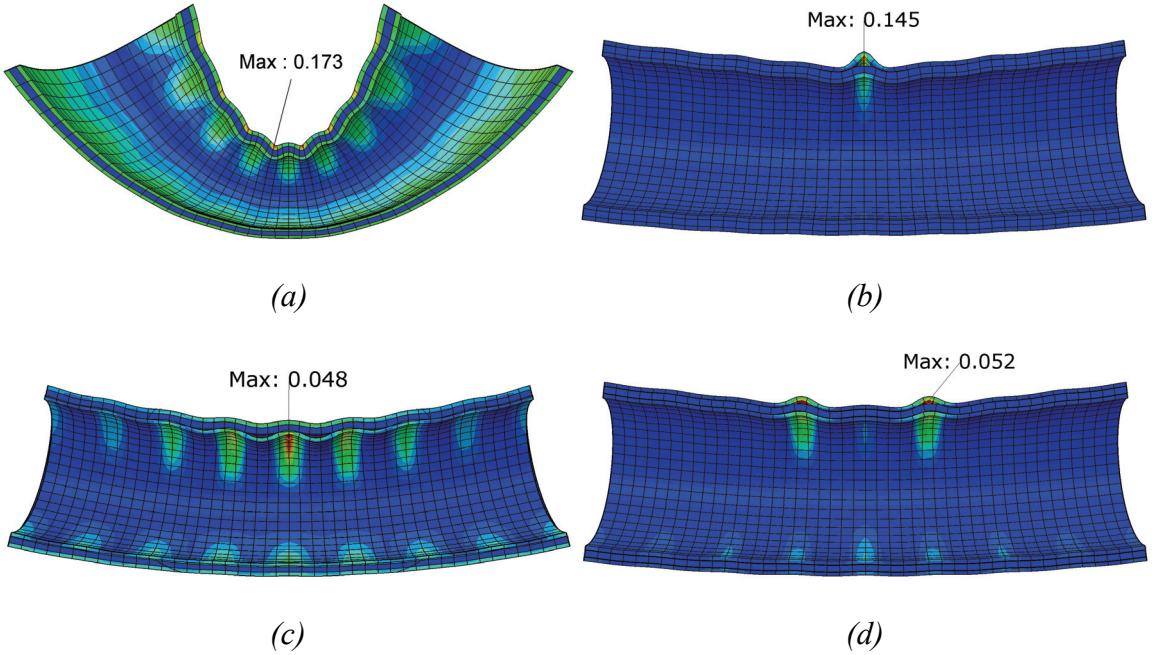

Figure 8.16. The deformed shape and maximum plastic strain of the sandwich pipe with various intra-layer configurations: (a) FB, (b) OU, (c) IU and (d) BU intra layer adhesion configurations.

The normalized moment and curvature capacities of SP systems with a core stiffness ratio of 0.001 and various intra-layer adhesion configurations are compared in Figure 8.17. It should be mentioned that the moment and curvature capacities of the SPs in this figure are normalized with respect to their external pipe's capacity. In a sense, these normalized values present the contribution of the sandwich system to an otherwise single-walled system. As can be seen in Figure 8.17.a, the efficiency of the sandwich structure decreases as the core thickness for SPs with relatively soft cores is increased. In such systems, the FB configuration would develop the largest moment capacity, while the OU and BU configurations would have almost similar capacities and present the least efficient configurations.

Figure 8.17.a shows changes in the curvature capacity by altering the interface adhesion condition. In contrast to the bending capacity, increasing the core thickness improves the deformation capacity of the system. A comparison of the moment and

curvature capacities of various configurations reveals that the systems whose core layer is unbonded from the external pipe would not receive any benefit from the sandwiching mechanism.

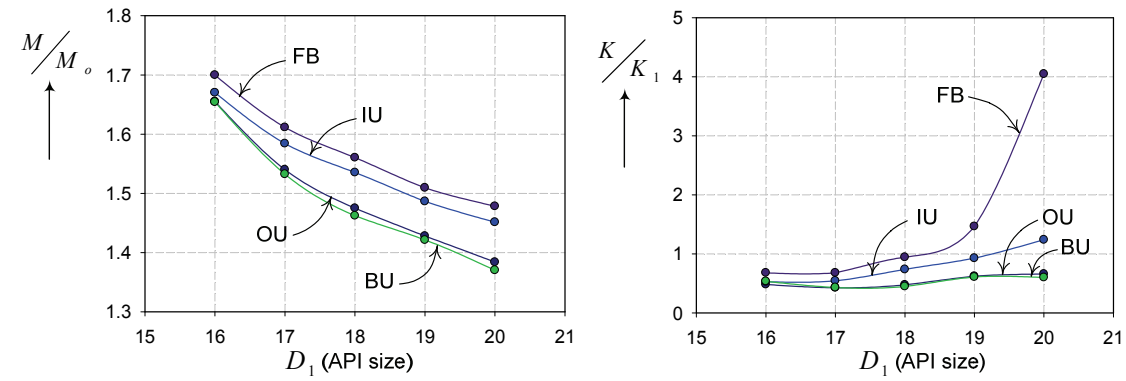

(a)

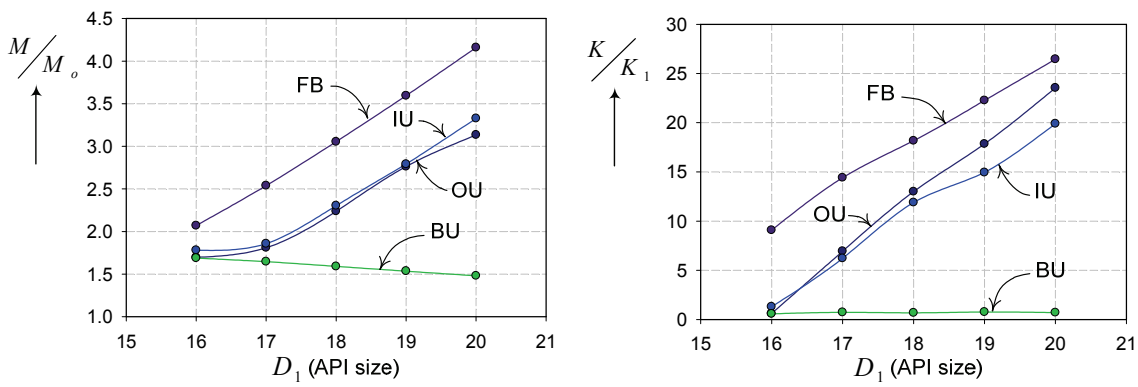

(b)

Figure 8.17. Influence of the intra-layer interaction configuration on the Moment capacity and Curvature capacity of a SP with (a) $E_c/E_p = 0.001$. *(b)* $E_c/E_p = 0.01$.

The same figures also illustrate the efficiency of the sandwich structure in an SP system with a core stiffness ratio of 0.01 and various intra-layer adhesion configurations. As can be seen in Figure 8.17.b, the efficiency of the sandwich system (load and deformation capacities) improves by increasing the core layer thickness. Comparing the results of the OU configurations with a relatively soft core with those having a relatively stiff core shows that enhancing core stiffness can significantly improve the capacity of

this configuration. As can be seen in Figure 8.17.b, the OU configuration, results in the same capacity as the IU configuration as long as a relatively stiff core layer is employed.

Effect of the internal and external pipes' materials yield anisotropy

As stated earlier, material yield anisotropy is an inherent property of cold-formed pipelines. It occurs as a result of the Baushinger effect and the large plastic deformation that is applied to the pipe during its manufacturing process [8.31]. Due to the increasing popularity of such pipelines, it is important to characterize the effect of material yield anisotropy on the bending response of such pipeline systems. Investigating the influence of material yield anisotropy would lead to a better understanding of the behavior of SPs with high-grade internal or external steel pipes. It should be noted that the yield properties of high-grade steel pipes are different when evaluated in different directions.

In this study, the influence of the degree of anisotropy on either the internal or external pipe's materials was investigated by employing Hill's material model [8.32]. The Hill yield potential function is a quadratic function of the stress components while the yield criterion of Hill's plasticity model is an extension of the von Mises yield potential. This model can be represented in the polar coordinate system by:

$$f(\sigma) = \{F(\sigma_{\theta\theta} - \sigma_{zz})^2 + G(\sigma_{zz} - \sigma_{rr})^2 + H(\sigma_{rr} - \sigma_{\theta\theta})^2 + 2L\sigma_{\theta z}^2 + 2M\sigma_{zr}^2 + 2N\sigma_{r\theta}^2\}^{1/2} \tag{8.8}$$

where F, G, H, L, M and N are the material constants, which should be calculated based on the ratio of the yield strength measured in the principal orientations with respect to the reference direction. Material yield anisotropic properties in the normal directions can also be expressed with respect to the material properties in pipeline's longitudinal axis direction as:

$$S_r = \frac{\sigma_{rr-y}}{\sigma_{zz-y}} \tag{8.9.a}$$

$$S_\theta = \frac{\sigma_{\theta\theta-y}}{\sigma_{zz-y}} \tag{8.9.b}$$

where σ_{zz} is the yield stress of the pipe's material in the longitudinal direction (which was taken as the yield stress of API X65-grade steel). In this study, the material yield anisotropy was only considered for normal directions. It was assumed however that the shear yield stresses would be isotropic in all directions.

The effect of the internal pipe's anisotropy parameters S_r and S_θ on the calculated moment capacity of an SP system is illustrated in Figure 8.18. The studied system has API size 14 and 16 as the internal and external pipes, respectively. The diameter-to-thickness ratios (D/t) of the pipes are 37.43 and 42.78, respectively. As can be seen in Figure 8.18.a, the moment capacity of the SP with a relatively soft core ($E_c/E_p = 0.001$) is relatively insensitive to the internal pipe's material anisotropy. Figure 8.18.b shows the effect of the yield anisotropy on an SP system with a relatively stiff core ($E_c/E_p = 0.01$). As can be seen in this figure, increasing either S_r or S_θ would improve the moment capacity. However, the maximum magnitude of the enhancement would only be 2%.

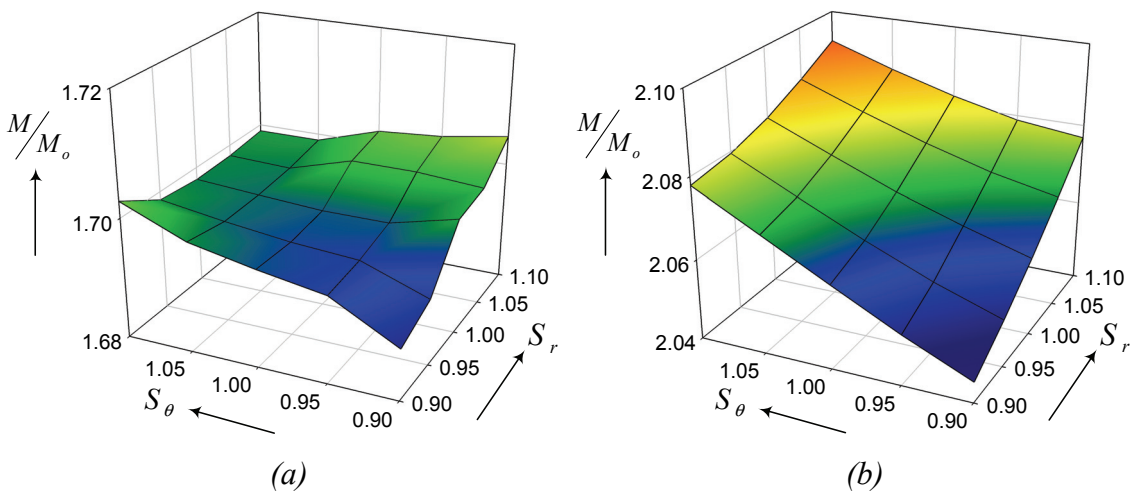

Figure 8.18. Influence of the internal pipe's material yield anisotropy on the bending moment capacity of a SP system having core stiffness ratio of: (a) 0.001. (b) 0.01.

Figure 8.19 illustrates the effect of the external pipe's material anisotropy parameters on the bending moment capacity of the above-mentioned SP system. As can be seen in Figure 8.19.a, the moment capacity of the system with a core stiffness ratio of 0.001 increases by either decreasing S_r or increasing S_θ for an anisotropic parameter range of $S_r < 1$ and $S_\theta > 1$. Nonetheless, the bending moment capacity is insensitive to the anisotropy parameters for the other values of S_r and S_θ. Figure 8.19.b illustrates a similar graph for a system with a relatively stiff core ($E_c/E_p = 0.01$). As can be seen in the figure, the moment capacity of the system is relatively insensitive to S_θ, while it increases

for $S_r > 1$ and decreases for $S_r < 1$. The maximum influence of the external pipe's material yield anisotropy for the studied case is however merely 3%.

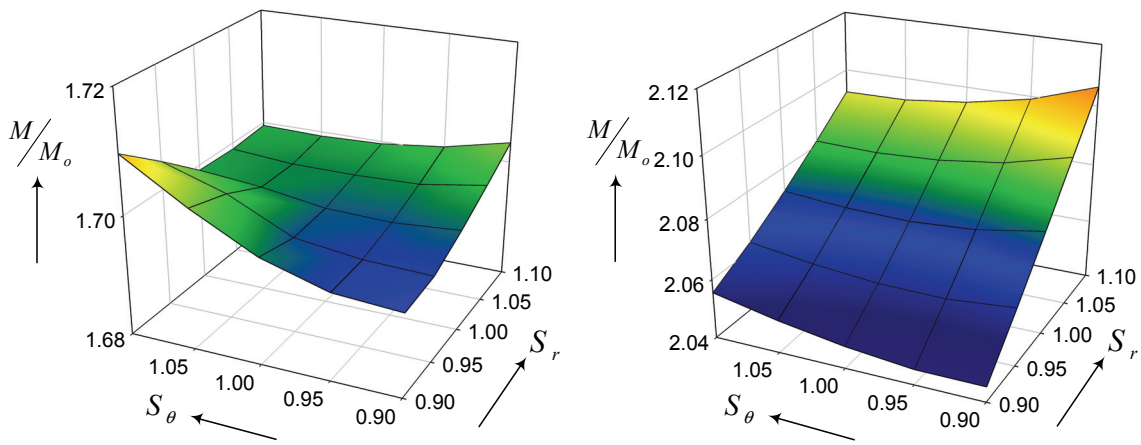

(a) *(b)*

Figure 8.19. Influence of the external pipe's material yield anisotropy on the bending moment capacity of a SP system having core stiffness ratio of: (a) 0.001. (b) 0.01.

8.7. CONCLUSION

The response of sandwich pipe systems subject to pure bending was investigated through a set of numerical parametric studies. The buckling response of the systems was evaluated by using the linear eigenvalue buckling analysis method, while nonlinear analysis was used to calculate the pre-buckling, buckling and post-buckling response. By employing nonlinear finite element analysis, the effect of significant geometrical parameters, material properties and the intra-layer interaction mechanism on the characteristic response of the systems was established. Notable conclusions of this research can be summarized as follows:

- The buckling analysis results revealed that, similar to single-walled pipes, SP systems buckle from the Brazier's effect or the formation of shortwave wrinkles along the pipe. However, owing to their inherently more complex structural interaction, categorizing the instability mode of an SP is more involved. This study shows that SPs with a relatively long length are more susceptible to

becoming unstable due to Brazier's effect, while shorter SPs become unstable due to the growth of short wavelength wrinkles along the pipeline.

- Linear eigenvalue analysis was used to investigate the influence of the core thickness and stiffness ratio on the buckling mode and the capacity of the system. It was found that, while the core thickness parameter does not have a significant effect on the longitudinal wavelengths, it does have a significant influence on the buckling moment. Moreover, it was found that if optimization of the steel used in the system is a matter of interest, an optimum core thickness can be established. As an important structural parameter, the influence of the core stiffness ratio was also studied. The results of this study indicate that the core stiffness ratio has a significant effect on both the buckling mode and buckling moment of the system.
- The post-buckling nonlinear analysis results revealed that, depending on their structural properties, SP systems would have two types of characteristic responses. SP systems with relatively soft cores would behave like typical single-walled pipes, with their characteristic path constituting a linear regime followed by the instability point. In contrast, SPs with relatively stiff cores would exhibit a bilinear characteristic response before reaching the instability limit.
- The efficiency of the sandwich structure was investigated by comparing the moment capacity of the SP system with the external pipe's capacity. It was found that in the case of relatively soft-cored SPs, increasing core thickness would not have a significant effect on the moment capacity of the system; however, for relatively stiff-cored SPs, the core thickness would have a significant effect. Moreover, for any core stiffness, increasing the core thickness would increase the curvature capacity of the system.
- The effect of the pipeline length on the moment and curvature capacity of the system was also investigated. It was found that in the studied length range (SPs categorized as short pipes), the length of the pipeline affects neither the moment capacity nor the curvature that would cause pipe's instability.
- The intra-layer adhesion condition of an SP system is a significant parameter in governing their structural response. This study revealed that the intra-layer adhesion condition can affect the moment capacity, the deformation capacity and

the instability mode of an SP system. It was found that Brazier's effect was more prevalent in governing the instability response of SPs with an FB (i.e., fully-bonded) configuration than SPs with the other intra-layer configurations.

- Comparing the moment capacity of the systems with various intra-layer configurations revealed that the FB configuration yielded the maximum bending moment capacity. After the FB configuration, IU and OU were found to be the most efficient configurations, respectively, while the BU configuration was the least efficient configuration. The difference between the moment capacities of a system with different intra-layer mechanisms is also highly dependent on the other structural parameters. It was shown that for the SP systems studied in this research, improving the intra-layer adhesion configuration could improve the moment capacity of the system by up to 38 times.
- The deformation capacity of the system was also significantly affected by the intra-layer adhesion configuration. It was found that the FB and BU configurations were, respectively, the most and least efficient configurations, from a deformation capacity prospective. The deformation capacity of an OU configuration was found to be highly sensitive to the core stiffness ratio. This study showed that the OU configuration was more efficient than the IU configuration, as long as a relatively stiff core was employed; in contrast, it could exhibit as low as efficiency as BU, if it were configured with a soft core.
- The influence of material yield anisotropy parameters was also investigated in this research. It was found that the moment capacity of soft-core SPs was relatively insensitive to both the internal and external pipes' anisotropy parameters, whereas for hard-core SPs, the material yield anisotropy affected the moment capacity of the system. The analysis results showed that increasing S_r always improves SPs' moment capacity, while the effect of S_θ alters the influence of the other investigated parameters. It should be noted, however, that with a fully isotropic material, the maximum influence of the material yield anisotropy parameters was 2% of the same system.

8.8. REFERENCES

8.1. Brush, D. O. and Almroth, B. (1975). Buckling of bars, plates and shells. McGraw-Hill, New York, USA.

8.2. Sato, M. and Patel, M. H. (2007). Exact and simplified estimations for elastic buckling pressures of structural pipe-in-pipe cross sections under external hydrostatic pressure. *Journal of Marine Science and Technology, 12*(4), 251-262.

8.3. Sato, M., Patel, M. H. and Trarieux, F. (2008). Static displacement and elastic buckling characteristics of structural pipe-in-pipe cross-sections. *Structural Engineering Mechanics, 30*(3), 263-278.

8.4. Arjomandi, K. and Taheri, F. (2010). Elastic buckling capacity of bonded and unbounded sandwich pipes under external hydrostatic pressure. To appear in the *Journal of Mechanics of Materials and Structures*.

8.5. Estefen, S. F., Netto, T. A., and Pasqualino, I. P. (2005). Strength analyses of sandwich pipes for ultra deep-waters. *Journal of Applied Mechanics, 72*(4), 599-608.

8.6. Castello, X., Estefen, S. F., Leon H. R., Chad L. C. and Souza J. (2009). Design Aspect and Benefits of Sandwich Pipes for Ultra Deepwaters. *International Conference on Offshore Mechanics and Arctic Engineering, OMAE2009-79528,* Hawaii, USA.

8.7. Castello, X. and Estefen, S. F. (2006). Adhesion effect on the ultimate strength of sandwich pipes. *International Conference on Offshore Mechanics and Arctic Engineering, OMAE2006-92481,* Hamburg, Germany.

8.8. Castello, X., and Estefen, S. F. (2008). Sandwich pipes for ultra deep-water applications. *Offshore Technology Conference,* OTC 197041*,* Houston, Texas, USA.

8.9. Arjomandi, K. and Taheri, F. (2009). Stability and Post-buckling Response of sandwich pipes under hydrostatic external pressure. Submitted to the *International Journal of Pressure Vessels and Piping*.

8.10. Kyriakides, S. and Netto, T. A. (2002). Dynamic propagation and arrest of buckles in pipe-in-pipe systems. *Proceedings of the International Conference on Offshore Mechanics and Arctic Engineering* - OMAE, 4, 199-205.

8.11. Kyriakides, S. and Vogler, T.J. (2002). Buckle propagation in pipe-in-pipe systems. Part II. Analysis. *International Journal of Solids and Structures, 39*(2), 367-392.

8.12. Kyriakides, S. (2002). Buckle propagation in pipe-in-pipe systems. Part I. Experiments. *International Journal of Solids and Structures, 39*(2), 351-366.

8.13. Kyriakides, S. and Netto, T. A. (2004). On the dynamic propagation and arrest of buckles in pipe-in-pipe systems. *International Journal of Solids and Structures, 41*(20), 5463-5482.

8.14. Arjomandi, K. and Taheri, F. (2010). Influence of the Material Plasticity on the Characteristic Behavior of Sandwich Pipes. Submitted to the *8th International Pipeline Conference*. *IPC2010-31518*, Alberta, Canada.

8.15. Arjomandi, K. and Taheri, F. (2010). External Pressure Capacity of Sandwich Pipes. Submitted to the *journal of Marine Structures*.

8.16. Arjomandi, K. and Taheri, F. (2010). The Influence of Interface Layer Adhesion Properties on the Pressure Capacity and Optimized Configurations of Sandwich Pipes. Accepted (Conditionally, pending minor revision) to the *journal of Ocean Engineering*.

8.17. Carr, M., Matheson, I., Peek, R., Saunders, P. and George, N. (2004). Load and resistance modeling of the Penguins pipe-in-pipe flowline under lateral buckling. *International Conference on Offshore Mechanics and Arctic Engineering – OMAE*. 3, 39-47.

8.18. Corona, E., Lee, L. H. and Kyriakides, S. (2006) Yield anisotropy effect on buckling of circular tubes under bending. *International Journal of Solids and Structures,* 43, 7099-7118.

8.19. Suzuki, N., Kondo, J., Ishikawa, N., Okatsu, M., and Shimamura, J. (2007). Strain capacity of X80 high-strain line pipes. *Proceedings of the 26th International Conference on Offshore Mechanics and Arctic Engineering - OMAE*, 3, 475.

8.20. Brazier, L. G. (1927). On the flexure of thin cylindrical shells and other 'thin' sections. Proceeding of Royal Society of London, Series A, 104-114.

8.21. Farshad, M. (1994). *Stability of structures*. Elsevier, Amsterdam, The Netherlands.

8.22. Fuchs, J. P., Hyer, M. W., Starnes, J. H. (1993). Numerical and Experimental Investigation of the bending Response of Thin-Walled Composite Cylinders.

Department of Engineering Science and Mechanics, NASA Gran NAG-1-343, Interim Report 95, The NASA-Virhina Tech Composite Program.

8.23. Seide, P. and Weingarten, V. I. (1961). On the Buckling of Circular Cylindrical Shells Under Pure Bending. *Journal of Applied Mechanics*, 28, 112-116.

8.24. Kyriakides, S. and Ju, G. T. (1992). Bifurcation and localization instabilities in cylindrical shells under bending. I. Experiments. *International journal of solids and structures,* 29(9), 1117-1142.

8.25. Ju, G. T. and Kyriakides, S. (1992). Bifurcation and localization instabilities in cylindrical shells under bending. II. Predictions. *International journal of solids and structures,* 29(9), 1143-1171.

8.26. Axelrad, E. L. (1965). Pinpointing the Upper Critical Bending Load of a Pipe by Calculating Geometric Nonlinearity. Akademy Nauk SSSR, Izvestiya Mekhanika, 4, 133-139.

8.27. Calladine, C. R. (1983). Theory of Shell Structures, Cambridge University Press, Cambridge, U. K., 614-621.

8.28. ABAQUS User's and Theory Manuals. (2008). Version 6.8, Dassault Systèmes, RI, USA.

8.29. API SPECIFICATION 5L. (2000). *Specification for line pipe*. API Publishing Services, Washington, D.C.

8.30. MATLAB (2008). Version 7, The MathWorks Inc., MA, USA.

8.31. Kyriakides, S. and Corona, E. (2007). *Mechanics of Offshore Pipelines. Volume 1: Buckling and Collapse.* Elsevier, Oxford, UK.

8.32. Hill, R. (1950). *Mathematical theory of plasticity*. New York: Oxford University Press.

CHAPTER 9
CONCLUSION

9.1. CONCLUSIONS

Within this thesis, the stability behavior of Sandwich Pipe systems under two governing loading scenarios has been investigated. External hydrostatic pressure as a governing condition for offshore pipelines and pure bending loads as a governing condition for either offshore or onshore pipelines were also considered in this study.

An analytical approach was used to develop an innovative solution for calculating the elastic buckling capacity of Sandwich Pipes with various intra-layer adhesion configurations. The elastic and plastic characteristic behavior as well as the buckling and collapse pressure of sandwich pipelines was studied using the numerical finite element method. Based on the finite element results, a practical set of equations was developed to calculate the plastic and elastic buckling pressure of SPs with enhanced accuracy. Using the pressure capacity equations developed in this study and recommended simplified manufacturing cost function, a minimum-seeking algorithm was proposed to establish the optimized SP configurations for preferred water depths.

In addition, the behavior of Sandwich Pipes under pure bending was also considered in this research. This included studying the influence of various structural design parameters, such as the pipeline geometrical and material properties as well as the intra-layer adhesion configuration between layers, on the characteristic behavior and bending capacity of the system. In order to perform this research, versatile finite element numerical models and several pre- and post-processing codes for creating the models and post-processing the results were developed. Notable conclusions of this research can be summarized as follows:

1) In contrast to single-walled pipes, where the pipe always buckles in the first mode corresponding to the growth of ovalities in the pipe's cross-section, Sandwich Pipes could buckle in higher modes, depending on the pipeline's geometrical, material and intra-layer configuration properties. Moreover, to the best of the author's knowledge, the influence of intra-layer adhesion condition was accounted for the first time in the semi-analytical solutions developed in this study. The results obtained from the

developed numerical parametric study and the developed analytical equations revealed that the interaction properties between layers in SPs would have a significant effect on both the buckling mode and the buckling pressure capacity.

2) The simplified solutions developed in this research for predicting the elastic buckling pressure of Sandwich Pipes are accurate for the limited range of the SP's parameters considered here. The accuracy of the proposed solution and the solution recommended by Sato and Patel (2007) were examined by comparing the predicted buckling pressure values with those obtained through finite element analysis. This comparison revealed that the solution proposed by Sato and Patel could provide results with higher accuracy for Sandwich Pipes with relatively stiff and thin core layers, while the simplified solutions developed in this study provided more accurate results for SPs with thicker and less stiff cores. Therefore, to attain the highest accuracy, the use of either equation is recommended, depending on the Sandwich Pipe's geometrical and material properties. The appropriate choice of the simplified solutions is facilitated by the graph produced in this study, which can be used to gain a sense of the degree of error margin one should expect when using the proposed simplified equation within a practical range.

3) The finite element numerical investigation of SP models assuming linear material models revealed that, unlike the practical single-walled steel pipes, Sandwich Pipes exhibit two different forms of stability response, depending on their structural properties. Therefore, understanding these responses is important for (i) distinguishing between linear and nonlinear buckling responses, (ii) appropriately analyzing the buckling and buckle propagating phenomena in SPs, and (iii) proper consideration of the ductility of the pipeline before reaching the limit pressure capacity.

4) It was found that in SP systems made from idealized elastic materials, one of the most significant parameters affecting the limit pressure is the core material's properties. Increasing the stiffness of the core material could significantly increase the limit pressure capacity. However, Poisson's ratio of the core material does not

have a significant influence on the buckling pressure capacity. It can be concluded from the numerical results that the use of less compressible core materials would slightly decrease the limit pressure capacity. Core layer thickness would also have a significant effect on both pressure capacity and ductility of the system before reaching the limit. The results of the numerical studies showed that increasing the core thickness would always improve the pressure capacity of the pipe.

5) Several FE models of SPs under hydrostatic external pressure were developed to study the influence of the material model used in the numerical models. The models were constructed incorporating steel with various degrees of hardening and Lüders bands. The comparison of the characteristic response of the considered SP systems revealed that the material plastic stress-strain profile did not have a significant effect on the pipe's buckling capacity.

6) Investigation of several practical PIP and SP configurations revealed that, as a general rule of thumb, adopting a core layer with stiffness ratio (E_c/E_p) of 10% would suffice to create an effective SP structure in which the internal pipe, core layer and external pipe work as an integral unit, whereas multi-layered pipes consisting of a core layer with 0.1% core stiffness ratio may be categorized as PIP configurations where only the external pipe would be effective in resisting external pressure.

7) The computational investigation carried out in this thesis, which accounted for the material and geometrical nonlinearities, revealed that the methods which do not consider material nonlinearity produce a large margin of error in evaluating the external pressure capacity of SPs. This conclusion was validated by comparing the computational results with the results obtained through our earlier linear perturbation FE buckling analysis as well as by using the simplified equations proposed by other investigators.

8) The parametric study results presented here revealed that increasing the t/r ratio of either the internal or external pipes could significantly improve the pressure capacity of the system. However, the comparison of the characteristic paths of the studied SPs revealed that even though increasing the t/r ratio of the external pipe would improve

the pressure capacity of the system, it would decrease the deformability of the system before reaching buckling pressure. On the other hand, employing an internal pipe with greater t/r ratio would improve both the pressure capacity and deformability of the system. It should be mentioned that the core stiffness ratio is an important structural parameter which significantly affects the efficiency of the internal pipe.

9) In this thesis, the influence of high-grade steel (used as the internal and/or external pipes) on the external pressure capacity of SPs was investigated. It was found that upgrading the steel grade of either the internal or external pipes would significantly improve the SP's pressure capacity. However, the influence of the internal pipe's steel grade would also be dependent on the structural properties of the core. That is, for SP configurations with soft core layers, an improvement in the internal pipe's steel grade would not markedly improve the external pressure capacity of the pipe. The parametric study results also revealed that employing high-grade steel pipes in SP systems would exhibit the highest attribute in the FB configuration. For other configurations, the influence of the steel grade would be affected by other parameters; in fact, in some cases, enhancing the steel grades of either the internal and/or external pipes would not improve the pressure capacity of the system at all.

10) Depending on their mechanical and physical properties, SPs exhibit three distinct characteristic responses when subjected to a hydrostatic external pressure. Most of the SP configurations fall under the first and second categories, which would, respectively, exhibit linear and bilinear characteristic paths before reaching their ultimate pressure capacity. However, the third category would include SPs that never become unstable under an external pressure. As an example, a SP with a relatively stiff core layer, unbonded to both the internal and external pipes, would fall under the third category.

11) The results of the parametric studies revealed that the FB (see sections 3.6 and 4.8 for definitions of FB, BU, OU and IU) configuration would offer the greatest pressure capacity and the BU configuration would yield the smallest capacity for an

SP with similar configuration. A comparison of the capacities of OU and IU configurations revealed that SPs with OU and IU configurations and other similar parameters would exhibit almost identical pressure capacities.

12) The results of the buckling analysis of SPs under pure bending revealed that, similar to single-walled pipes, SP systems would buckle due to Brazier's effect or the formation of shortwave wrinkles along the pipe. However, due to the more complex mechanical nature of SPs in comparison to regular single-walled pipes, compartmentalization of SPs' instability mode would be more involved. This study shows that SPs with a relatively long length are more susceptible to becoming unstable due to Brazier's effect, while the relatively short SPs become unstable due to the growth of short wavelength wrinkles along the pipeline's length.

13) The linear eigenvalue analysis was used to investigate the influence of the core thickness and stiffness ratio on the bending buckling mode and system capacity. It was found that, while the core thickness parameter did not have a significant effect on longitudinal wavelengths, it did have a significant influence on the buckling moment. Moreover, it was found that if optimization of the steel used in the system would be of interest, then an optimum core thickness could be established to minimize the overall cost-to-capacity value of the system. As an important influencing structural parameter, the effect of the core stiffness ratio was also studied. The results of this study showed that the core stiffness ratio had a significant effect on both the buckling mode and buckling moment of the system.

14) The post-buckling nonlinear analysis results revealed that, depending on the structural properties of SP systems, they would have two types of characteristic behaviors when subjected to pure bending. SP systems with relatively soft cores would behave like typical single-walled pipes and their characteristic path would consist of a linear regime followed by an instability regime. In contrast, SPs with relatively stiff cores exhibit a bilinear characteristic behavior before reaching the instability limit.

15) The efficiency of the sandwich structure was investigated by comparing the moment capacity of the SP system with the external pipe's capacity. It was found that in the case of relatively soft-cored SPs, increasing the core thickness would not have a significant effect on the system's efficiency from the prospective of its moment capacity. However, for relatively stiff-cored SPs, the core thickness would have a significant influence on the load capacity of the system. Moreover, for any core stiffness, increasing core thickness improves the system's ductility.

16) A comparison of the moment capacity of SPs with various intra-layer configurations revealed that the FB configuration would offer the maximum bending moment capacity. After the FB configuration, IU and OU would be the most efficient configurations, respectively, while the BU configuration would be the least efficient. The difference in the moment capacities of systems with different intra-layer mechanisms would also be highly dependent on the other structural parameters. It was shown that for the SP systems studied in this project, improving the intra-layer adhesion configuration could significantly improve the capacity of the system (up to 38 times).

17) The ductility of the system would also be significantly affected by the intra-layer adhesion configuration. It was found that the FB and BU configurations were, respectively, the most and least efficient configurations, from a ductility prospective. The deformation capacity of an OU configuration was found to be highly sensitive to the core stiffness ratio. This study showed that the OU configuration could be more efficient than the IU configuration, if a relatively stiff core is employed, or it would exhibit the lowest efficiency (as in the case of BU system) if a soft core were used.

18) The influence of the material yield anisotropy parameters on the bending capacity of the pipe was also investigated in this research. It was found that the moment capacity of SPs with a soft core would be relatively insensitive to both the internal and external pipes' anisotropy parameters, whereas for SPs with a hard core, the material yield anisotropy would affect the moment capacity of the system. The analysis results showed that increasing S_r would always improve the system's

moment capacity, while the effect of S_θ would be influenced by other parameters as well (see sections 9.5 for definitions of S_r and S_θ). However, the maximum influence of material yield anisotropy parameters on the bending capacity was 2% of the same system without considering the material yield anisotropy.

9.2. RECOMMENDATIONS FOR FUTURE WORK

This thesis investigated the stability behavior of SPs under two governing loading conditions with the use of analytical and numerical tools. The consideration of the following tasks is recommended for the continuation of this work:

- An investigation of the structural response of SPs under combined loading scenarios as experienced by these pipelines during their installation and/or operation would provide an optimal research extension to the work carried out in this thesis.

- Conducting a comprehensive series of experimental studies is highly recommended. This would enable us to better understand the response of SPs under various loading conditions. Moreover, the results of such experimental investigations could be used to further verify the analytical and numerical results developed in this thesis.

- Advancements in the field of composite materials have introduced a wide range of materials with a versatile range of structural and thermal properties. Investigating the influence of employing such materials for forming the internal and/or external pipes on the structural behavior of SPs could be a valuable extension to this work.

- Engineers are constantly striving to design more optimized and cost-efficient pipelines. In this thesis, a simplified cost function and optimization algorithm was used to establish cost-efficient and resilient systems for use in various water depths. Inclusion of a more precise cost function and a more robust constraint function and optimization method would be extremely valuable to the pipeline industry.

- One of the main challenges in designing SPs is selecting an appropriate core material which can offer both optimal structural and thermal properties. Investigating the best options for the core layer, including consideration of new

hybrid materials, would produce a significant contribution to the future use of SPs.

- The SP systems considered in this study consisted of internal and external pipes and a core layer. Investigating the effect of bulkheads on the structural behavior of the system would serve as a valuable extension to this research.

- SPs used in ultra-deep water may undergo buckle propagation. This phenomenon would be affected by the intra-layer adhesion condition in SPs. The development of a numerical and experimental study to characterize the buckle propagation of SPs by considering the interaction mechanism between the layers is also recommended for future work.

REFERENCES

ABAQUS User's and Theory Manual. (2008). Version 6.8, Dassault Systèmes, RI, USA.

API SPECIFICATION 5L. (2000). *Specification for line pipe*. API Publishing Services, Washington, D.C.

Axelrad, E. L. (1965). Pinpointing the Upper Critical Bending Load of a Pipe by Calculating Geometric Nonlinearity. AkademyNauk SSSR, IzvestiyaMekhanika, 4, 133-139.

Bardi, F. C., and Kyriakides, S. (2006). Plastic buckling of circular tubes under axial compression-part I: Experiments. *International Journal of Mechanical Sciences, 48*(8), 830.

Bardi, F. C., Kyriakides, S., and Yun, H. D. (2006). Plastic buckling of circular tubes under axial compression-part II: Analysis. *International Journal of Mechanical Sciences, 48*(8), 842.

Brazier, L. G. (1927). On the flexure of thin cylindrical shells and other 'thin' sections. *Proceeding of Royal Society of London*, Series A, 104-114.

BREDERO SHAW, 2010. *PU Foam Insulated Pipe-In-Pipe.* [online] Available at: < http://www.brederoshaw.com/solutions/Pipe-In-Pipe.htm> [Accessed 16 September 2010].

Brush DO. and Almroth, B. (1975). *Buckling of bars, plates and shells*. McGraw-Hill, New York.

Calladine, C. R. (1983). Theory of Shell Structures, Cambridge University Press, Cambridge, U. K., 614-621.

Canadian Standards Association (2002). *Steel Line Pipe*, Oil and Gas Industry Systems and Materials Standard CSA-Z245.1.

Carr, M., Matheson, I., Peek, R., Saunders, P. and George, N. (2004). Load and resistance modeling of the Penguins pipe-in-pipe flowline under lateral buckling. *International Conference on Offshore Mechanics and Arctic Engineering – OMAE*.3, 39-47.

Castello, X. and Estefen, S. F. (2006). Limit strength and reeling effects of sandwich pipes with bonded layers. *International Journal of Mechanical Sciences*, 49, 577–588.

Castello, X. and Estefen, S. F., 2006. Adhesion effect on the ultimate strength of sandwich pipes. *International Conference on Offshore Mechanics and Arctic Engineering, OMAE2006-92481,* Hamburg, Germany.

Castello, X., and Estefen, S. F., 2008. Sandwich pipes for ultra deep-water applications. *Offshore Technology Conference,* OTC 197041*,* Houston, Texas, USA.

Castello, X., Estefen, S. F., Leon H. R., Chad, L. C. and Souza, J. (2009). Design aspects and benefits of sandwich pipes for ultra deepwaters. *Proceedings of the 28th International Conference on Ocean, Offshore and Arctic Engineering,* OMAE2009 -79528, Hawaii, USA.

C-CORE, Colt Engineering Corporation Tri Ocean Engineering Ltd., AGRA Earth & Environmental. (2000). *An Engineering Assessment of Double Wall versus Single Wall Designs for Offshore Pipelines in an Arctic Environment*. C-CORE publication. St John's NF.

Corona, E. (2006). Yield anisotropy effects on buckling of circular tubes under bending. *International Journal of Solids and Structures*, 43(22), 7099.

DNV Offshore Standard Det Norske Veritas, (2000). *Dnv-Os-F101, Submarine Pipeline Systems*. GCS AS, Norway.

Estefen, S. F., Netto, T. A., and Pasqualino, I. P. (2005). Strength analyses of sandwich pipes for ultra deepwaters. *Journal of Applied Mechanics, 72*(4), 599-608.

Farshad, M. (1994). *Stability of structures*. ELSEVIER, Amsterdam.

Fuchs, H. P., Hyer, M. W. (1992). The nonlinear bending response of thin-walled laminated composite cylinders. *Proceedings of the 33rd Structures, Structural Dynamics, and Materials Conference*, AIAA 92-2230, Dallas, TX, USA.

Fuchs, J. P., Hyer, M. W., Starnes, J. H. (1993). Numerical and Experimental Investigation of the bending Response of Thin-Walled Composite Cylinders. *Department*

of Engineering Science and Mechanics, NASA Gran NAG-1-343, Interim Report 95, The NASA-Virhina Tech Composite Program.

Gill, P. E., Murray W. M., Saunders M. A. and Wright. M. H. (1986). User's guide for NPSOL (version 4.0): A FORTRAN package for nonlinear programming. Technical Report SOL 86-2. Stanford University: Department of Operations Research.

Hill, R. (1950). *Mathematical theory of plasticity*. New York: Oxford University Press.

Ju, G. T., Kyriakides, S., (1992). Bifurcation and localization instabilities in cylindrical shells under bending. II. Predictions. *International journal of solids and structures,* 29(9), 1143-1171.

Kardomateas, G. A. and Simitses, G. J. (2002). Buckling of long, sandwich cylindrical shells under pressure. *Proceedings of the International Conference on Computational Structures Technology*, 327-328.

Kardomateas, G. A. and Simitses, G. J. (2005). Buckling of long sandwich cylindrical shells under external pressure. *Journal of Applied Mechanics, 72*(4), 493-499.

Kedward, K. T. (1987). Nonlinear collapse of thin-walled composite cylinders under flexural loading. *Proceeding of the 2nd International Conference on Composite Materials (ICCM2)*, 353-365, Toronto, Canada.

Kuwabara, T., Comsa, D. S., Banabic, D. and Iizuka, E. (2002). Modeling anisotropic behavior for steel sheets using different yield criteria. *Key Engineering Materials, 233*, 841.

Kyriakides, S. (2002). Buckle propagation in pipe-in-pipe systems. Part I. Experiments. *International Journal of Solids and Structures, 39*(2), 351-366.

Kyriakides, S. and Corona, E. (2007). *Mechanics of offshore pipelines* (1st ed.). Elsevier, Amsterdam.

Kyriakides, S. and Corona, E. (2007). *Mechanics of offshore pipelines* (1st ed.). Elsevier, Amsterdam.

Kyriakides, S. and Netto, T. A. (2002). Dynamic propagation and arrest of buckles in pipe-in-pipe systems. *Proceedings of the International Conference on Offshore Mechanics and Arctic Engineering* – OMAE2002, 4, 199-205.

Kyriakides, S. and Netto, T. A. (2004). On the dynamic propagation and arrest of buckles in pipe-in-pipe systems. *International Journal of Solids and Structures, 41*(20), 5463-5482.

Kyriakides, S. and Vogler T.J. (2002). Buckle propagation in pipe-in-pipe systems. Part II. Analysis. *International Journal of Solids and Structures, 39*(2), 367-392.

Kyriakides, S., Bardi, F. C., and Paquette, J. A. (2005). Wrinkling of circular tubes under axial compression: Effect of anisotropy. *Journal of Applied Mechanics, 72*(2), 301.

Kyriakides, S., Corona, E. and Fischer, F.J. (1991). On the effect of the UOE manufacturing process on the collapse pressure of long tubes. *Proceeding of Offshore Technology Conference*, OTC 6758, 531-543.

Kyriakides, S., Ju, G. T. (1992). Bifurcation and localization instabilities in cylindrical shells under bending. I. Experiments. *International journal of solids and structures,* 29(9), 1117-1142.

Liberty Development Project (1999). *Evaluation of Pipeline System Alternatives: Executive Summary*, BP.

Liu, M. and Wang, Y. (2007). Advanced modeling of plasticity of linepipe steels with anisotropic texture and complex loading history. *Proceedings of the International Offshore and Polar Engineering Conference-ISOPE,* 3093.

Liu, M., and Wang, Y. (2006). Modeling of anisotropy of TMCP and UOE linepipes. *Proceedings of the International Offshore and Polar Engineering Conference-ISOPE,* 221.

Liu, M., and Wang, Y. (2007). Modeling of anisotropy of TMCP and UOE linepipes. *International Journal of Offshore and Polar Engineering, 17*(4), 288.

Martinez, M. and Brown, G. (2005). Evolution of pipe properties during reel-lay process: Experimental characterization and finite element modeling. *Proceedings of the*

International Conference on Offshore Mechanics and Arctic Engineering - OMAE, 419-429.

Mathematica. (2008). Version 7. *Wolfram Research Inc,* IL, USA.

Meyer, K. J. (1999). Colville River Crossing. *Presented to: Alaskan Arctic Pipelines Workshop*, November 8-9, Anchorage, AK.

Ohga, M., SanjeewaWijenayaka, A. and Croll, J. G. A. (2005). Reduced stiffness buckling of sandwich cylindrical shells under uniform external pressure. *Thin-Walled Structures, 43*(8), 1188-1201.

Paquette, J. A., and Kyriakides, S. (2006). Plastic buckling of tubes under axial compression and internal pressure. *International Journal of Mechanical Sciences, 48*(8), 855. Corona, E. Yield anisotropy effects on buckling of circular tubes under bending. International Journal of Solids and Structures, 43(22), 7099.

Pontremoli, M. (2005). A new generation of ultra-high strength X100/120 pipelines: A breakthrough for economic long-distance gas transportation. *Proceedings of the International Offshore and Polar Engineering Conference - ISOPE, 2005*, 31.

Reddy, J. N. (2003). *Mechanics of laminated composite plates and shells, theory and analysis, second edition*. CRC Press, Boca Raton.

Sato, M. and Patel, M. H. (2007). Exact and simplified estimations for elastic buckling pressures of structural pipe-in-pipe cross sections under external hydrostatic pressure. *Journal of Marine Science and Technology, 12*(4), 251-262.

Sato, M., Patel, M. H., and Trarieux, F. (2008). Static displacement and elastic buckling characteristics of structural pipe-in-pipe cross-sections. *Structural Engineering Mechanics, 30*(3), 263-278.

Seide, P., Weingarten, V. I. (1961). On the Buckling of Circular Cylindrical Shells Under Pure Bending. *Journal of Applied Mechanics*, 28, 112-116.

Spinelli, C., and Marchersani, F. (2004). TAP project. *Proceedings of the Biennial International Pipeline Conference, IPC, 1*, 757.

SPSS (2008). Version 17, SPSS Inc., IL, USA.

Suzuki, N., Kondo, J., Ishikawa, N., Okatsu, M., and Shimamura, J. (2007). Strain capacity of X80 high-strain line pipes. *Proceedings of the 26th International Conference on Offshore Mechanics and Arctic Engineering - OMAE, 3*, 475.

Tanguy, B., Luu, T. T., Perrin, G., Pineau, A. and Besson, J. (2008). Plastic and damage behavior of a high strength X100 pipeline steel: Experiments and modeling. *The International Journal of Pressure Vessels and Piping, 85*(5), 322.

Timoshenko, S., and Goodier, J. N. (1970). *Theory of elasticity* (3rd ed.). McGraw-Hill, New York; Toronto.

Vries G. D., Brennodden H., Meer, J. V. D., Wendel S. (2009). Ormen Lange Gas Field: Immediate Settlement of Offshore Rock Supports. *Journal of Offshore Mechanics and Arctic Engineering*. 131, 1-4.

Appendix A

Inner and Outer Pipes Stiffness Matrix

External pressure's effect is considered in the pipes stiffness matrix.

$$K_p = \begin{bmatrix} c_{11} & c_{12} & 0 & 0 \\ c_{21} & c_{22} & 0 & 0 \\ 0 & 0 & c_{33} & c_{34} \\ 0 & 0 & c_{43} & c_{44} \end{bmatrix} \tag{A-1}$$

$$a_1 = r_1 - \frac{t_1}{2} \tag{A-2}$$

$$a_2 = r_2 + \frac{t_2}{2} \tag{A-3}$$

$$\alpha_1 = \frac{E_p t_1}{r_1\left(1 - \upsilon_p^2\right)} \tag{A-4}$$

$$\alpha_2 = \frac{E_p t_2}{r_2\left(1 - \upsilon_p^2\right)} \tag{A-5}$$

$$c_{11} = \alpha_1 \left[1 + \frac{1}{12}\left(\frac{t_1}{r_1}\right)^2 n^4\right] + q(n^2 - 1) \tag{A-6}$$

$$c_{12} = -c_{21} = \alpha_1 \left[n\left(1 + \frac{1}{12}\left(\frac{t_1}{r_1}\right)^2 n^2\right)\right] \tag{A-7}$$

$$c_{22} = \alpha_1 \left[n^2\left(-1 + \frac{1}{12}\left(\frac{t_1}{r_1}\right)^2\right)\right] \tag{A-8}$$

$$c_{33} = \alpha_2 \left[1 + \frac{1}{12}\left(\frac{t_2}{r_2}\right)^2 n^4\right] \tag{A-9}$$

$$c_{34} = -c_{43} = \alpha_2 \left[n\left(1 + \frac{1}{12}\left(\frac{t_2}{r_2}\right)^2 n^2\right)\right] \tag{A-10}$$

$$c_{44} = \alpha_2 \left[n^2\left(-1 + \frac{1}{12}\left(\frac{t_2}{r_2}\right)^2\right)\right] \tag{A-11}$$

Appendix B

Core Material Stiffness Matrix

$$K_c = L\widetilde{K}_c \tag{B-1}$$

$$L = \begin{bmatrix} 1 & 0 & 0 & 0 \\ -nt_1/2r_1 & 1 - t_1/2r_1 & 0 & 0 \\ 0 & 0 & 1 & 0 \\ 0 & 0 & nt_2/2r_2 & 1 + t_2/2r_2 \end{bmatrix} \tag{B-2}$$

$$\widetilde{K}_c = \begin{bmatrix} \tilde{c}_{11} & \tilde{c}_{12} & \tilde{c}_{13} & \tilde{c}_{14} \\ \tilde{c}_{21} & \tilde{c}_{22} & \tilde{c}_{23} & \tilde{c}_{24} \\ \tilde{c}_{31} & \tilde{c}_{32} & \tilde{c}_{33} & \tilde{c}_{34} \\ \tilde{c}_{41} & \tilde{c}_{42} & \tilde{c}_{43} & \tilde{c}_{44} \end{bmatrix} \tag{B-3}$$

$$R = \frac{a_2}{a_1} \tag{B-4}$$

$$\tilde{c}_{ij} = \frac{A_{ij}}{\psi} \tag{B-5}$$

$$\Lambda = 4\nu_c - 3 \tag{B-6}$$

Core is fully bonded to both inner and outer pipes. (nonvanishing entries only).

$$\psi = (7 + \Lambda)\{\Lambda^2(1 + R^{4n}) - R^{2n-2}[(-1 + n^2)(-1 + R^2)^2 + (1 + R^4)\Lambda^2]\} \tag{B-7}$$

$$\begin{aligned} A_{11} = 2\mathrm{E_c}\{&\Lambda[-1 + n(-1 + \Lambda) - \Lambda] - R^{4n}\Lambda[1 + n(-1 + \Lambda) + \Lambda] \\ &+ 2R^{2n-2}[2(-1 + \Lambda) + n^2(-1 + R^2)(-2 + R^2 + \Lambda) \\ &+ R^2(3 - \Lambda + R^2(-1 + \Lambda^2))]\} \end{aligned} \tag{B-8}$$

$$\begin{aligned} A_{21} = A_{12} = -2\mathrm{E_c}\{&\Lambda[1 + n + (-1 + n)\Lambda] + R^{4n-2}\Lambda(-1 + n + \Lambda \\ &+ n\Lambda) - 2nR^{2n-2}[(-1 + n^2)(-1 + R^2)^2 + \Lambda + R^4\Lambda^2]\} \end{aligned} \tag{B-9}$$

$$\begin{aligned} A_{31} = A_{13} = -2\mathrm{E_c}\,(&\Lambda \\ &- 1)\{R^{3n-1}[(-1 + n^2)(-1 + R^2) - (1 + n + (-1 \\ &+ n)R^2)\Lambda] \\ &+ R^{n-1}[(-1 + n^2)(-1 + R^2) + (-1 + n + (1 \\ &+ n)R^2)\Lambda]\} \end{aligned} \tag{B-10}$$

$$\begin{aligned} A_{41} = A_{14} = -2\mathrm{E_c}(&\Lambda \\ &- 1)\{R^{3n-1}[(-1 + n^2)(-1 + R^2) - (+1 + n - (-1 \\ &+ n)R^2)\Lambda] \\ &+ R^{n-1}[-(-1 + n^2)(-1 + R^2) + (1 - n + (1 \\ &+ n)R^2)\Lambda]\} \end{aligned} \tag{B-11}$$

$$\begin{aligned} A_{22} = 2\mathrm{E_c}\{&\Lambda[-1 + n(-1 + \Lambda) - \Lambda] - R^{4n}\Lambda[1 + n(-1 + \Lambda) + \Lambda] \\ &+ 2R^{2n-2}[n^2\Lambda - (-1 + n^2)R^2(1 + \Lambda) + R^4(-1 + n^2 \\ &+ \Lambda^2)]\} \end{aligned} \tag{B-12}$$

$$A_{32} = A_{23} = -2\mathrm{E_c}\,(-1 + \Lambda)\{-R^{3n-1}[(-1+n^2)(-1+R^2) + (1+n+R^2 - nR^2)\Lambda] + R^{n-1}[(-1+n^2)(-1+R^2) + (1+R^2+n(-1 + R^2))\Lambda]\} \tag{B-13}$$

$$A_{33} = 2\mathrm{E_c}\{-R^{4n}[-1+n(-1+\Lambda)-\Lambda]\Lambda + \Lambda[1+n(-1+\Lambda)+\Lambda] + 2R^{2n-2}[1+n^2(-1+R^2)(1+R^2(-2+\Lambda)) + R^2(-3 + \Lambda) - 2R^4(-1+\Lambda) - \Lambda^2]\} \tag{B-14}$$

$$A_{34} = A_{43} = 2\mathrm{E_c}\{R^{4n}\Lambda[1+n+(-1+n)\Lambda] + \Lambda(-1+\Lambda+n(1+\Lambda)) - 2nR^{2n-2}[(-1+n^2)(-1+R^2)^2 + R^4\Lambda + \Lambda^2]\} \tag{B-15}$$

$$A_{44} = 2\mathrm{E_c}\{-R^{4n}[-1+n(-1+\Lambda)-\Lambda]\Lambda + \Lambda[1+\Lambda+n(\Lambda-1)] - 2R^{2n-2}[(1+\Lambda)(-1+R^2+\Lambda) + n^2(-1+R^2)(-1 + R^2\Lambda)]\} \tag{B-16}$$

Core can slide on the outer pipe but it is bonded to the inner pipe. (nonvanishing entries only).

$$\psi = (7+\Lambda)\{\Lambda[-1-\Lambda+n(-1+\Lambda)] - R^{4n}\Lambda[1+\Lambda+n(-1+\Lambda)] + 2R^{2n-2}[n^2\Lambda - (-1+n^2)R^2(1+\Lambda) + R^4(-1+n^2 + \Lambda^2)]\} \tag{B-17}$$

$$A_{21} = A_{12} = A_{22} = A_{32} = A_{23} = A_{42} = 0 \tag{B-18}$$

$$A_{11} = 8\mathrm{E_c}(-1+n^2)\{-\Lambda - R^{4n}\Lambda + R^{2n-2}[2R^2 + n^2(-1+R^2)^2 + R^4(-1+\Lambda^2)]\} \tag{B-19}$$

$$A_{31} = A_{13} = -4\mathrm{E_c}(n^2-1)(\Lambda - 1)\{R^{3n-1}[n(1-R^2) + R^2(-1+\Lambda)] + R^{n-1}[n(-1+R^2) + R^2(-1+\Lambda)]\} \tag{B-20}$$

$$A_{41} = A_{14} = 4\mathrm{E_c}(n^2-1)(\Lambda - 1)\{R^{n-1}[n(-1+R^2) - R^2(1+\Lambda)] + R^{3n-1}[n(-1+R^2) + R^2(1+\Lambda)]\} \tag{B-21}$$

$$A_{33} = 2\mathrm{E_c}\{-2R^{2n-2}[2R^4(2-2\Lambda+n^2(-2+\Lambda)) - 2n^2\Lambda - (-1 + n^2)R^2(-3+\Lambda)(1+\Lambda)] + [n^2(-1+\Lambda)^2 - (1+\Lambda)^2] + R^{4n}[n^2(-1+\Lambda)^2 - (1+\Lambda)^2]\} \tag{B-22}$$

$$A_{43} = A_{34} = 2\mathrm{E_c}\{-R^{4n}[\Lambda+1+n(-1+\Lambda)][1-\Lambda+n(1+\Lambda)] + [-\Lambda-1+n(-1+\Lambda)][-1+\Lambda+n(1+\Lambda)] + 4nR^{2n-2}[n^2\Lambda - (-1+n^2)R^2(1+\Lambda) + R^4(-1+n^2 + \Lambda)]\} \tag{B-23}$$

$$A_{44} = 2\mathrm{E_c}\{[n^2(-1+\Lambda)^2 - (1+\Lambda)^2] + R^{4n}[n^2(-1+\Lambda)^2 - (1+\Lambda)^2] + 2R^{2n-2}[2n^2\Lambda(1+R^4) - (-1+n^2)R^2(1+\Lambda)^2]\} \tag{B-24}$$

Core can slide on the inner pipe but it is bonded to the outer pipe. (nonvanishing entries only).

$$\psi = (7+\Lambda)\{\Lambda[1+\Lambda+n(-1+\Lambda)] - R^{4n}\Lambda[-1-\Lambda+n(-1+\Lambda)] - 2R^{2n-2}[(1+\Lambda)(-1+R^2+\Lambda)+n^2(-1+R^2)(-1+R^2\Lambda)]\} \tag{B-25}$$

$$A_{41} = A_{14} = A_{42} = A_{24} = A_{43} = A_{34} = A_{44} = 0 \tag{B-26}$$

$$A_{11} = 2\mathrm{E_c}\{[n^2(-1+\Lambda)^2-(1+\Lambda)^2] + R^{4n}[n^2(-1+\Lambda)^2-(1+\Lambda)^2] + 2R^{2n-2}[4(-1+\Lambda)-R^2(-3+\Lambda)(1+\Lambda)+n^2(4-2\Lambda+2R^4\Lambda+R^2(-3+\Lambda)(1+\Lambda))]\} \tag{B-27}$$

$$A_{21} = A_{12} = -2\mathrm{E_c}\{\mathrm{a1}^{4n}R^2[1+n(-1+\Lambda)+\Lambda][1+n+(-1+n)\Lambda] - R^2(\mathrm{a1}R)^{4n}[-1+n(-1+\Lambda)-\Lambda][-1+n+\Lambda+n\Lambda] - 4\mathrm{a1}^{2n}n(\mathrm{a1}R)^{2n}[-1+\Lambda+R^2(1+\Lambda)+n^2(-1+R^2)(-1+R^2\Lambda)]\} \tag{B-28}$$

$$A_{21} = A_{12} = -2\mathrm{E_c}\{\mathrm{a1}^{4n}R^2[1+n(-1+\Lambda)+\Lambda][1+n+(-1+n)\Lambda] - R^2(\mathrm{a1}R)^{4n}[-1+n(-1+\Lambda)-\Lambda][-1+n+\Lambda+n\Lambda] - 4\mathrm{a1}^{2n}n(\mathrm{a1}R)^{2n}[-1+\Lambda+R^2(1+\Lambda)+n^2(-1+R^2)(-1+R^2\Lambda)]\} \tag{B-29}$$

$$A_{31} = A_{13} = -4\mathrm{a1}^{n}\mathrm{E_c}(-1+n^2)(-1+\Lambda)\{R^{3n-1}(-1+\Lambda+n(1-R^2)) + R^{n-1}[\Lambda-1+n(-1+R^2)]\} \tag{B-30}$$

$$A_{22} = 2\mathrm{E_c}\{[n^2(-1+\Lambda)^2-(1+\Lambda)^2] + R^{4n}[n^2(-1+\Lambda)^2-(1+\Lambda)^2] + 2R^{2n-2}[2n^2\Lambda+2n^2R^4\Lambda-(-1+n^2)R^2(1+\Lambda)^2]\} \tag{B-31}$$

$$A_{32} = A_{23} = -4\mathrm{E_c}(n^2-1)(\Lambda-1)\{R^{n-1}[-1-\Lambda+n(-1+R^2)] + R^{3n-1}[1+\Lambda+n(-1+R^2)])\} \tag{B-32}$$

$$A_{33} = 8\mathrm{E_c}(n^2-1)\{\Lambda(-1-R^{4n}) + R^{2n-2}[-1+2R^2+n^2(-1+R^2)^2+\Lambda^2]\} \tag{B-33}$$

Core can slide on the both inner and outer pipes. (nonvanishing entries only).

$$\psi = (7+\Lambda)\{[n^2(-1+\Lambda)^2-(1+\Lambda)^2] + R^{4n}[n^2(-1+\Lambda)^2-(1+\Lambda)^2] + 2R^{2n-2}[2n^2\Lambda(1+R^4)-(-1+n^2)R^2(1+\Lambda)^2]\} \tag{B-34}$$

$$A_{21} = A_{12} = A_{41} = A_{14} = A_{22} = A_{32} = A_{23} = A_{42} = A_{24} = A_{43} = A_{34} = A_{44} = 0 \tag{B-35}$$

$$A_{11} = -8\mathrm{E_c}(-1+n^2)\{-R^{4n}[-1-\Lambda+n(-1+\Lambda)] + [1+\Lambda+n(-1+\Lambda)] - 2R^{2n-2}[R^2(1+\Lambda)+n^2(-1+R^2)(-1+R^2\Lambda)]\} \tag{B-36}$$

$$A_{11} = -8\mathrm{E_c}(-1+n^2)\{-R^{4n}[-1-\Lambda+n(-1+\Lambda)] + [1+\Lambda+n(-1+\Lambda)] - 2R^{2n-2}[R^2(1+\Lambda)+n^2(-1+R^2)(-1+R^2\Lambda)]\} \tag{B-37}$$

$$A_{31} = A_{13} = -8\mathrm{E_c} n\,(-1+n^2)(\Lambda-1)\{R^{n-1}[-1-n+(-1+n)R^2] + R^{3n-1}[1+R^2+n(-1+R^2)]\} \tag{B-38}$$

$$A_{33} = -8\mathrm{E_c}(-1+n^2)\{[-1-\Lambda+n(-1+\Lambda)] - R^{4n}[1+\Lambda+n(-1+\Lambda)] + 2R^{2n-2}[n^2R^4+n^2\Lambda-(-1+n^2)R^2(1+\Lambda)]\} \tag{B-39}$$

Appendix C

Copyright Agreement Forms

Journal of Mechanics of Materials and Structures
Copyright Agreement Form for

Kaveh Arjomandi

Elastic Buckling Capacity of Bonded and Unbounded Sandwich Pipes under External Hydrostatic Pressure

A formal Consent to Publish is required (see item 6 below). It is also strongly recommended that Authors provide a Transfer of Copyright to the Publisher. The signed Consent to Publish gives the Publisher the Author(s)' permission to publish the Work. The signed Transfer of Copyright empowers the Publisher on behalf of the Author(s) to protect the Work and its image against any unauthorized use and to properly authorize dissemination of the Work by means of printed publications, offprints, reprints, electronic files, licensed photocopies, microform editions, translations, document delivery and secondary information sources such as abstracting, reviewing and indexing services, including converting the Work into machine readable form and storing it in electronic databases.

The Publisher hereby requests that the Author(s) complete and return this form promptly so that the Work may be readied for publication.

1. The Author(s) hereby consents that the Publisher publishes the Work.

2. The Author(s) warrants that the Work has not been published before in any form except as a preprint, that the Work is not concurrently submitted to another publication, that all Authors are properly credited, and generally that the Author(s) has the right to make the grants made to the Publisher complete and unencumbered. The Author(s) also warrants that the Work does not libel anyone, infringe anyone's copyright, or otherwise violate anyone's statutory or common law rights.

3. The Author(s) hereby transfers to the Publisher the copyright of the Work named above whereby the Publisher shall have the exclusive and unlimited right to publish the said Work and to translate (or authorize others to translate) it wholly or in part throughout the World during the full term of copyright including renewals and extensions and all subsidiary rights as indicated above subject only to item 4.

4. The Work may be reproduced by any means for educational and scientific purposes by the Author(s) or by others without fee or permission with the exception of reproduction by services that collect fees for delivery of documents. The Author(s) may use part or all of this Work or its image in any future works of his/her (their) own. In any reproduction, the original publication by the Publisher must be credited in the following manner: "First published in [Publication] in [volume and number, or year], published by the Journal of Mechanics of Materials and Structures," and the copyright notice in proper form must be placed on all copies. Any publication or other form of reproduction not meeting these requirements will be deemed to be unauthorized.

5. In the event of receiving any request to reprint or translate all or part of the Work, the Publisher shall seek to inform the Author(s).

6. If the Author(s) wishes to retain copyright of the content and image of this Work, in the Author(s)' name(s) or the name of a third party (e.g., employer), the Author(s) may strike out items 3, 4, and 5 above. In this case the Author(s) nevertheless gives the Publisher unlimited rights to publish and distribute the Work in any form and to translate (or allow others to translate) the Work wholly or in part throughout the World and to accept payment for this. The copyright holder retains the right to duplicate the Work by any means and to permit others to do the same with the exception of reproduction by services that collect fees for delivery of documents. In each case of authorized duplication of the Work, the Author(s) must still ensure that the original publication by the Publisher is properly credited. If the Author(s) does not choose, or is unable, to assign copyright to the Publisher, the Author(s) agrees that the JOMMS is not responsible for protecting the Work from misuse by others, and the copyright holder agrees to hold the Journal of Mechanics of Materials and Structures harmless in all matters concerning copyright. If copyright is not to be transferred to the Publisher, please indicate how the copyright line should read:

Please note: If the Work was created by U.S. Government employees in the scope of their official duties, the Work is not copyrightable and all provisions of this agreement relating to copyright (other than item 2) are void and of no effect. The Consent to Publish provisions remain in effect, however, and must be signed.

7. This form is to be signed by the Author(s) or, in the case of a "work-made-for-hire," by the employer. If there is more than one Author, then all authors must sign the Consent to Publish and Copyright Agreement, either on the same form or on different copies of the same form.

2009-10-30

Signature: _____

Kaveh Arjomandi

Please mail the signed form to:
Mathematical Sciences Publishers
Department of Mathematics
University of California
Berkeley, CA 94720-3840
United States